Studies of the *Drosophila* Rho G protein regulators, *pebble* and *RacGAP50C*.

by
W. G. Somers, B. Sc., M. Sc. (first class honours)
November 2002

This thesis is submitted in fulfilment of the requirements for a Doctor of Philosophy (PhD) in the Faculty of Science at the University of Adelaide.

Centre for the Molecular Genetics of Development
Department of Molecular Biosciences
University of Adelaide

Declaration

This thesis contains no material which has been accepted for the award of any other degree or diploma in any other university or tertiary institute and, to the best of my knowledge and belief, contains no material previously published or written by another person, except where due reference has been made in the text.

I give consent to this copy of my thesis, when deposited in the University Library, being available for loan and photocopying.

Greg Somers, November 2002.

Acknowledgments

I would like to start by saying an indebted thankyou to Rob Saint. For firstly, giving me the opportunity to conduct this work in his laboratory and allowing me to learn the wonders of fly genetics. Your encouragement and enthusiasm throughout my research has been admirable and greatly appreciated.

Thanks to all past and present Saint lab. members, both in Adelaide and Canberra for their support. I am particularly grateful for the time and patience Louise had while teaching me the basics in fly pushing. Thankyou to my summer-students, Rena and Sharon. I hope the mindless molecular techniques I taught you will be helpful in the future.

I would like to thank everyone who acknowledged my stress as I wrote this thesis, particularly those who fed me, so that I did not have to leave the computer. Thankyou to Pen, Masha, Peter, Duka and Rob, for helpful suggestions in writing this thesis.

I would like to thank Adelaide University for granting me a scholarship, and the Centre for Molecular Genetics of Development (CMGD), for their support in attending international conferences.

I would finally like to say a big thankyou to Penelope for always being there and for patiently waiting for me to finish that 'last experiment', for three and a half years. Well, I can now finally say ..... "its done"!

Abstract

Cytokinesis is the final step in mitosis, requiring the formation and constriction of an actin-myosin-based contractile-ring. In both *Drosophila* and mammalian cells the stimulatory signal that positions the contractile-ring and coordinates F-actin and microtubule bundling is derived from the central spindle. The nature of this signal is currently unknown. The *Drosophila* gene *pebble* (*pbl*) encodes a Rho family guanine nucleotide exchange factor that is essential for cytokinesis. PBL is localised to the inner face of the furrowing cortex during anaphase/telophase and to the nucleus of non-dividing cells. While it is likely that the role of the cytoplasmically localised PBL is to activate Rho1, to regulate actin cytoskeleton dynamics during cytokinesis, the function of the nuclear localised PBL is unknown. PBL also contains two consensus BRCA1-C terminal (BRCT) domains which, from studies of other proteins, are implicated in DNA damage repair. The role of the N-terminal BRCT domains were examined in this thesis.

A yeast two-hybrid screen identified that the Rho family GTPase protein, RacGAP50C, was capable of strongly interacting with the N-terminal domains of PBL. Like its mammalian ortholog MgcRacGAP and *C. elegans* ortholog CYK-4, RacGAP50C was shown to be essential for cytokinesis. Throughout mitosis RacGAP50C colocalises with the kinesin-like motor protein, Pavarotti (PAV). During anaphase/telophase this RacGAP50C-PAV complex was observed to localise to the midzone region of cortically associate microtubules. It is here that RacGAP50C localises adjacent to the cortically localised PBL. I propose that upon arrival of the RacGAP50C-PAV complex to the central spindle, RacGAP50C then interacts with PBL. The RacGAP50C-PAV complex may recruit PBL to the equatorial cortex, thereby specifying the cleavage plane. The formation of this RacGAP50C-PBL complex is then able to stimulate cytokinesis, by regulating the assembly and constriction of the contractile-ring.

TABLE OF CONTENTS

Chapter One: Introduction.....1

Chapter Two: Materials and Methods.....33

Chapter Eight: General discussion and future directions..... 165

Abbreviations

A_{600}: optical absorbance at the wavelength 600nm
AED: after egg deposition
AP: alkaline phosphatase
APF: after pupal formation
APS: ammonium persulphate
β-mercaptoethanol: 2-mercaptoethanol
BCIP: 5-bromo-4-chloro-3-indolyl-phosphate
BDGP: Berkley *Drosophila* Genome Project
bisacrylamide: N,N'-methylene-bisacrylamide
Blotto: 5% skim milk powder in PBT
bp: base pairs
BSA: bovine serum albumin
CDS: coding sequence
CIP: calf intestinal alkaline phosphatase
CNS: central nervous system
DIG: digoxigenin
DAB: 3,3'-diaminobenzidine
DMSO: dimethylsulphoxide
DNA: deoxyribonucleic acid
DNaseI: deoxyribonuclease I
dNTP: deoxyribonucleoside triphosphate
DTT: dithiothreitol
ECL: enhanced chemiluminescense
EDTA: ethylenediaminetetraacetic acid
EMS: ethyl methane sulfonate
EST: expressed sequence tag
EtBR: ethidium bromide
GFP: green fluorescent protein
GST: glutathion-S-transferase
HRP: horse-radish peroxidase
IPTG: isopropyl ß-D-thiogalactopyranoside
kb: kilobase pairs
kDa: kilodaltons
LiOAc: lithium acetate
Luminol: 5-amino-2,3-dihydro-1,4-phthalazinedione
MQ: MilliQ
MT: microtubule
NBT: 4-nitro blue tetrazolium chloride
NGS: Normal goat serum
PAGE: polyacrylamide gel electrophoresis
PEG: polyethylene glycol
PBS: phosphate buffered saline
PCP: planar cell polarity
PI: protease inhibitor
PNS: peripheral nervous system
RNA: ribonucleic acid
RNAi: RNA interference
RNaseA: ribonuclease A
rpm revolutions per minute
RT: room temperature
S2: Schneider 2
SDS: sodium dodecyl sulphate
ssDNA: sonicated salmon sperm DNA
TEMED: N,N,N',N-tetramethylenediamine
Tris: tris (hydroxymethyl) aminoethane
U: unit of enzyme activity
UAS: upstream activating sequence
UV:ultra violet light
WT: Wild type
X-gal: 5-bromo-4-chloro-3-indolyl-β-D-galactopyranoside

Chapter One: Introduction

Cytokinesis is the final step in mitosis and is the process that generates two daughter cells from a single cell. Although cytokinesis has been observed for well over a century, the signalling and regulatory mechanisms involved remain poorly understood. The initiation of cytokinesis is tightly regulated with respect to earlier events in the cell cycle to ensure proper chromosome segregation and to prevent premature mitotic exit. In all systems studied, cytokinesis requires the coordinated reorganisation of both actin filaments and microtubules. In animal cells, the stimulatory signal that positions the contractile-ring and initiates cytokinesis is generated from the central spindle microtubules. The nature of the stimulus is unknown but appears to involve the combined interactions of a number of proteins. The well-characterised cellular events that occur during *Drosophila melanogaster* development, the ease of genetic manipulation and the significant level of gene conservation with higher organisms makes *Drosophila* an excellent model organism for the study of eukaryotic cytokinesis.

1.1 The eukaryotic cell cycle

The cell cycle is a term used to describe the replication of both cellular mass and genetic material. All stages within the cell cycle must be tightly regulated to prevent developmental abnormalities. A typical cell cycle can be broken down into four stages. Beginning with the Gap phase one (G1), cells then progress through to the S phase, Gap phase two (G2), M phase and then re-enter the next G1 phase. The G1 and G2 phases are considered to be a 'resting state', in which cells remain metabolically active. The genomic DNA is replicated during S phase and mitosis occurs during the M phase of the cell cycle. Mitosis involves the equal segregation of the replicated DNA, followed by cytokinesis to produce two identical daughter cells. Modified versions of the cell cycle exist in certain tissues during development. For example, in

endoreplicative tissues, such as the salivary glands of *Drosophila,* the M phase is absent and during *Drosophila* syncytial blastoderm development there are no G phases.

1.1.1 CDKs and cyclins

Progression through the cell cycle is controlled by a family of cyclin dependent serine/threonine kinases (CDKs). The association of a CDK with an appropriate cyclin protein regulates the activity of the CDK. The abundance of CDKs remains fairly stable throughout the cell cycle, while the abundance of the regulatory cyclin subunits fluctuates dramatically due to ubiquitin-mediated proteolysis. CDK/cyclin complexes selectively phosphorylate target proteins involved in cell cycle progression into and through different stages. For example, in mammalian cells Cyclin A and/or Cyclin B complex with Cdk1 for the G2 to M phase transition; Cyclin D1, D2 or D3/Cdk4 or Cdk6 and Cyclin E/Cdk2 are required for the G1 to S phase transition; and Cyclin A/Cdk2 is required for progression through S phase (reviewed by Reed, 1996). In *Drosophila*, cyclin D (Duronio and O'Farrell, 1995) and cyclin E (Knoblich *et al.,* 1994) are required for S phase transition. Cyclin A degradation facilitates chromosome disjunction, cyclin B destruction is required for anaphase B and cytokinesis, while cyclin B3 degradation is required for proper spindle reorganization (Parry and O'Farrell, 2001).

1.1.2 Mitosis (M phase)

Mitosis involves the duplication of genetic material which is then equally segregated into two daughter cells by a process known as cytokinesis. Mitosis can be divided into five sub-phases: prophase, pro-metaphase, metaphase, anaphase and telophase. Chromatin condensation occurs during prophase and the chromosome kinetochores are captured by mitotic microtubules at pro-metaphase. Metaphase is characterised by the alignment on the equatorial region of the paired sister chromatids, now attached by their kinetochores to either polar centrosome. Anaphase involves the separation of the sister chromatids and the initiation of cytokinesis. Anaphase can be further subdivided into two sequential stages: anaphase A, where sister chromatids separate and travel to either pole and anaphase B, where the spindle poles increase their separation so that they are in closer proximity to the cell cortex. Telophase then sees the reforming of the

nuclear envelope, the continued ingression of the cortical furrow (except in plants) and the resolving of the cell membrane to generate two daughter cells.

1.2 Cytokinesis

Cytokinesis is accomplished by the placing of a cell membrane between the separated sister chromatids. The specification of the division plane and partitioning of the daughter cells is coordinated with nuclear events to ensure proper chromosome segregation. Depending on the model organism being studied, this can occur through a number of different ways. Nevertheless, many similarities appear to exist in the basic mechanisms involved. Animal and yeast cells appear to divide using very similar mechanisms. Both cell types construct a contractile-ring at the equatorial cell cortex, comprised predominantly of filamentous actin (F-actin) and non-muscle myosin.

1.2.1 Plant cytokinesis

Unlike animal cells, cytokinesis in plant cells proceeds in the absence of a contractile-ring. Instead, plant cells divide by the accumulation of new cell wall material (cell plate), midway between the separated daughter nuclei (Figure 1.1, A). Golgi-derived vesicles are transported along antiparallel arrays of actin and microtubules that are part of a structure known as the phragmoplast and are used to synthesis the new cell wall. The phragmoplast is also involved in directing the assembly of actin filaments and microtubules into an equatorial ring known as the preprophase band, which disappears prior to metaphase, but has marked the site for the upcoming division (Smith, 2001).

1.2.2 Fission yeast

Cytokinesis in the fission yeast, *Schizosaccharomyces pombe*, occurs like the name suggests, via medial fission and involves the combined actions of two separate but equally essential pathways (Figure 1.1, C). One pathway involves the formation of a medial positioned acto-myosin ring that constricts part way. Following constriction of the acto-myosin ring, septin proteins are then deposited in the intervening medial zone and are required for the final step in septation. A signaling pathway, known as the septation initiation network (SIN), has been identified to function to initiate mitotic exit and cytokinesis at the end of anaphase (McCollum and Gould, 2001). The GTPase Spg1p, is central to the SIN regulatory pathway and controls the onset of septation.

Ectopic expression of Spg1p is capable of inducing ectopic septation independent of nuclear events (Schmidt *et al.,* 1997). Spg1p localises to the spindle pole body and is maintained in an inactive state by the action of two proteins (Cdc16p and Byr4p), which together act as a GTPase activating protein (GAP). Loss of either of these proteins also results in continuous rounds of septation (Minet *et al.,* 1979; Song *et al.,* 1996).

The mitotic spindles of *S. pombe* appear to play no role in positioning the cleavage plane. Instead the position of the nucleus appears to specify the cleavage plane (Chang *et al.,* 1996). The polo-like kinase Plo1 plays many roles during mitosis, one of which is the formation of the medial ring. Localisation of Plo1 to the cortex recruits the forming-homology protein Mid1p, thus determining the medial point (Bahler *et al.,* 1998).

1.2.3 Budding Yeast

Cytokinesis in the yeast *Saccharomyces cerevisiae* occurs via budding (for a review see Palmieri and Haarer, 1998) (Figure 1.1, B). Like in the fission yeast, this is accomplished by the combined efforts of an acto-myosin ring and septins (Bi *et al.,* 1998). Myosin is assembled as a ring at the mother-bud neck, in an actin-independent/septin-dependent manner and remains there until F-actin is recruited in late anaphase in a myosin II-dependent manner (Bi *et al.,* 1998). Like *S. pombe,* septins are required for cytokinesis in *S. cerevisiae*, however, unlike *S. pombe*, myosin is not essential for cytokinesis (Bi *et al.,* 1998). The division site in *S. cerevisiae* is pre-determined and is formed adjacent to the prior division site (Longtine *et al.,* 1996). Mitotic exit and the initiation of cytokinesis is regulated in *S. cerevisiae* with an analogous signalling pathway to the *S. pombe* SIN pathway, known as the mitotic-exit network (MEN). The MEN pathway promotes mitotic exit by linking spatial information with the mitotic machinery. The GTPase, Tem1p, is associated with the spindle pole and is capable of initiating mitotic exit, once the spindle pole has grown into the bud and has come into contact with its activator Lte-1 (Bardin *et al.,* 2000). Once activated, Tem1p activates the release of Cdc14p from the nucleolus, which dephosphoylates a number of CDK substrates (Shou *et al.,* 1999), leading to the initiation of cytokinesis.

1.2.4 Dictyostelium discoidium

Cytokinesis in the slime mould *D. discoidium* appears to occur using mechanisms more similar to animal cells than to either yeast or plant cells. Early studies of *D. discoidium* provided important information on the involvement of type II myosin in cell division. *D. discoidium* can divide in either a myosin II independent fashion when adhered to a substrate, or a myosin II dependent fashion when grown in suspension (Zang *et al.,* 1997). Myosin II deficient *D. discoidium* cells grown on a substrate can form an ingressing cleavage furrow and undergo cellular division via an alternative mechanism referred to as attachment-assisted mitotic cleavage.

1.2.5 Animal cell cytokinesis

The specification of the division plane and the assembly of an acto-myosin equatorial ring occurs during anaphase in animal cells. The site at which the contractile-ring is positioned is determined by the bundled microtubule (MT) structure known as the central spindle (For a review see Gatti *et al.,* 2000). Constriction of the contractile-ring results in furrow ingression, which continues until the cortex has constricted down upon the thick MT bundle known as the midbody (Figure 1.1, D). The midbody is then resolved to produce two separate cells. Both mitotic exit and initiation of cytokinesis are controlled by the inactivation of the cyclin-dependent kinase, Cdk1, via the timed degradation of Cyclin B. Ectopic expression of stable forms of Cyclin B disrupts both late stages of mitosis as well as cytokinesis (Murray *et al.,* 1989; Sigrist *et al.,* 1995; Yamano *et al.,* 1996; Parry and O'Farrell, 2001).

1.2.5.1 Completing cytokinesis in animal cells

The final step in cytokinesis, abscission, involves the severing of the link between the daughter cells and is possibly the least understood process of cytokinesis. At this final step the cleavage furrow has fully ingressed and the daughter cells must resolve the shared

Figure 1.1 Cytokinesis in different model organisms

Diagrammatic representations of cytokinesis in (A) plant cells, (B) *S. cerevisiae*, (C) *S. pombe* and (D) animal cells. Nuclei are represented in blue, microtubules in green and the contractile-ring in red. (A) Plant cells exhibit no furrowing of the cell wall, but instead deposit new cell wall material in the medial region. This medial site is specified by a microtubule/F-actin structure known as the phragmoplast. (B) The budding yeast, *S. cerevisiae* constricts the cell membrane by the actions of a contractile-ring positioned at the mother-bud neck. Septins are then involved in completing cytokinesis. (C) The fission yeast *S. pombe* divide via the constriction of a medially positioned contractile-ring. Like the budding yeast, *S. pombe* also requires septins for the completion of cytokinesis. (D) Microtubules in animal cell specify the site for the formation of the contractile-ring. Constriction of the contractile-ring results in cortical furrowing; at the same time microtubules are bundled to form the central spindle.

A

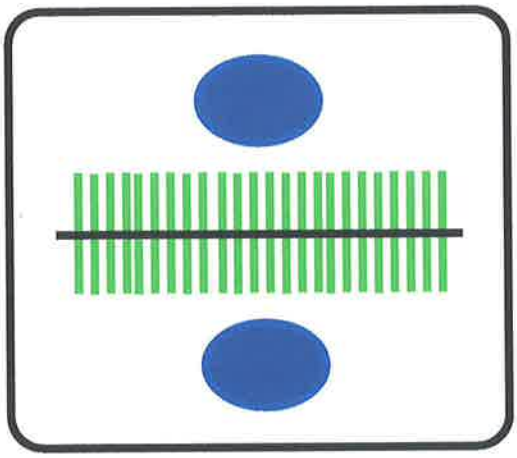

B

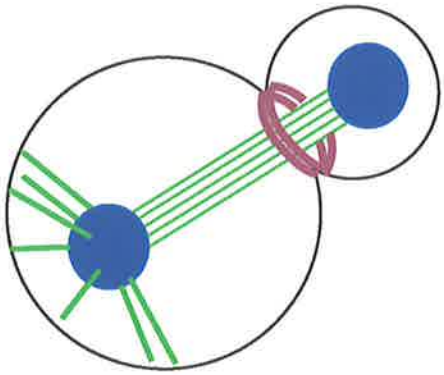

C

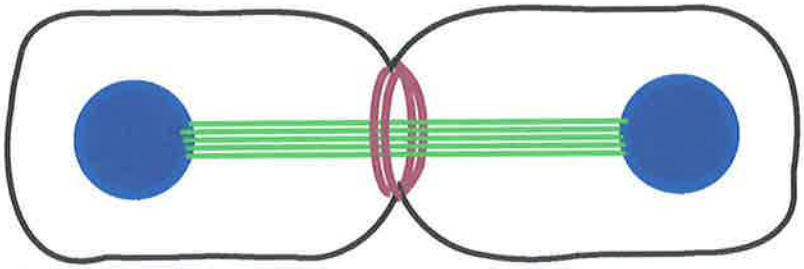

D

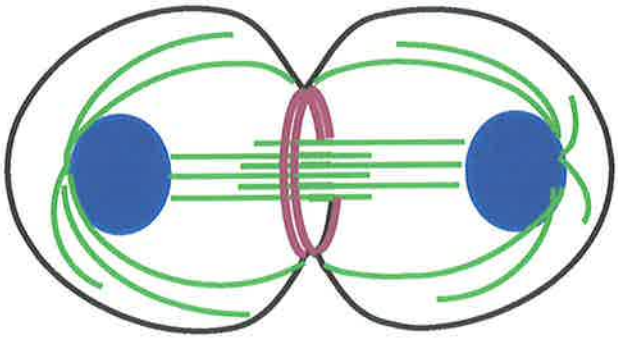

plasma membrane and midzone MTs, in a process that appears to require the targeting of membrane vesicles to the cleavage furrow. It has been appreciated for some time that *Xenopus* embryos accomplish cytokinesis by the insertion of new membrane at the cleavage furrow (Bluemink and Laat, 1973). Recently, other model organisms, *Drosophila*, *C. elegans* and sea urchin embryos have also been shown to require membrane addition for this late event of cytokinesis. Disruption of Rab proteins (small GTPases implicated in vesicle trafficking) have been shown to interfere with late events in cytokinesis (Skop *et al.,* 2001). The *D. melanogaster* Lava lamp (*Lva*), is a Golgi associated protein that is required for membrane trafficking during cellularisation, is also essential for cytokinesis (Sisson *et al.,* 2000). Disruption of vesical secretion in *C. elegans* embryos has no effect on midbody formation or the initiation of furrowing, but does interfere with a late event in cytokinesis (Skop *et al.,* 2001). Skop and collegues (2001) proposed that the midzone MTs are the functional equivalent of the plant phragmoplast, and act to target membrane vesicles to the cleavage region.

The fusion of vesicles with their target membranes is mediated by a complex of proteins, one of which is the cleavage furrow associated protein syntaxin. Disruption to the *C. elegans* Syntaxin-4 results in a failure in cytokinesis (Jantsch-Plunger and Glotzer, 1999), without effecting the formation of the contractile machinery. Similarly, disruption of the sea urchin *syntaxin* (Conner and Wessel, 1999) and *Drosophila syntaxin 1* result in a failure in cytokinesis (Burgess *et al.,* 1997). Mutations in the *Arabdopsis thaliana* cytokinesis-specific syntaxin Knolle (KN) also disrupt cytokinesis, producing seedlings with multinucleate cells and incomplete cell walls (Waizenegger *et al.,* 2000). Ectopic expression of KN results in aberrant membrane targeting, suggesting that a cell cycle dependent activation of this protein is required to ensure correct vesical secretion (Volker *et al.,* 2001).

1.3 The contractile-ring

Furrow ingression in animal cells is believed to be accomplished in part by the actions of two predominant molecules, non-muscle myosin II and filamentous actin. Both the actin and myosin assemble into a structure known as the acto-myosin ring on the

equatorial cell cortex and are believed to function in a way similar to that observed in skeletal muscle.

1.3.1 Non muscle myosin-II

Using fluorescently labeled antibodies, Fujiwara and Pollard (1978) observed that non-muscle myosin accumulated at the equatorial cell cortex at the time of cytokinesis. The first evidence for the requirement of non-muscle myosin-II in cytokinesis came from studies involving the injection of anti-myosin antibodies into starfish blastoderms, which inhibited subsequent cleavages (Mabuchi and Okuno, 1977). Loss of myosin function has since been shown to disrupt cytokinesis in *Drosophila*, *Dictyostelium*, budding yeast and fission yeast (De Lozanne and Spudich, 1987; Karess *et al.,* 1991; Bezanilla *et al.,* 1997; Bi *et al.,* 1998).

The non-muscle myosin II motor is composed of a dimer of two heavy chains each associated with an essential light chain and a regulatory light chain. Disruption of the *D. melanogaster* regulatory light chain, *spaghetti squash (sqh)*, causes a failure in cytokinesis in imaginal tissues resulting in a polyploid larval mutant phenotype (Karess *et al.,* 1991). Phosphorylation of Ser19 of myosin light chain (MLC) by myosin light chain kinase (MLCK) stimulates the ATPase activity of Myosin II and is believed to activate cortical contractility (Somlyo and Somlyo, 1994). MLC phosphatase acts antagonistically to MLCK, thus preventing actin-myosin contractility. It is believed that Rho Kinase, the downstream effector molecule of the Rho1 small GTPase, inhibits MLC phosphatase activity during cytokinesis, thus promoting the active form of MLC (Kimura *et al.,* 1996).

However in some cases myosin activity is observed not to be an absolute requirement for cytokinesis. For example, as mentioned above, *S. cerevisiae* are viable in the absence of the only myosin II gene (Bi *et al.,* 1998), also, *Dictyostelium* can still complete cytokinesis in the absence of myosin II when grown on a substrate (Gerisch and Weber, 2000). The non-essential role for myosin in cytokinesis has also been demonstrated in cultured mammalian cells. In strongly adhered rat kidney epithelial cells, cell division can still occur in the absence of myosin II, while in other less strongly adhered cell-lines cytokinesis is disrupted (O'Connell *et al.,* 1999). These studies identified the importance that cell adhesion plays during cytokinesis.

1.3.2 F-actin

Actin is a highly conserved eukaryotic protein, capable of polymerisation to form filamentous actin (F-actin) structures. Ultrastructural studies have been used to study the assembly of actin during cytokinesis. A complex arrangement of actin filaments running in parallel arrays around the circumference of the equatorial cortex and also perpendicular to the mitotic spindle were observed in mammalian cells (Opas and SoÇtyÑska, 1978; Fishkind and Wang, 1993). The barbed ends of the actin filaments attach to the plasma membrane at many sites around the equator of the dividing cell and overlap with opposite polarities. The use of various chemicals to interfere with actin, has identified the actin cytoskeleton to be extremely dynamic. The stability of the F-actin cytoskeleton during cell division is dependent on the stability of MTs (Fishkind *et al.,* 1996). Evidence now suggests that the formation of the acto-myosin contractile-ring and central spindle are interdependent in animal cells (Gatti *et al.,* 2000; Somma *et al.,* 2002).

1.3.2.1 Actin binding proteins

The *Drosophila* genes *chickadee* and *twinstar* encode profilin and cofilin respectively, both are actin binding proteins believed to regulate F-actin structures, that are essential for cytokinesis (Verheyen and Cooley, 1994; Gunsalus *et al.,* 1995; Giansanti *et al.,* 1998). Under certain circumstances profilin can sequester actin monomers to inhibit filament growth (Carlsson *et al.,* 1977), whilst under other conditions profilin releases actin monomers to promote filament growth (Goldschmidt-Clermont *et al.,* 1991; Pantaloni and Carlier, 1993). Cofilin on the other hand has been shown to promote actin filament disassembly (Gunsalus *et al.,* 1995; Bamburg 1999). Cofilin has been observed to localise to the cleavage furrow in mammalian cells (Nagaoka *et al.,* 1995), and the *Drosophila* ortholog is regulated by the Rho1 GTPase effector, LIM-kinase, to induce reorganisation of the actin cytoskeleton (Ohashi *et al.,* 2000).

Another actin-binding protein that is essential for cytokinesis is anillin (Oegema *et al.,* 2000). The *Drosophila* anillin is also observed to accumulate in the cleavage furrow during embryonic divisions (Field and Alberts, 1995). It appears that profilin, cofilin and anillin and most probably various other actin-binding proteins, are required in the regulation of contractile-ring assembly and constriction.

1.3.2.2 Cortexillins

Cortexillins are a pair of actin-bundling proteins required for normal cleavage in *Dictyostelium* (Weber *et al.,* 1999). Cortexillins show a highly dynamic cellular localisation throughout the cell cycle, enriching at the cleavage furrow during anaphase. The two cortexillin isoforms (I and II) are composed of an amino terminus actin binding domain, a central coiled coil domain (required for parallel dimerisation) and a carboxyl terminus basic phosphatidylinositol 4,5-bisphophate (PIP2)-binding sequence. These actin-binding proteins are capable of bundling and cross-linking actin filaments *in vitro*. The carboxyl terminus of the cortexillins is essential for both translocation and cytokinetic function. Surprisingly, the amino terminus, which contains the putative actin-binding domain, is functionally dispensable.

1.3.2.3 Septins

Septins are a family of novel proteins named after their involvement in septation or cell division, in a wide range of organisms. Septins were first identified in screens using *S. cerevisiae*. Electron microscopy analysis revealed a highly organised ring structure around the bud site, comprised of 10 nm filaments spaced at 28nm intervals (Byers and Goetsch, 1976). *In vitro* studies have shown that they are capable of forming long filaments (Field *et al.,* 1996) and have GTPase activity (Kinoshita *et al.,* 1997). Septins have now been identified in most eukaryotes (except plants) and have a conserved function in cell division (for a review see Field and Kellogg, 1999).

The four *S. cerevisiae* septins, CDC3, CDC10, CDC11 and CDC12, interact with each other, colocalising at the mother-bud neck. Mutations in any of these budding yeast genes results in multinucleate cells and abnormal bud growth. In addition, disruption of any of these septins results in the loss of the other septin molecules from the bud neck (Frazier *et al.,* 1998). Gin4p kinase is capable of directly binding to these septins (Longtine *et al.,* 1998) and is believed to function in maintaining the septin ring, as the septins fail to organise into the parallel filaments at the mother-bud axis in *gin4* mutant cells.

Drosophila possess five septins, Peanut (PNUT), SEP1, SEP2, SEP4 and SEP5 (Adam *et al.,* 2000). PNUT, SEP1 and SEP2 are capable of forming a stable complex *in vitro*

(Field *et al.*, 1996). Mutations in *pnut* result in a failure in cytokinesis (Neufeld and Rubin, 1994). PNUT localises to the cortex at interphase and is recruited to the cleavage furrow during anaphase, before accumulating in the midbody.

It is unclear what role septins play in cytokinesis. Their persistence in the midbody region and the evidence that yeasts are capable of completing cytokinesis using a septin-dependent mechanism in the absence of contractile-ring activity, suggests a role in the final step of cytokinesis. Along with their ability to bind actin, septins are also capable of binding MTs. This dual binding activity may provide a direct link between the contractile-ring and the central spindle late in cytokinesis once extensive furrowing has occurred (Glotzer, 1997).

1.4 Microtubules

MTs play many essential roles during mitosis and cytokinesis in all cell types. Some of these processes include vesical and organelle transportation, sister chromatid separation, cell migration and cytokinesis. The bundled MTs produced during anaphase in animal cells generates a stimulatory signal that positions the contractile-ring and initiates cortical furrowing. Evidence now suggests that the integrity of the mitotic spindle structures and the contractile-ring are interdependent as demonstrated in *Drosophila* S2 cultured cells (Somma *et al.*, 2002). Thus, it is not surprising then that an increasing number of reports have identified interactions between the actin and MT cytoskeletons during cytokinesis.

1.4.1 Microtubule organisation

MTs function both as intracellular 'highways' for various motor proteins, as well as playing structural cytoskeletal roles. MTs are composed of alternate alpha and beta tubulin subunits, arranged in a cylindrical shape and are in a constant equilibrium of growth and depolymerisation. Each tubulin monomer binds a guanosine triphosphate (GTP) molecule, but only the beta subunits are able to hydrolyse the GTP to GDP.

MT formation in animal cells first begins with nucleation from the centrosomes. Centrosomes are comprised of two structures known as the centrioles, arranged perpendicular to each other. During interphase, the single pair of centrioles split, travel

to opposite ends of the cell and replicate, giving rise to two new centrosomes. Centrosomes have been shown to play an essential role late in cytokinesis in mammalian cultured cells (Piel *et al.,* 2001). In normal cells it was observed that the mother centrosome transiently travels to the midbody and appear to be required to signal the final step in cytokinesis. Centrosomes are surrounded by a material of largely unknown composition, termed the pericentriolar material. One component that is known is gamma tubulin, which is able to bind the alpha-beta heterodimers allowing nucleation. Growth of MTs proceeds by the addition of tubulin monomers onto what are termed the 'plus' or 'fast-growing' end. If MT polymerisation proceeds faster than GTP hydrolysis, a structure termed a GTP cap is formed and the MT filament is stabilised.

MTs are highly dynamic. They are in a constant state of growth and disassembly depending on the stage of the cell cycle. During prophase, a large proportion of the structural MTs depolymerise, providing material for the three types of mitotic MT structures seen later on. The kinetochore MTs that extend from the centrosome to the chromosome kinetochores, the astral MTs that extend from the centrosome to the periphery and the bundled midzone MTs that are located between the two centrosomes that are organised into an anti-parallel structure. At pro-metaphase, mitotic spindle nucleation begins. Some MTs attach to the kinetochores of the chromosomes, while others interdigitate with MTs generated by the other pole. At metaphase, the MTs align the chromosomes on the equatorial plane and then shorten during anaphase, separating the sister chromatids. During the metaphase/anaphase stage another MT structure, termed the central spindle, begins to form in the central region of the cell. The central spindle is thought to originate from the existing mitotic spindles detaching from the centrosome and sliding to the central region, or through *de novo* nucleation. Gamma tubulin which is present at the spindle poles, can now be detected at the minus ends of the central spindle in mammalian cells (Julian *et al.,* 1993). Depletion of the gamma tubulin prevents central spindle assembly, resulting in a failure of cytokinesis (Julian *et al.,* 1993; Shu *et al.,* 1995; Hendrickson *et al.,* 2001). As furrow constriction progresses during telophase, the central spindle MTs are bundled, producing a dense MT structure known as the midbody. The bundling of the central spindle MTs is likely to occur as the result of the actions of a recently identified conserved complex, termed

'centralspindlin'. This protein complex, comprised of a kinesin-like motor protein dimer and a Rho family GTPase activating protein dimer, is capable of bundling MTs *in vitro* (Mishima *et al.,* 2002). During the severing of the daughter cells the midbody is resolved by an unknown mechanism, that appears to require vesical transport and membrane deposition as mentioned previously.

1.4.2 Microtubules are the source for the cytokinetic stimulatory signal

MTs play an essential role in animal cell cytokinesis. The first evidence to suggest such a role came from the studies of Conklin (1917). These studies revealed that cortical furrowing could be induced in *Crepidula* eggs by displacing the spindle closer to the cortex using centrifugation. Subsequent studies in various organisms, have since demonstrated that the anaphase/telophase MTs generate a stimulatory signal that is responsible for both establishing the contractile-ring and initiating cortical furrowing. Depending on the model system studied, differences exist between which set of MTs produce the stimulatory signal. In the larger embryonic cells of *Echinoderms* and *C. elegans*, the astral MTs appear to be responsible for producing the signal, while in most other smaller animal cells, the central spindle MTs are essential for initiating cortical furrowing (Discussed by Murata-Hori and Wang, 2002).

The involvement of astral MTs in cytokinesis was first shown through the classical studies performed by Rappaport on *Echinoderm* embryos. Manipulation of sand dollar (*Echinarachnius parma*) embryos to produce two independent spindles within a single cell, revealed that cortical furrowing could be induced midway between the asters of the individual spindles (Rappaport, 1961). It was therefore proposed that the asters were the primary source for generating cortical furrowing in animal cells. This proposal was further supported by experiments that showed that cortical furrowing was not inhibited by the placement of an artificial barrier between the central spindle and the cortex (Rappaport and Rappaport, 1983), but was inhibited if the asters were relocated further from the equator (Rappaport, 1968; Rappaport, 1985). Similarly, the initiation of cytokinesis in *C. elegans* embryos appears to rely on signals generated by the astral MTs, while the central spindle appears to play an essential role late in cytokinesis. The *cyk-4* and *zen-4 C. elegans* mutant embryos display a disrupted central spindle but

normal astral MT arrays. These mutant embryos are still capable of initiating extensive cortical furrowing, however cytokinesis ultimately fails (Raich *et al.,* 1998; Jantsch-Plunger *et al.,* 2000).

In contrast, in other animal cells, including mammalian cultured cells and *Drosophila* embryonic cells, the central spindle MTs are thought to produce the stimulatory signal. Repeating the barrier experiments in cultured cells, similar to that performed in the *Echinoderm* embryos, revealed that furrowing was disrupted at the cortex adjacent to the barrier (Cao and Wang, 1996). This was presumably due to the signal generated by the central spindle being unable to reach the cortex. If the barrier was created once anaphase had progressed, cytokinesis could proceed normally, suggesting that the signal does not have to be continually transmitted to the cell cortex. As in the *Echinoderm* embryos, it was observed that ectopic furrows could be generated between asters of separate spindles in cultured mammalian cells (Wheatley and Wang, 1996). Although similar to the *Echinoderm* results, it was observed that these ectopic furrows could only be produced if a central spindle structure was generated between the asters. Depolymerisation studies revealed that the pre-anaphase spindles including the astral MTs, were dispensable for cytokinesis (Rieder and Salmon, 1998). Furthermore, cultured cells were capable of undergoing a normal cytokinesis in the presence of just the central spindle (Wheatley and Wang, 1996). The non-essential role for astral MTs in cytokinesis was further supported by observations that normal cytokinesis can occur in *Drosophila asterless (asl)* mutants (Bonaccorsi *et al.,* 1998; Giansanti *et al.,* 2001). *asl* mutants produce no detectable astral MTs, but are still capable of a normal cytokinesis in spermatocytes and neuroblasts.

The studies mentioned above have clearly shown that MTs generate a stimulatory signal that is capable of initiating furrow ingression. However differences exist as to which set of MTs produce this stimulatory signal (Discussed by Murata-Hori and Wang, 2002). Both the *C. elegans* and *Echinoderm* embryos are relatively large cells compared to mammalian cultured cells and *Drosophila* embryonic cells and appear to generate the stimulatory signal from the astral MTs. This is likely due to the fact that the central spindle is a significant distance from the cell cortex in these embryos. Therefore, it is thought that the signal that stimulates furrowing travels out along the

astral MTs to the equatorial region to reach the cortex. On the other hand, in smaller animal cells the central spindle appears to occupy a large proportion of the equatorial volume and due to the close proximity of the central spindle to the cell cortex, these MTs are capable of stimulating cortical furrowing.

1.4.3 Relationships between microtubules and the actin cytoskeleton

Cooperation between the MT and actin cytoskeletons is necessary for a wide range of processes including vesical transport, cell migration, spindle orientation, nuclear migration and cleavage site specification. Few reports have documented these interactions due to the dynamic nature of both cytoskeletons and the belief that they play separate cellular functions. Recent evidence suggests otherwise. A number of proteins involved in cytokinesis have been identified to be capable of binding both MTs and microfilaments, including the *Drosophila* KLP3A, Anillin, Septins and Dynamin (Sisson *et al.,* 2000). In animal cells the central spindle MTs and contractile-ring also appear to behave in an interdependent fashion to coordinate cytokinesis.

As will be discussed later, the chromosomal passenger protein INCENP localises to the central spindle MTs, but also associates with the equatorial cell cortex in early anaphase (Cooke *et al.,* 1987). Destabilisation of MTs results in a general cortical staining of INCENP (Wheatley *et al.,* 2001), suggesting that actin/MT interactions are important in regulating protein localisation to the cleavage furrow. An alternative isoform of the mammalian MT motor protein, MKLP1, known as CHO1, can interact with both MT and actin cytoskeletons (Kuriyama *et al.,* 2002). Disrupting the actin-binding capability of CHO1 does not affect the early stages of cytokinesis, but does prevent the final step of resolving the two daughter cells. Therefore, CHO1 is likely to be involved in stabilising a MT/actin cytoskeleton structure late in cytokinesis, or involved in some other late cytokinetic role, such as transportation of membrane vesicles to the cleavage site.

MT dynamics are also important in controlling actin polymerisation through the regulation of GTPase exchange factor (GEF) activity. RhoGEF-H1 localises to MTs and mutants that are defective in MT binding have a higher GEF activity, resulting in

Rho dependent actin reorganisation (Krendel *et al.,* 2002). The Rho family GEF, TrioGEF1, has not been shown to associate with MTs, but still requires an intact MT structure for activity (Bateman and Van Vactor, 2001). Depolymerisation of MTs has been shown to result in an increase in the amount of active RhoA and the formation of contractile actin bundles. MT polymerisation results in an increase in the amount of active Rac1 and the formation of lamelliopodia (Ren *et al.,* 1999; Waterman-Storer *et al.,* 1999). RhoA however, also mediates selective MT stabilisation (Cook *et al.,* 1998), as does its downstream effector mDia (Palazzo *et al.,* 2001). The Rac/Cdc42 effector PAK on the other hand, activates the MT destabiliser Strathmin (Daub *et al.,* 2001).

The central spindle MTs and contractile-ring also interact through an unknown mechanism (for a review see Gatti *et al.,* 2000). Several studies, particularly in *Drosophila* have observed that a disruption to either the central spindle or contractile-ring results in a disruption of the other structure. *Drosophila* mutants of *chikadee* (*chic*), *diaphanous* (*dia*), *spaghetti squash* (*sqh*), *KLP3A*, *pavarotti* (*pav*) and *polo* all appear to have a disruption to both structures (Karess *et al.,* 1991; Williams *et al.,* 1995; Adams *et al.,* 1998; Carmena *et al.,* 1998; Giansanti *et al.,* 1998; Herrmann *et al.,* 1998). Depletion of *RacGAP50C, pebble* (*pbl*), *Rho1, pav* and *sqh* by RNA interference in *Drosophila* S2 cells has also been shown to result in a disruption of both the central spindle and contractile-ring (Somma *et al.,* 2002). In the case of *chicadee* and *sqh*, which encode an actin-binding protein and the regulatory light chain myosin respectively and are likely to be involved in contractile-ring activity, suggests that disruptions to the assembly of the contractile-ring can have a secondary effect on the stability of the central spindle. On the other hand mutations in the MT bundling motor-proteins *pav* and *KLP3A*, demonstrate that the disruption of the central spindle can interfere with the formation of the contractile-ring.

The former idea that MT and actin cytoskeletons are separate structures serving different roles is clearly untrue. It is now obvious that the MTs and actin filaments function together in a wide range of processes including cytokinesis. In fact a mechanical linkage between the plasma membrane and the central spindle appears to exist. Studies involving the displacement of the spindle via micro-manipulation, showed that the spindle returned to its original position (Lutz *et al.,* 1988). It is

currently unclear whether the interdependence observed between the central spindle and contractile-ring as observed in *Drosophila* is a common feature of all animal systems.

1.4.4 Central spindle associated proteins

Successful cytokinesis requires the correct localisation of a number of proteins to the central spindle/midbody region. Studies primarily using *Drosophila* and *C. elegans* have identified a number of these proteins and have shown their importance in midbody formation and cytokinesis. The isolation of midbodies from mammalian cells have identified around 35 proteins that localise to this electron dense structure (Mullins and McIntosh, 1982).

1.4.4.1 Chromosomal passengers

Chromosome passenger proteins are defined as proteins that decorate the chromosomes before translocating to the central spindle at anaphase. Three well-characterised chromosome passengers conserved among studied species are the *Drosophila* Aurora B serine-threonine kinase (*C. elegans* AIR-2, human AIRK2), inner centromeric protein (INCENP)(*C. elegans* Icp-1; yeast Ipl1p) and Survivin (*C. elegans* BIR-1). These proteins have been shown to interact with each other and with the kinesin-like motor proteins. They are essential for a broad range of events throughout mitosis including cytokinesis.

Chromosome passenger proteins are implicated in a range of mitotic activities including chromosome condensation, chromosome segregation, MT bundling and cytokinesis. As these proteins appear to play a wide range of roles during mitosis, the later defects observed in cytokinesis may be the result of a secondary effect caused by disruptions to chromosome condensation/segregation. However, specific disruptions in chromosome segregation in *C. elegans* embryos still allowed cytokinesis to proceed, suggesting that chromosomal passenger proteins do play an essential role in cytokinesis (Severson *et al.*, 2000).

Chromosomal passengers interact to form an evolutionary conserved protein complex. The *C. elegans* AIR-2 and INCENP are capable of interacting *in vitro* and the human

orthologs were observed to exist in an *in vivo* complex (Kaitna *et al.,* 2000). The human Survivin, Aurora-B and INCENP were also shown to interact in a yeast two-hybrid and *in vitro* pull-down assays (Wheatley *et al.,* 2001) and the yeast homologs of AIR-2 (Sli15) and INCENP (Ipl1p) also genetically interact (Kim *et al.,* 1999). The correct localisation of the chromosome passenger proteins is reliant on all other members. AIR-2 localisation to the central spindle was shown to be disrupted in the absence of either INCENP or Survivin, in both *C. elegans* and vertebrate cells (Kaitna *et al.,* 2000; Speliotes *et al.,* 2000). INCENP was further shown to be required for the transfer of Survivin to the mitotic spindles (Wheatley *et al.,* 2001). The conserved protein complex that forms between Aurora B and INCENP is now referred to as the ABI complex (Kim *et al.,* 1999).

Chromosome passenger proteins are also involved in maintaining the integrity of the central spindle. Disruptions to MT bundling are observed in *air-2* mutants (Severson *et al.,* 2000). The correct localisation of the *C. elegans* kinesin-like motor protein ZEN-4, to the central spindle, is reliant on *air-2* and *icp-1* (Kaitna *et al.,* 2000; Severson *et al.,* 2000). Similarly, localisation of the *Drosophila* ortholog of ZEN-4, Pavarotti (PAV), to the central spindle is disrupted in *aurora B* depleted cells (Giet and Glover, 2001). AIR-2 and ZEN-4 are capable of directly binding *in vitro* (Severson *et al.,* 2000), suggesting that the kinesin–like motor protein is targeted to the central spindle via a direct association with the ABI complex. Temperature shift assays involving temperature sensitive mutant alleles of *air-2*and *zen-4* revealed that AIR-2 is required at metaphase and early anaphase, while ZEN-4 is required after anaphase, and throughout cytokinesis (Severson *et al.,* 2000). AIR-2 was needed for the initial localisation of ZEN-4 to the central spindle, but not for maintaining it there. This is not a functional interdependence, as AIR-2 is still capable of localising to the central spindle in the absence of ZEN-4 (Schumacher *et al.,* 1998; Jantsch-Plunger *et al.,* 2000).

Chromosomal passenger proteins play a number of functions throughout mitosis to ensure proper chromosome segregation and cell division. The disruption to cytokinesis observed in the absence of chromosome passenger proteins is likely to be the result of not localising the centralspindlin complex to the central spindle, resulting in the failure

to bundle the central spindle MTs and thus an inability to produce the stimulatory signal required for cytokinesis.

1.4.4.2 Kinesin motor proteins

Kinesin motor proteins are responsible for intracellular trafficking of organelles, vesicles, movement of chromosomes and the assembly and function of the mitotic spindle. They can be classified by the direction they travel on MTs, either plus end or minus end moving.

The *Drosophila* kinesin-like motor protein PAV and the *C. elegans* and human orthologs ZEN-4 and MKLP1/CHO1 respectively, all localise to the midbody in telophase and cause a failure in cytokinesis when disrupted (Adams *et al.,* 1998; Raich *et al.,* 1998; Kuriyama *et al.,* 2002). However, a significant difference exists between the mutant phenotypes of the *Drosophila pav* and *C. elegans zen-4. pav* mutants fail to organise components of the contractile-ring, such as anillin, actin and septins (Adams *et al.,* 1998), and thus have no cortical furrowing. In contrast, *zen-4* mutant embryos are able to organise a contractile ring and have extensive cortical furrowing. This cortical furrow eventually regresses, producing a much later cytokinetic mutant phenotype (Raich *et al.,* 1998). These discrepancies may simply reflect intrinsic differences in the mechanisms used to initiate cytokinesis. These kinesin-like motor proteins are required for MT bundling during cytokinesis. MKLP1 is capable of bundling MTs into anti-parallel arrays, in an ATP-dependent manner (Nislow *et al.,* 1992) and over-expression of the mammalian CHO1 in insect Sf9 cells can induce MT bundling (Kuriyama *et al.,* 1994). As discussed previously, the centralspindlin protein complex, comprised of a kinesin-like motor protein and a Rho family GAP protein, exists in *C. elegans* and humans and is capable of bundling MTs *in vitro* (Mishima *et al.,* 2002). Disrupting either component of the centralspindlin complex interferes with the bundling of the central spindle MTs and a failure in cytokinesis (Jantsch-Plunger *et al.*, 2000; Raich *et al.*, 1998).

1.5 The Ras superfamily of GTPases

1.5.1 Background

The Ras superfamily of guanine-nucleotide binding proteins function as critical molecular switches in a wide number of signalling pathways. The ability to bind and hydrolyse GTP regulates the activity of all members. With over 60 known mammalian family members and almost 50 known and predicted in *D. melanogaster,* these proteins function in a diverse range of biological pathways including cell proliferation, membrane trafficking and cytoskeletal organisation. Not surprisingly, mutations in many members of this superfamily are responsible for a high percentage of cancers.

The Ras superfamily of small GTPases (20-25 kDa) belongs to an even broader family of GTPases, which include the heterotrimeric G proteins involved in mediating signals from cell membrane bound receptors. The Ras superfamily members share significant similarity at the amino acid level (30-55%) and on the basis of both structural and functional similarities can be subdivided into even smaller families (Ras, Rho, Rab, Arf, Ran and RGK). Ras sub-family members (H-Ras, K-Ras, N-Ras, R-Ras, TC21, Rap1A/Rap1B and Rap2A/Rap2B) are implicated in cell proliferation and differentiation (Lowy and Willumsen, 1993), while Rab and Arf in vesicular transport (Balch, 1990). Rho members (Cdc42/G25K, Rac1, Rac2, RhoA, RhoB, RhoC, RhoG and TC10) are involved in cytoskeletal organisation (Ridley and Hall, 1992; Ridley *et al.,* 1992) as are the RGK members (Pan *et al.,* 2000), while Ran members are involved in nuclear protein transport (Moore and Blobel, 1993).

1.5.2 GTPase cycling

Along with sharing considerable sequence homology, members of the Ras superfamily share the common feature of being able to bind guanine-nucleotides, which consequently regulates their activity. Three conformational states exist in all GTPase superfamily members: an active (GTP-bound) state, an inactive (GDP-bound) state and an 'empty' state. The active form reverts back to an inactive state through hydrolysis of the GTP. Removal of the GDP converts an inactive G-protein to an 'empty' state. As a consequence of cytoplasmic molar ratios, GTP is more likely to bind to the empty site than GDP and in doing so converts the protein back to an active form. The exchange of

hydrolysed GDP for GTP results in conformational changes in the GTPases, unmasking structural domains, thus allowing downstream effector molecules to bind (Bourne *et al.,* 1990). The rate of guanine nucleotide exchange and GTP hydrolysis controls the balance between active and inactive states. Various effectors further regulate these events. The intrinsic GTPase activity of the Ras family members is very slow, unless catalysed by proteins known as GTPase activating proteins (GAPs). These effectors act as positive regulators for the GTP/GDP exchange, resulting in an inactive GDP-bound G-protein. The exchange of GDP for GTP is also extremely slow, unless stimulated by a guanine nucleotide exchange factor (GEF, also referred to as guanine nucleotide releasing protein, GNRP, or guanine nucleotide dissociation stimulator, GDS). These effectors act as positive regulators for the GDP/GTP exchange, catalysing the dissociation of GDP. The small GTPase protein then has a higher affinity for the GTP nucleotide over the bound GEF protein, resulting in the displacement of the GEF (Lenzen *et al.,* 1998). Rab and Rho family members also possess a further class of effectors, termed guanine nucleotide dissociation inhibitors (GDIs), which bind to GTPases in the GDP-bound form, maintaining their inactive state.

1.5.3 The Rho family of GTPases

Cells constantly reorganise the actin cytoskeleton in response to extracellular and intracellular signals. Early studies using cultured mammalian cells revealed that the Rho family of GTPases are implicated in actin based cytoskeletal remodelling. The correct activation of Rho family members is important for the regulation of the actin cytoskeleton (Figure 1.2). Each Rho family member appears to signal the formation of unique actin structures. The activation of RhoA in Swiss 3T3 fibroblasts results in the bundling of actin filaments to form actin stress fibres (Ridley and Hall, 1992). Microinjection of Rac1 resulted in membrane ruffles or lamellipodia (large sheets of actin under the cell membrane) (Ridley *et al.,* 1992). This was later followed by the appearance of stress fibres. Activation of Cdc42 induced the formation of filopodia (microspikes, comprised mainly of F-actin) (Nobes and Hall 1995), followed by the formation of lamellipodia and then stress fibres. Thus, a unidirectional activation amongst the Rho family members appears to exist in mammalian cultured cells, starting

Figure 1.2 GEFs, GAPs and GDIs regulate the activity of Rho GTPase family members.

Rho family GTPases cycle between an active (GTP-bound) state and an inactive (GDP-bound) state. GTP exchange factors (GEFs) promote the formation of the active state by binding to the GTPase and displacing the bound GDP. In the active state, Rho family members are able to signal to downstream effectors to regulate the actin cytoskeleton. GTPase activating proteins (GAPs) inactive Rho family members by binding to and catalysing their intrinsic GTPase activity. GTP dissociation inhibitors (GDIs) are capable of binding the inactive state (GDP-bound form), maintaining it in this inactive state.

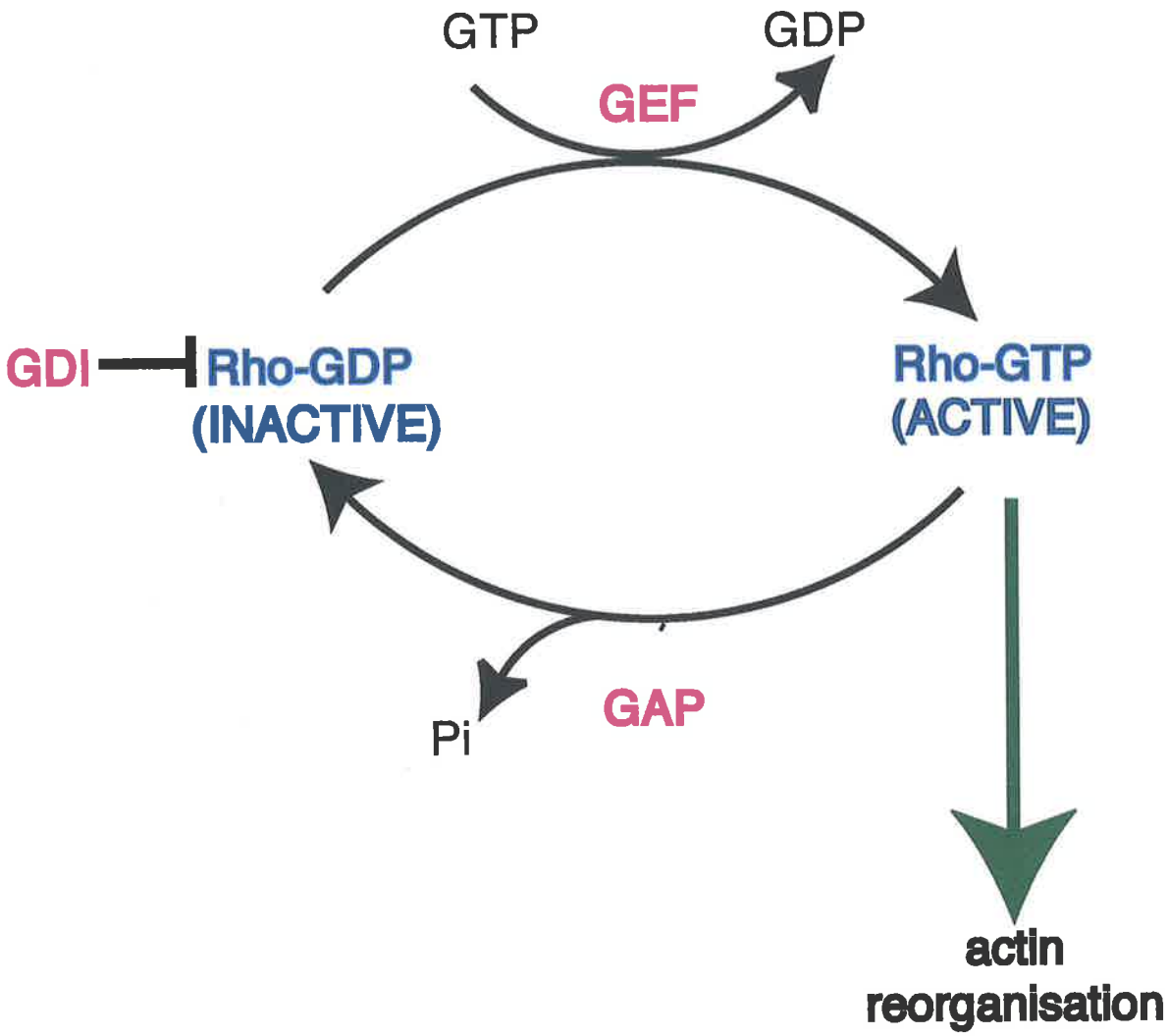
GTP
GDP
GEF
GDI
Rho-GDP
(INACTIVE)
Rho-GTP
(ACTIVE)
Pi
GAP
actin
reorganisation

with Cdc42 which activates Rac1, which in turn activates RhoA (Chant and Stowers, 1995).

1.5.4 Interactions between Rac1 and Rho1

Cross-activation and repression has been observed between the members of the Rho family of GTPases. As described above, the activation of Rac1 can lead to the activation of RhoA. However, studies performed with other cell lines have shown that Rho family members are able to repress as well as activate other members. Rac1 and RhoA appear to have opposing actions during cell movements (Ory *et al.,* 2000). Various biochemical experiments have demonstrated that RhoA and Rac1 have opposing effects on myosin light chain (MLC) phosphorylation (Sanders *et al.,* 1999) and therefore possibly acto-myosin contractile-ring function. The Rho effector molecule Rho kinase is able to phosphorylate myosin phosphatase (Kimura *et al.,* 1996), inhibiting its activity, thus increasing the phosphorylated state of MLC. In contrast, PAK1, the effector molecule of Rac1 and Cdc42, specifically targets myosin II light chain kinase (MLCK), decreasing MLC contractility (Sanders *et al.,* 1999). PAK and Rho-kinase have also been shown to act oppositely in epithelial-mesenchymal cell shape changes (Royal *et al.,* 2000). Activation of Rac1 and Cdc42 leads to the downregulation of active RhoA in NIH3T3 fibroblasts, while the activation of RhoA has no effect on Rac1 activity (Sander *et al.,* 1999; Zondag *et al.,* 2000). In some other instances, activation of RhoA is capable of inhibiting Rac1 signalling (Yamaguchi *et al.,* 2001). Thus, biochemical evidence has supported the idea of cross-talk occurring between the signalling pathways of Rho family members. Nevertheless, it now appears to be even more complicated than what was first thought.

1.5.5 Involvement of Rho GTPases in cytokinesis

Evidence for the requirement of Rho GTPases in cytokinesis first came from studies involving the use of the botulinum C3 toxin, which specifically inhibits the Rho1 GTPase. Subsequent studies have identified that Rho1 is essential for cytokinesis in *Xenopus* (Kishi *et al.,* 1993; Drechsel *et al.,* 1997), sea urchin embryos (Mabuchi *et al.,* 1993), human cultured cells (O'Connell *et al.,* 1999), *Drosophila* (Prokopenko *et al.,* 1999) and *C. elegans* (Jantsch-Plunger *et al.,* 2000). The other Rho family members have also been shown to be involved in cytokinesis in various systems. Ectopic

expression of a modified form of *Cdc42* is capable of inhibiting cytokinesis in both human cultured cells and *Xenopus* (Dutartre *et al.,* 1996; Drechsel *et al.,* 1997). The *Dictyostelium RacE* is essential for cytokinesis (Larochelle *et al.,* 1996) and overexpression of constitutively active or dominant negative forms of *Rac1A, Rac1B and Rac1C* has been shown to also disrupt cytokinesis in *Dictyostelium* (Dumontier *et al.,* 2000; Palmieri *et al.,* 2000).

The effector proteins of RhoGTPases have also been shown to be involved in cytokinesis. Ect2, a RhoGEF that targets Rho, Rac and Cdc42 (Miki *et al.,* 1993), is essential for cytokinesis (Tatsumoto *et al.,* 1999). The *Drosophila* ortholog of *ect2*, *pebble* (*pbl*), is also essential for cytokinesis (Prokopenko *et al.,* 1999). PBL has been shown to specifically interact with Rho1 and not Rac1 or Cdc42 (Prokopenko *et al.,* 1999) and genetically interacts with the FH protein Diaphanous, a downstream effector of Rho1 (O'Keefe, 2001). The *C. elegans* Rho family GAP, *cyk-4*, has also been shown to play an essential role in cytokinesis (Jantsch-Plunger *et al.,* 2000). Similarly, the mammalian ortholog of *cyk-4*, MgcRacGAP, (Hirose *et al.,* 2001; Van de Putte *et al.,* 2001) and more recently the *Drosophila* ortholog, *RacGAP50C,* (Somma *et al.,* 2002) have all been shown to be essential for cytokinesis. This RacGAP has a much higher specificity for targeted inactivation of Rac1 and Cdc42 than it does for Rho1. As described earlier, this RacGAP is required for bundling the central spindle MTs during anaphase/telophase (Jantsch-Plunger *et al.,* 2000; Mishima *et al.,* 2002). Recently, an essential requirement for a RhoGDI in *Dictyostelium* cytokinesis has been observed (Rivero *et al.,* 2002).

1.5.6 *Drosophila* Rho family members

Drosophila Rho family members were identified based on conserved sequence similarity with mammalian orthologs. Subsequent analysis discovered similar roles in regulation of the actin cytoskeleton. Analysis of the *Drosophila* genome sequence data has identified eight Rho family members (*Rho1, RhoL, Rac1, Rac2, Mig2-like (Mtl), Cdc42, RhoBTB* and *CG12102*).

The recent generation of null mutants of the three Rac alleles *Rac1*, *Rac2* and *Mtl* has demonstrated a functional redundancy. They have been implicated in epithelial

morphogenesis, axon guidance and myoblast fusion, events that all require actin cytoskeleton reorganisation (Hakeda-Suzuki *et al.,* 2002; Ng *et al.,* 2002). However, no disruption to cytokinesis was reported. Lethal alleles of *Cdc42* have pointed to a requirement in actin filament assembly (Genova *et al.,* 2000), but again no reported disruption to cytokinesis. Null alleles of *Rho1* have identified a role in maintaining tissue polarity (Strutt *et al.,* 1997), morphogenesis and segmentation (Magie *et al.,* 1999), cellularisation (Crawford *et al.,* 1998), gastrulation (Barrett *et al.,* 1997), dorsal closure (Harden *et al.,* 1999) and cytokinesis (Prokopenko *et al.,* 1999). The fact that Rho family members have been shown to regulate many cellular processes suggests that the coordination of the correct signalling pathways may require the differential action of various GEFs and targeted downstream effectors.

1.5.7 Downstream effectors of the Rho family

Rho family GTPases clearly play an important role in regulating the actin cytoskelton. Clues to how these GTPases actually signal such reorganisations came via the identification of downstream targets through biochemical and yeast two-hybrid studies. The down-stream targets fall into three classes: serine/threonine (Ser/Thr) kinases, lipid kinases and scaffold proteins. This review will only discuss the Rho1 downstream effectors; Rho-kinase, Citron kinase, IQGAP and PAK.

1.5.7.1 Rho kinase

Rho-associated kinase (also known as Rho kinase, ROK or ROCK) is a Ser/Thr kinase that localises to the cleavage furrow, once activated by Rho (Kosako *et al.,* 1999). Rho kinase interacts with a number of other proteins essential for cytokinesis, suggesting Rho kinase may simply transduce the signal from the activated Rho1 to further downstream target proteins required for cytokinesis (Figure 1.3). One of the targets of Rho kinase is the myosin regulatory light chain kinase (Amano *et al.,* 1996). Rho kinase activates the myosin regulatory light chain via phosphorylation, which is proposed to stimulate myosin activity needed for cortical furrowing. Rho kinase can also stimulate myosin activity indirectly by inactivating myosin phosphatase through phosphorylation (Kimura *et al.,* 1996). Rho kinase also targets and phosphorylates LIM kinase (LIM is an acronym of the three gene products Lin-11, Isl-1 and Mec-3) (Maekawa *et al.,* 1999). Not only is LIM kinase regulated by Rho signalling, but it is

Figure 1.3 Rho1 signalling pathways involved in cytokinesis

Rho GTPases cycle between an inactive (GDP-bound) state and an active (GTP-bound) state. In the active state Rho GTPases can signal to downstream effectors to regulate both actin (indicated in green) and myosin (indicated in red) based systems to coordinate contractile-ring activity. Several effector molecules have been identified to act downstream of actived-Rho1. The activation of citron kinase is thought to stimulate contractile-ring activity, although the signalling pathway is yet to be defined. Activation of Rho kinase (ROCK) can lead to the stimulation of a number of pathways to initiate cytokinesis. ROCK can phosphorylate and activate myosin regulatory light chain (MRLC), which stimulates the ATPase activity of myosin II. ROCK can also inactivate myosin phosphates by phosphorylation, thus increasing the activity of myosin. ROCK can also activate LIM kinase by phosphorylation, which in turn inactivates cofilin by phosphorylation. Inactivation of cofilin, along with activation of the profilin, via Rho mediated activation of formin-homology proteins, promotes the formation of filamentous actin (F-actin).

Adapted from Glotzer, (2001).

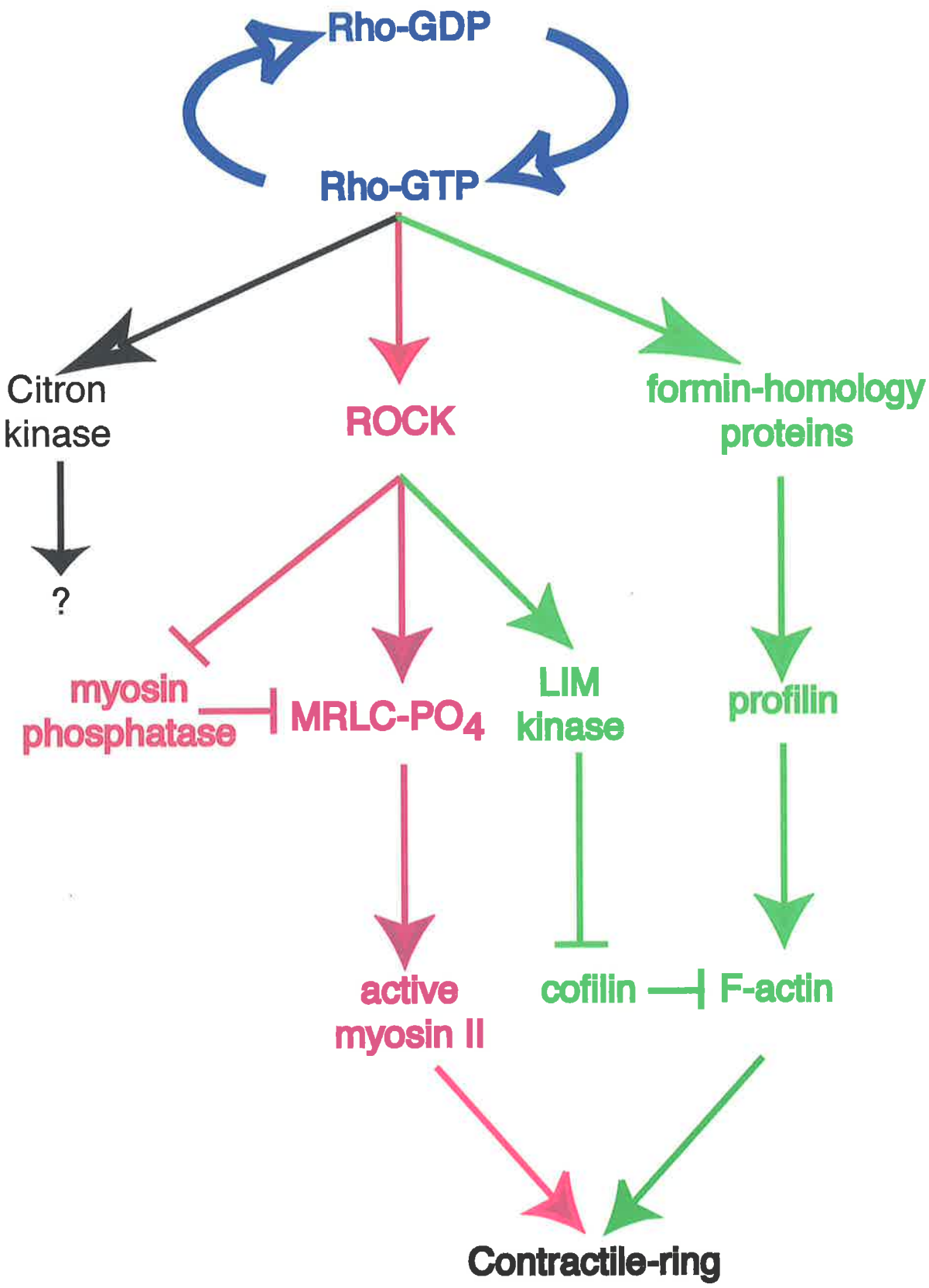
Rho-GDP
Rho-GTP
Citron kinase
?
ROCK
formin-homology proteins
myosin phosphatase
MRLC-PO4
LIM kinase
profilin
active myosin II
cofilin
F-actin
Contractile-ring

also activated by both Rac1/Cdc42 signalling pathways (Edwards *et al.,* 1999). Activated LIM kinase is capable of phosphorylating and inactivating cofilin (Moriyama *et al.,* 1996; Sumi *et al.,* 1999), thus stabilising F-actin structures. Therefore, Rho kinase, once activated by Rho1 appears to induce acto-myosin contractility through a number of pathways involving the regulation of F-actin assembly and myosin activity.

1.5.7.2 Citron kinase

Another target of activated Rho1 is citron kinase. Citron kinase localises to the cleavage furrow (Eda *et al.,* 2001) and is essential for cytokinesis in mammalian tissue culture cells (Madaule *et al.,* 1998). Citron kinase knock-out mice display phenotypes characteristic of disrupted cytokinesis in some tissues (Di Cunto *et al.,* 2000). Although it is not yet clear which regulatory signalling pathway citron kinase is involved in, it is possible that it functions in a similar manner to Rho kinase, to regulate acto-myosin contraction.

1.5.7.3 IQGAP

The family of proteins known as the IQGAPs are implicated in connecting cell signalling pathways to the actin cytoskeleton and are shown to be downstream targets of Rac and Cdc42 (Kuroda *et al.,* 1996). IQGAP members are defined as having a number of domains, including a RasGAP-homology domain (GRD), a calponin homology (CH) domain, a SH3-mimicking domain (WW), internal repeats (IR) and calmodulin binding motifs (IQ), not all of which are conserved between species. Originally identified as putative Ras GTPase activating proteins (RasGAP) based on amino acid sequence, these proteins do not appear to bind Ras or have GAP activity. IQGAPs have since been shown to be required for cytokinesis in *Dictyostelium* (Adachi *et al.,* 1997) and *S. cerevisiae* (Epp and Chant, 1997).

The *S. cerevisiae* IQGAP homologue, Iqg1p/Cyk1p, binds actin filaments and is recruited to the bud neck during anaphase where it plays an active role in recruiting F-actin to the contractile-ring (Shannon and Li, 1999). The *S. pombe* IQGAP (Rng2p) functions similarly to Iqg1p, but requires actin for its proper localisation. It is suggested that having such a variety of domains, IQGAP1 serves as a scaffold organiser for the formation of a larger protein complexes (Hart *et al.,* 1996).

1.5.7.4 p21-activated kinases (PAKs)

The PAK Ser/Thr protein kinases are downstream targets of activated Rac and Cdc42. Null alleles of *Dictyostelium paka* have demonstrated that these proteins also play a role in cytokinesis (Chung and Firtel, 1999). *Drosophila PAK* mutants have not been shown to effect cytokinesis, but do display a disruption to dorsal closure (Harden *et al.*, 1996) and axon guidance (Newsome *et al.*, 2000).

1.6 RacGAP50C

The *Drosophila* gene *RacGAP50C* (also referred to as *acGAP, DRacGAP and RacGAP50C14*) encodes a putative Rho family GAP, which has recently been identified to be essential for cytokinesis (Somma *et al.*, 2002). Depletion of *RacGAP50C* with RNA interference in *Drosophila* S2 cells causes a disruption in the formation of both the central spindle and contractile-ring. *RacGAP50C* is the ortholog of the *C. elegans* gene *cyk-4* and mammalian gene *mgcRacGAP*, both of which are essential for cytokinesis (Jantsch-Plunger *et al.*, 2000; Hirose *et al.*, 2001). This suggests that the inactivation of a Rho family GTPase may be necessary for cytokinesis.

C. elegans cyk-4 mutant embryos exhibit a disorganised central spindle, containing a significant reduction in the number of bundled MTs (Jantsch-Plunger *et al.*, 2000). *cyk-4* mutant embryos are capable of initiating cytokinesis and can achieve extensive cortical furrowing, which ultimately regresses (Jantsch-Plunger *et al.*, 2000). This suggests that CYK-4 plays an essential role during the late stages of cytokinesis. The disrupted central spindle phenotype observed in *cyk-4* mutant embryos is strikingly similar to the phenotype seen when the kinesin-like motor protein *zen-4* is disrupted (Raich *et al.*, 1998). CYK-4 and ZEN-4 have also been observed to have an interdependence for localising to the central spindle (Jantsch-Plunger *et al.*, 2000). More recently, ZEN-4 and CYK-4 have been identified to physically associate *in vivo* in both humans and *C. elegans*, forming a tetrameric complex, termed 'centralspindlin'. This centralspindlin was observed to be capable of bundling MTs *in vitro* (Mishima *et al.*, 2002).

The *C. elegans* CYK-4 and mammalian MgcRacGAP have a conserved localisation during mitosis, which is also consistent with a functional role in MT bundling and cytokinesis (Jantsch-Plunger *et al.,* 2000; Hirose *et al.,* 2001). Both CYK-4 and MgcRacGAP accumulate on the mitotic spindle during metaphase, then enrich at the central spindle during anaphase, before becoming restricted into the midbody at late telophase. Both proteins are also observed to localise to the nucleus in interphase cells.

CYK-4 has a significantly higher specificity for targeted inactivation of Rac1 and Cdc42 compared with RhoA, as assayed *in vitro* (Jantsch-Plunger *et al.,* 2000). This is consistent with exchange assays performed with MgcRacGAP, which show little or no activity towards RhoA (Toure *et al.,* 1998; Kawashima *et al.,* 2000). RacGAP50C also genetically interacts with Rac1 and Cdc42, but not Rho1 during wing development (Sotillos and Campuzano, 2000). However, in these model systems Rac1 does not appear to play an essential role in cytokinesis, whereas Rho1 does (O'Connell *et al.,* 1999; Prokopenko *et al.,* 1999; Jantsch-Plunger *et al.,* 2000). Jantsch-Plunger and colleagues (2000) proposed that CYK-4 targets Rho1 *in vivo*. It is proposed that the intrinsically lower targeted GAP activity CYK-4 has for Rho1 is overcome *in vivo* due to the temporal/spatial accumulation of both proteins at the cleavage furrow.

1.7 Pebble

The *Drosophila* gene *pebble* encodes a putative GEF for the Rho family of GTPases. *pebble* was first identified in a screen for mutations that affected the larval cuticle morphology (Jurgens *et al.,* 1984). Subsequent analysis of *pbl* mutant embryos revealed it was essential for cytokinesis, with homozygous *pbl* mutant embryos failing cytokinesis during the 14th (first *Drosophila* embryonic cycle that requires cytokinesis) and subsequent mitoses, resulting in larger cells with multiple nuclei (Hime and Saint, 1992; Lehner, 1992). The cloning of the *pbl* locus was facilitated by the identification of a *P*-element insertion allele generated in a screen for mutations that affected PNS development (Salzberg *et al.,* 1997). Sequence analysis by Prokopenko *et al.,* (1999) revealed that PBL was a multidomain protein. The amino terminus of PBL contained a RADECL and two tandem BRCT (BRCA1 carboxyl terminus) domains, followed by a nuclear localisation signal (NLS) (Harley, 2002). The RADECL domain was so called due to its similarity with regions present in RAD4-like and Ect2, hence RAD4-like

Ect2 like region (Harley, 2002). The RADECL domain is invariably found associated with a BRCT domain and may represent a specialised subfamily of BRCT domains. BRCT domains are generally found in proteins shown to play a role in DNA repair and cell cycle checkpoint control (Bork *et al.,* 1997) and function in protein-protein interactions. The carboxyl terminus of PBL contains a tandem Dbl Homology (DH) and Pleckstrin homology (PH) domain, characteristic of a Rho family GEF. The *pbl* gene is orthologous to the mouse proto-oncogene, *Ect2*. *Ect2* was originally identified as an N-terminally truncated gene product capable of transforming NIH/3T3 fibroblasts (Miki *et al.,* 1993).

Although *pbl* mutants fail to assemble a contractile-ring and exhibit no cortical furrowing (Prokopenko *et al.,* 1999), other aspects of mitosis, including nuclear envelope breakdown, chromosome condensation and spindle assembly remain unaffected (Lehner, 1992). The sub-cellular localisation of PBL is reported to be highly dynamic during mitosis (Prokopenko *et al.,* 1999). PBL is associated with the cell cortex in early anaphase, before becoming enriched on the inner cortex of the ingressing furrow. During progressing into telophase, PBL remains associated with the ingressing furrow, as well as accumulating within the daughter nuclei. This reported intracellular localisation of PBL differs substantially from that reported for Ect2 (Tatsumoto *et al.,* 1999). Ect2, unlike PBL, is associated with the mitotic spindle at metaphase, concentrating in the central spindle during anaphase and becoming restricted to the midbody during late telophase. The amino terminus of Ect2 is important for the correct localisation to the midbody and also for the regulation of Ect2 activity (Tatsumoto *et al.,* 1999). Over-expression of the amino terminus of both Ect2 or PBL inhibits cytokinesis and is predicted to function as a dominant negative (Prokopenko *et al.,* 1999; Tatsumoto *et al.,* 1999; Kimura *et al.,* 2000; Sakata *et al.,* 2000).

The presence of a GEF domain and the localisation to the equatorial region during cytokinesis, is highly suggestive of PBL regulating the activity of a Rho family GTPase during cytokinesis. In fact, PBL has been identified to physically interact with Rho1 but not Rac1 or Cdc42, in a yeast two-hybrid assay, as well as genetically (Prokopenko *et al.,* 1999). As discussed previously, Rho1 is known to be essential for the formation

and function of the contractile-ring. Thus, PBL appears to act as the GEF that specifically regulates Rho1 during cytokinesis.

Along with the predicted cytoplasmic function of PBL in regulating cytokinesis by modulating the activity of Rho1 at the cleavage furrow, evidence also suggests PBL has a nuclear role. PBL possesses an NLS and is localised to the nucleus during interphase. PBL also possess tandem BRCT domains, which have previously only been identified in proteins that function in DNA damage sensing. Recently it has been shown that the N-terminus of PBL (RADECL/BRCT domain region) is essential for cytokinesis (Harley, 2002). The focus of this thesis centred around investigating the biological function of the N-terminal domains of PBL.

1.8 This study

Although cytokinesis has been studied for many years, surprisingly little is known regarding the molecular mechanisms involved. The use of a number of model organisms has identified a growing number of proteins involved in actin-myosin based contractility and MT dynamics that are essential for cytokinesis. The *Drosophila* putative RhoGEF PBL is essential for cytokinesis and is implicated in modulating Rho1 activity at the contractile-ring at the time of cortical furrowing. The presence of N-terminal BRCT domains and observations that PBL localises to the nucleus, suggests PBL may also have a nuclear function. The subject of this thesis centred on understanding the molecular functions of these N-terminal RADECL and BRCT domains of PBL.

A yeast two-hybrid screen identified a strong interaction between the N-terminal region of PBL and the Rho family GAP, RacGAP50C. The PBL-RacGAP50C complex was shown to exist *in vivo* and the human orthologs, Ect2 and MgcRacGAP, were also identified to be capable of interacting. Strong genetic interactions were observed between *pbl* and *RacGAP50C*, confirming the importance of this *in vivo* interaction. Depletion of *RacGAP50C* was shown to disrupt cytokinesis in both *Drosophila* tissues and S2 cultured cells. Immunocytochemical studies revealed that RacGAP50C has a conserved subcellular localisation compared to its orthologs, CYK-4 and MgcRacGAP. RacGAP50C was also identified to form a conserved protein complex with the kinesin-

like motor protein Pavarotti. The RacGAP50C-PAV complexes were observed to colocalise to MTs throughout mitosis. During anaphase/telophase the majority of the RacGAP50C-PAV complexes were observed at the midzone region of cortically associated MTs. Genetic interactions confirmed that RacGAP50C, like CYK-4 and MgcRacGAP, was capable of targeting Rac1 for inactivation. This has allowed me to propose a model whereby the localisation of PAV-RacGAP50C-PBL complexes to the midzone region of cortically associated MTs at anaphase/telophase, stimulates the formation and/or contractility of the acto-myosin ring. The localisation of PAV-RacGAP50C complexes may be necessary for the recruitment of PBL to the equatorial cortex. The association of RacGAP50C with PBL would then regulate the activity of Rho family members to stimulate cytokinesis.

Chapter Two: Materials and Methods

2.1 Materials

2.1.1 Antibiotics

Ampicillin	Sigma
Chloramphenicol	Sigma

2.1.2 Antibodies

Primary Antibodies	**Dilution used**	**Source**
anti-Tubulin (mouse monoclonal)	1:1 000 (tissue)	Sigma
anti-Anillin (rabbit)	1: 1 000 (tissue)	C. Field (Harvard, Boston)
anti-c-myc (mouse monoclonal 9E 10)	1:250 (tissue)	DSHB
anti-Pavarotti (rabbit Rb3301)	1:100 (tissue)	D. Glover (Uni. Of Cambridge)
anti-Pebble (rat R9)	1:500 (tissue)	S. Prokopenko (Baylor, Houston)
anti-β-galactosidase (rabbit)	1:1 000 (tissue)	Rockland
anti-Lex-A (mouse monoclonal)	1:2 000(Western)	Clontech
anti-DIG-AP (sheep)	1:2 000 (tissue)	Roche

Secondary Antibodies		
anti-rat-biotin (goat)	1:200 (tissue)	Jackson Laboratories
anti-rabbit-HRP (goat)	1:2 000 (Western)	Jackson Laboratories
anti-rat-HRP (goat)	1:2 000 (Western)	Jackson Laboratories
anti-mouse-HRP (rat)	1:2 000 (Western)	Jackson Laboratories
anti-rat-AP (goat)	1.200 (tissue)	Jackson Laboratories
anti-mouse-AP (goat)	1.:200 (tissue)	Jackson Laboratories
anti-rat-Rhodamine Red (goat)	1:200 (tissue)	Jackson Laboratories
anti-rat-FITC (goat)	1:200 (tissue)	Jackson Laboratories

Tertiary Complexes		
Strepavidin-Alexa 488	1:200 (tissues)	Molecular Probes
Strepavidin-Cy5	1:200 (tissues)	Jackson Laboratories
Strepavidin-Rhodamine Red	1:200 (tissues)	Jackson Laboratories
Strepavidin-AP	1:500 (tissues)	Jackson Laboratories
Strepavidin-HRP	1:500 (tissues)	Jackson Laboratories

2.1.3 Bacterial Strains

DH5α: F⁻,f80, *lac*ZΔM15, *rec*A1, *end*A1, *gyr*A96, *thi*-1, *hsd*R17, (r_{K-}, M_K+), *sup*E44, *rel*A1, *deo*R, Δ(*lac*ZYA-*arg*F) U169

2.1.4 Chemicals

All chemicals were of analytical grade, or the highest grade available, and were purchased from Sigma unless otherwise stated.

2.1.5 Constructs

	Source	
pKS+-pbl1A	L. O'Keefe	(University of Adelaide)
pKS+-3'pbl	C. McLeod	(University of Adelaide)
pSK+-3'pbl	C. McLeod	(University of Adelaide)
pMB-hmgcRacGAP	T. Kitamura	(Hokkaido University, Japan)
pGEX-2T-Rac1	B. Dickson	(I.M.P., Vienna)
pGEX-2T-Rac2	B. Dickson	(I.M.P., Vienna)
pGEX-2T-RhoA	B. Dickson	(I.M.P., Vienna)
pGEX-2T-RhoL	B. Dickson	(I.M.P., Vienna)
pGEX-2T-Cdc42	B. Dickson	(I.M.P., Vienna)
pGEX-2T-Mtl	B. Dickson	(I.M.P., Vienna)

2.1.6 *D. melanogaster* stocks

w^{1118} were obtained from laboratory stocks. pbl^{2} and pbl^{3} alleles (originally referred to as pbl^{5D} and pbl^{7O} respectively (Jurgens *et al.*, 1984)) correspond to nonsense mutations that result in truncated protein products of 37 and 185 amino acids respectively (Prokopenko *et al.*, 1999), were obtained from L. O'Keefe. The *GMR-pbl* and *GMR-*$pbl^{\Delta DH}$ stocks were obtained from L. O'Keefe (Prokopenko *et al.*, 1999). The *UAS::*$pbl^{\Delta RADECL/BRCT1}$ stock was obtained from A. West, the *UAS::*pbl^{1-298} stock was obtained from S. Prokopenko, the *UAS::pbl-GFP* stock was obtained from P. Smibert. The *GMR::Gal4* and *en::Gal4* drivers were obtained from L. O'Keefe. $Rho1^{72R}$ and $Rho1^{72O}$ null alleles were obtained from M. Mlodzik. $Cdc42^{3}$ and $Cdc42^{4}$ lethal alleles were obtained from R. Fehon. dia^{2} was provided by S. Wasserman. rok^{2} were provided by L. Luo. $chic^{221}$ was provided by L. Jones. pav^{B200}, $PKN^{l(2)06736}$ and $pnut^{XP}$ were obtained from Bloomington stocks centre. *UAS::mCD8-GFP* stock came from the L. Luo. *Pak, dock* and *trio* alleles and stocks were obtained from B. Dixon.

sqh^{1} was obtained from Umea stock centre. The mutant *Rac* alleles, *Rac1*^{J11}, *Rac1*^{J10}, *Mtl*$^{\Delta}$ and *Rac2*$^{\Delta}$ as well as the triple mutant stocks were obtained from L. Luo (Hakeda-Suzuki *et al.*, 2002; Ng *et al.*, 2002). The expression constructs *UAS::DRac1* and *UAS::DRac1*^{N17} were also obtained from L. Luo. All other fly stocks were obtained from the Bloomington stock centre.

2.1.6.1 Constructs generated for fly transformation

UAS::Myc-RacGAP50C was generated by PCR amplification of the *RacGAP50C* ORF from the #28 yeast two-hybrid clone, with the RacGAPEco-5' and RacGAPXho-3' primers. This PCR fragment was cloned into the pCS2+MT vector. The Myc-tag and *RacGAP50C* fragment was excised as a *Bam*HI/*Xba*I fragment and cloned into the pUASP expression vector. The *Myc-RacGAP50C* fragment was then excised from the pUASP vector as a *Not*I/*Xho*I fragment and cloned into pUAST.

UAS::Myc-RacGAP50C$^{\Delta EIE}$ was generated by site directed mutagenesis of a pKS+-*RacGAP50C*(#28) clone with the RacGAP(ΔEIE)-5' and RacGAP(ΔEIE)-3' primers. The *RacGAP50C* ORF was PCR amplified from mutagenised clones with the RacGAPEco-5' and RacGAPXho-3' primers. Subcloning then proceeded as described for *UAS::Myc-RacGAP50C.*

UAS::Myc-RacGAP50C$^{\Delta YRL}$ was generated by site directed mutagenesis of a pKS+-*RacGAP50C*(#28) clone with the RacGAP(ΔYRL)-5' and RacGAP(ΔYRL)-3' primers. The *RacGAP50C* ORF was PCR amplified from mutagenised clones with the RacGAPEco-5' and RacGAPXho-3' primers Subcloning then proceeded as described for *UAS::Myc-RacGAP50C.*

UAS::RacGAP50C^{RNAi} was generated by a head to head cloning of two overlapping PCR fragments, generated with the RacGAPEco-5'/ RacGAPDAGBam-3' and RacGAPBssHEco-5'/ RacGAPDAGBam-3' primer pairs. Both fragments were cloned into a *Bam*HI digested pBluescript KS+ vector in a three-way ligation. The ligated fragments were then excised as a *Bam*HI fragment and cloned into pUAST.

2.1.7 Enzymes

Enzymes were obtained from the following sources

Restriction enzymes	New England Biolabs
DNase I (RNase–free)	Roche
T4 DNA ligase	Roche
CIP	Roche
T7, T3 polymerases	Roche
Taq Polymerase	Perkin Elmer
Pfu	Stratagene
Pfu turbo	Stratagene
RNase A	Roche
Klenow	New England Biolabs

2.1.8 EST's

		Source
pav	LD24535	(Berkley Drosophila Genome Project)

2.1.9 Kits

	Source
QIAquick Gel Extraction Kit	Qiagen
QIAquick PCR Purification Kit	Qiagen
QIAprep Spin Miniprep Kit	Qiagen
QIAfilter Plasmid Midi Kit	Qiagen
QuikChange Site-Directed Mutagenesis kit	Stratagene
Western Blot Recycling Kit	Alpha Diagnostic
ECL Western Blotting Detection Reagents	Amersham Pharmacia Biotech

2.1.10 Molecular Weight Markers

	Source
DNA: 1KB Ladder	New England Biolabs
Prestained Protein Standard	New England Biolabs
Kaleidoscope prestained standards	Bio-Rad

2.1.11 Plasmids

	Source
pGEM-T easy	Promega
pBluescript SK+	Stratagene
pBluescript KS+	Stratagene
pCS2-MT	S.Prokopenko (Baylor, Houston)
pLitmus28	New England Biolabs
pUAST	H. Richardson (Uni. Of Adelaide)
pUASP	A. Brand (Uni. Of Cambridge)
pGEX-3X	S. O'Connell (Uni. Of Adelaide)
pπ25.7*wc*(Δ2-3)	R. Saint (Uni. Of Adelaide)
pNLX	S. Parkhurst (Fred Hutchinson Research Centre)
pVP-16	S. Parkhurst (Fred Hutchinson Research Centre)

2.1.12 Primers

(Oligonucleotide primers were obtained from Geneworks (formerly Bresatec) (Thebarton, SA) or Genset Pacific (formerly Pacific Oligos)(Lismore, QLD)).

PblBam-5'	5'-cgcggatcctgatggaaatggagaccattgaagag-3'
PblBam-3'	5'-cgcggatcctcaaaagtccataaagtgattaaagcgc-3'
PblBRCT1aBam-3'	5'-cgcggatcctcatgtctgtttcatctcggccgcgta-3'
PblBRCT1aBam-5'	5'-ccggggatccgttacgcggccgagatgaaacagaca-3'
PblBRCT2.EBam-5'	5'-cgcggatcccaccgaacacagatcgtcgggattc-3'
PblNLSBam-5'	5'-cgcggatccgctatgccaatgagatggactatctg-3'
PblDHBam-5'	5'-cgcggatcctgttgcatgccgagccggaggcg-3'
PblDHBam-3'	5'-cgcggatcctcatggcgattttgcagtgttgaatcc-3'
PblDH5'Bam-3'	5'-cgcggatcctcagtccataaagtgattaaagcgcatcga-3'
PblPHBam-5'	5'-cgcggatccacatcaacgaggataaaaggcgg-3'
PblRadEClBam-3'	5'-cgggatccgatgcgtcttggtgaaattctc-3'
hEct2Bam-5'	5'-cgggatccgtatggctgaaaatagtgtattaaca-3'
hEct2Bam-3'	5'-cgggatcctcatgacactgatttcttgagctg-3'
PavEco-5'	5'-ggaattcatgaaggcagtacccaggacgccg-3'
PavEco-3'	5'-ggaattcttagattttcgacttcttgctgct-3'
RacGAPEco-5'	5'-ggaattcaatggcgctctccgcattggcgtcc-3'
RacGAPBam-5'(Y2-H)	5'-ttggatccccatggcgctctccgcattggcgtcc-3'
RacGAPBam-5'	5'-cgggatccatggcgctctccgcattggcgtcc-3'
RacGAPBam-3'	5'-cgggatccttatttcttgtgcgcagatgccgg-3'
RacGAPXho-3'	5'-ccgctcgagttatttcttgtgcgcagatgccgg-3'
RacGAP#21Eco-5'	5'-ggaattcactggagggcaaactctttcac-3'
RacGAPN-termBam-3'	5'-ccggatcctcaagtggcgttccggattcagcgaca-3'
RacGAPC-termBam-5'	5'-ttggatccttgtcgctgaatccggaacgccact-3'

RacGAPCUT3Bam-3'	5'-cgggatcctcaagattttgatgtgcgcacatcgag-3'
RacGAPCUT3endBam-5'	5'-cgggatcccctcgatgtgcgcacatcaaaatc-3'
RacGAPDAG5'Bam-3'	5'-cgggatcctcagggtatggtgaccttggtggtggc-3'
RacGAPDAGBam-5'	5'-cgggatccttgtgccaccaccaaggtcaccatac-3'
RacGAPDAGBam-3'	5'-cgggatcctcacgtcgtcggtgttcccgtttgcgg-3'
RacGAPBssHBam-5'	5'-cgggatccaggcgcgccgccaggcgg-3'
RacGAPBssHEco-5'	5'-cggaattcgcgcgccgccaggcggaacac-3'
RacGAPSfiBam-5'	5'-cgggatcccggccgagacggccagg-3'
RacGAPSfiBam-3'	5'-cgggatccttactcggccgcgtagcccgcgc-3'
RacGAPBglBam-3'	5'-cgggatccttacagatctgccacagccatg-3'
RacGAP(delta21)-5'	5'-tcgacatggagatcaagctgctgcgacacgagcgc-3'
RacGAP(delta21)-3'	5'-gcgctcgtgtcgcagcagcttgatctccatgtcga-3'
RacGAP(delta38)-5'	5'-tgaccaaaatgggcgacctgctgcgacacgagcgc-3'
RacGAP(delta38)-3'	5'-gcgctcgtgtcgcagcaggtcgcccattttggtca-3'
RacGAP(ΔEIE)-5'	5'-cccggcactgattgtgcactgcgtaaatgcccgcggcctg accgaggttggcc-3'
RacGAP(ΔEIE)-3'	5'-ggccaacctcggtcaggccgcgggcatttacgcagtgca caatcagtgccggg-3'
RacGAP(ΔYRL)-5'	5'-ccgcggcctgaccgaggttggcctctcctcgtcggaggag cgggagtacaaggc-3'
RacGAP(ΔYRL)-3'	5'-gccttgtactcccgctccgacgaggagaggccaacctcgg tcaggccgcgg-3'
RacGAPseq.mutagen-5'	5'-ctgtgtgccgcaaacggg-3'
hMgcRacGAPEco-5'	5'-cggaattcatggatactatgatgctgaat-3'
hMgcRacGAPBam-3'	5'-cgggatccttacttgagcattggagaagcaaa-3'
SP6	5'-atttaggtgacactatagaatac-3'
T7	5'-taatacgactcactatagggcga-3'
pVP16-F	5'-gagtttgagcagatgttta-3'
pVP16-R	5'-gttgtaaaacgacggccagt-3'
pGEX-3X-5'	5'-cccacaaattgataagtacttgaaatccagc-3'

2.1.13 Libraries

A 0-4 hour *Drosophila* embryonic library obtained from S. Parkhurst was used in the yeast 2-hybrid screen. Randomly primed cDNAs were ligated into the pVP16 vector. The library provided had a complexity of 2×10^6 and an average insert size of ~1kb.

A human Testis library (Stratagene-939202) was obtained from T. Cox.

2.1.14 Yeast strains

The L40 yeast strain (MATa his3Δ200 trp1-901 leu2-3,112 ade2 LYS2::$(lexAop)_4$-HIS3 URA3::$(lexAop)_8$-lacZ GAL4 gal80) was obtained from Susan Parkhurst (Fred Hutchinson Research Centre, Seattle).

2.2 Buffers and solutions

Agarose gel loading buffer 10X	2.5ml glycerol 2.4ml 0.5M Na_2EDTA 0.025g bromophenol blue (SIGMA)
Amino Acids	100X Histidine 0.2% 100X Leucine 0.5% 100X Uracil 0.2% 100X Adenine 0.2% (dissolve with 0.4ml NaOH(5M) per 10 ml) 100X Tryptophan 0.5% (filter sterilised, and kept at 4°C in dark)
Ampicillin	50μg/ml for liquid culture 100μg/ml for agar plates
AP staining buffer	100mM Tris-HCl (pH 9.0), 100mM NaCl, 50mM $MgCl_2$, 0.1% Tween-20, 1mM levamisole, 8.24ml MQ
BCIP	50mg/ml in 100% DMF
Brower Fix Buffer	0.15M PIPES, 3mM $MgSO_4$, 1.5mM EGTA, 1.5%NP-40, adjust pH to 6.9.
Buffer B	100mM KH_2PO_4/K_2HPO_4 (~25:20) pH 6.8, 450mM KCl, 150mM NaCl, 20mM $MgCl_2$.
Devitellinising Buffer	Buffer B: 37% formaldehyde: MQ H_2O (1:1:4)
EBR (Ringers Solution)	130mM NaCl, 4.7mM KCl, 1.9mM $CaCl_2$, 10mM HEPES (pH 6.9).
ECL solutions	Solution A: 5ml 100mM Tris-HCl (pH 8.5), 22µl 90mM para-coumaric acid, 50µl 250mM luminol Solution B: 5ml 100mM Tris-HCl (pH 8.5), 3µl hydrogen peroxide.
Grape juice agar plates	3% agar, 25% dark grape juice, 1.25% sucrose.
Hoechst 33258 (1000X)	10mg/ml in 1X PBS
HEN fix buffer (10X)	1M HEPES, 0.5M EGTA, 0.1% NP-40 (pH 6.9)
Injection buffer (10X)	50mM KCl,1 mM $NaPO_4$ pH 6.8

In-situ prehybridisation buffer	50% deionised formamide, 5X SSC, 50µg/µl Heparin, 100µg/ ml ssDNA, 0.1% Tween-20
In-situ transcription buffer (10X)	400mM Tris-HCl (pH 8.0), 60mM $MgCl_2$, 100mM NaCl, 20mM Spermidine, 100mM DTT
NBT	50mg/ml in 70% DMF
PBS NaCl	7.5mM Na_2HPO_4, 2.5mM NaH_2PO_4, 145mM
PBT	1 x PBS, 0.1% Tween 20
Phenol/chloroform:	50% phenol 48% chloroform 2% isoamyl alcohol stored under TE in the dark
Protein gel running buffer	1.5% Tris Base, 7.2% Glycine, 0.5% SDS
Protein sample buffer (3X) (pH 6.8),	3% SDS, 30% glycerol, 0.15 M Tris-HCl 3% β-mercaptoethanol added fresh. Bromophenol Blue added to colour.
Protein gel stain solution	10% acetic acid, 1:1 v/v (methanol:MQH_2O), 0.25% Coomassie Blue R-250.
Protein gel destain solution	10% acetic acid, 1:1 v/v (methanol:MQH_2O),
RIPA buffer	50mM Tris-HCl (pH 7.4), 150mM NaCl, 5mM EDTA, 0.1% NP-40 and 5mM PMSF
SSC(20X)	175.3g NaCl, 88.2g sodium citrate, pH 7.0 with HCl and adjust volume to 1L.
TAE	40mM Tris-acetate 20mM sodium acetate 1mM EDTA pH 8.2
Taxol (1 000X)	5mg/ml in DMSO
TE	10mM Tris-HCl pH 7.4 1 mM EDTA
Western transfer buffer	50 mM Tris, 0.3% glycine, 0.04% SDS, 20% methanol.

Yeast Transformation Cocktail	35% PEG(3400), 10mM LiOAc, 0.05X TE,14μg ssDNA

2.2.1 Media

All media were prepared with distilled and deionised water and sterilised by autoclaving, except heat labile reagents, which were filter sterilised, unless otherwise stated. Antibiotics were added from sterile stock solutions after the media had been autoclaved.

2.2.1.1 Bacterial media

L-Broth: 1% (w/v) bactotryptone, 0.5% yeast extract, 1% NaCl, pH 7.0.

SOC: 2% bactotryptone, 0.5% yeast extract, 10mM NaCl, 2.5 mM KCl,10mM $MgCl_2$, 10 mM $MgSO_4$, 20mM glucose.

2.2.1.2 Fly culturing media

Fortified (F1) *Drosophila* medium

10% Treacle, 20% yeast, 1% agar, 10% polenta, 2.5% tegosept and 1.5% propionic acid.

Harvard fly food

Dissolve 47.4g Agar, 165g Torula yeast and 312g maize meal in 1.3 litres of tap water, and add 3.3 litres of boiled water, stir and add 660g glucose. Boil to dissolve, before cooling to 80°C, add 54ml TEGOSEPT (23.8g tegosept, 91.8ml ethanol), pour into bottles. Leave bottles to air-dry overnight, add 2-3 grains of active yeast, and stopper.

Grape-juice agar plates

25% grape juice, 3% sucrose, 3% tegosept and 3% agar

2.2.1.3 Yeast media

Yeast minimal media (YNB): 0.17% yeast nitrogen base, 0.5% ammonium sulphate, 2% glucose (amino acids were added as required).

YPD: 1% Yeast extract, 2% Bactopeptone, 2% glucose.

YPAD YPD, 0.01% adenine

Plates: Liquid broth with 2% bactoagar.

2.3 Methods

2.3.1 DNA manipulation

Standard molecular genetic techniques were performed as described in Sambrook *et al.* (1989); Ausubel *et al.* (1994).

2.3.2 Agarose gel electrophoresis

Molten 0.8 to 1.2% SeaKem LE grade agarose (FMC Bioproducts, Rockland, ME), dissolved in 1x TAE, was poured onto a glass plate and set. The gels were placed in an electrophoresis tank and submerged in 1x TAE. The samples were mixed with sample buffer and loaded alongside a suitable size marker, and then separated by applying 40-100V to the tank. The gel was stained with ethidium bromide to visualise the DNA under UV light.

2.3.3 Purification of DNA from agarose gels

QIAquick gel extraction kits from Qiagen (Hilden, Germany) were used to purify DNA bands cut from agarose gels, following the manufactures protocol.

2.3.4 Dephosphorylation of vector DNA

Recircularisation of vectors with compatible ends was prevented by dephosphorylation. During or after restriction enzyme digestion, 1-2 U CIP was added to the reaction and incubated for at least 1 hr at 37°C.

2.3.5 Ligation

A reaction mix of purified insert and vector DNA fragments (typically in a ration of 3:1 insert:vector), 1 U T4 DNA ligase (Boehringer Mannheim), and 1x ligation buffer (Boehringer Mannheim) was incubated at 18°C overnight. For transformation by electroporation, the ligation was phenol/chloroform extracted and precipitated with 1/10 volume 3 M Sodium acetate (pH 5.2) and 2.5 volumes ethanol. The pellet was washed in 70% ethanol and resuspended in10µl of MQH_2O.

2.3.6 Bacterial transformation

Electrocompetent cells were made by inoculating one litre of L-broth 1/500 from an overnight culture of DH5α. This was then grown to an optical density at A_{600} of 0.4 to 0.5. Cells were chilled on ice for 15 minutes, and kept at 0-4°C throughout the following protocol. The cells were pelleted by centrifugation at 3000 rpm for 10 minutes at 4°C, and the pellet gently resuspended in 500 ml ice cold dH_20. The cells were again pelleted by centrifuging at 4000 rpm for 10 minutes and resuspended in 20 ml ice-cold 10% glycerol. The cells were centrifuged again, and the final cell pellet resuspended in 1.5 ml 10% glycerol. Aliquots of 50 μl were snap-frozen in liquid nitrogen and stored at -80°C. Ligations were electroporated into the electrocompetent cells using BioRad electroporation cuvettes with a 2mm gap. The ligation was incubated with the thawed cells for 1 minute on ice, then transferred into a chilled cuvette, which was electroporated with the BioRad Gene Pulser set at 2.5 V, 200Ω, 25 μFD and the Capacitance Extender set to 500 μFD. Immediately after electroporation, cells were revived by incubation in 1 ml SOC at 37°C for 1 hour before plating on the appropriate selective antibiotic plate.

2.3.7 Automated sequencing

DNA templates were prepared for sequencing using a Qiagen purification kit. Big Dye (Perkin-Elmer) chemistry was used to generate sequence fragments, as per the manufactures instructions. Reactions were cycled through 25 cycles of: 95°C for 10 seconds, 50°C for 5 seconds, and 60°C for 5 minutes in a PTC-200 DNA engine (MJ research). The 20µl sequence reactions were precipitated with 80µl freshly prepared 70% isopropanol for 15 minutes at RT, and the reactions pelleted by spinning for 30

minutes at 14000rpm. The pellet was washed in 250µl of 70% isopropanol and dried at 100°C for 30 seconds. Automated sequencing equipment at the Department of Molecular Pathology, IMVS, Adelaide, was used to analyse the sequencing reactions.

2.3.8 *In vitro* site-directed mutagenesis

Mutagenesis primers were designed and used following the instructions provided in Statagene's QuikChange Site-Directed Mutagenesis kit. The reaction was set up and cycled in an MJ Research thermal cycler PCR machine. The reaction was then cooled to <37°C, and 1μl of *Dpn*I (10U/μl) was added to the reaction and mixed and allowed to incubate at 37°C for 1 hour to digest the parental (nonmutated) template. The reaction was then phenol/$CHCl_3$ extracted and ethanol precipitated, before resuspending in 10μl of water, and transforming into DH5α using electroporation. Restriction digest analysis was used to identify mutated clones where possible. All mutations were confirmed by sequence analysis before use in subsequent experiments.

2.3.9 Bacterial recombinant protein expression

The PCR amplified product of full length RacGAP50C was ligated into the expression vector pGEX-3X (Amersham Pharmacia Biotech), in frame to the Glutathione-S-transferase protein. Protein expression was induced in DH5α. An overnight culture was used to seed 1/50 a fresh 100ml L-broth. Once an OD_{600} ~0.8 was reached, IPTG was added to a concentration of 1mM. The cells were grown for a further 3 hours. Cultures were spun down at 4800rpm at 4°C, and the pellet resuspended in an equal volume of cold PBS and repeated. Pellets were then resuspended in 2 ml PBS (which included protease inhibitors (Complete-mini (Roche)) and sonicated on ice (medium setting, 3 times 15 seconds, with a 1 minute gap between each cycle). The supernatant was then removed by spinning down at maximum speed for 10 minutes, and the insoluble pellet (where the majority of RacGAP50C resided), was resuspended in 1x reducing buffer and frozen.

2.3.10 Antibody generation

The insoluble sonicated protein pellet, from the induced recombinant fusion protein was added to protein sample buffer and boiled for 5 minutes. Proteins were separated on a 12% polyacrylamide gel with a 4% stacking gel, and the gel stained in 0.25%

Coomassie in MQH_2O. The gel was destained in RO H_2O until bands could be visualised. The induced protein band at the correct size was cut out as a gel slab. Gel slabs were crushed by passing them through an 18 gauge followed by a 21 gauge needle several times. Anti-RacGAP50C antibodies were generated using the recombinant GST-RacGAP50C fusion protein antigen at the Institute of Medical and Veterinary Sciences. Two rats and two rabbits were injected according to the following schedule. A prebleed was taken one day before the first injection, and subsequent injections performed at three, six and nine weeks after the first injection. The host animals were terminally bleed 11 days after the final booster injection. The antigen injected into the rabbits contained Freuds complete adjuvant, which was absent in the rat injections.

2.3.11 IgG purification

IgG was purified from the rabbits and rats serum using a 5ml or 1ml HiTrap Protein-G Sepharose column (Amersham Pharmacia Biotech) respectively. Preimmune and postimmunised serum according to the manufactures protocol. The columns were washed with 20mM sodium phosphate (pH 7.0). The serum was mixed 1:1 with 20mM sodium phosphate, and passed into the column using a syringe. The column was washed with 10bed volumes of 20mM sodium phosphate (pH 7.0), and the IgG eluted with 0.1M glycine-HCl (pH 2.7), in 5 fractions of the bed volume, into tubes containg $1/10^{th}$ the eluted volume of 1M Tris-HCl (pH 8.0). The majority of the IgG was collected in the second fraction.

2.3.12 SDS-polyacrylamide gel electrophoresis

The Bio-rad Mini-Protean II gel electrophoresis system was used to cast and run protein gels. Protein samples were boiled at $100^{o}C$ for 5 minutes in protein sample buffer and loaded and run on the gels at 180-200V. Separated protein samples were then transferred to a nitrocellulose filter (Schleicher and Schuell, Germany), using a Bio-rad Transblot SD Semi-dry transfer cell according to manufacturer's guidelines. In general, a current of 0.3 mA per cm^3 of gel was applied for 30 min. After transfer, the nitrocellulose filter was stained with 2% Ponceau S stain (Sigma) for 20 minutes, to quantify the protein transfer. The Ponceau S was then rinsed off in dH_20.

2.3.13 Co-immunoprecipitations

Staged embryo lays were collected from grape juice agar plates, washed with PBT and stored in ~50-100µl lots, at –80°C, until use. When required, the samples were thawed on ice and homogenised with a glass rod in 500µl of 50mM Tris-HCl (pH7.5), 1mM EDTA, 0.1%NP-40 containing a cocktail of protease inhibitors (Complete Mini EDTA-free, Roche). The homogenised sample was spun at 14000rpm for 10 minutes at 4°C and the supernatant collected and centrifuged again. The soluble protein extract was split equally into the immunoprecipitation tubes, and the soluble protein samples made up to 500µl with the homogenisation buffer. The primary antibodies were added to the protein extract and incubated with gently rocking for 3 hours at 4°C. While the primary antibody was incubating with the extract, the Protein A Sepharose TM CL-4B slurry (Amersham Pharmacia Biotech), was washed several times in PBT followed by two washes in the homogenisation buffer. The Protein A Sepharose was then spun at 2000rpm for 2 minutes to settle. Following the primary antibody incubation, ~100µL of the Protein A Sepharose was added to each sample tube containing extract and antibody and incubated for a further 3 hours at 4°C. At the completion of the incubation, the tubes containing the samples were spun at 14000rpm for 10 seconds and washed with 1ml of the homogenisation buffer (without the Protease Inhibitors) for 10 minutes at 4°C twice. Samples were spun at 14000rpm for 10 seconds for a final time, before adding 1X protein sample buffer to the pelleted protein complex and boiling for 5 minutes. The samples were then spun at 14000rpm for 5 minutes and the supernatant extracted. Typically 10-20µl was loaded on a SDS polyacrylamide gel for electrophoresis.

2.3.14 Western blotting

Nitrocellulose membranes, containing the separated proteins, were blocked in PBT/5% Blotto for one hour with agitation. The primary antibody was incubated with the membrane in the same block overnight at 4°C. The filter was then rinsed repeatedly with PBT at room temperature. A HRP-conjugated secondary antibody, diluted in the same block, was incubated with the membrane for 2 hours at room temperature. The secondary antibodies were detected with either the commercial Enhanced Chemiluminescence Kit (Amersham) or by mixing 5ml of the ECL solution A with 5ml

of solution B. The membrane was incubated in this solution for one minute, blotted dry, wrapped in glad-wrap and exposed to autoradiographic film (Kodak, X-Omat).

2.3.15 Yeast transformation

Yeast cultures were inoculated in 10ml of the appropriate selective media (YNB+/- appropriate amino acids, or YPD) and grown for ~20 hours at 30°C with shaking. The next morning a fresh 10ml culture was inoculated to an OD_{A600} of ~0.1, and grown for 3-5 hours or until OD_{A600} was ~0.5. The cultures were then pelleted at 2800 rpm for 5 minutes in a bench-top centrifuge, resuspended in 4ml 1X TE, pelleted again and then resuspended in 200µl 1X TE. The suspended yeast cells were transferred to an eppendorf tube and spun at 14000 rpm for 10 seconds, before resuspending in 100 mM LiOAc/0.5X TE (in enough volume for approximately 50µl/transformation). The cells were then incubated in a 30°C water-bath for 15 minutes, then 50µl aliquoted into individual eppendorf tubes. The cells were pelleted at 14000rpm for 10 seconds, and resuspended in 350µl (35% 4000 PEG/0.1 M LiAc/0.5 x TE/50µg denatured sonicated salmon sperm DNA). 1-2µg of the plasmid to be transformed was added to the resuspended cells, briefly vortexed and incubated at 30°C for 30 minutes. The tubes were then heat-shocked at 42°C for 15 minutes. The transformed yeast cells were pelleted once again at 14000 rpm for 10 seconds, resuspended in ~200µl 1X TE and plated onto YNB selective media and grown for ~3 days placed at 30°C .

2.3.16 Yeast two-hybrid library screen

The L40 yeast strain, transformed with the bait plasmid *pNLX-pbl*$_{1\text{-}308}$, was grown in 10ml of YNB-trp+leu+his+ade, overnight at 30°C. The transformation efficiency of these yeast was determined using a titratable amount of the plasmid library, and a concentration selected that would allow ~40000 transformants per 150mm plate. The large-scale library transformations were done en mass, i.e. the transformation volumes were not proportionally increased to create a larger transformation volume, but rather many small transformations were performed simultaneously. After the yeast were transformed with the library plasmid and heat-shocked, the cells were allowed to recover in YPAD at 30°C for 1 hour, plated onto YNB-trp-his-leu+ade selection plates and grown for five days at 30°C. Colonies appeared from three days onwards and by five days numerous satellite colonies started appearing. Individual colonies were

picked and streaked onto YNB-trp-leu-his+ade, YNB-trp-leu+ade and YNB to reconfirm the primary colony interaction.

2.3.17 Rescue of yeast library plasmids

The library plasmid from individual interacting yeast clones selected from the screen was then isolated by scraping a sample of the interacting clone with a sterile toothpick and resuspended in 200µl Back Extraction Buffer (0.1 M Tris/HCl (pH 9.0), 0.1 M NaCl, 0.5% SDS, 1 mM EDTA). Glass beads (425-600µm) were added to just below the surface and vortexed for three minutes, before spinning at 14000 rpm for five minutes. The supernatant was transferred to a new eppendorf tube, phenol/chloroform extracted three times then ethanol precipitated. The pelleted DNA was resuspended in 20µl of MQ H2O and 5µl was transformed into *E.coli* and selected for *Amp.* resistance. Individual bacterial colonies were screened to identify the yeast library plasmid, which is significantly larger than the bait plasmid.

2.3.18 Yeast protein extraction protocol

50ml yeast cultures were set up in the appropriate selective media and allowed to grow overnight at 30°C with shaking, to an OD_{600} of approximately 0.8. The yeast were pelleted at 2800 rpm for 5 minutes. The pellet was resuspended in 200-400µl of ice-cold lysis RIPA buffer and transferred to a cold screw cap eppendorf tube. Glass beads were added to the tubes to make up half the volume. The tubes were then placed into a "bead beater" at 4°C (Dalton Lab, Dept. of Biochemistry, University of Adelaide, Australia) and beat 3X 20 seconds, with a 20 second break in between cycles. The tubes were then spun at 14000 for 15 minutes at 4°C, and the supernatant separated and stored at -80°C before western blot analysis.

2.3.19 *Drosophila* cultures

Flies were maintained at 18°C or 25°C, with 70% humidity, on F1 or Harvard medium. Experimental fly crosses were performed at 18°C, 25°C or 30°C.

2.3.20 Collection and fixation of *Drosophila* embryos

Embryos were collected on grape-juice agar plates and washed thoroughly with MQ H_2O in a basket. The embryos were then de-chorionated in 100% commercially

available bleach, White King (2% sodium hypochlorite), for 1 minute 15 seconds. The embryos were then thoroughly washed in PBT. Embryo fixations were performed using several methods. For AP and HRP detections the embryos were transferred to a glass scintillation vial containing 540μl 37% formaldehyde (Sigma ACS reagent), 500μl 10X HEN fix buffer, 3.9ml dH_20 and 5 ml n-heptane, and shaken vigorously for 25 minutes. The embryos were then devitellinised by removing the aqueous phase and replacing it with 5 ml of methanol, and shaking the vial vigorously for 1 minute. Embryos that sank from the interface were collected, rinsed twice in methanol and stored under ethanol at -20°C. For immuofluorescent stainings, embryos were fixed for 2 minutes in 100mM PIPES/K+ (pH 6.4), 1mM EGTA (pH 7.25), 2mM $MgSO_4$, 33% formaldehyde, in an equal volume of heptane. For microtubule preservation the embryos were then devitellinised for 30 seconds in methanol, while devitellinisation to preserve the F-actin was performed in 80% ethanol.

2.1.21 Whole mount immuno-staining of *Drosophila* embryos

Fixed embryos were rehydrated by replacing the ethanol with methanol, followed with a 50% methanol/PBT mix. Embryos were then rinsed several times with PBT. The embryos were then blocked in PBT/0.2% BSA/5% NGS for at least 1 hour. The embryos were then incubated with the primary antibody diluted in fresh blocking solution, overnight at 4°C. The next day the antibody solution was removed and embryos were washed several times with PBT over a couple of hours. Embryos were then incubated with secondary antibodies in fresh blocking solution for at least two hours at room temperature with gentle agitation. If needed, the embryos were again washed several times in PBT over a couple of hours, then incubated with a strepavidin tertiary complex (either an AP conjugated streptavidin for colour reaction, or a flurochrome conjugated strepavidin for fluoresence detection). Embryos were again washed in PBT over a period of 2 hours. Generally, DNA was also detected with Hoechst 33258, for 1 minute, followed by repeated washes in PBT. The embryos were then cleared in 80% glycerol/PBT. Embryos were then examined using a Zeiss Axiophot, epifluorescence Olympus or Delta Vision (Applied Precision) microscope and photographed using a CCD camera. Images were then edited using Adobe Photoshop 6.0 or 7.0.

2.1.22 Alkaline phosphatase staining of *Drosophila* embryos

Drosophila embryos were fixed, blocked and incubated with the primary antibody as described in 2.3.20. The embryos were repeatedly washed in PBT and then incubated with an AP-conjugated secondary antibody for 2 hours, before repeated washing in PBT. The embryos were then equilibrated in AP buffer (3X 10 minutes), and then colour detected with the addition of 3.5µl BCIP and 4.5µl NBT in 1 ml of AP buffer. Colour development was monitored under a dissecting microscope and stopped when the desired level of colour had been achieved by repeated washes in PBT.

2.1.23 Immunostaining of *Drosophila* ovaries

Immunostaining of *Drosophila* ovaries was performed as conducted by L. Cooley (http://info.med.yale.edu/cooley/protocols/protocol3.html). Wild-type *Drosophila* ovaries were dissected in Ringers solution (EBR) and transferred to an eppendorf tube containing100ul of devitellinizing buffer and 600µl heptane and agitated gently for 10 minutes. The solution was removed from the ovaries and washed three times in PBS over 30 minutes. The ovaries were then incubated in PBT for 10 minutes and blocked in PBT/0.2% BSA/5%NGS for 1 hour. Standard *Drosophila* tissue immunostaining (2.3.21) then followed. The egg chambers were dissected apart in PBS:glycerol (1:1) and mounted in PBS/80% glycerol.

2.1.24 Pupal wing dissection

Pupal wing preparations were performed using a modified protocol from that described by Winter *et al.* (2001). Hatches of 36 hour-old pupal cases were removed and the pupae fixed in 4% formaldehyde in PBT for 1 hour. The wings were then dissected off the pupae and incubated with 200nM Phalloidin-Rhodamine in PBS for 30 minutes and DNA detected with Hoechst 33258. The wings were then washed once in PBS and then cleared in 80% glycerol before mounting.

2.1.25 Dissociation of wing disc cells

Larval wing discs were dissected out in 1X PBS and incubated in 200µl of PBTH (55µl 10x PBS, 100µl 2.5% trypsin, 0.5µl Hoechst 33258, 395µl MQ H_2O) for three hours at

room temperature, with gentle rocking. Approximately 30µl of this solution was mounted directly onto a slide for fluorescent microscopic analysis.

2.3.26 Immunodetection in larval wing and eye imaginal discs

Wing and eye imaginal discs were dissected out of third instar larvae, and fixed in 4% formaldehyde diluted in 1X Browers, for 30 minutes. The discs were then washed several times in PBT, before incubating in 0.5% NP-40 for 30 minutes. The discs were then washed several times in PBS/0.1% seponin, and blocked in PBS/0.2% BSA/0.01% seponin/5% NGS. Primary antibodies were incubated with the discs over night at 4°C, in the same block. The next day, discs were repeatedly washed in PBS/0.01% seponin, and then incubated with a biotin-conjugated secondary antibody. The discs were again repeatedly washed in PBS/0.01% seponin, and then incubated with a streptavidin conjugated horseradish peroxidase for 2 hours. The embryos were again repeatedly washed in PBS/0.01% seponin and colour detection was performed. The DAB solution was diluted to 0.5 mg/ml in PBT, and 200 μl was added to the imaginal disks. If a blue/black staining was desired, rather than a brown, a 1/100 dilution of 8% $NiCl_2$ solution and then, 3 μl of 3% H_2O_2 were added to the imaginal discs. Colour development was monitored under a dissecting microscope. Once the desired level of colour had been achieved the embryos were immediately rinsed 4-8 times in PBT, followed by one 5 minutes wash. Embryos were cleared in 80% glycerol in PBT and mounted for viewing.

2.3.27 *In situ* probe synthesis

RacGAP50C sense and antisense transcripts were synthesised using T7 RNA polymerase from linerarised plasmids containing full-length *RacGAP50C* in either direction. 1µg of the linerarised plasmid was added to 2µl 10X *in-situ* transcription buffer, 2µl NTP mix (65mM ATP, 65mM CTP, 65mM GTP, 65mM UTP, 3.5mM digoxygenin-UTP) and 40U RNA polymerase and made up to 20µl. The reaction was incubated at 37°C for 2 hours and stopped with the addition of 2µl 200mM EDTA. Synthesised transcripts were precipitated with 2.5µl LiCl (4M) and 75µl chilled ethanol. This was placed at –80°C for 1 hour and then spun for 20 minutes at 13000rpm. The pellet was washed with 50µl 80% prechilled ethanol and spun again,

finally resuspending in 30µl *in-situ* prehybridisation buffer. The probes were then analysed by dot blot detection. A serial dilution of the probes from 1/10 to 1/10 000 was made in 10 fold increments and 1µl from each dilution was spotted onto a nitrocellulose filter. The filter was UV cross-linked, washed in PBT for 10 minutes, blocked in PBT+ 0.5% blotto for 3X 10 minutes. The filter was then incubated with anti-DIG-AP 1:2000 at room temperature for 30 minutes. The filter was then washed in PBT 2X 15 minutes and then equilibrated for 2 minutes in AP buffer. The reaction was carried out in 5ml of AP buffer containing 22.5µl of NBT and 17.5µl BCIP in the dark and stopped with 10mM Tris-HCl (pH 7.0), 1mM EDTA. Probe dilutions were selected as judged to give a corresponding equal intensity in colour between sense and anti-sense.

2.3.28 Whole mount *in situ* detection of *Drosophila* embryos

An overnight lay (0-17hrs) of embryos was collected on grape juice agar plates from w^{1118} stock, de-chorionated, and fixed as stated in 2.3.20. Embryos were gradually rehydrated with 5 minute incubations of (7:3)ME:PP, followed by (1:1) ME:PP, followed by (3:7) ME:PP, then 20 minutes in PP (ME: 90% methanol/10% 0.5M EGTA; PP: 4% formaldehyde in PBS). The embryos were then washed repeatedly in PBS. Fixed embryos were incubated in pre-warmed solutions (55°C) of 1:1 in-situ prehybridisation buffer:PBT for 20 minutes at room temperature, followed by 20 minutes in 100% prehybridisation buffer. Fresh prehybridisation buffer was then added to the embryos and incubated for at least 1 hour at 55°C. The *in-situ* probe was denatured at 80°C for 2-3 minutes, added to the embryos in the pre-hybridisation buffer and incubated over-night at 55°C. The next day the embryos were washed in 100% prehybridisation buffer (pre-warmed to 55°C for 20 minutes, followed by 1:1 buffer:PBT (prewarmed) for 20 minutes, followed by 5X 20 minute washes of PBT moving from 55°C to room temperature during the washes. The embryos were incubated with 1:2000 anti-DIG-AP in PBT at room temperature for 1 hour, and washed 4X 20 minutes in PBT. The embryos were equilibrated in AP buffer for 2X 5 minutes, and then the colour developed in 1ml AP buffer containing 4.5µl NBT and 3.5µl BCIP. Colour development was monitored under a dissecting microscope and

stopped with repeated washes of PBT. The embryos were cleared and mounted in 80% glycerol in PBT for viewing under the microscope.

2.3.29 Scanning electron micrographs

Adult eyes were dehydrated progressively through an acetone series (25%, 50%, 75%, 100%), dried, sputter coated with gold and viewed with a field emission scanning electron microscope (Hitachi S2250N, EMU unit, Australian National University). Digital images were collected and analysed in Adobe Photoshop 7.0.

2.3.30 P-element mediated transformation of *Drosophila*

High purity DNA (Qiagen) was prepared for embryo injections. The construct DNA, at 700ng/µl, and the transposase activity plasmid, pπ25.7*wc*(Δ2-3), at 300ng/µl, were combined in injection buffer. w^{1118} embryos, aged between 15-30 minutes were dechorinated in 100% bleach for 1 minute 15 seconds and washed thoroughly with PBT. The dechorinated embryos were then aligned on a strip of non-toxic rubber cement (Earth) within 5 minutes to prevent desiccation and then covered with light paraffin oil. The posterior end of each embryo was micro-injected with the above DNA mixture. After injecting the embryos were surrounded by a circle of yeast and kept moist at 18°C overnight. Once hatched, the larvae were collected with thin strips of Whatman paper and placed into fresh vials. Emerging adults were crossed to w^{1118} flies, and the progeny scored for *mini-white*$^{+}$ eye pigmentation phenotype, indicating a germ-line transformation. Independent transformants were crossed to the doubly balanced stock, w^{1118};*Gla/CyO*;*Df(3R)ro*^{XB3}/*TM6B,Hu*. Male transformant flies carrying the *CyO* and *TM6B* chromosomes were selected and back-crossed to w^{1118} virgins to determine the chromosomal insertion through segregation patterns. Once the chromosome of insertion was determined, balanced stocks of the insert were generated.

2.3.31 Ethyl methane sulfonate mutagenesis

Adult males were mutagenised by providing them with a sucrose solution laced with EMS, as reported by Grigliatti, (1986). Males were aged for 3-5 days post-eclosion, at 25°C and starved for approximately 6 hours prior to administering the EMS. 26 µl of EMS solution (Sigma) was added to 10 ml of 1% sucrose solution. Approximately 1 ml of the EMS/sucrose solution was drawn up into a syringe and injected through the lid

of the bottle onto filter paper stuck to the bottom of the bottle. The flies were kept in this bottle overnight. The mutagenised males were then turned onto fresh food and left for 8 hours to overnight, before virgin females were added. Once females were added, the flies were turned into a fresh bottle every 1-2 days to maximise laying and minimise over-crowding.

2.3.32 Growth and maintenance of *Drosophila* S2 cells

Drosophila Schneider 2 (S2) cells were grown in 1X Schneider's *Drosophila* media (GIBCO) supplemented with 10% Foetal Calf Serum (FCS) in 75-cm2 flasks (Falcon®) or in a 6-well plate (Falcon®) containing a 22 x 22 mm cover slip, and grown at 25°C in normal air.

2.3.33 *Drosophila* S2 cell culture immunostaining

Immunostaining was performed on *Drosophila* S2 cells adhered to cover slips in the 6-well plates. The S2 cells were gently washed several times with PBS, before fixing with 3.7% Formaldehyde (Sigma) in PBT for 15 minutes at room temperature. The S2 cells were then washed 3-4 times in PBS over a 10 minute period. The S2 cells were then blocked at 37°C in PBT/0.2%BSA/5% NGS for 30 minutes in a humid chamber. The fixed S2 cells were then incubated with the primary antibodies in the same block solution for 1.5 hours at 37°C, before washed 3-4 times in PBS. The S2 cells were then incubated with secondary antibodies for 1.5 hours at 37°C in a light-tight container and again washing 3-4 times in PBS. Incubation with tertiary-complexes followed if needed, conducted in the same way as the secondary antibodies. DNA was detected with 10μg/ml Hoechst 33258 for 1 minute. The cells were again washed several times in PBS, before mounting face down on a slide containing 10μl 80% glycerol/PBT and sealed with nail-varnish.

2.3.34 Generation of double-stranded RNA (dsRNA)

cDNA fragments (700bp-1kb) of the target gene were cloned into either pBluescript KS+ or SK+ (Stratagene) or pLitmus28 (New England Biolabs). Approximately 1μg of linearised plasmid, dissolved in 14μl of MQ H_2O, was used in a single RNA transcription reaction. The transcription mix (2μl solution of 10mM ATP, CTP, GTP and UTP, 2μl of 400mM Tris-HCl (pH 8.0), 60mM $MgCl_2$, 100mM DTT, 20mM

Spermidine, 100mM NaCl, and 2µl (40U) T7 RNA polymerase) was then added to each tube of linearised template and incubated at 37°C for 2 hours. The reaction was then DNAse treated with 2µl of RNAse-free DNAse (Roche) and incubated at 37°C for 15 minutes. The completed reaction was phenol/chloroform extracted and ethanol/sodium acetate precipitated. The pellet was washed in 50µl 70% ethanol and resuspended in 20µl 1mM Tris-HCl (pH7.5)/1mM EDTA (pH 8.0). Complementary RNA transcripts were annealed in 50µl at a final concentration of 50µM for either transcript. This was incubated at 100°C for 1 minute, followed by a slow cooling to room temperature.

2.3.35 RNAi treatment of *Drosophila* S2 cells

Drosophila S2 cells were treated with dsRNA as described by (Clemens *et al.*, 2000). S2 cells were plated out to a concentration of 1x 10^6 cells/ml in 1X Schneider's *Drosophila* media + 10%FCS. The cells were then incubated with ~15µg dsRNA in 1 ml 1X Schneider's *Drosophila* media (serum free) for 1 hour at room temperature. An additional 1 ml of media, supplemented with FCS, was then added to the cells and the cells grown at 25°C for 2-3 days.

2.3.36 Regulatory considerations

All manipulations involving recombinant DNA was carried out in accordance with the regulations and approval of the Genetic Manipulation Advisory Committee and the University Council of Adelaide University. All manipulations involving animals were carried out in accordance with the regulations and approved by the Animal Ethics Committee and the University Council of Adelaide University.

Chapter Three: Identification of proteins that interact with the N-terminus of Pebble, and the characterisation of RacGAP50C.

3.1 Introduction

Pebble (PBL) is a multidomain protein essential for cytokinesis. The initial clue to the role of PBL in cytokinesis came from the analysis of its domain structure. The carboxyl terminus of PBL contains a tandem Dbl oncogene homology (DH) domain and a Pleckstrin homology (PH) domain, categorising PBL as a Rho family GEF. GEF-mediated activation of Rho family members is needed for the remodelling of the actin cytoskeleton, a process needed for cytokinesis. Of the Rho family members tested, PBL physically associates with, as well as genetically interacts with, Rho 1 (Prokopenko *et al.,* 1999). PBL localises to the cytoplasmic face of the contractile ring during the telophase furrow ingression (Prokopenko *et al.,* 1999), and it is here that PBL is likely to regulate Rho1 activity.

PBL may also be involved in a separate nuclear function. PBL possesses a nuclear localisation sequence (NLS), and tandem N-terminal BRCT domains. BRCT domains were originally identified in the BRCA1 breast cancer tumour suppressor protein (Koonin *et al.,* 1996), and have now been identified in a range of proteins, all of which have a function in DNA damage sensing and repair (Bork *et al.,* 1997; Callebaut and Mornon, 1997). A *pbl* hypomorphic mutant has been shown to be sensitive to X-irradiation (Harley, 2002). In addition, PBL accumulates in the nucleus during telophase, remaining there until metaphase of the next mitotic cycle (Prokopenko *et al.,* 1999). The BRCT domains of PBL may therefore play a yet to be defined role in the nucleus.

To elucidate a possible function for the BRCT domains of PBL, a yeast two-hybrid screen was conducted to identify proteins that physically associate with the N-terminus of PBL. A number of candidate interactors with potential cytoplasmic and nuclear roles were identified from the screen. One strongly interacting candidate, RacGAP50C, was chosen for further analysis. The initial characterisation of this PBL-RacGAP50C interaction is presented in this chapter.

3.2 Results

3.2.1 Identification of proteins that bind the N-terminus of PBL.

Approximately 1.5×10^6 colonies from a 0-4 hour *Drosophila* embryonic cDNA library were screened for an interaction with the N-terminus of PBL (PBL_{1-308}). This region contains two tandem BRCT domains as well as a conserved N-terminus. This N-terminus region shares similarity with the Rad4-like and Ect2 proteins, and was thus named the RADECL (**Rad**4-like and **Ec**t2 **l**ike) domain. The strength of the interaction was determined by the amount of growth on the selective medium YNB-Trp-Leu-His+Ade, and ranged from very weak to very strong. A total of 401 interactors were selected from the primary library screening plates and replica streaked on various nutrient selective media. Contaminating yeast were identified and avoided by selecting only colonies auxotrophic for adenine (the parental L40 genotype), reducing the number of candidates down to ~150 individual colonies. The majority of these clones were sequenced from the 5' end, and the insert identified through BLAST sequence homology searches against the sequenced *Drosophila* genome from the Berkeley *Drosophila* Genome Project. Interactors were assigned as a possible candidate or a false positive based on published data and a compiled list of common false positives maintained by Erica Golemis (http://www.fccc.edu/research/labs/golemis/InteractionTrapInWork.html). Plasmids of potential candidates were isolated from yeast and purified, before retransforming them to re-test the interaction with the PBL bait construct. The results of the identified interactors are summarised in Table 3.1.

Sequence analysis revealed that the majority of interacting clones contained solely the linker sequence used to clone the amplified cDNAs, and therefore catergorised as false

positives. Mitochondrial 16SrRNA and genomic DNA as well as various transcription components have been identified in other yeast two-hybrid screens, and are likely to represent false positive interactors.

The strongest candidate interactor identified in the yeast two-hybrid screen was RacGAP50C. Two independent RacGAP50C clones (#21 and #28) were identified from the screen and found to interact equally strongly. RacGAP50C orthologs exist in *C. elegans* (*cyk-4*), human and mouse (*mgcRacGAP*). The cDNA of clone #28 began within the 5'UTR (generating an additional 8 amino acids in the fusion protein product) and terminating in the 3'UTR at bp 1993. Clone #21 had an in-frame N-terminus truncation, so that it started 195base pairs into the coding sequence and also contained 3'UTR, finishing at base pair 1899. BLAST sequence homology searches (http://www.ncbi.nlm.nih.gov/BLAST/) and Clustal sequence alignments (http://www.ch.embnet.org/software/ClustalW.html) revealed that RacGAP50C possesses a consensus Rho family GTPase activating protein (GAP) domain in the C-terminus, comprised of three conserved subdomains (Boguski and McCormick, 1993), shown as I, II and III (Figure 3.1). Significant homology exists between well-characterised GAP proteins, the human N-Chimaerin and *D. melanogastor* Rotund. Rotund shares the highest similarity to RacGAP50C (47% identity, 63% similarity), and is homologous to the entire GAP domain region of RacGAP50C. RacGAP50C also contains another prominent domain, identified as a Phorbol ester/diacylglycerol binding domain (also known as the Protein kinase C conserved region 1 C1 domain) situated centrally in the protein. Part of this C1 domain region also contains a cysteine rich region. This domain is implicated in Phorbol ester/diacyglycerol-binding. The COILS prediction programme (http://www.ch.embnet.org/software/COILS_form.html) strongly predicts the presence of a coiled coil structure in the N-terminus at residues 36-122 (Figure 3.2).

Figure 3.1 Sequence alignment of RacGAP50C

The entire protein sequence of RacGAP50C (NP_610912) was aligned with that of Human MgcRacGAP (NP_037409) and N-Chimaerin (P15882), mouse MgcRacGAP (NP_036155), *C. elegans* CYK-4 (NP_499845) and *D. melanogaster* Rotund (P40809), using the Clustal W sequence alignment program and processed with Boxshade. Black highlighting of amino acid residues indicates a 50% or greater amino acid conservation within this group of proteins, while grey highlighting represents a conservation of amino acid residues with similar properties. The consensus amino acid sequence is displayed below the alignment. Uppercase letters in the consensus alignment indicate amino acid residues that are conserved between all sequences, while lower case letters indicate conservation of similar amino acids. Conserved domains are indicates on the consensus sequence. A coiled-coil domain (green box) is predicted to exist in the N-terminus, a phorbol ester/diacylglycerol binding domain (brown box) and cysteine rich region (orange box) are centrally located, while a highly conserved GAP domain, comprised of three conserved subdomains (I, II and III) (red boxes) is located at the C-terminus. Two clusters of three residues, essential for the catalytic activity of GAP proteins, are highlighted (Blue) in the consensus sequence of the GAP subdomain I. The start point of the N-terminally truncated RacGAP50C clone #21 is also indicated, starting part way through the conserved N-terminal coiled-coil domain.

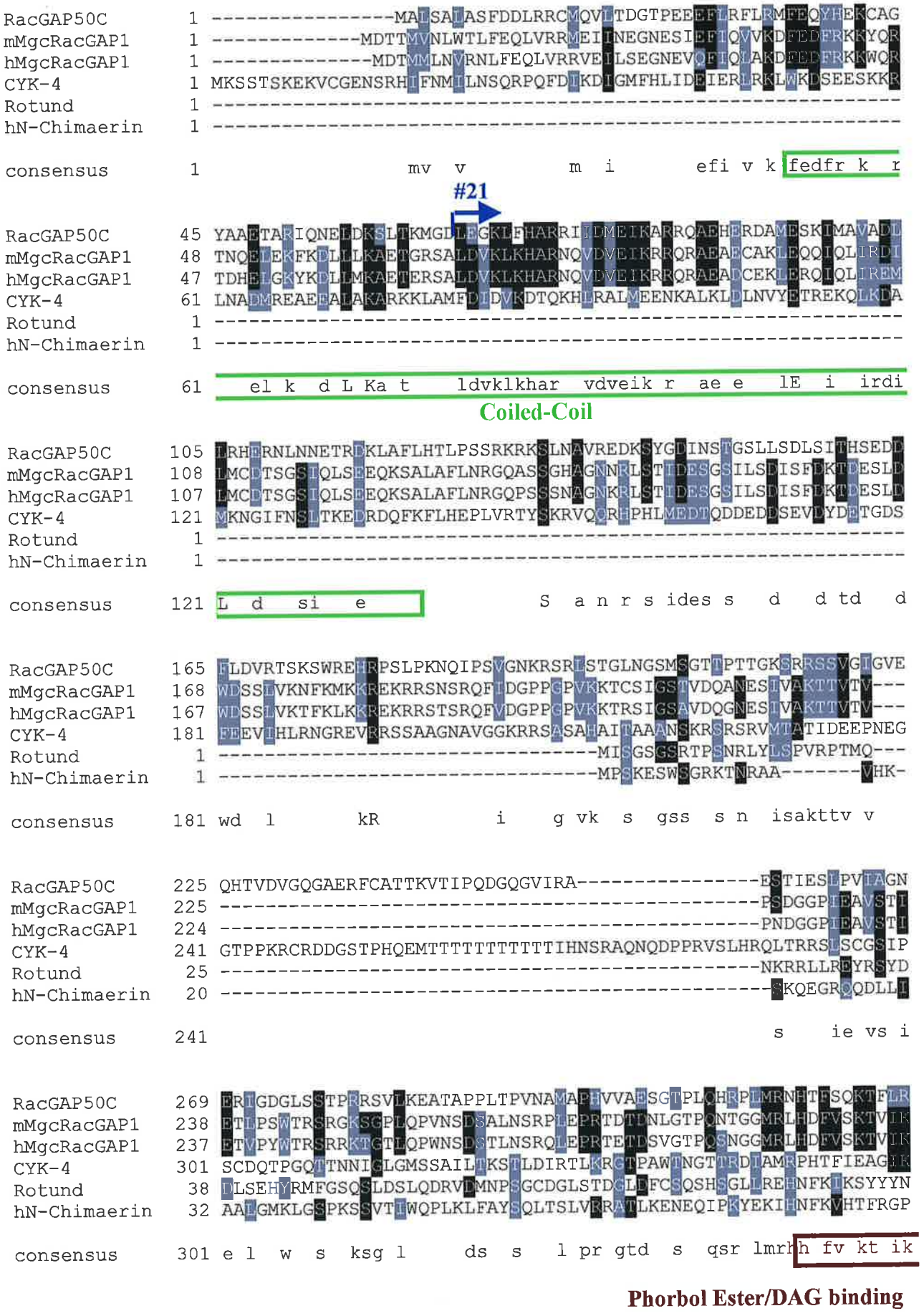
#21
Coiled-Coil
Phorbol Ester/DAG binding

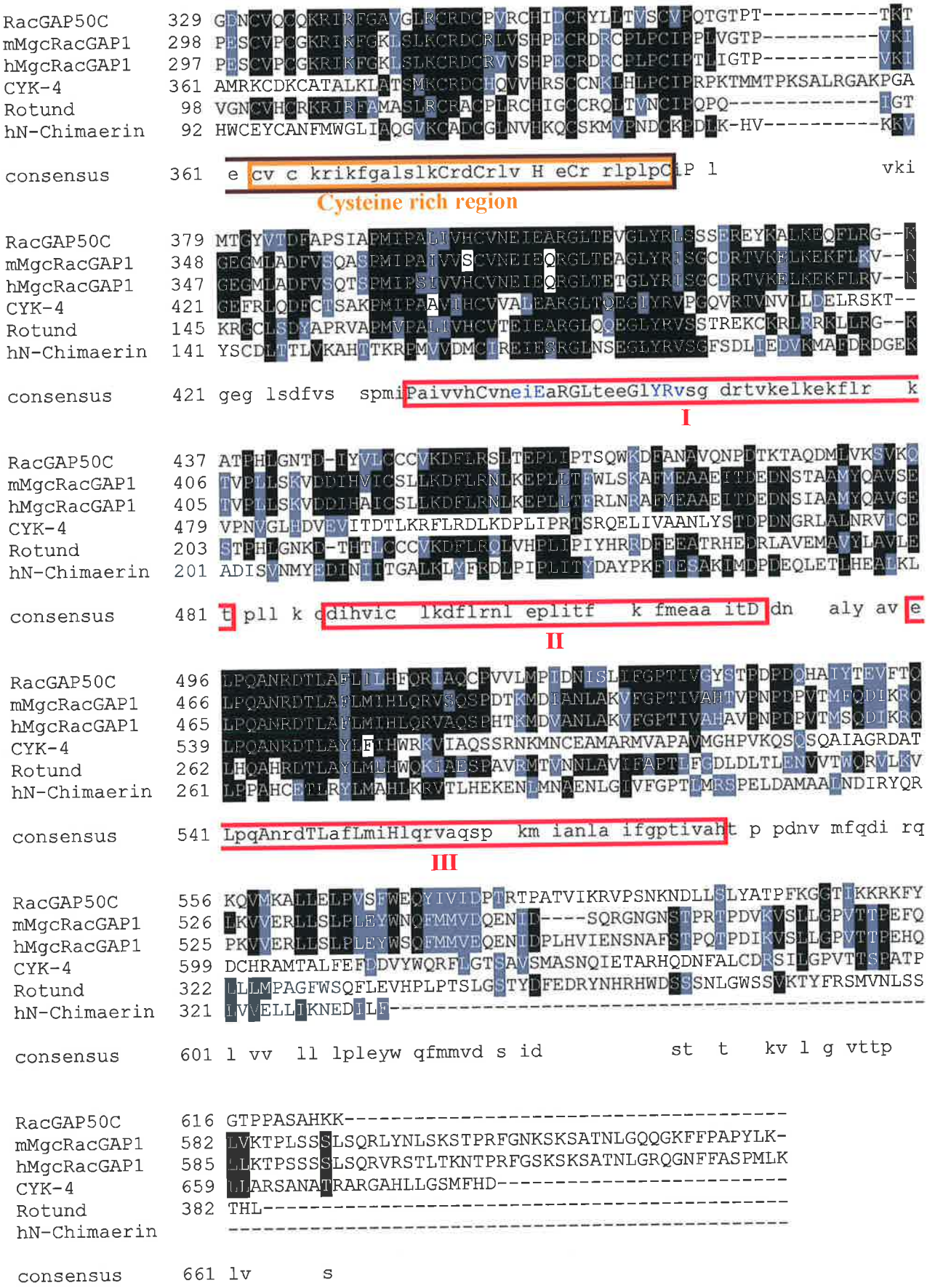
RacGAP50C
mMgcRacGAP1
hMgcRacGAP1
CYK-4
Rotund
hN-Chimaerin
consensus
Cysteine rich region
I
II
III

Table 3.1

Proteins identified from the yeast two-hybrid screen capable of interacting with the N-terminus of Pebble

Gene		No. of interactors	ID No.	Strength of Interaction
Candidate Interactors				
Potential Nuclear Interaction				
CG1966	*Acf-1*	1	196	++
CG7917	*Nlp*	1	365	++
CG4584	(DNA repair protein)	1	300	+
Potential Cytoplasmic Interaction				
CG1453	*Klp10A*	1	282	+
Potential Cytoplasmic and/or Nuclear Interaction				
CG13345	*RacGAP50C*	2	21, 28	+++/+++
CG5784	*Mapmodulin*	2	190, 359	+/+
CG11579	*Armadillo*	1	352	+
Unknown				
CG14897		1	313	++
CG11931		1	160	+
CG9894		1	26	+
(+: weak interaction ,++: moderate interaction , +++: strong interaction)				
Probable False Positives				
Polylinker (No Insert)		45	25, 40, 75, 104, 109, 118, 120, 138, 150, 158, 159, 161, 186, 189, 191, 200, 202, 214, 215, 234, 248, 257, 262, 263, 265, 268, 270, 273, 277, 280, 287, 294, 291, 294, 297, 306, 318, 321, 322, 331, 332, 338, 390, 397, 401	
16SrRNA		27	2, 29, 30, 49, 61, 76, 79, 82, 105, 107, 115, 162, 187, 201, 205, 228, 230, 233, 237, 241, 284, 289, 290, 291, 324, 329, 363	
Mitochondrial Genomic DNA		7	134, 137, 258#2, 261, 276, 281, 367	
CG8989	*Histone 3.3B*	4	59, 90, 119, 309	
Mitochondrial *Cytochrome C Oxidase*		3	114, 203, 275	
CG10161	*eIF-3p66*	1	22	
CG4954	*eIF-3S8*	1	222	
CG6418	(Helicase)	1	110	
CG11660	*RIO1*	1	88	

Sequence analysis of clones #190 and #359, identified the uncharacterised *D. melanogaster* ortholog of Mapmodulin (CG5784). Similar proteins are found in *C. elegans*, Human and mouse. Mapmodulin, which is located at 54F6-55A1, is implicated in MT binding, and contains leucine rich repeats (LRR), which are implicated in a diverse range of cellular functions and localisations, as well as protein-protein interactions. Clone #190 has an N-terminal truncation resulting in the loss of the first 142 amino acids, including the LRR, but contains the rest of the ORF. Clone #359 similarly has an N-terminal truncation resulting in the loss of the first 146 amino acids, and contains the remainder of the ORF. Both *mapmodulin* clones weakly interacted with the PBL bait construct.

Sequence analysis of clone #365, a moderately interacting candidate clone, revealed that it encoded the majority of the ORF of *D. melanogaster* Nucleoplasmin (NLP) (CG7917) (also known as chromatin remodelling protein, CRP1, located on the right arm of chromosome 3 (99D3-D4). Clone #365 has an N-terminal truncation resulting in the loss of the first two amino acids, but contains the remainder of the ORF and some 3'UTR sequence. *D. melanogaster* NLP contains no conserved motifs.

Sequence analysis of the weak interactor of clone #282 revealed that it was the kinesin motor protein, Klp10A (CG1453). Clone #282 lacks the most of the 5' coding sequence, resulting in the loss of the first 651 amino acids. This clone encodes the remaining 152 amino acids and has a 3'UTR that extends at least 200bp further than the mRNA sequence predicted by the *Drosophila* genome analysis.

Clone #196 encodes part of the ATP-dependent chromatin assembly factor large subunit, Acf-1 (CG1966), and is capable of moderate interactive growth with the PBL bait construct. Clone #196 has an N-terminal truncation, resulting in the loss of the first 880 amino acids. Clone #196 was not fully sequenced and therefore it was not confirmed if it contained the remainder of the ORF. Acf-1 contains a putative bromodomain (typically found in chromatin associated proteins), and a PHD-finger. It is a component of the chromatin accessibility complex (CHRAC), which is involved in ISWI mediated chromatin remodelling (Eberharter *et al.*, 2001).

Clone #352 was a weak PBL interactor, and sequence analysis revealed that it encodes the *Drosophila* beta-catenin protein, Armadillo (Arm) (CG11579). Clone #352 has an N-terminus truncation resulting in the absence of the first 702 amino acids, but contains the remaining 138 amino acids as well as 3'UTR sequence.

Clone #300 encodes a putative DNA repair protein/dUTP pyrophosphatase (CG4584), and was capable of only weak interactive growth with the PBL bait construct. Sequence analysis revealed clone #300 lacks the 5' CDS resulting in the loss of the first 16 amino acids, but contains the remaining 172 amino acids as well as having 3'UTR sequence.

Clone #26 encodes a novel protein (CG9894). Clone #26 lacks 5' coding sequence resulting in a 90 amino acid N-terminal truncation, but contains the remaining sequence encoding the last 62 amino acids. This region shares homology with the Astrovirus capsid protein precursor.

Figure 3.2 RacGAP50C contains a predicted coiled-coil domain

Output window from the COILS prediction program, showing the result of the entire RacGAP50C ORF. A coiled-coil domain is predicted to exist in the N-terminus of RacGAP50C, from amino acid 36 to 122. The analysis indicates potentially two adjacent coiled-coil domains in this region. A weak coiled-coil domain is also predicted to exist towards the C-terminus.

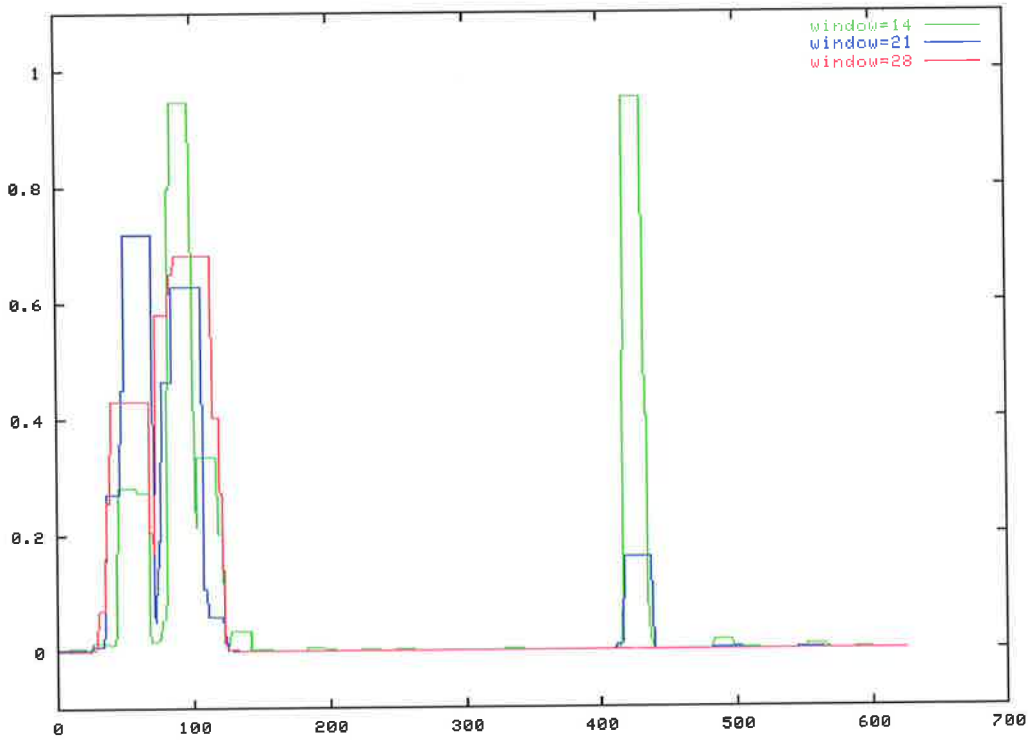
window=14
window=21
window=28
1
0.8
0.6
0.4
0.2
0
0
100
200
300
400
500
600
700

3.2.2 Genetic interaction between *pbl* and the candidate interactors

A number of interactors capable of interacting with the N-terminus of PBL were identified from the yeast two-hybrid screen (Table 3.1). The *in vivo* significance of these interactions was explored by looking at dominant genetic modifier interactions with *pbl*. Ectopic expression of *pbl* constructs in the eye using the GMR (glass minimal region) promoter (*GMR>pbl* and *GMR>pblΔDH*), produce a rough eye phenotype (Prokopenko *et al.,* 1999). The *UAS::pblΔDH* construct encodes a dominant negative PBL that is capable of inhibiting cytokinesis, while ectopic expression of full length wild type *pbl* has been shown to inhibit apoptosis (Prokopenko *et al.,* 1999; O'Keefe *et al.,* 2001). These rough eye phenotypes can be dominantly enhanced or suppressed by removal of one copy of upstream and downstream components known to be involved in Rho signalling and cytokinesis, for example, *Rho1*, *pbl*, *rok*, *dia*. The candidate PBL-interacting proteins identified from the yeast two-hybrid screen were tested for a dominant genetic modifier interaction with these PBL constructs.

For all candidates, apart from *armadillo*, specific mutant alleles were not available, therefore deficiencies that removed the candidate gene were used. Deficiency stocks are available that cover a large percentage of the genome, but a significant disadvantage with these stocks is that they disrupt more than one gene. This limits the interpretation of the resulting phenotype as, for example, a second gene removed by the deficiency could interact with *pbl* masking the interaction of the candidate gene.

The genetic interactions are summarised in Table 3.2. Genetic interactions involving the deficiencies Df(3R)B81 and Df(2L)sc19-8 could not be determined due to the region being haplo-insufficient. Various degrees of genetic interactions were scored ranging from a very strong enhancement of the *GMR-pbl* rough eye by Df(2L)J39 to a very strong suppression of the *GMR-pblΔDH* rough eye by Df(2L)C144.

Table 3.2
Genetic interactions of candidate yeast two-hybrid interactors with *GMR-pbl* and *GMR-pblΔDH*

Deficiency	Breakpoints	Gene disrupted	*GMR-pbl*	*GMR-pblΔDH*
Df(3R)B81	98F14; 99D9-E1	*Nlp*	ND	ND
Df(2L)sc19-8	24C02-08; 25C08-09	*CG11931*	ND	ND
Df(2R)Pcl7B	54E8-F1; 55B9-C1	*Mapmodulin*	E+	-
Df(3R)P115	89B07-08; 89E07-020	*CG14897*	E++	E+
Df(2L)C144	22F03-04; 23C03-05	*CG9894*	E+	S+++
Df(2L)J39	31C-D; 32D-E	*CG4584*	E+++	S++
Df(1)v-N48	9F; 10C03-05	*Klp10A*	-	S++
Df(2R)CX1	49C01-04;50C23-D02	*RacGAP50C*	-	semi-lethal (-)
Df(3R)faf-BP	100D;100F05	*Acf-1*	E+++	lethal
Arm Allele				
Arm^{YD35}	2B14	*Arm*	-	E+

E+ mild enhancement, E++ moderate enhancement, E+++ strong enhancement, S++ moderate suppression, S+++ strong suppression, - no effect, ND not determined.

3.2.3 The N-terminus of Pebble interacts with the N-terminus of RacGAP50C

The yeast two-hybrid screen identified a number of candidate PBL interacting proteins, involved in a diverse range of biological activities. From these, RacGAP50C was chosen for further study. The yeast two-hybrid screen identified two clones of RacGAP50C, both of which interacted strongly. Shortly after the screen was completed, published research revealed that the *C. elegans RacGAP50C* ortholog (*cyk-4*) was essential for cytokinesis (Jantsch-Plunger *et al.*, 2000).

The regions of PBL and RacGAP50C that were necessary for an interaction were dissected using the yeast two-hybrid assay. Various LexA-PBL fusion constructs were generated and analysed for an interaction with RacGAP50C, including PBL_{1-101}, PBL_{1-206}, PBL_{94-206}, PBL_{94-308}, $PBL_{197-308}$, $PBL_{369-651}$, $PBL_{369-853}$ and $PBL_{571-853}$. Firstly, these

constructs were transformed into yeast and assayed to confirm that the LexA fusion proteins were expressed. Protein extracts from the transformed yeast were separated by SDS/PAGE, and anti-LEX-A monoclonal antibodies used to detect the fusion protein (Figure 3.3).

The VP16-fused full length RacGAP50C clone (#28) was assayed for an interaction with the PBL constructs listed above (Figure 3.4 A). The construct containing the RADECL and first BRCT domain (PBL_{1-206}) interacted with full length RacGAP50C as strongly as the original PBL bait construct (PBL_{1-308}) (Figure 3.5). However, separately neither the first BRCT domain (PBL_{94-206}) or N-terminal RADECL domain (PBL_{1-101}) constructs were capable of interacting with RacGAP50. The N-terminus PBL construct (PBL_{1-101}) was capable of autoactivation of the histidine reporter. Therefore interactions were tested in the presence of 3AT, to inhibit the autoactivating growth, and shown to be incapable of interacting with PBL. Full length RacGAP50C was also unable to interact with any of the other PBL constructs, including the two BRCT domains (PBL_{94-308}), the second BRCT domain ($PBL_{197-308}$) and various constructs in the C-terminus. The above results clearly indicate that the first BRCT domain of PBL and its associated conserved N-terminal extension, the RADECL domain, are necessary for the interaction with RacGAP50C.

A complementary set of experiments was used to identify the region of RacGAP50C that interacted with PBL. Various RacGAP50C constructs were generated and tested for an interaction with the PBL bait construct, PBL_{1-308} (Figure 3.4 B). Firstly two RacGAP50C constructs comprised respectively of the N-terminal ($RacGAP50C_{N\text{-}term\ 1\text{-}309}$) half and the C-terminal half ($RacGAP50C_{C\text{-}term\ 303\text{-}625}$) of RacGAP50Cwere generated. Only the N-terminal construct of RacGAP50C was capable of interacting with PBL. This N-terminal region was again cut into three regions, according to potential domain containing regions: the N-terminus ($RacGAP50C_{1-173}$), which contains a coiled coil domain, the C1 domain ($RacGAP50C_{232-309}$) and the region between these two domains ($RacGAP50C_{166-240}$). Of these three constructs only the coiled coil containing construct interacted with PBL. Using fortuitous restriction enzyme sites (*Bgl*II, *BssH*II and *Sfi*I), C-terminal truncations of the $RacGAP50C_{1-173}$ construct were

Figure 3.3 Expression of Pebble-LexA fusion proteins in yeast

Protein extracts were prepared from yeast transformed with various PBL-LexA fusion constructs, and separated by SDS-PAGE. Western analysis with anti-LexA antibodies identified proteins of the expected sizes. pNLX (empty vector) (lane1) expressing the ~27kDa LexA protein, PBL-$LexA_{1-101}$(lane2), PBL-$LexA_{1-206}$ (lane 3), PBL-$LexA_{1-308}$(lane 4), PBL-$LexA_{94-206}$ (lane 5), PBL-$LexA_{94-308}$ (lane 6), PBL-$LexA_{197-308}$ (lane 7), PBL-$LexA_{283-393}$ (lane 8), PBL-$LexA_{571-853}$ (lane 9), PBL-$LexA_{369-651}$ (lane 10), PBL-$LexA_{283-651}$ (lane 11). Molecular weights in kDa are indicated on the left.

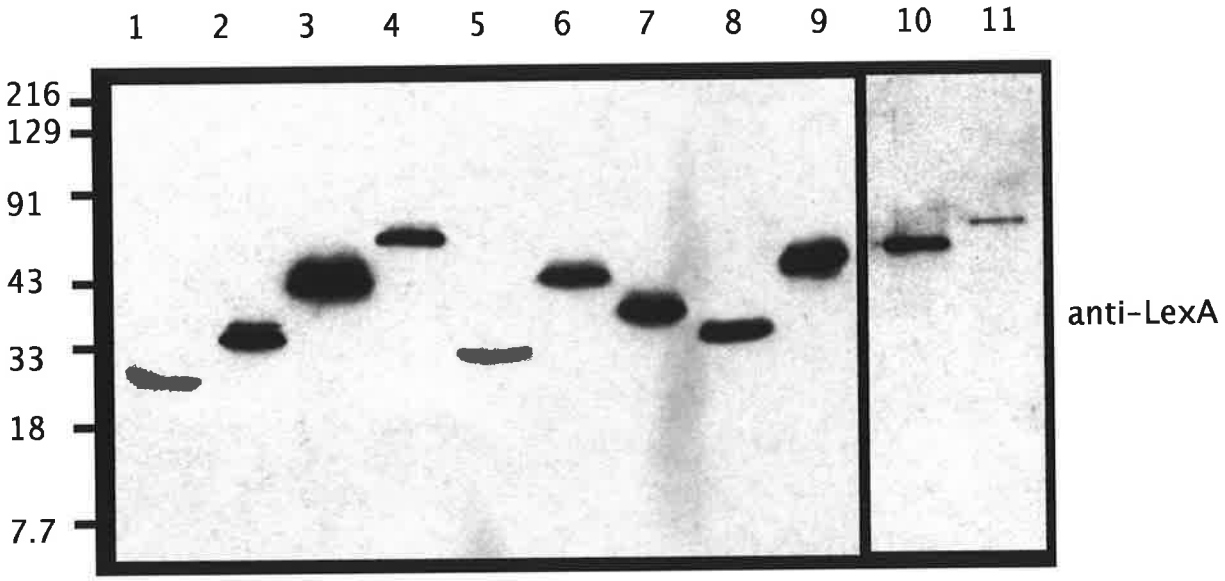
1
2
3
4
5
6
7
8
9
10
11
216
129
91
43
33
18
7.7
anti-LexA

Figure 3.4 Schematic representation of PBL-RacGAP50C yeast two-hybrid assay.

Constructs used in the interaction tests are shown diagrammatically, with full-length proteins displayed at the top with domains labelled as following: RADECL: Rad4-like/Ect2-like; BRCT: BRCA1 C-terminal domain; NLS: nuclear localisation sequence, DH: Dbl homology; PH: Pleckstrin homolgy; CC: coiled coil domain; C1: phorbol ester/diacylglycerol-binding domain; GAP: GTPase activating domain. The strength of the interaction is indicated on the right, with +++ denoting a strong interaction and – denoting no interaction. (A) The N-terminus of PBL, containing the RADECL and first BRCT domain is sufficient to interact with full-length RacGAP50C. (B) The coiled coil domain of RacGAP50C is necessary for an interaction with PBL.

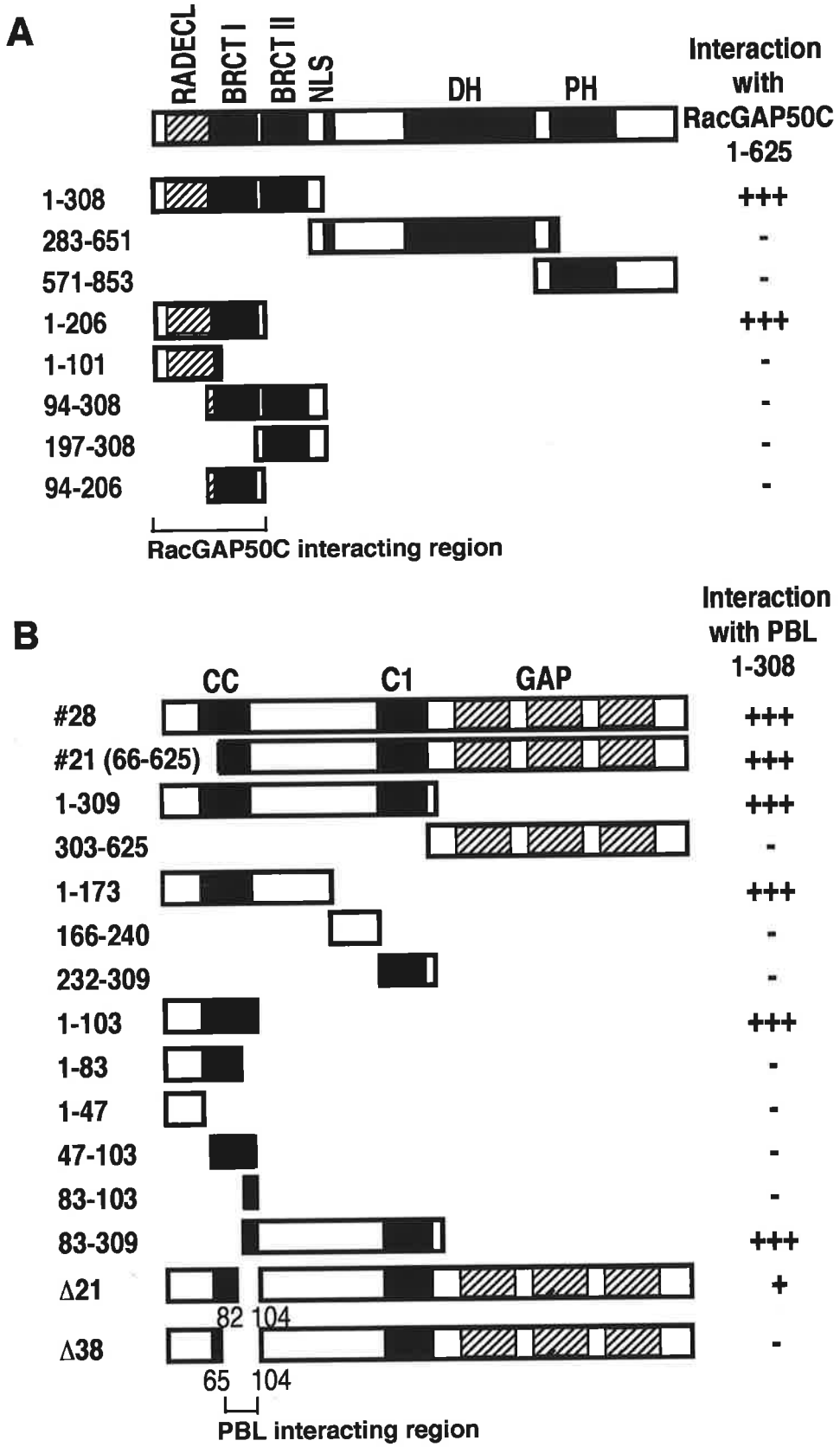
A
RADECL
BRCT I
BRCT II
NLS
DH
PH
Interaction with RacGAP50C 1-625
1-308
+++
283-651
-
571-853
-
1-206
+++
1-101
-
94-308
-
197-308
-
94-206
-
RacGAP50C interacting region
B
Interaction with PBL 1-308
CC
C1
GAP
#28
+++
#21 (66-625)
+++
1-309
+++
303-625
-
1-173
+++
166-240
-
232-309
-
1-103
+++
1-83
-
1-47
-
47-103
-
83-103
-
83-309
+++
Δ21
+
82 104
Δ38
-
65 104
PBL interacting region

Figure 3.5 The N-terminus of Pebble and RacGAP50C interact.

To assay the region of interaction between PBL and RacGAP50C, transformed yeast were streaked onto the selective medium YNB-trp-leu (A, B and C) or YNB-trp-leu-his (A', B' and C').

(A and A') Transformed PBL-LexA fusion protein constructs (1) PBL_{1-308}, (2) PBL_{1-206}, (3) PBL_{94-308}, (4) PBL_{94-206}, (5) $PBL_{197-308}$ were tested for an interaction with full-length RacGAP50C. The N-terminus of PBL, specifically the RADECL and first BRCT domain, were capable of interacting with full-length RacGAP50C (A', 2.).

(B, B', C and C') RacGAP50C-VP-16 fusion constructs (1) RacGAP50C #28, (2) $RacGAP50C_{303-625}$, (3) $RacGAP50C_{1-309}$, (4) $RacGAP50C_{1-173}$, (5) $RacGAP50C_{166-240}$, (6) $RacGAP50C_{232-309}$, were assayed for an interaction with PBL_{1-308} (B and B') and PBL_{1-206} (C and C'). The N-terminus of RacGAP50C was capable of interacting with the N-terminus of PBL.

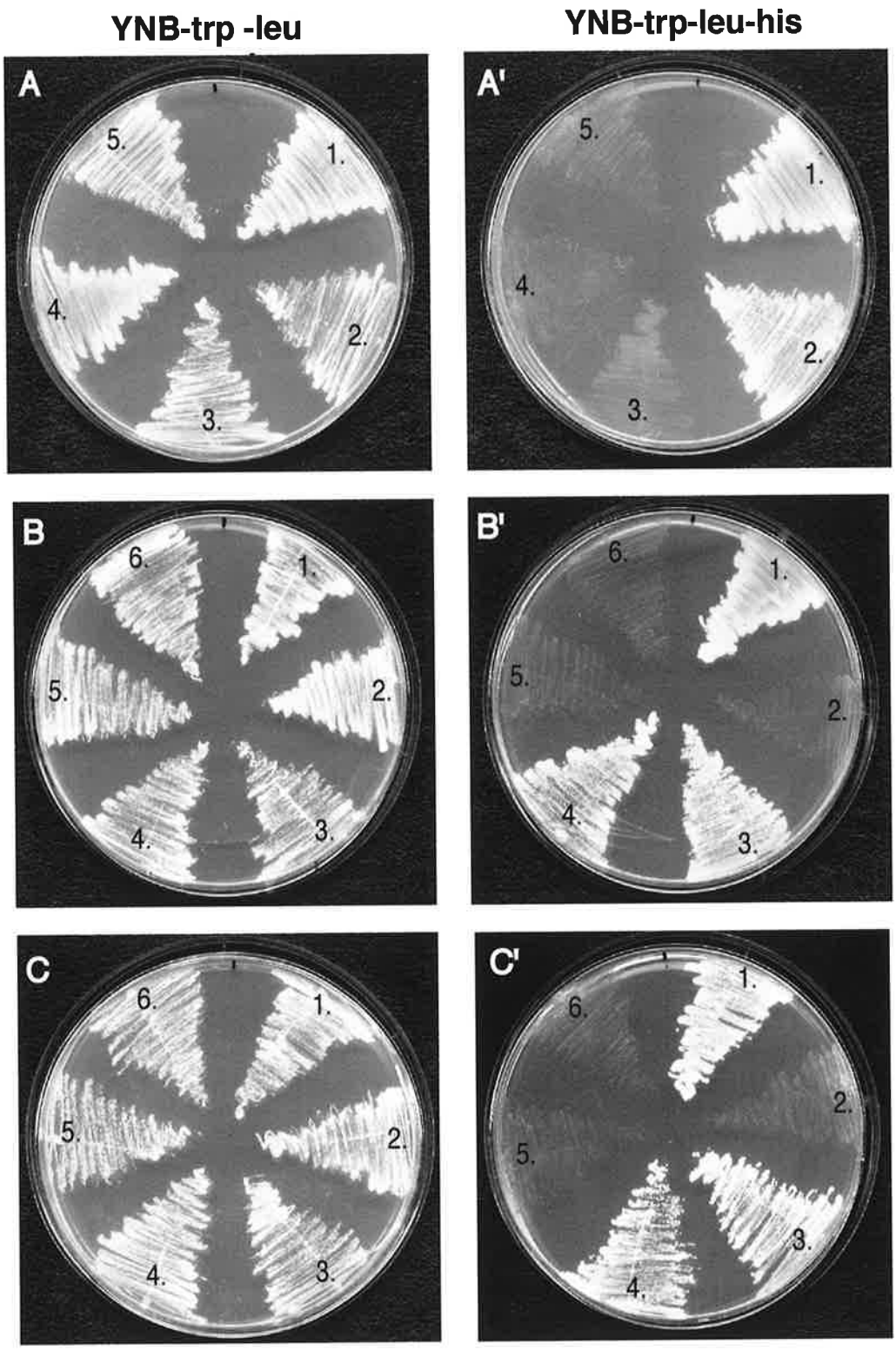
YNB-trp -leu
YNB-trp-leu-his
A
5.
1.
4.
2.
3.
A'
5.
1.
4.
2.
3.
B
6.
1.
5.
2.
4.
3.
B'
6.
1.
5.
2.
4.
3.
C
6.
1.
5.
2.
4.
3.
C'
1.
6.
2.
5.
3.
4.

created, generating the clones RacGAP50C$_{1-103}$, RacGAP50C$_{1-83}$ and RacGAP50C$_{1-47}$ respectively. Two-hybrid interaction tests with PBL revealed that only clone RacGAP50C$_{1-103}$ interacted.

Interpretation of the RacGAP50C deletion constructs, as well as the fact that the RacGAP50C yeast two-hybrid interactor #21 has an N-terminal truncation, narrows down the most likely region of interaction to somewhere between the start of #21 (amino acid 65) and the *Bgl*II site (amino acid 103). Smaller constructs (RacGAP50C$_{47-104}$ and RacGAP50C$_{83-104}$) within this region were generated but both of these failed to interact, possibly due to an inability to form the required structure because of their small size. Deletion constructs were generated in an attempt to produce full length RacGAP50C that abolished the interaction with PBL, while trying not to disturb other functional domains. Two constructs were generated, RacGAP50CΔ21 and RacGAP50CΔ38, that deleted amino acids 83-103 and 66-103 respectively. The region deleted in RacGAP50CΔ21 construct removed the amino acids found between the non-interacting RacGAP50C$_{1-83}$ construct and the interacting RacGAP50C$_{1-103}$ construct. The deleted region of RacGAP50CΔ38 covered the same region as the RacGAP50CΔ21 but included an additional 17 amino acids towards the amino terminus, which includes residues conserved between RacGAP50C homologs. Deleting the 21 amino acids in RacGAP50CΔ21 abolished most interactive growth with PBL (a small amount of growth was seen after 3 days of growth at 30°C). On the other hand, RacGAP50CΔ38 had no detectable interactive growth with PBL. This indicates that the majority of the critical interacting residue(s) of RacGAP50C are found in the 21 amino acid region deleted in the RacGAP50CΔ21 construct, but residues taken out in the 38 amino acid deletion of RacGAP50CΔ38 also play a role in the interaction with PBL.

3.2.4 Pebble RhoGEF and RacGAP50C form a complex *in vivo*

To test if the PBL RhoGEF/RacGAP50C complex identified in the yeast two-hybrid forms *in vivo*, rat and rabbit polyclonal anti-RacGAP50C antibodies were generated and used to perform co-immunoprecipitations. Western blot analysis revealed that all anti-RacGAP50C antibodies generated detect an expected ~70kDa band from

Drosophila early embryonic extracts (data not shown). The specificity of the antibodies were confirmed by performing western blot analysis on protein samples generated treated with and without *RacGAP50C* dsRNA (Figure 3.6 A). Probing the western with anti-RacGAP50C antibodies (Rat#2), a protein of the expected size, (~70kDa) was detected only in the untreated lane. The western blot was stripped and reprobed with anti-alpha-tubulin, to confirm similar sample loadings, and thus prove the specificity of the anti-RacGAP50C antibodies. These anti-RacGAP50C antibodies were then used in a coimmunoprecipitation (Figure 3.6 B). Anti-RacGAP50C antibodies were capable of immunoprecipitating RacGAP50C from early embryonic protein extracts (Figure 3.6 B, lane 2), as well as detect RacGAP50C in the embryonic extract (Figure 3.6 B, lane 5). Immunoprecipitations with anti-PBL IgG (Prokopenko *et al.,* 1999) also precipitated the ~70kDa RacGAP50C protein (Figure 3.6 B, lane 4), indicating the presence of a PBL RhoGEF-RacGAP50C complex *in vivo*.

3.2.5 The RhoGEF-RacGAP complex is evolutionarily conserved

Orthologs of RacGAP50C are highly conserved (see Figure 3.1), sharing domains that are also spatially conserved within the protein. To test if the RhoGEF-RacGAP complex can potentially form in other organisms, a physical association between the human proto-oncogene Ect2 and MgcRacGAP were assayed using a yeast two-hybrid assay. The N-terminus of Ect2 (amino acids 1-333), corresponding to the PBL bait construct used in the yeast two-hybrid screen, was shown to interact strongly with a full-length clone of MgcRacGAP, suggesting that the interaction is conserved during animal development.

3.2.6 RacGAP50C is essential for cytokinesis

The use of dsRNA in *Drosophila* S2 cells has recently enabled researchers to conduct fast and efficient genome wide screens to identify genes involved in particular aspects of mitosis, including cytokinesis. Using a slightly modified procedure to that used by

Figure 3.6 RacGAP50C and Pebble form an *in vivo* complex.

(A) Protein samples were prepared from *Drosophila* S2 cell culture cells, treated with (+) and without (-) 15ug of *RacGAP50C* dsRNA for 60 hours at 25°C. These protein samples were separated by SDS/PAGE, and analysed by western blot. Anti-RacGAP50C antibodies (Rat#2) detect a single ~70kDa band in the untreated lane. The western blot was subsequently stripped and probed with anti-alpha-tubulin, which served as a loading control. An expected 50kDa tubulin band was detected in both protein samples.

(B) RacGAP50C coimmunoprecipitates with PBL from 0-5 houur embryonic extracts. Samples were immunoprecipitated with antibodies indicated above each well, or with no antibody (No IgG) before being electrophoresed. The right lane (lane 5) was loaded with total embryonic protein extract. Following separation and transfer, anti-RacGAP50C antibodies were used to probe the membrane. The ~70kDa RacGAP50C protein is detected in the total protein extract as well as in both the RacGAP50C and PBL immunoprecipitations.

A

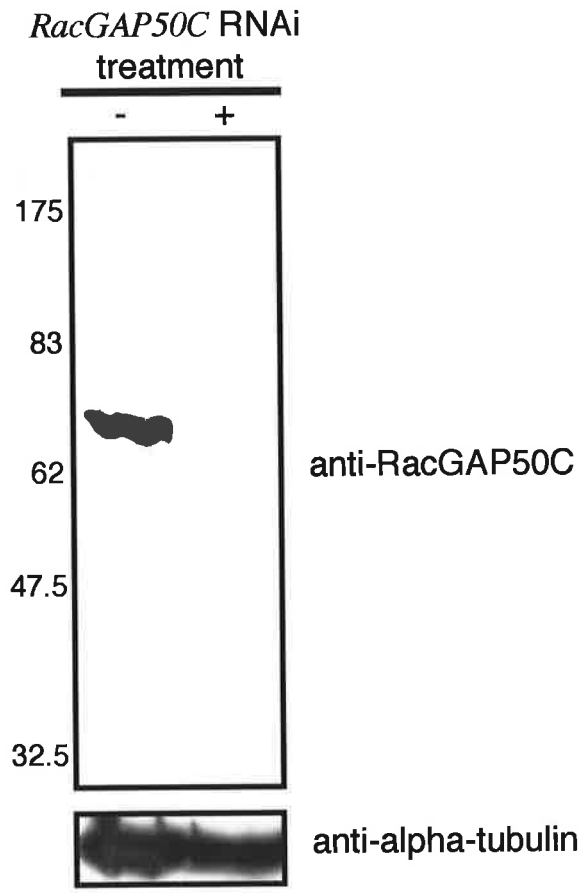
RacGAP50C RNAi
treatment
-
+
175
83
62
47.5
32.5
anti-RacGAP50C
anti-alpha-tubulin

B

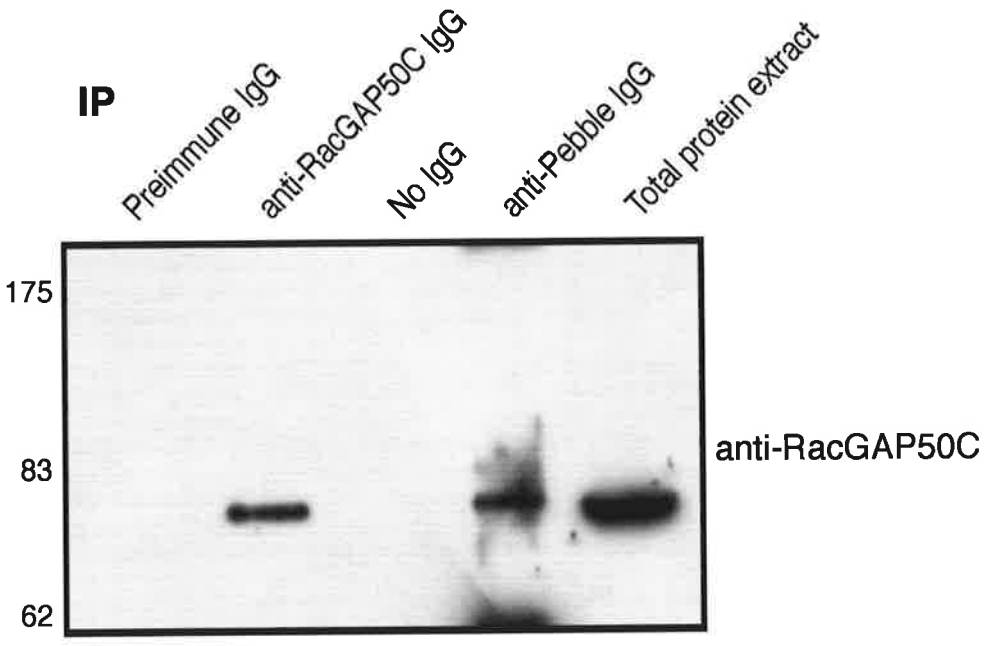
IP
Preimmune IgG
anti-RacGAP50C IgG
No IgG
anti-Pebble IgG
Total protein extract
175
83
62
anti-RacGAP50C

Figure 3.7 *RacGAP50C* is required for cytokinesis in *Drosophila* S2 cultured cells

DNA stained with Hoechst 33258 (Blue), anti-alpha-tubulin (green). *Drosophila* S2 cells were treated with 10ug of *RacGAP50C* dsRNA for 2 days. Cytokinesis was disrupted in a significant number of these cells after this time (asterisk indicate multinucleate cells).

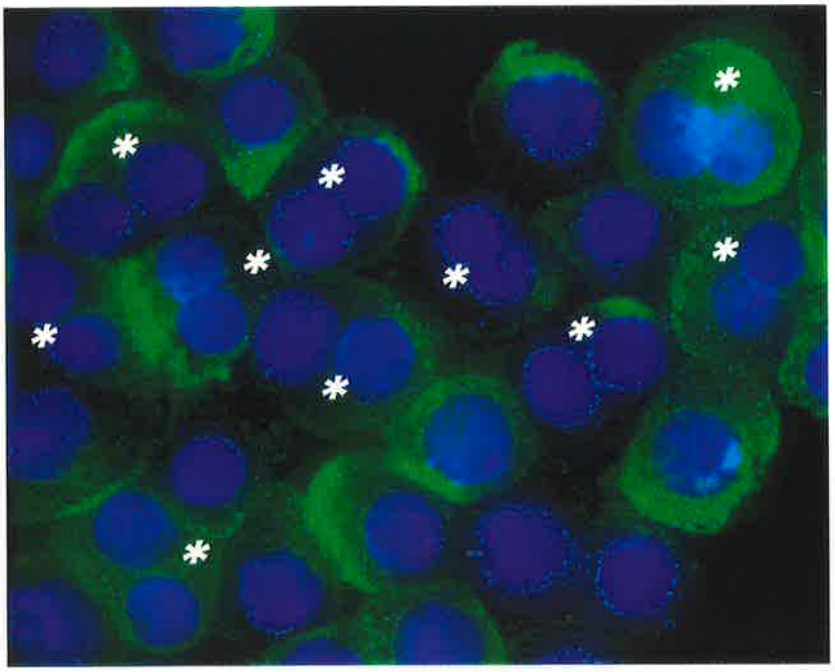

C lemens *et al.*, (2000), *Drosophila* S2 cells were treated with 15μg of dsRNA specific to *RacGAP50C*. Within 24 hours of growth an observable number of cells had already become multinucleate, and within 48 hours the majority (75-80%) of cells were multinucleate (Figure 3.7). This multinucleate phenotype was also seen when S2 cells were incubated with dsRNA against *pbl* and *Rho1*, but not *RhoL*, *rac1*, *rac2*, *cdc42*, *mtl* or a combination of dsRNAs against both *rac1* and *rac2*. Similar results were recently published, revealing the essential role that *pbl*, *RacGAP50C* and *Rho1* play during cytokinesis in *Drosophila* S2 cell (Somma *et al.*, 2002).

3.3 Discussion

A yeast two-hybrid screen was conducted to identify proteins that interact with the BRCT domain-containing N-terminus of PBL (PBL_{1-308}). A number of candidate proteins were identified that possessed a mixture of nuclear and cytoplasmic functions as based on sequence similarity to other characterised proteins. The PBL bait construct interacted with these candidate proteins in the yeast two-hybrid assay with varying intensity, ranging from a strong interaction with RacGAP50C, to weak interactions with clones such as Armadillo and Klp10A. Although yeast two-hybrid screens are renowned for their identification of false positive interactors, the weak interactions observed with some candidates may solely reflect that these clones had partial ORF's, possibly removing part of the PBL interacting region. Alternatively, the PBL bait construct used for the screen may not contain the entire interacting region. Further analysis is needed to confirm whether the candidate interactors identified in the yeast two-hybrid screen also form a complex with PBL *in vivo*.

3.3.1 Candidate nuclear interactors

From telophase until interphase of the following cell cycle, PBL is found localised in the nucleus. This localisation, as well as the possession of tandem N-terminal BRCT domains, is suggestive of a nuclear role for PBL. The identification of the candidate interactors dUTP pyrophosphatase, Nlp and Acf-1, that also have putative nuclear roles, may provide clues to the function of nuclear accumulated PBL.

The *Drosophila* dUTP pyrophosphatase (Clone #300) encodes a putative DNA repair protein. The dUTP pyrophosphatase may associate with PBL after DNA damage,

preventing the completion of the cell cycle until the damage is repaired. Disruption of dUTP pyrophosphatase using dsRNA on *Drosophila* S2 cell culture cells did not interfere with cytokinesis (C. McLeod, personal communication). If this interaction with PBL occurs *in vivo*, it is likely therefore to be associated with a non-cytokinetic function of PBL. Further studies of this interaction could include identifying the protein complexes that associate with PBL in the presence and absence of DNA damage.

Drosophila nucleoplasmin (Nlp) (Clone #365) is a nuclear protein that is present throughout embryo development and is involved in chromatin binding and decondensation (Crevel *et al.,* 1997). PBL accumulates in the nucleus following nuclear envelope reformation and during chromatin decondensation, ideally positioning PBL to interact with Nlp. Depletion of Nlp using dsRNA on *Drosophila* S2 cell culture cells, again was observed not to interfere with cytokinesis (C. McLeod, personal communication).

Acf-1 (Clone #196), is a component of the chromatin accessibility complex (CHRAC), which is involved in ISWI mediated chromatin remodelling (Eberharter *et al.,* 2001). Similar proteins are found in humans, mouse, *C. elegans* and yeast. Like Nlp, an interaction with Acf-1 suggests that PBL interacts with chromatin remodelling proteins in the nucleus. These proteins may be part of a complex involved in DNA damage sensing/repair (linking a DNA damage check-point to later stages in mitosis via PBL). Alternatively, PBL may associate with these chromatin remodelling proteins to regulate targeted gene expression.

3.3.2 Candidate cytoplasmic interactors

Given PBLs role in cytokinesis, the association with cytoplasmically localised candidate proteins is expected. However, what was not expected was that these proteins interacted with the normally nuclear functioning N-terminal BRCT domains.

Klp10A (Clone #282) is a microtubule associated kinesin motor protein. The Xenopus orthologue (XKCM1) localises to centromeres and spindle poles and is required for both establishing and maintaining the mitotic spindles. Interference with this kinesin

motor results in abnormally long microtubules (Walczak *et al.,* 1996). The mouse orthologue (KIF2b) is a plus end-directed microtubule motor that is involved in translocating lysosomes from the MTOC to the cell periphery (Santama *et al.,* 1998). The arrival of PBL to the equatorial cortex is through an unknown mechanism. The association of PBL with the microtubule motor protein Klp10A, provides a possible mechanism by which PBL is transported to the equatorial cortex during anaphase.

Mapmodulin is a putative cytoskeletal protein, possessing a leucine-rich repeat domain, commonly observed in proteins involved in cell adhesion. A protein of similar sequence in humans (I1PP2A/PHAP1), acts as a protein phosphatase 2A (PP2A) inhibitor. PP2A plays a key role in regulating cellular growth/tumorigenic transformation and cell cycle progression and cytokinesis. An interaction between PBL and mapmodulin could provide a regulatory link to coordinate mitosis with cytokinesis.

The *Drosophila* beta-catenin protein, Armadillo (Arm) (Clone #352), is involved in segment polarity, transducing signals from the Wingless/Wnt (WG) family of proteins. WG signalling alleviates the negative regulation of cytoplasmic Armadillo by repressing the activity of Shaggy/ZW3 (Peifer *et al.,* 1994). Cytoplasmic Armadillo is then able to complex with the nuclear factor Pangolin to modulate the transcription of target genes. beta-catenin also complexes with cadherins to mediate cell adhesion. A conserved region comprised of multiple repeats is able to interact with the intracellular portion of E-cadherin (Peifer 1993), while an N-terminal domain binds alpha-catenin, which is associated with the actin cytoskeleton (Oda *et al.,* 1993). PBL is thus capable of potentially interacting with Armadillo in both the nucleus, to regulate WG transduced gene expression, and in the cytoplasm, playing a role in cytoskeleton regulation through interactions involving the cadherin-catenin complex. PBL has also previously been identified as a genetic interactor in a large scale screen for modifiers of an overexpression and underexpression Arm phenotype. Loss of one copy of *pbl* strongly enhanced the overexpression of Arm and strongly suppressed the under expression phenotype (Greaves *et al.,* 1999), supporting an *in vivo* role for this interaction.

The RacGAP50C clones (#28 and #21) were by far the strongest interactors identified. Subsequent reports revealed that the *C. elegans* and mammalian orthologs of RacGAP50C (*cyk-4 and mgcRacGAP*) were essential for cytokinesis (Jantsch-Plunger *et al.,* 2000; Hirose *et al.,* 2001; Van de Putte *et al.,* 2001), making RacGAP50C a prime candidate for further analysis.

3.3.3 The nature of the Pebble-RacGAP50C interaction

Two independent clones of *RacGAP50C* were identified from the screen, capable of interacting with the N-terminus of PBL. This interaction was further confirmed through co-immunoprecipitation experiments from early embryonic protein extracts. A yeast two-hybrid assay was used to identify residues within the RADECL and first BRCT domains of PBL were necessary for the interaction with RacGAP50C. The assay also identified the coiled-coil domain of RacGAP50C was necessary for the interaction with PBL. This coiled coil domain has previously been shown to be necessary for both homo-dimerisation, as well as for interacting with the kinesin motor protein ZEN-4 (Mishima *et al.,* 2002). Depletion of *RacGAP50C* in *Drosophila* S2 culture cells with RNA interference results in a polyploidy phenotype, same as that reported when the *C. elegans* ortholog *cyk-4* or mammalian ortholog *mgcRacGAP* are disrupted (Jantsch-Plunger *et al.,* 2000; Hirose *et al.,* 2001; Van de Putte *et al.,* 2001; Mishima *et al.,* 2002). The intracellular localisation of these RacGAP50C orthologs has also been reported (Jantsch-Plunger *et al.,* 2000; Hirose *et al.,* 2001), and appears strikingly similar to that reported for PBLs mammalian ortholog, Ect2 (Tatsumoto *et al.*, 1999). In these organisms the RacGAP orthologs localise to the mitotic spindles during metaphase and become restricted to the central spindle and midbody during anaphase and telophase respectively. Late in telophase MgcRacGAP accumulates within the nucleus. PBL has not been reported to be associated with MT structures, but instead localises to the contractile-ring during late telophase. A clear possibility is that the PBL-RacGAP50C interaction occurs once the cortex has furrowed and come into contact with the central spindle, where the formation of the PBL-RacGAP50C complex is then capable of stabilising or further regulating the constriction of the contractile-ring. As both proteins localise to the nucleus, the interaction may also occur there. Although Rho family members have been shown to play a role in signalling to the nucleus to regulate gene expression (Hill *et al.,* 1995), the proposal that both proteins

are involved in regulating cytokinesis at the contractile-ring/central spindle is far more satisfying as both PBL and RacGAP50C are putative Rho family regulators, that are essential for cytokinesis.

Chapter Four: RacGAP50C localises to cortical microtubules of the central spindle and the midbody during cytokinesis.

4.1 Introduction

The previous chapter described the identification of a strong direct interaction between the N-terminus of PBL and the Rho family activating protein, RacGAP50C. Co-immunoprecipitation experiments also revealed the existence of an *in vivo* PBL-RacGAP50C complex. In addition, yeast two-hybrid assay results demonstrated that the human orthologs of PBL and RacGAP50C are also capable of interacting. To gain a better understanding of the functional significance of this PBL RhoGEF-RacGAP50C interaction, the intracellular localisation of RacGAP50C was investigated.

The expression pattern of *RacGAP50C* has previously been reported on whole-mount embryos and imaginal tissues (Sotillos and Campuzano, 2000). *RacGAP50C* transcripts were shown to be ubiquitous during early embryonic stages, then restricted to the central and peripheral nervous systems during germ-band retraction. The protein localisation of the RacGAP50C orthologs, *C. elegans* CYK-4 and mammalian MgcRacGAP, has also been reported (Jantsch-Plunger *et al.,* 2000; Hirose *et al.,* 2001; Mishima *et al.,* 2002). Both CYK-4 and MgcRacGAP localise to mitotic microtubules. During metaphase both proteins are associated with the mitotic spindle, appearing on the central spindle midzone region at early anaphase and becoming restricted to the midbody during telophase, before localising into the nucleus. Disruption of either *cyk-4* or *mgcRacGAP* interferes with cytokinesis, resulting in the formation of multinucleate cells. *cyk-4* mutant embryos are capable of initiating cortical furrowing, which ingresses a significant way, reaching the central spindle before regressing.

This chapter describes the patterns of expression of the *RacGAP50C* transcript and the use of anti-RacGAP50C antibodies to characterise the RacGAP50C protein expression pattern and intra-cellular localisation.

4.2 Results

4.2.1 *RacGAP50C* is expressed in highly proliferating tissues

Identifying the expression pattern of a gene provides important information on potential developmental roles. The expression pattern of *RacGAP50C* has been briefly reported by (Sotillos and Campuzano, 2000). *RacGAP50C* was shown to have ubiquitous expression in early syncytial development, later becoming restricted to the central and peripheral nervous system, then to the imaginal discs during larval development (Sotillos and Campuzano, 2000).

Whole mount *in-situ* staining of wild-type embryos, using a DIG-labelled *RacGAP50C* probe transcribed from the full-length yeast two-hybrid clone (#28), supports these reported observations. *RacGAP50C* transcripts were seen to be ubiquitous during cellularisation and blastoderm stages of development (Figure 4.1 A, B). The apparent hexagonal staining of the *RacGAP50C* transcript in cellularising embryos (Figure 4.1 B), is the result of nuclear exclusion of the transcript. Later during embryonic development *RacGAP50C* transcripts were detected at higher levels in cells in and around the ventral midline and cephalic furrow (Figure 4.1 C). These ventral mesodermal cells undergo apical flattening, which involves the apices of these cells constricting and elongating, driving the cytoplasm and nuclei basally, resulting in the elongation of the cells. The cells then shorten, causing the bases of the cells to become larger as the apical surface is still constricted, and this is believed to generate the main force needed for invagination.

Figure 4.1 *RacGAP50C* is expressed in highly proliferative tissues during early embryogenesis.

RacGAP50C transcript distribution was examined in wholemount wild-type *Drosophila* embryos using *in situ* hybridisation. (A) Lateral view of a stage 4 cellularising embryo, showing ubiquitous staining. (B) Lateral view of a stage 5 cellularising embryo shows nuclear exclusion of the transcript. (C) Lateral view of a stage 6 embryo, showing strong staining in the cephalic and ventral furrows. (D) Stage 12 embryo showing strong staining in the brain-lobes and epidermal expression in a regular repeated pattern. (D') Lateral view of a stage 14 embryo showing high levels of *RacGAP50C* transcript in the brain lobes and CNS. (E) Ventral view of a stage 14 embryo showing strong staining in the brain lobes, and a regular pattern of expression along the CNS. (E') Dorsal view of a stage 15 embryo showing strong expression in the brain-lobes, as well as staining in the visceral mesoderm and gonads (arrows). In all figures anterior is to the left.

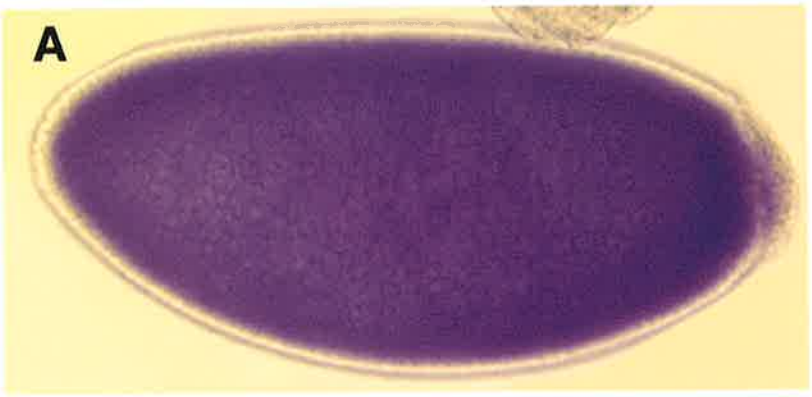
A

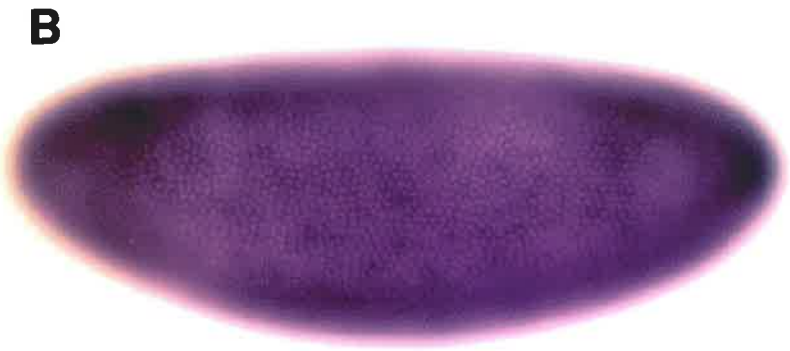
B


C


D


D'

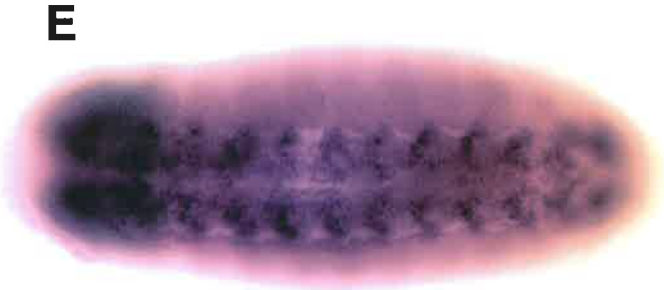
E

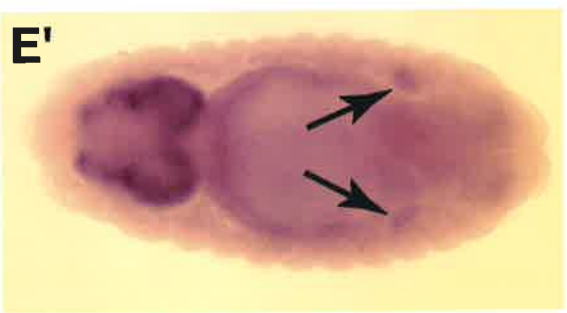
E'

This process requires the cells to undertake highly dynamic cell shape changes that involve extensive reorganisation of the actin and microtubule cytoskeletons. Figures 4.1 D, D', E and E' are various embryonic stages during and following germ-band retraction. Figures 4.1 D and D' show a high level of *RacGAP50C* transcript in the brain-lobes and nervous systems. Figure 4.1 D is a lateral view of the epidermis of a stage 11 embryo, showing *RacGAP50C* transcripts in a regularly repeated stripe pattern, consistent with PNS staining. *RacGAP50C* expression was also detected in high levels in the CNS and brain-lobes (Figure 4.1 D'). Figure 4.1 D' is a lateral view of a stage 14 embryo showing strong staining in the CNS, in a regular repeated pattern, indicating higher expression in a sub-set of neural cells. The restriction of *RacGAP50C* expression in the CNS is also seen in the ventral view of Figure 4.1 E. Figure 4.1 E' is a dorsal view of a stage 15 embryo revealing *RacGAP50C* expression in the visceral mesoderm and gonads (arrows).

RacGAP50C expression was detected in tissues undergoing rapid proliferation (brain-lobes and CNS during stage 11-14) and in tissues undergoing dynamic cell shape changes (ventral and cephalic furrows, stage 7), and is consistent with that reported by (Sotillos and Campuzano, 2000). In addition, no staining was detected with the corresponding sense-probe (data not shown), suggesting that the *RacGAP50C* expression data shown here is specific.

4.2.2 Anti-RacGAP50C antibodies detect variable sized protein products.

The anti-RacGAP50C antibodies were used to study the expression levels of RacGAP50C in protein samples from different developmental stages of *D. melanogaster*, using western blot analysis (Figure 4.2). The anti-RacGAP50C antibodies (rat#2) detect the 70kDa RacGAP50C protein in embryonic protein samples. It was present in high amounts during the rapidly proliferating early stages of development (0-8 hours), with levels declining later in embryogenesis. During later developmental stages, larger molecular weight proteins were detected. A 110kDa protein band was detected by the anti-RacGAP50C antibodies in third instar larval, pupae and adult fly protein extracts. Also, a prominent ~80kDa protein was detected in the pupal protein extract, and weakly throughout embryonic development.

Figure 4.2 Anti-RacGAP50C antibodies detect various sized proteins throughout development.

Protein samples were prepared from specific embryonic stages, and several later developmental stages throughout the life cycle, and separated by SDS/PAGE. Western analysis was performed with anti-RacGAP50C (Rat#2) antibodies, and detected by chemiluminesence (ECL) (Amersham Pharmacia Biotech). A prominent 70kDa band was present in high amounts during early embryogenesis. At later developmental stages (larval, pupal and fly) higher molecular weight bands (80 and 110kDa) were detected. Molecular weight standards are indicated on the left. Sample loading was standardised by Bradford assay, and proteins visualised by Ponseau S.

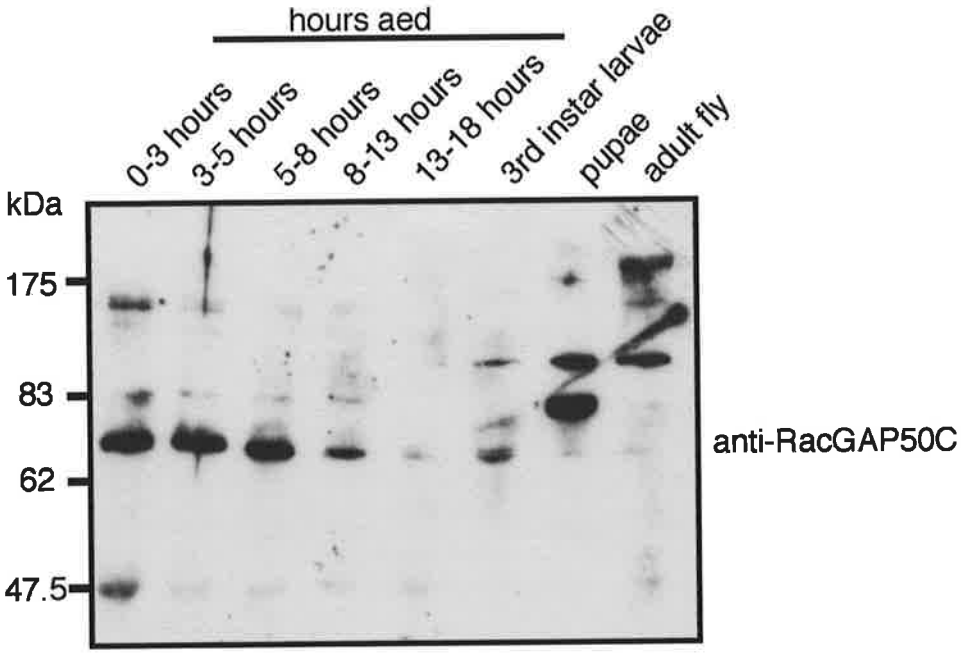
hours aed
0-3 hours
3-5 hours
5-8 hours
8-13 hours
13-18 hours
3rd instar larvae
pupae
adult fly
kDa
175
83
62
47.5
anti-RacGAP50C

The highly dynamic expression patterns of RacGAP50C are fairly consistent with the published microarray expression data (Arbeitman *et al.*, 2002) (http://genome.med.yale.edu/Lifecycle/query_gen.php?input1=CG13345). The apparent high molecular weight 80kDa and 110kDa RacGAP50C isoforms could be explained by a number of possibilities. Firstly, these higher molecular weight bands could be non-specific proteins detected by the polyclonal anti-RacGAP50C antibodies. Alternatively post-translational modification may be a necessary event for regulating the activity of RacGAP50C at various stages of development. Phosphorylation of MgcRacGAP localised to the midbody has been reported (Kitamura *et al.*, 2001). Therefore regulation of RacGAP50C through various forms of post-translational modification, possibly glycosylation, prenylation or acylation, may produce these higher molecular weight protein bands. Splice variants that are developmentally regulated, may also produce larger RacGAP50C transcripts. Although all anti-RacGAP50C antibodies generated detect the 70kDa RacGAP50C protein product, in further studies the Rat#2 and Rabbit#2 were used predominantly since they gave consistently cleaner results.

4.2.3 The RacGAP50C protein and transcript distribution patterns are similar.

The distribution of RacGAP50C was analysed in whole-mount *D. melanogaster* embryos using immunochemical detection. Although minor inconsistencies were observed between the staining patterns with the various anti-RacGAP50C antibodies, the general expression patterns were consistent. Figure 4.3 shows the distribution of RacGAP50C in wild type embryos, as detected with Rat#2 anti-RacGAP50C antibodies (A, B, C, E, G and J), Rabbit#2 anti-RacGAP50C antibodies (F, K and L), and Rabbit #1 anti-RacGAP50C antibodies (D, H and I). During syncytial and cellularising stages of development, RacGAP50C had a ubiquitous expression pattern (A and B). During germ-band extension the anti-RacGAP50C antibodies detected high levels of expression in the ventral furrow (D, E and F). Later in embryonic development RacGAP50C was detected at high levels in a restricted subset of cells in the CNS (G, H, J and K) as well as the PNS (I). These expression patterns of RacGAP50C are consistent with the high levels of expression

Figure 4.3 Anti-RacGAP50C antibodies detect an expression pattern consistent with *in situ* results.

Wholemount wild-type embryos during early embryogenesis were immunostained with anti-RacGAP50C antibodies generated from Rat#2 (A, B, C, E, G, J), Rabbit #2 (F, K, L) or Rabbit #1 (D, H, I). (A and B) preblastoderm and cellularising embryos have a ubiquitous RacGAP50C expression pattern. (C-F) germ band extending embryos showing prominent RacGAP50C expression in the ventral furrow. (G and H) Ventral views of later embryos, showing a subset of CNS cells expressing RacGAP50C. (I) Lateral view of the epidermis showing RacGAP50C expression in a repeated pattern along the epidermis. (J and K) Germ band retracted embryos showing high levels of RacGAP50C expression in the brain lobes and CNS. (L) a syncitial blastoderm showing the Rabbit#2 anti-RacGAP50C antibodies strongly detect nuclear accumulate RacGAP50C.

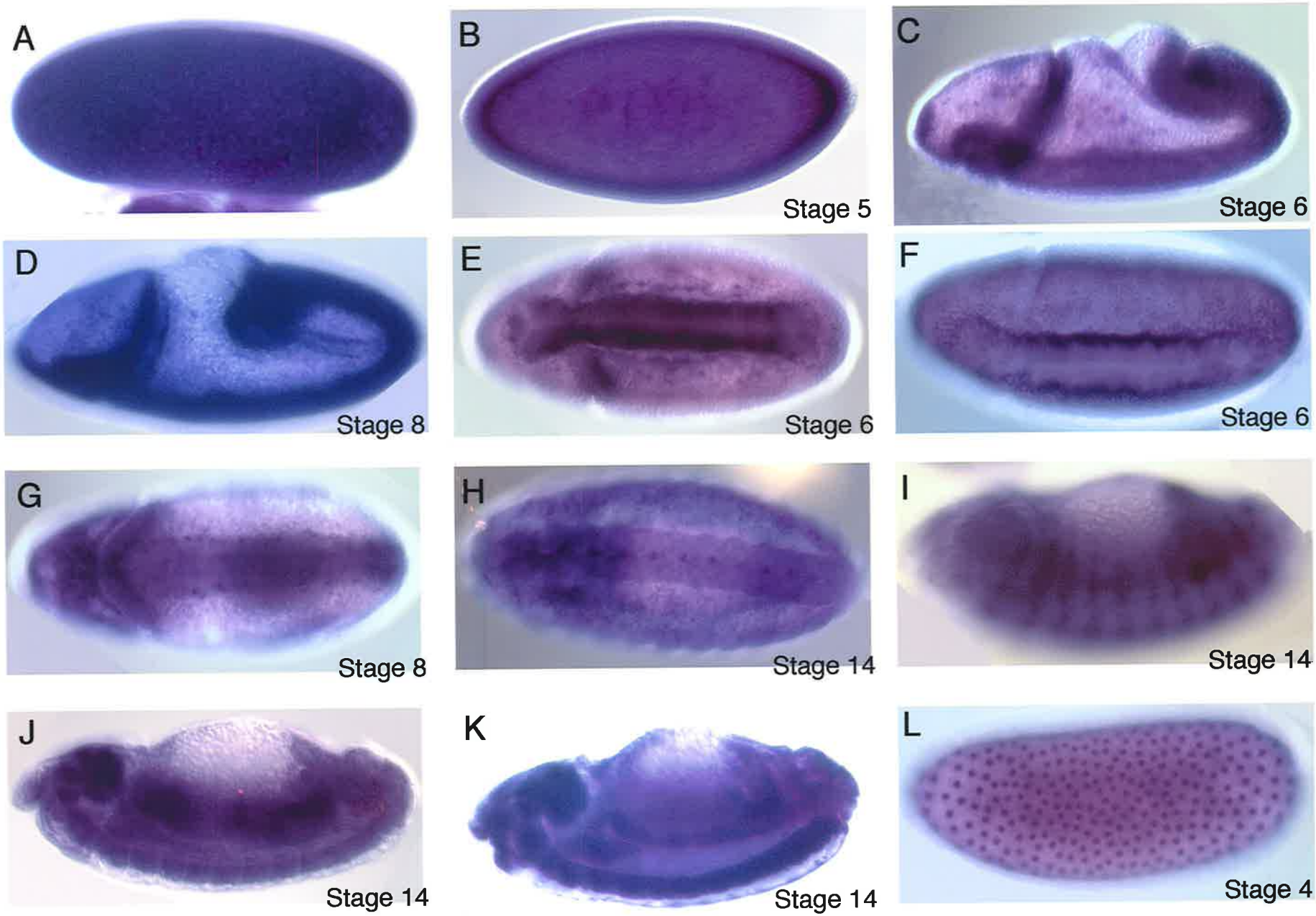
A
B
Stage 5
C
Stage 6
D
Stage 8
E
Stage 6
F
Stage 6
G
Stage 8
H
Stage 14
I
Stage 14
J
Stage 14
K
Stage 14
L
Stage 4

detected on the developmental western. Also, the localisation of RacGAP50C to tissues undergoing rapid proliferation and major morphological changes is consistent with RacGAP50C playing a role during mitosis/actin cytoskeletal rearrangement. The anti-RacGAP50C antibodies generated by Rabbit#2 produced a slightly different staining pattern compared with the other anti-RacGAP50C antibodies. This antibody detected strong RacGAP50C staining in the syncitial nuclei (Figure 4.3, L) in a cell-cycle dependent manner, while the other anti-RacGAP50C antibodies failed to detect a significant nuclear accumulation during syncitial development.

The distribution of RacGAP50C was also determined in third instar larval eye and wing imaginal discs, using the Rat#2 anti-RacGAP50C antibodies. During imaginal eye development a synchronous dorsal-ventral wave, known as the morphogenetic furrow (MF), can be traced as it moves anteriorly. Most cells within and posterior to this wave have entered into a synchronous cell cycle. Proliferating cells are therefore seen scattered in the tissue ahead of the MF as well as in a tight band directly behind the furrow. Anti-RacGAP50C antibodies detect two bands of RacGAP50C expressing cells, one band anterior of the MF and the other directly posterior to the MF (Figure 4.4 A). These two bands are presumably in the mitotically active band of cells either side of the MF. This suggests that RacGAP50C expression is cell cycle dependent.

Previously, *RacGAP50C* transcripts has been reported to localise in the presumptive interveins during late third instar of the wing discs and persist in the vein/intervein boundaries of pupal wings (Sotillos and Campuzano, 2000). Anti-RacGAP50C antibodies (Rat#2) detected expression on both the presumptive dorsal and ventral wing surfaces (Figure 4.4 B). The RacGAP50C expressing cells were restricted to two medial horizontal stripes (arrows), possibly corresponding to cells bordering the wing margin, and several vertical stripes on both the dorsal and ventral wing surface (arrowheads), possibly the intervein or vein tissue.

Figure 4.4 RacGAP50C expression in late larval eye and wing imaginal discs.

Third instar larval eye (A) and wing discs (B) were dissected and probed with anti-RacGAP50C antibodies (Rat#2). (A) RacGAP50C detects two stripes of expression in the eye imaginal disc, one anterior to and one posterior to the morphogenetic furrow (MF) (arrow). (B) RacGAP50C is detected in perpendicular stripes on the pre-dorsal/ ventral wing surface. The stripes are likely to represent cells either side of the wing margin (arrows) and cells either in the vein or intervein territories (arrowheads).

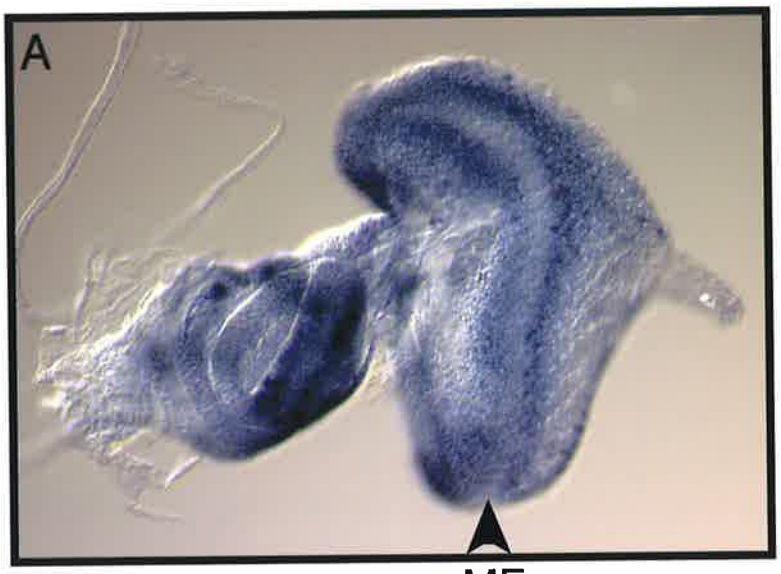
A
MF

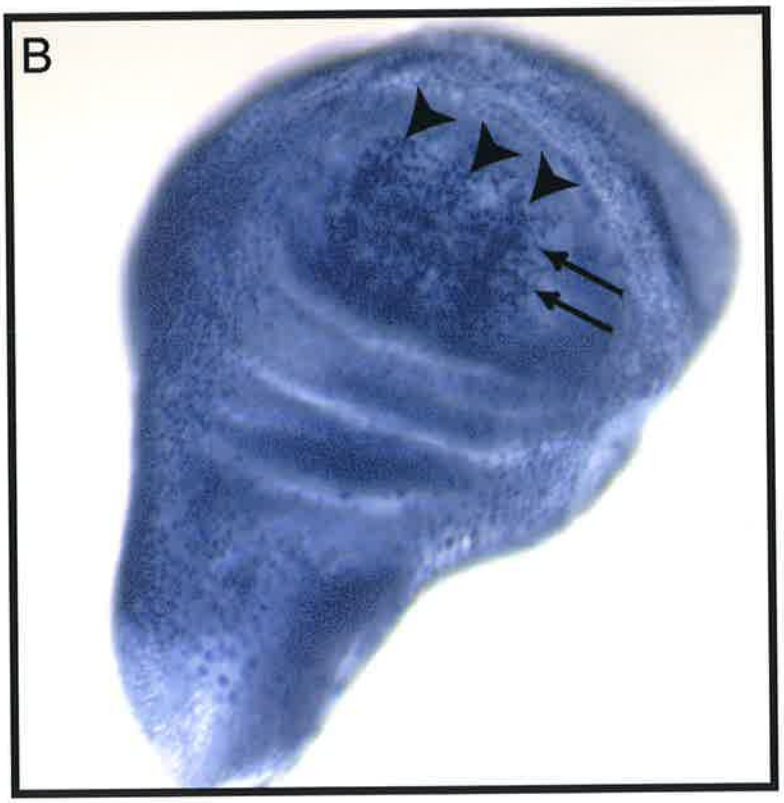
B

Figure 4.5 RacGAP50C localises to the central spindle and midbody during cytokinesis in *Drosophila* S2 cultured cells

Immunostaining of *Drosophila* S2 cultured cells stained for DNA with Hoechst 33258 (first column, blue in merge), anti-alpha-tubulin (second column, green in merge) and anti-RacGAP50C (third column, red in merge), the fourth column is a merge of the detected fluorescence from the three filter channels. RacGAP50C is seen to associate with microtubules in S2 cells. The stages of mitosis are indicated on the left. RacGAP50C is associated with the mitotic microtubules during metaphase, accumulates on the central spindle during anaphase A and B, restricted to the midbody during telophase, and accumulates in the nucleus in interphase.

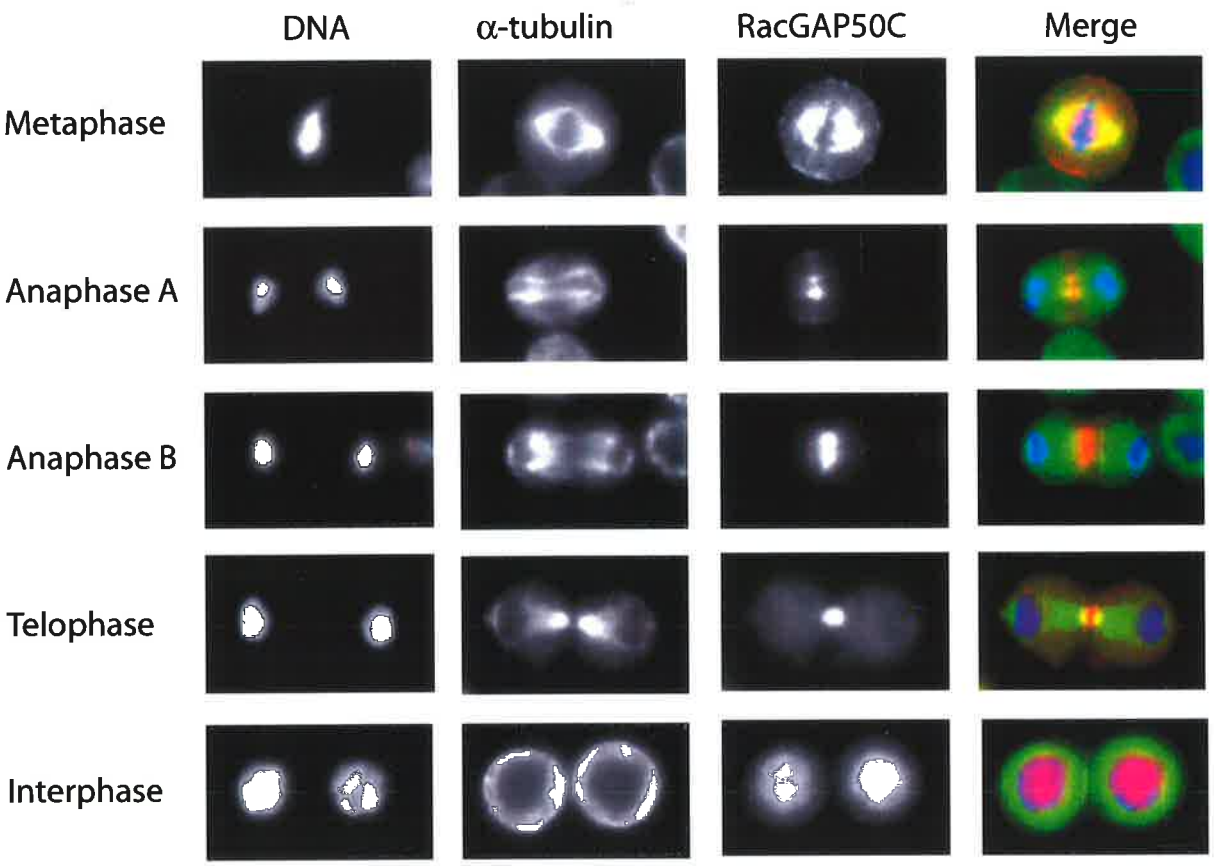
DNA
α-tubulin
RacGAP50C
Merge
Metaphase
Anaphase A
Anaphase B
Telophase
Interphase

Figure 4.6 RacGAP50C localises to the central spindle and midbody in dividing *Drosophila* embryonic epithelial cells

Immunostainings of dividing wild-type *Drosophila* embryonic epithelial cells stained for DNA with Hoechst 33258 (A, and blue in D and E), anti-RacGAP50C (B, and red in D and E), anti-alpha-tubulin (C, and green in D and E). D is a coloured merge of A-C and E is a separate field of dividing *Drosophila* epithelial cells. As shown by the different mitotic domains in D and E, RacGAP50C is detected as a diffuse punctate staining on the central spindle during early anaphase (white arrows in E), becomes more concentrated in the midzone region during a later anaphase stage (black arrows in E), and concentrates in the midbody of telophase cells (asterisk in E).

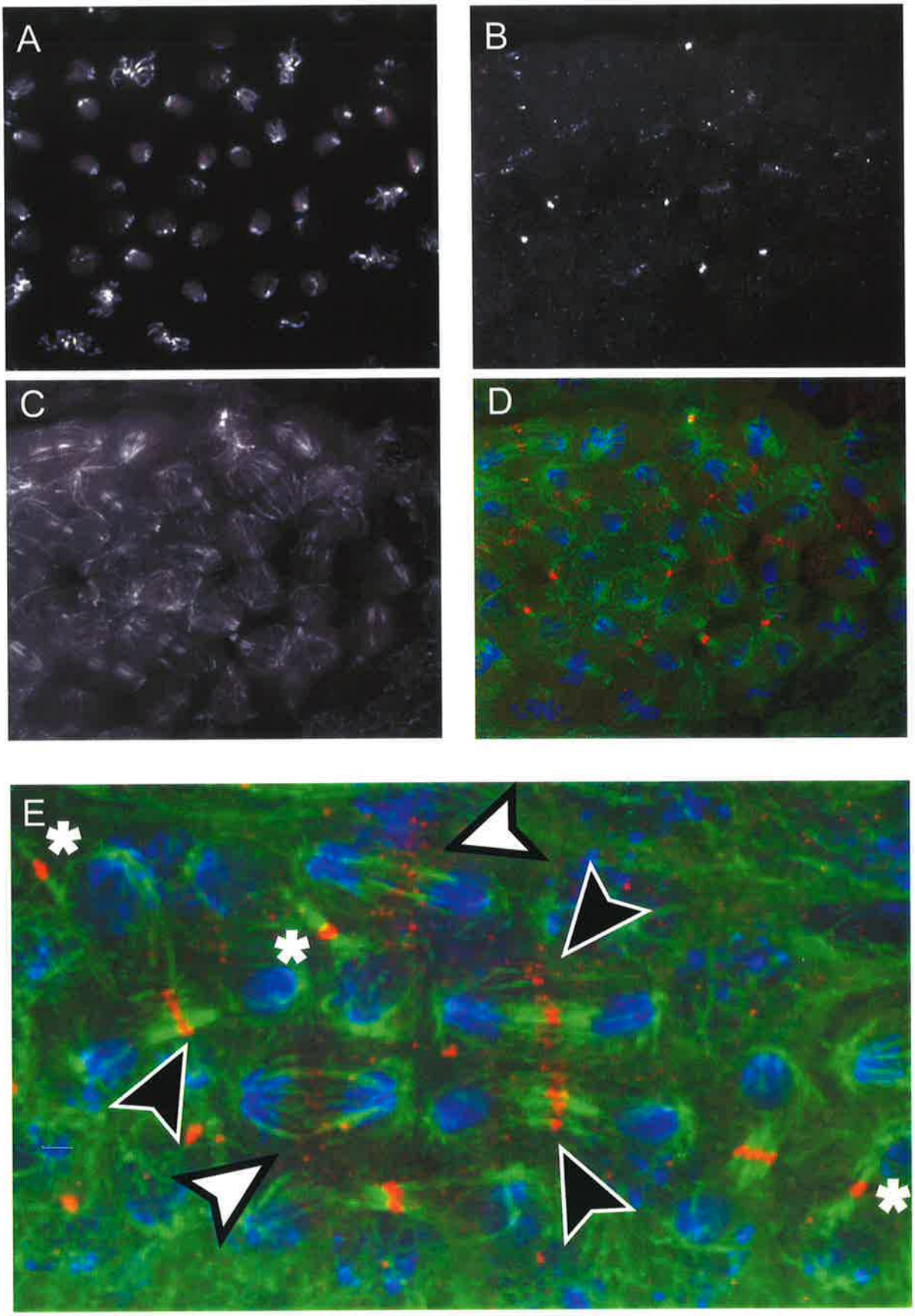
A
B
C
D
E

4.2.4 RacGAP50C colocalises with the mitotic spindle during mitosis.

To investigate the intracellular localisation of RacGAP50C, anti-RacGAP50C antibodies were used in immunocytochemical studies using both *Drosophila* S2 cultured cells (Figure 4.5) as well as dividing *Drosophila* embryonic cells (Figure 4.6). In both cases RacGAP50C was weakly detected along the entire length of the mitotic spindles during metaphase. Upon entering anaphase the signal increased in the central spindle region and become restricted to the midbody during telophase. Upon completion of cytokinesis, RacGAP50C was detected within the nucleus. This localisation is consistent with that reported for the *C. elegans* ortholog CYK-4 and mammalian ortholog MgcRacGAP (Jantsch-Plunger *et al.*, 2000; Hirose *et al.*, 2001).

Although this expression pattern is consistent with that reported for RacGAP50C orthologs, one significant difference was observed. Three-dimensional rotations of mitotic figures in late anaphase/early telophase revealed that the majority of the RacGAP50C localised to the midzone of cortically localised MT bundles, and thus formed a ring adjacent to the cleavage furrow (Figure 4.7). RacGAP50C was also detected in the midzone region of the classical MT bundled structure of the central spindle.

Colocalisation studies between RacGAP50C and PBL were carried out using a C-terminally GFP-tagged PBL transgene to monitor the PBL localisation. In fixed tissues GFP was observed to localise to the cell cortex and nucleus (Figure 4.8 A), in a manner similar to that reported for the endogenous PBL protein (Prokopenko *et al.*, 1999). Colocalisation studies using the anti-RacGAP50C antibodies and the PBL-GFP construct revealed that RacGAP50C appeared as a ring more cytoplasmic than the cortical PBL-GFP ring (Figure 4.8, A). GFP was also detected in the midzone of the central spindle, a localisation for PBL that has not been previously reported (Prokopenko *et al.*, 1999). Due to the current lack of PBL-specific antibodies, this localisation cannot be confirmed to be a true reflection of the endogenous protein, rather than an artefact caused by the ectopic expression. Colocalisastion studies between RacGAP50C and components of the

Figure 4.7 3D rotations of anaphase/telophase cells reveal that RacGAP50C localises to cortical as well as midzone microtubules.

(A) Three *Drosophila* embryonic epithelial cells at various stages of anaphase were stained for RacGAP50C (red), anti-alpha-tubulin (green), and DNA (Hoechst 33258) (Blue). (B-H) z-series rotation, in 15° increments projected around the Y-axis, of the anti-RacGAP50C-stained cells shown in (A). The majority of RacGAP50C is detected in a cortical ring, while some staining is detected on the central midzone MTs.

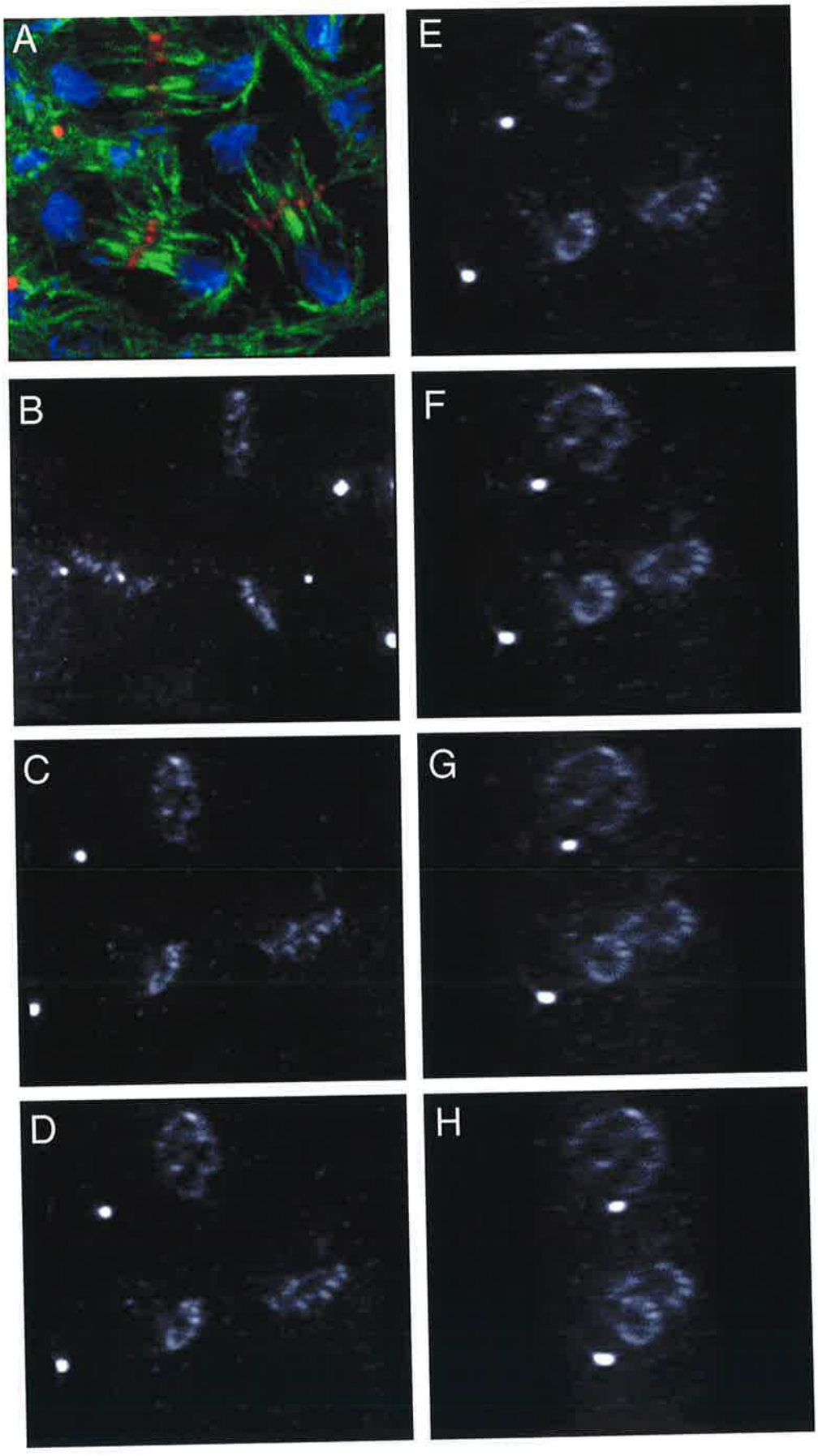
A
E
B
F
C
G
D
H

Figure 4.8 RacGAP50C localises as a ring internally to the cortical contractile-ring components.

(A) A *Drosophila* embryonic epithelial anaphase/telophase cell expressing PBL-GFP with the *prd-Gal4* driver. Anti-GFP immunostaining (first column, and green in merge), anti-RacGAP50C immunostaining (second column, and red in merge), and DNA stained with Hoechst 33258 (Blue in first row merge). Both PBL and RacGAP50C are detected as equatorial rings. The RacGAP50C ring appears internally and adjacent to the PBL ring. (B and C) anti-RacGAP50C (red), anti-anillin (green) and anti-alpha-tubulin (only in B) (blue). RacGAP50C is observed to stain internally and adjacent to the contractile-ring component anillin, in both a cross-section of a dividing *Drosophila* embryonic epithelial cell (B), as well as in a 90° three-dimension rotation (C).

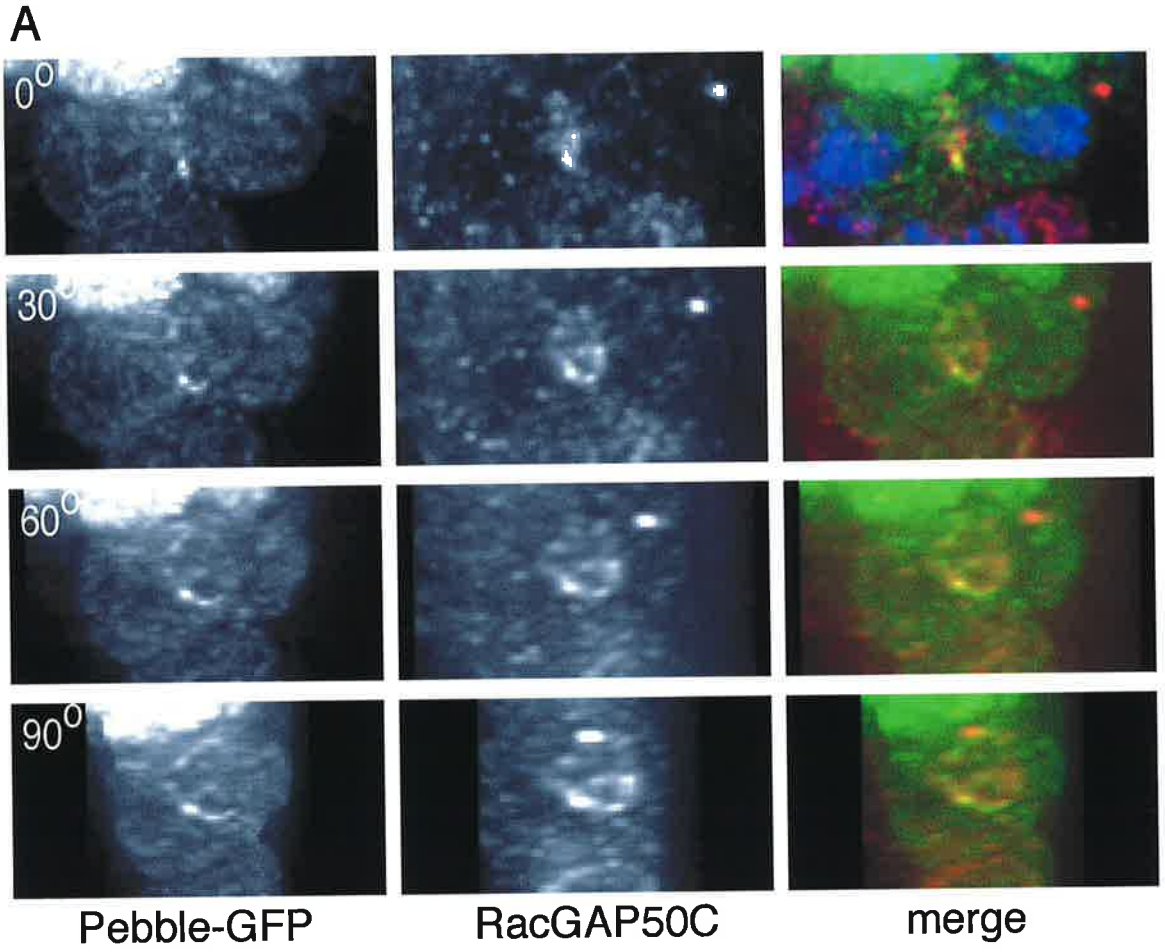
A
0°
30°
60°
90°
Pebble-GFP
RacGAP50C
merge

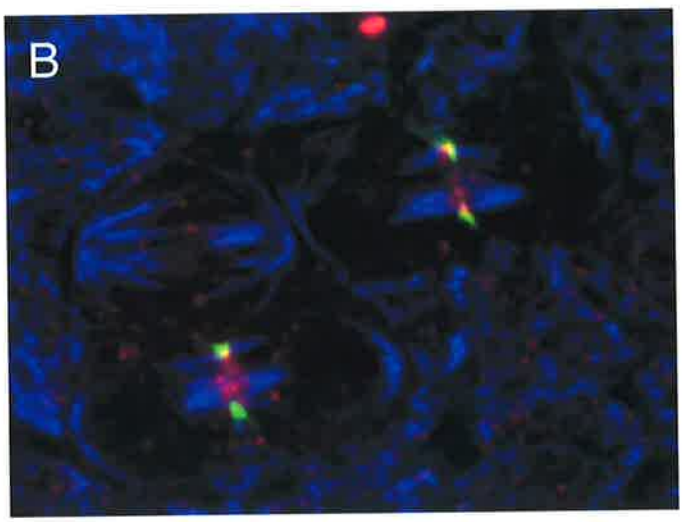
B

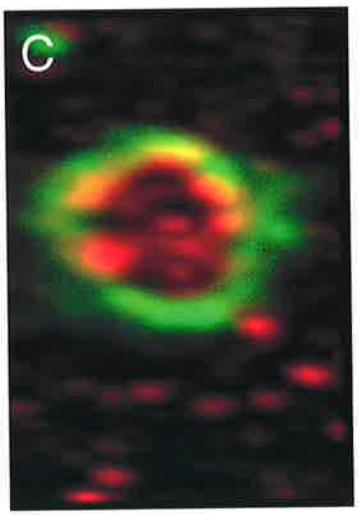
C

contractile apparatus were also performed. RacGAP50C was seen as a separate ring internal but adjacent to the actin-binding protein anillin (Figure 4.8, B).

4.2.5 Localisation of RacGAP50C at the midzone is maintained in the absence of Pebble.

RacGAP50C and PBL, two Rho family regulators essential for cytokinesis, have been shown here to colocalise and form an *in vivo* complex. While the subcellular localisations seem to indicate that PBL and RacGAP50C only interact during cleavage furrow constriction and/or midbody abscission, the mammalian orthologs, MgcRacGAP and Ect2, appear to co-localise on the MTs throughout mitosis. To address wether the localisation of PBL on the contractile-ring is necessary to correctly localise RacGAP50C to the central spindle midzone, the localisation of RacGAP50C was determined in cells which were disrupted for *pbl*.

Incubation of *Drosophila* S2 cells with *pbl* dsRNA results in a strong multinucleate phenotype (Figure 4.9 A), similar to that observed with *RacGAP50C* RNAi treatment. Immunostaining of these cells with anti-RacGAP50C and anti-α-tubulin, identified cells with abnormal mitotic structures. However, these cells still maintained RacGAP50C localisation to the bundled central spindle MTs (Figure 4.9 B). Similarly, RacGAP50C was also observed to localise correctly to the midzone of the central spindle/midbody in homozygous *pbl* null embryos, even in the presence of highly abnormal microtubule structures present in later divisions (Figure 4.9 C). These results clearly demonstrate that RacGAP50C can localise normally to the central spindle, even when *pbl* is disrupted. One interesting observation is that bundled central spindle MTs can still occur in the absence of PBL. This is inconsistent with observations made by Gatti and colleagues, who observed that the contractile-ring and central spindle were interdependent for correct formation (Somma *et al.*, 2002).

Figure 4.9 RacGAP50C does not require PBL for correct midzone localisation.

(A and B) *Drosophila* S2 cultured cells treated with *pbl* dsRNA. RacGAP50C is immunostained red (only in B), anti-alpha-tubulin is immunostained green and DNA is stained with Hoechst 33258 (Blue). (C) a homozygous pbl^2 mutant embryonic mitotic cell, immunostained with anti-RacGAP50C (red), anti-alpha-tubulin (green), and DNA stained with Hoechst 33258. (A) *Drosophila* S2 cells treated with 15ug of *pbl* dsRNA for 60 hours results in many cells becoming polyploid. (B) a highly abnormal mitotic *Drosophila* S2 cell treated with *pbl* dsRNA, forms a central spindle and has RacGAP50C localises correctly to the midzone region. (C) an epithelial cell in the 15 mitosis in a *pbl* null embryo, can still form a complex array of central spindles, with RacGAP50C localising correctly to the midzone region of all of these MTs.

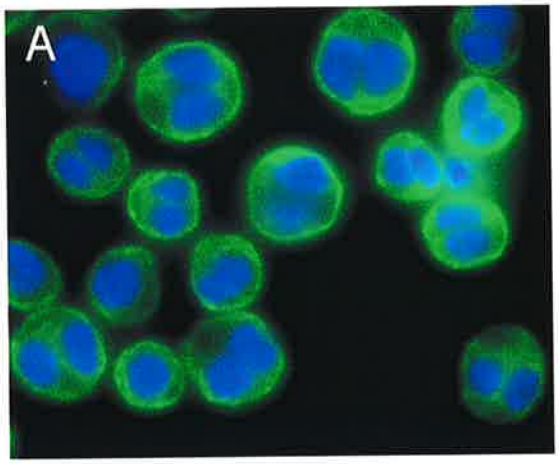
A

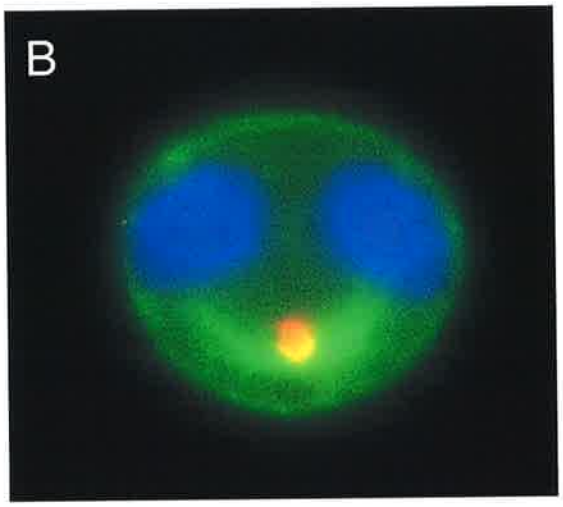
B

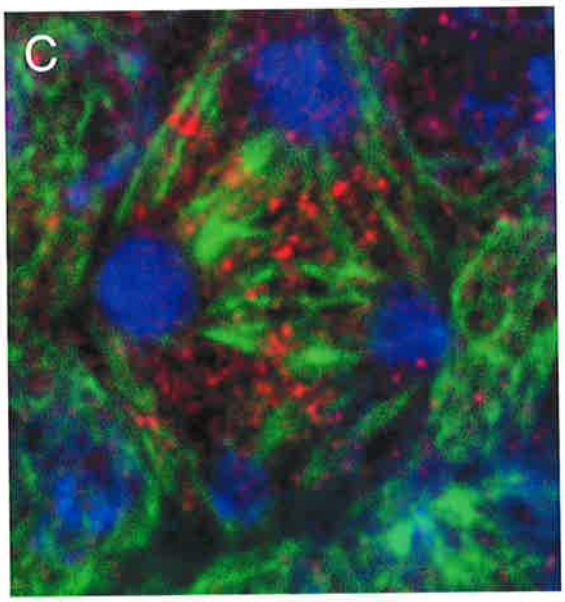
C

4.3 Discussion

To gain some insight into the significance of the PBL-RacGAP50C interaction, the expression patterns and sub-cellular localisation of RacGAP50C were investigated. RacGAP50C is dynamically expressed throughout embryonic development and adult life-cycle stages. Anti-RacGAP50C antibodies detected a prominent 70kDa band, the predicted size for the 625 amino acid RacGAP50C protein. This result is in agreement with the range of detected sizes in mammalian tissues. In HeLa cells MgcRacGAP has been detected as a 85kDa protein (Hirose *et al.*, 2001), while anti-MgcRacGAP antibodies detect a 70kDa protein in murine tissues and a 58kDa protein in human tissues (Arar *et al.*, 1999). The varying sizes reported could be attributed to species and/or tissue specific differences. The nature of the higher molecular weight protein bands detected during the later stages of *Drosophila* development is currently unclear. The identity of these proteins could be determined through immunoprecipitation and mass-spectrophotometry analysis. This could provide more insight into the specificity of the antibodies, and perhaps identify alternative splice forms of RacGAP50C.

Both the *RacGAP50C* transcript and protein were detected in *Drosophila* embryonic tissues that are undergoing rapid proliferation. High level of RacGAP50C was detected in the dense tissues that comprise the CNS and brain-lobes. A restricted pattern of RacGAP50C expression was also seen along the length of the CNS, and may represent a developmentally regulated set of RacGAP50C expressing cells, or those CNS cells undergoing mitosis. Intracellularly, RacGAP50C has an apparently identical localisation to that reported for its orthologs MgcRacGAP and CYK-4 (Jantsch-Plunger *et al.*, 2000; Hirose *et al.*, 2001). During pro-metaphase RacGAP50C displayed a ubiquitous cytoplasmic distribution then decorated the metaphase MTs, concentrating on the central spindle midzone region during anaphase and being restricted into the midbody at telophase. Three-dimension rotations of anaphase/telophase mitotic cells revealed that RacGAP50C not only stained the bundled MTs of the central spindle but was also detected as a MT-associated ring adjacent to the cell cortex. These cortical MTs have recently been recognised in *Drosophila* larval neuroblasts and described as a 'cage' that surrounds the elongating central spindle (Savoian and Rieder, 2002). The localisation to the midzone region of these cortically-associated MTs ideally position

RacGAP50C to interact with the cortically localised PBL throughout cleavage furrow ingression.

4.3.1 Future Directions

4.3.1.1 Interactions between the actin and microtubule cytoskeletons

The identification of an interaction between a MT associated Rho family GAP and a contractile-ring associated RhoGEF, both of which are essential for cytokinesis, generates many intriguing questions. For instance, which Rho family G proteins do they target to coordinate cytokinesis? Although during anaphase/telophase RacGAP50C was shown to localise to cortically-associated MTs, and PBL to the equatorial cortex, due to the dynamic nature of both cytoskeletons, and their close physical association, a closer examination of the subcellular localisations of both RacGAP50C and PBL is needed. For instance, it is not clear whether RacGAP50C remains associated with the MTs throughout mitosis. Perhaps RacGAP50C translocates from the MTs to the contractile-ring after localising to the central spindle, via its interaction with PBL. It is likely that depolymerisation of MTs prior to anaphase would result in RacGAP50C failing to localise to the central spindle. However, if the MTs were depolymerised in cells arrested in anaphase with an inducible stable Cyclin B3, examination of the RacGAP50C localisation would determine whether PBL can maintain a RacGAP50C ring adjacent to the cortex. Also, with the recent availability of *RacGAP50C* mutants, it should now be possible to determine whether the localisation of cortical PBL and the formation of the contractile ring require RacGAP50C.

4.3.1.2 Positioning of the contractile ring and initiation of furrowing

The positioning of RacGAP50C to the equatorial central spindle region during anaphase, provides a mechanism enabling the cell to time the formation of the contractile-ring and/or initiate cytokinesis with respect to other events during mitosis. The arrival of RacGAP50C to the intervening region of cortically localised MTs, may specify the site for PBL localisation and the formation of the contractile-ring. If this model were to hold true, displacement of the midzone localised RacGAP50C would cause a similar displacement of PBL localisation and consequently the contractile-ring.

As mentioned in the previous chapter and reported by Somma *et al.,* (2002), the depletion of RacGAP50C in *Drosophila* S2 cells disrupts cytokinesis, similar to what was observed for its othologs *cyk-4* and *mgcRacGAP*. *C. elegans cyk-4* mutant (*t1689ts*) embryos were observed to have extensive cortical furrowing which ultimately regressed, suggesting a role in the late stages of cytokinesis (Jantsch-Plunger *et al.,* 2000). However, this temperature sensitive allele may possess some partial activity. Although, incomplete cytokinesis was also observed in *C. elegans* embryos treated with *cyk-4* dsRNA (Jantsch-Plunger *et al.,* 2000), there was no mention of the stability of the CYK-4 protein or variance in the phenotypes. In both cases partial CYK-4 activity may be enough to initiate but not complete cytokinesis. However, fundamentally different cytokinetic mechanisms may be involved in these two model systems. Unlike *Drosophila* and mammalian cell culture cells, the initial cortical furrowing in the nematode embryos is not reliant on the central spindle (Powers *et al.,* 1998; Raich *et al.,* 1998), but appears to be more reliant on the astral MTs (Discussed by Murata-Hori and Wang, 2002). Depletion of the kinesin-like motor protein ZEN-4 in *C. elegans* disrupts cytokinesis but not the initial cortical furrowing (Raich *et al.,* 1998), while disruption of the *D. melanogaster* ortholog, PAV, disrupts the formation of the contractile-ring, and consequently no furrowing is observed (Adams *et al.,* 1998). The coordination of MT bundling during cortical furrowing may be a significant difference between the *Drosophila* and *C. elegans* systems. Compared to *Drosophila* epidermal embryonic cells, the central spindle in *C. elegans* embryos is relatively small and is not in close proximity to the cell cortex prior to cortical constriction. Thus in *Drosophila*, the RacGAP50C-PBL interaction is likely to be necessary to initiate cortical furrowing, while in *C. elegans* CYK-4 only comes into contact with the cell cortex once extensive ingression has occurred, and only then is furrowing coordinated with MT bundling.

Chapter Five: RacGAP50C is found in a complex with the mitotic kinesin-like motor protein, Pavarotti.

5.1 Introduction

The previous chapter described the intracellular localisation of RacGAP50C in dividing *Drosophila* embryonic cells and *Drosophila* S2 cultured cells. RacGAP50C decorated the metaphase mitotic microtubules, before intensifying on the midzone region of the central spindle during anaphase. During late telophase RacGAP50C was seen restricted to the midbody. Three-dimensional imaging of anaphase/telophase mitotic figures revealed that RacGAP50C localised as a ring to cortically associated bundled MTs.

Another protein that travels along the MTs in a remarkably similar fashion to RacGAP50C is the *Drosophila* MKLP1, Pavarotti (PAV). PAV is a plus ended directed microtubule motor that is also essential for cytokinesis (Adams *et al.*, 1998). *pav* mutants exhibit a depletion in the number of bundled central spindle MTs during the 16th cell cycle, and a failure to localise essential contractile-ring components. The *C. elegans* ortholog of PAV, ZEN-4/CeMKLP-1, is also essential for cytokinesis, and requires the chromosome passenger protein AIR-2 for correct localisation to the central spindle (Severson *et al.*, 2000). In *C. elegans* embryos, the Rho family GTPase activating protein, CYK-4, colocalises with ZEN-4 and has an interdependence for localisation to the central spindle (Jantsch-Plunger *et al.*, 2000). Furthermore, a recent publication reported that both CYK-4 and ZEN-4 homodimerise, and together form a heterotetrameric complex *in vivo*. This complex, termed 'centralspindlin', is capable of bundling MTs *in vitro* (Mishima *et al.*, 2002).

This chapter describes the identification of the complex between *Drosophila* RacGAP50C and the kinesin-like motor protein PAV-KLP. Yeast two-hybrid assays and immunoprecipitations revealed that these proteins directly bind to each other. Co-

immunofluoresence studies revealed that RacGAP50C colocalises with PAV during the various stages of mitosis. This RacGAP50C-PAV complex is observed to localise to the midzone of cortical MTs during anaphase/telophase, where an interaction between RacGAP50C and PBL appears to occur.

5.2 Results

5.2.1 RacGAP50C and the kinesin-like motor protein Pavarotti colocalise.

To identify if the *Drosophila* RacGAP50C and kinesin-like motor protein PAV form an *in vivo* complex, co-immmunostainings were performed. Immunofluorescent stainings of dividing embryonic *Drosophila* cells (Figure 5.1, A), as well as dividing *Drosophila* S2 culture cells (Figure 5.1, B), revealed that RacGAP50C and PAV colocalised throughout the cell cycle. During metaphase both proteins decorated the mitotic spindles, concentrated to the central spindle during anaphase, before becoming restricted to the midbody during telophase. During anaphase of *Drosophila* S2 cell division, both proteins were seen to localise adjacent to the cell cortex (arrows, Figure 5.1, B). Three dimensional imaging of *Drosophila* embryonic early telophase mitotic figures revealed that PAV colocalised with RacGAP50C to a punctate ring associated with cortically localised MTs as well as to the bundled MTs of the central spindle.

Throughout *Drosophila* development, a host of structures undergo modified forms of cytokinesis. Studying these various modified forms of cell division allows identification of common unifying mechanisms necessary for cytokinesis. During oogenesis a stem cell at the tip of the germarium divides to produce a cystoblast, which then divides exactly four times, producing 16 cyst cells. Only one of these cells is selected to go on and develop into the oocyte, while the other 15 become nurse cells. However, none of the divisions are ever completed, and the daughter cystocytes remain interconnected through specialised cleavage furrows known as ring-canals, thus producing 16 cystocytes interconnected by 15 ring-canals. PAV has been reported to localise to the oocyte nucleus and the actin-rich ring canals, built from remnants of the

Figure 5.1 RacGAP50C colocalises with the Pavarotti mitotic kinesin-like motor protein.

(A) RacGAP50 C and PAV colocalise in dividing *D. melanogaster* embryonic epithelial cells (A) and in *D. melanogaster* S2 cell culture cells (B). (A) Immunofluoresence detection of RacGAP50C (left column, and blue in right column merge), PAV (middle column, and red in right column merge) and alpha-tubulin (green in right column merge). A three dimensional rotation in 30° increments of the stained dividing cell is presented in each column. The 3D rotation reveals that RacGAP50C and PAV colocalise to a cortical ring at the site of the spindle midzone, as well as to the midzone of bundled central spindle microtubules. (B) RacGAP50C and PAV colocalise throughout the cell cycle in *D. melanogaster* S2 cells. In the merge panel RacGAP50C is red, PAV is green and DNA, stained with Hoechst 33258, is blue. Both proteins are found predominantly on the mitotic spindle during metaphase, the central spindle during anaphase and midbody during telophase. During anaphase PAV and RacGAP50C are also observed associated with the cortex (arrows).

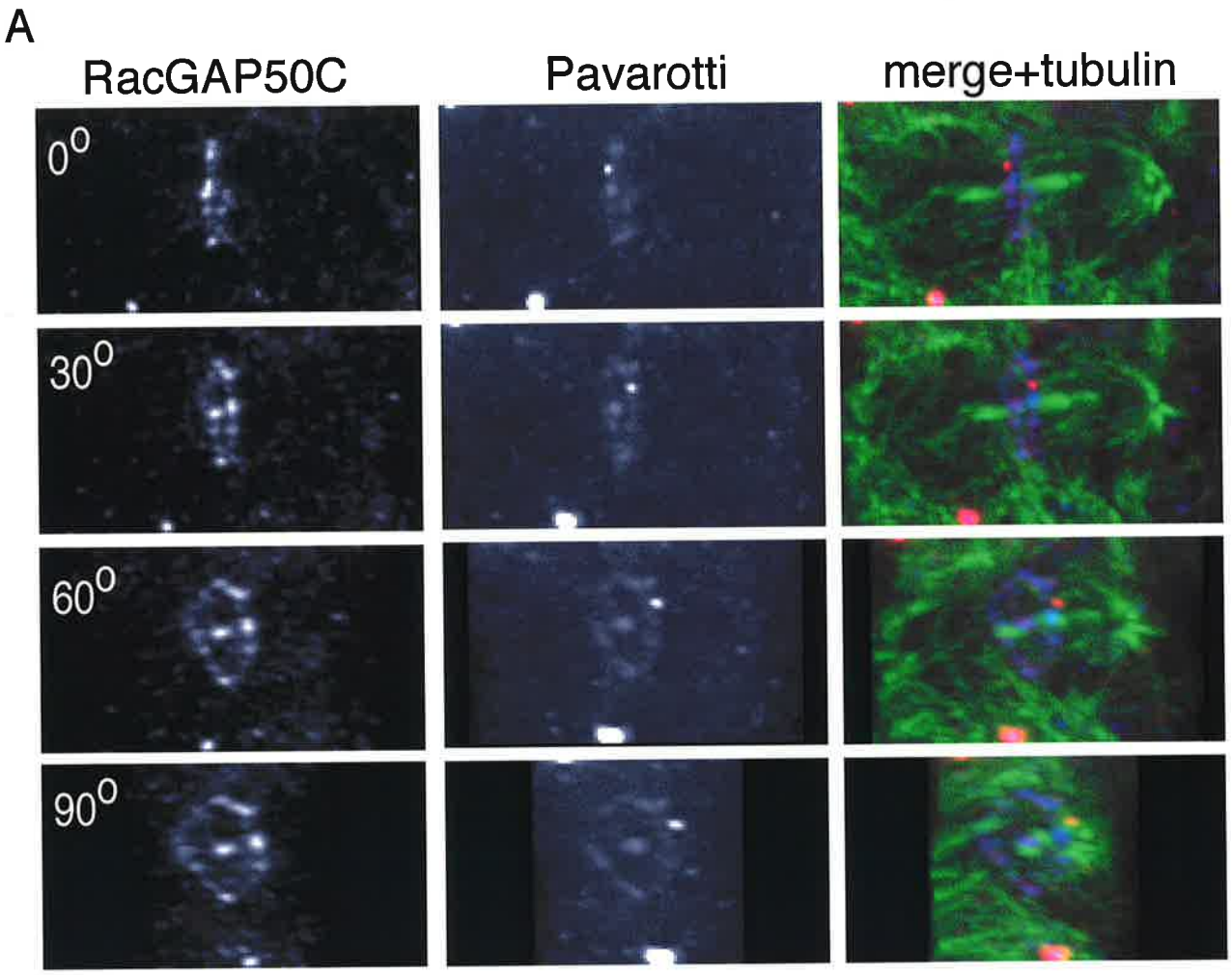
A
RacGAP50C
Pavarotti
merge+tubulin
0°
30°
60°
90°

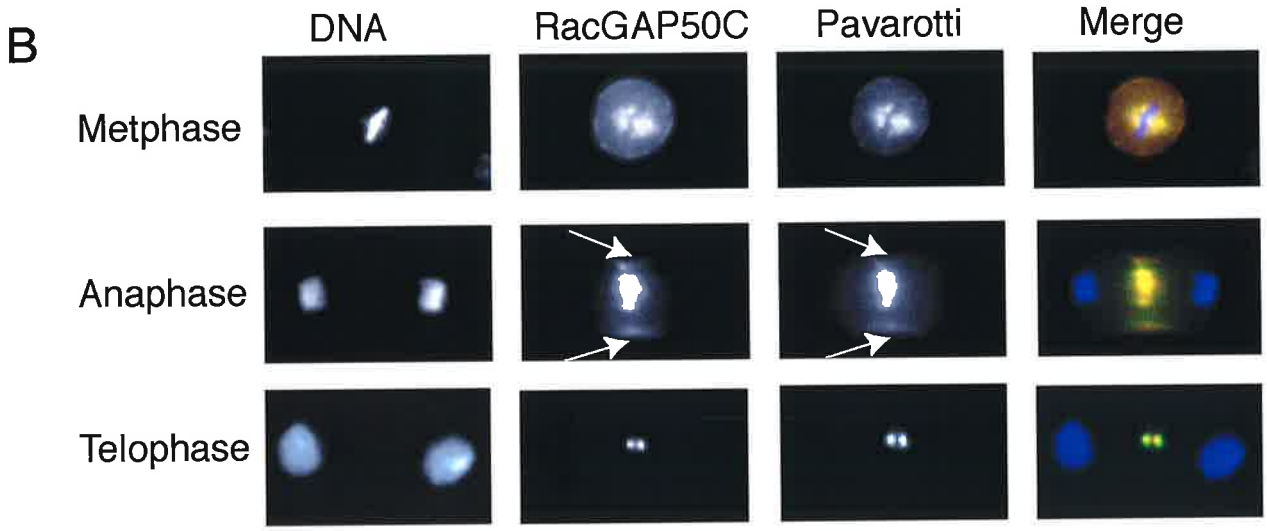
B
DNA
RacGAP50C
Pavarotti
Merge
Metphase
Anaphase
Telophase

Figure 5.2 RacGAP50C and Pavarotti colocalise to ovary ring-canals

Immunostaining of a wild-type stage 5/6 ovary detecting RacGAP50C (red), PAV (green) and DNA, stained with Hoechst 33258 (blue). A total of 80 z-series sections, spaced at 0.2μm, were taken throughout the ovary and merged. Thirteen of the fifteen ring canals are clearly visible, and reveal that both RacGAP50C and PAV colocalise to these modified contractile-ring structures.

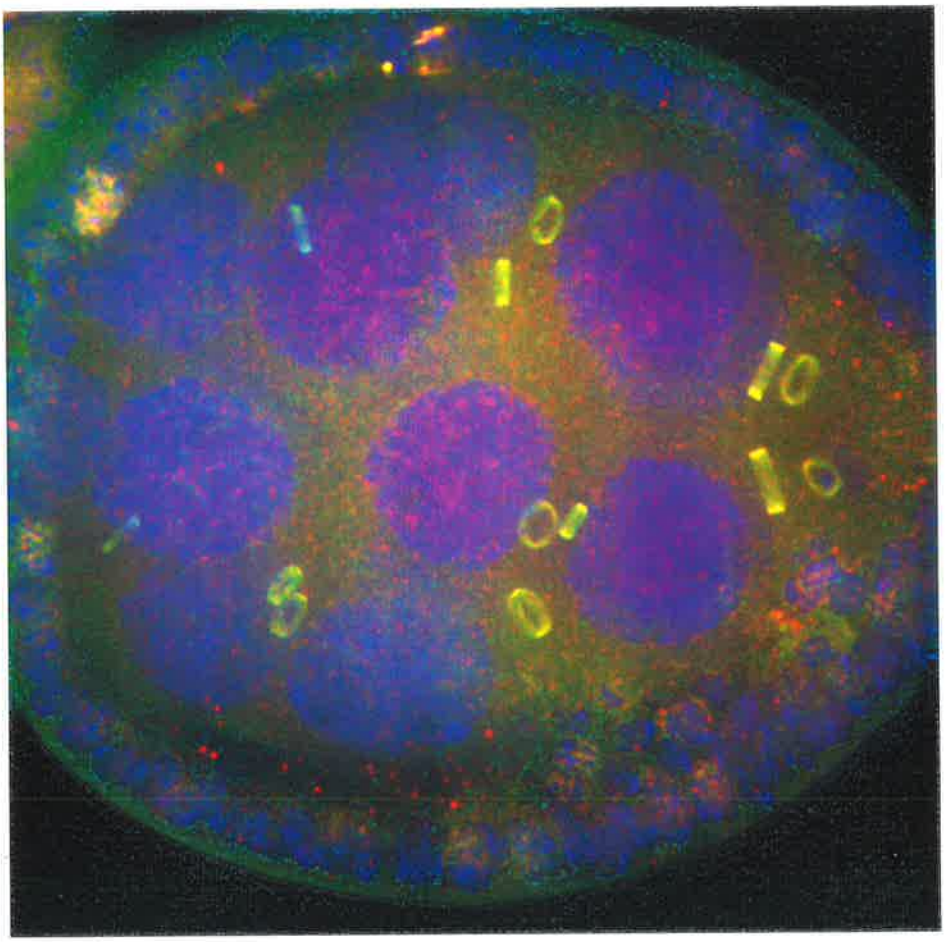

contractile-ring (Minestrini *et al.*, 2002). Co-immunostaining of wild-type ovaries with anti-RacGAP50C and anti-PAV showed that these two proteins colocalise on the stabilised ring-canals (Figure 5.2).

5.2.2 RacGAP50C and Pavarotti form a complex *in vivo.*

Recent studies have shown that CYK-4 and ZEN-4 physically bind each other, and that the coil-coiled domains of both proteins are essential for this interaction (Mishima *et al.*, 2002). In addition, a tetrameric complex comprised of a CYK-4 homodimer and ZEN-4 homodimer, has been shown to exist in *in vivo* extracts.

Coimmunoprecipitation experiments were performed to test whether the *Drosophila* RacGAP50C forms an *in vivo* complex with Pav-KLP. Protein extracts were generated from 0-5 hour AED wild-type embryos. Western blot analysis with anti-RacGAP50C antibodies detected a ~70kDa RacGAP50C band in the embryonic extracts (Figure 5.3, lane 5 top panel). The anti-RacGAP50C antibodies also detected a ~70kDa RacGAP50C band when anti-RacGAP50C or anti-PAV antibodies were used in the immunoprecipitation. The Western blot was stripped and probed with anti-PAV antibodies (Figure 5.3, bottom panel). The anti-PAV antibodies detected the expected ~110kDa PAV band in the total embryo extract. The ~110kDa PAV band was also detected in both the PAV and RacGAP50C immunoprecipitation, but not the negative control immunoprecipitations.

5.2.3 Pavarotti interacts with the N-terminus of RacGAP50C.

The coiled-coil domains of both CYK-4 and ZEN-4 have been shown to be necessary for both homodimerisation and formation of the tetrameric centralspindlin complex (Mishima *et al.*, 2002). To characterise the region of RacGAP50C that is necessary for the interaction with PAV, a yeast two-hybrid assay was conducted. The RacGAP50C yeast two-hybrid constructs used to identify the PBL interacting region (see Chapter 3), were tested for an interaction with a full-length PAV clone. The yeast two-hybrid interactions are summarised in Figure 5.4 (A). Of the two RacGAP50C clones identified from the original yeast two-hybrid screen, only the full-length clone (#28)

Figure 5.3 RacGAP50C and Pavarotti form a complex *in vivo*.

Anti-RacGAP50C, anti-PAV or non-specific IgG immunoprecipitates of 0-5 hour *D. melanogaster* embryonic extracts were separated by SDS/PAGE and transferred to a nitrocellulose filter. The IgG used for each immunoprecipitation is indicated at the top. The filter was probed with anti-RacGAP50C antibodies (top panel), and then stripped and probed with anti-PAV antibodies (bottom panel). Anti-PAV antibodies immunoprecipitated a 70kDa RacGAP50C protein (upper panel), and anti-RacGAP50C antibodies immunoprecipitated a 110kDa PAV protein (lower panel).

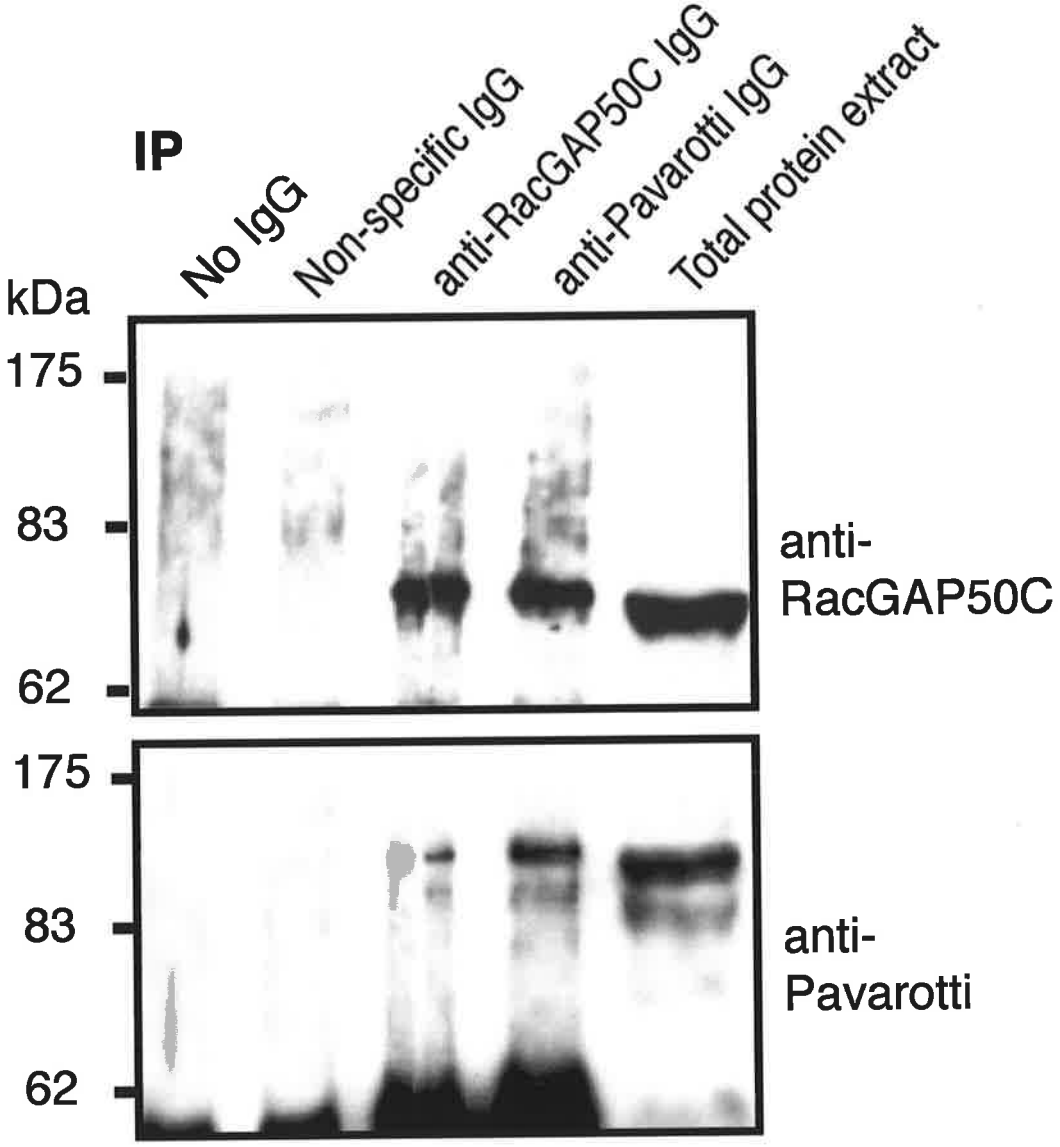
IP
No IgG
Non-specific IgG
anti-RacGAP50C IgG
anti-Pavarotti IgG
Total protein extract
kDa
175
83
62
anti-
RacGAP50C
175
83
62
anti-
Pavarotti

Figure 5.4 The amino terminus of RacGAP50C interacts with Pavarotti.

Yeast two-hybrid assay of RacGAP50C interactions with PAV. (A) Summary diagram showing that clone #21, which lacks the first 65 amino acids, is incapable of interacting with full-length PAV, while a construct containing only the first 47 amino acids of RacGAP50C is capable of strongly interacting with PAV. (B) YNB-trp-leu-his plates inoculated with yeast cotransformed with full-length PAV and various RacGAP50C constructs (1, #28 RacGAP50C; 2, $RacGAP50C_{303-625}$; 3, $RacGAP50C_{1-309}$; 4, $RacGAP50C_{1-173}$; 5, $RacGAP50C_{166-240}$; 6, $RacGAP50C_{232-309}$) were plated on selective growth media to test for a physical interaction. This assay showed that the N-terminus of RacGAP50C is necessary for the interaction.

A

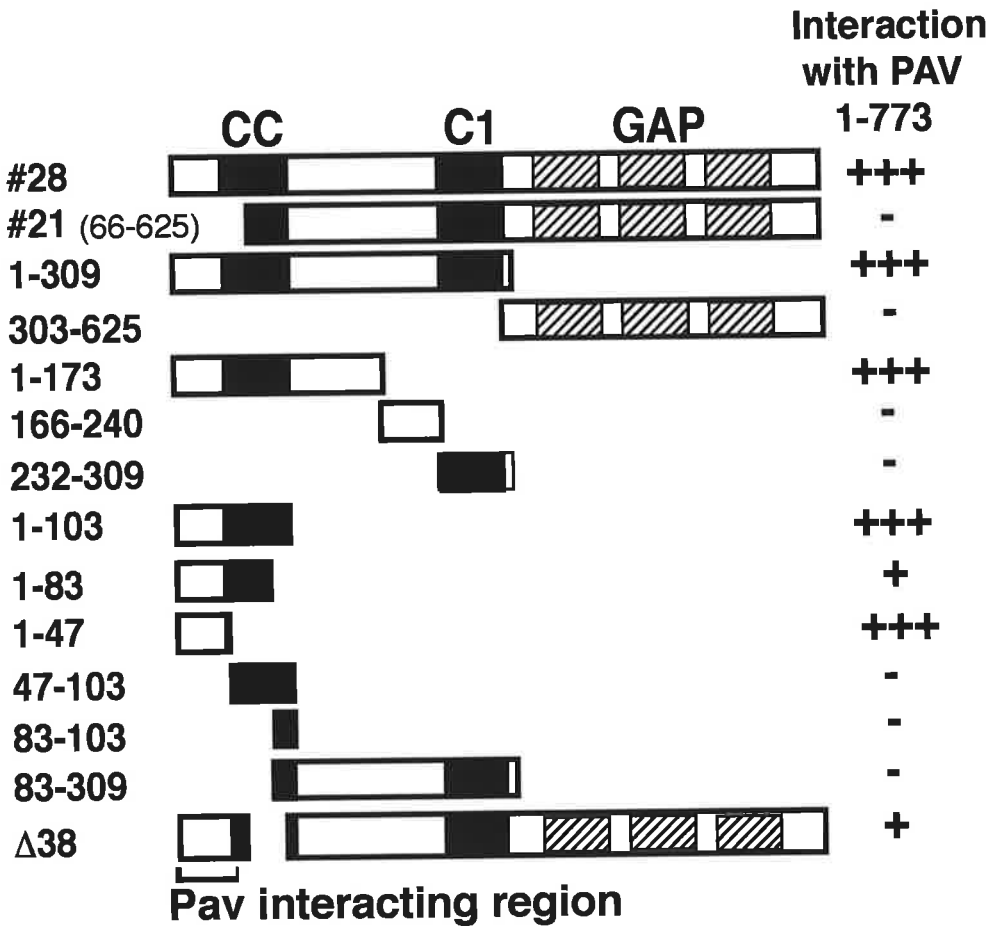
Interaction with PAV 1-773
CC
C1
GAP
#28
+++
#21 (66-625)
-
1-309
+++
303-625
-
1-173
+++
166-240
-
232-309
-
1-103
+++
1-83
+
1-47
+++
47-103
-
83-103
-
83-309
-
Δ38
+
Pav interacting region

B

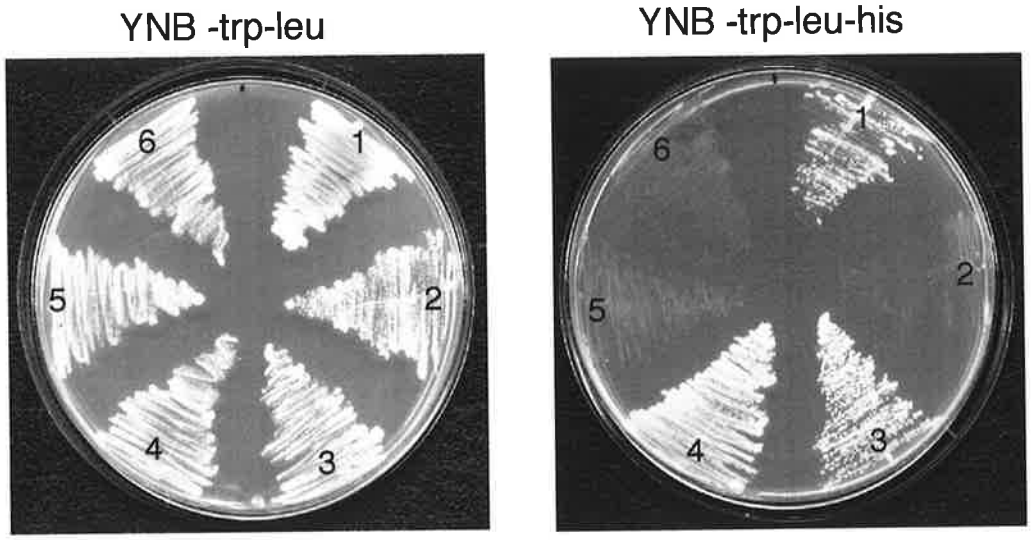
YNB -trp-leu
YNB -trp-leu-his
1
2
3
4
5
6

was capable of interacting with full-length PAV. Other RacGAP50C clones that interacted strongly with the PAV clone included RacGAP50C 1-309, 1-173, 1-103 and 1-47. Thus, it appeared that the extreme N-terminus of RacGAP50C, which was missing in clone #21, is necessary and sufficient for interacting with PAV. Figure 5.4, B shows the relative strengths of several of the interactions assayed using the yeast two-hybrid system, and grown on selective growth media.

The smallest RacGAP50C construct that was sufficient for full interactive capability contained amino acids 1-47. This region is adjacent to, yet separate from, the identified PBL interacting region within the coiled coil domain (amino acids 66-103). The corresponding N-terminus region of CYK-4 has also recently been reported necessary for interacting with the kinesin-like protein ZEN-4 (Mishima *et al.,* 2002).

5.2.4 Pavarotti is necessary for the correct localisation of RacGAP50C to the central spindle.

The *C. elegans* plus end directed microtubule motor protein, ZEN-4, has been shown to colocalise to the central spindle in an interdependent fashion with CYK-4 (Jantsch-Plunger *et al.,* 2000). The correct localisation of ZEN-4 to the central spindle is required for successful cytokinesis. Similarly, disruption of *pav* results in a failure of cytokinesis during mitotic cycle 16. In these *pav* mutant cells, components of the contractile-ring, including Peanut, actin and anillin fail to accumulate, and fewer bundles of MTs are seen in the central spindle (Adams *et al.,* 1998).

To address whether RacGAP50C has a conserved requirement for PAV to correctly localise it to the central spindle, immunofluoresence staining was performed on homozygous *pav* mutant embryos. Anti-RacGAP50C antibodies failed to detect RacGAP50C in the midzone region of MTs of anaphase/telophase cycle 16 dividing cells in homozygous *pav* mutants (Figure 5.5).

Figure 5.5 Pavarotti is required for the correct localisation of RacGAP50C

D. melanogaster embryonic pav^{B200} cells undergoing mitotic cycle 16 were stained with anti-RacGAP50C antibodies (red), anti-alpha-tubulin antibodies (green), and Hoechst 33258 (DNA, blue). The homozygous pav^{B200} mutant cells show a depletion of MTs that comprise the central spindle, and no cortical or midzone localised RacGAP50C.

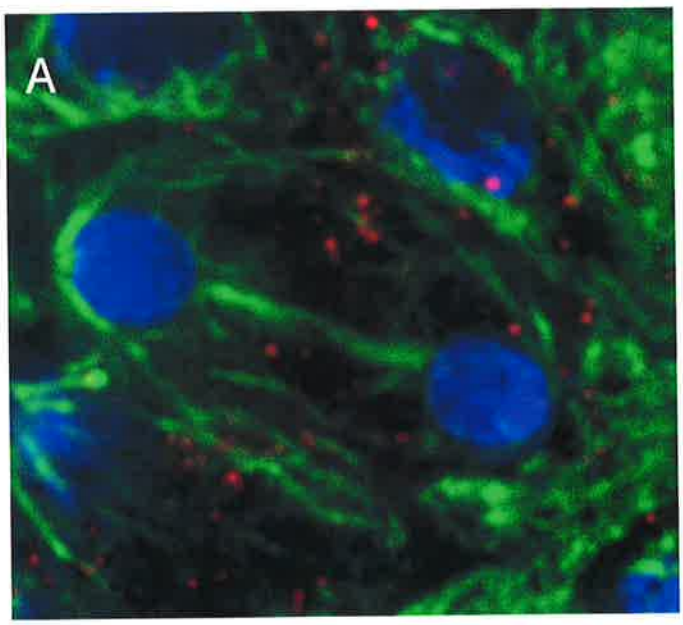
A

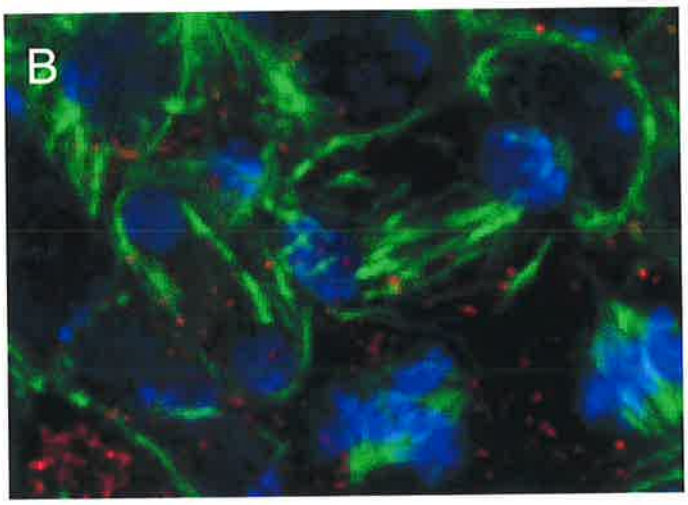
B

5.3 Discussion

In animal cells, the central spindle produces an unknown stimulus that is required to initiate cytokinesis. The integrity of bundled central spindle MTs during the late stages of mitosis is maintained by a mitotic kinesin-like motor protein. Orthologous proteins exist in *C. elegans*, *Drosophila* and human (ZEN-4/CeMKLP-1, PAV and CHO1 respectively). Disruption of any of these orthologs has a similar effect, resulting in a depletion of bundled MTs in the central spindle and a failure in cytokinesis (Adams *et al.,* 1998; Raich *et al.,* 1998; Matuliene and Kuriyama, 2002).

Co-immunostainings revealed that RacGAP50C and PAV colocalise throughout the mitotic cell cycle in both dividing *Drosophila* embryonic cells and S2 cultured cells. Both proteins were invariably found to colocalise, including to structures such as the ring canals in the *Drosophila* ovary. It has previously been reported that PAV localises to the interzonal region of the mitotic spindle during anaphase, remaining associated with the spindle during telophase (Adams *et al.,* 1998). Three-dimensional rotation of co-immunostained *Drosophila* embryonic anaphase/telophase mitotic figures revealed that like RacGAP50C, PAV was also localised to the interzonal region of cortically localised MTs. Thus, anti-PAV antibodies detected a ring structure that colocalised with RacGAP50C at the equatorial region of anaphase cells, and also on the bundled MTs of the central spindle. It is likely that other proteins previously reported to localise to the spindle midzone, will also be restricted to the cortically associated MTs in *Drosophila* epithelial cells. The *C. elegans* CYK-4 and ZEN-4 have an interdependence for correct localisation to the central spindle midzone. Immunostainings failed to detect RacGAP50C at the central spindle in the absence of *pav*, consistent with the behaviour of the *C. elegans* orthologs.

Confirming the observed immunostaining colocalisations, immunoprecipitation experiments using *Drosophila* embryonic protein extracts identified the existence of an *in vivo* RacGAP50C-PAV protein complex. Recently, an orthologous protein complex has been identified in both humans and *C. elegans*, termed 'centralspindlin' (Mishima *et al.,* 2002). A surprising observation reported by Mishima and collegues (2002) was

that the centralspindlin complex appears to only consist of the RacGAP and the kinesin-like motor protein. ZEN-4 and its orthologous kinesin-like motor proteins have been identified to bind a number of other proteins which are important for cytokinesis, therefore additional protein bands should have been detected in the immunoprecipitation experiments. For instance, AIR-2, the *C. elegans* ortholog of Aurora B, and PLK, the mammalian ortholog of Polo, are capable of binding ZEN-4 (Lee *et al.,* 1995; Severson *et al.,* 2000). Therefore, although studies have suggested that Pav and RacGAP50C only associate with each other, interactions with other proteins, including the RacGAP50C-PBL interaction, do occur. These interactions may only occur transiently during the cell cycle and so may not be consistently detected. Immunoprecipitation studies from mitotically synchronised cells may be more informative in identifying transient protein interactions at various stages of mitosis.

The yeast two-hybrid assay was used to determine that the N-terminus of RacGAP50C was sufficient and necessary for interacting with PAV. RacGAP50C clone #21, which lacks the first 65 amino acids, failed to interact with full-length PAV, while the RacGAP50C construct containing just the amino acids 1-47 was capable of strong interaction. This region of interaction is consistent with the region of CYK-4 (amino acids 1-120, which includes the N-terminus plus coiled coil domain) that has been shown to be necessary to interact with ZEN-4 (Mishima *et al.,* 2002).

This chapter has described the identification of a conserved animal complex consisting of the *Drosophila* mitotic kinesin-like motor protein PAV and the Rho family regulator RacGAP50C. Like the nematode ortholog CYK-4, RacGAP50C forms an *in vivo* complex with the kinesin-like motor protein, PAV, directly binding PAV through an N-terminal sequence. RacGAP50C also requires PAV for correct localisation to the central spindle region.

Chapter Six: *RacGAP50C* genetically interacts with *pbl* and *Rac1*.

6.1 Introduction

RacGAP50C has strong homology with other Rho family GTPase activating proteins (RhoGAPs). RhoGAPs inactivate specific Rho family members, by binding to and catalysing the intrinsic GTPase activity of the Rho family GTPases. Most eukaryotes possess several Rho family GTPases, which play roles in a range of processes. Considerable cross-talk exists between Rho family members, which can complicate interpretations of signalling pathways in which they are involved. For instance, mammalian cell culture studies have observed a hierarchy of activation among Rho family members Cdc42, Rac and Rho. The activation of Cdc42 leads to a reorganisation of the F-actin into filopodia. This is followed by the activation of Rac1 as judged by the formation of lamellopodia, followed further by the formation of stress fibres, a characteristic of RhoA activation (Chant and Stowers, 1995). However, under certain developmental contexts RhoA and Rac1 have been shown to act antagonistically. The activation of Rac1 and Cdc42 can lead to down-regulation of the levels of active RhoA in NIH3T3 fibroblasts (Sander *et al.,* 1999; Zondag *et al.,* 2000), while in other situations, the activation of RhoA can result in decreased levels of activated Rac1 (Yamaguchi *et al.,* 2001).

RacGAP50C has highest homology to other GAPs that specifically target Rac1. Genetic interactions involving *D. melanogaster* have shown that RacGAP50C interacts with *Rac1* and *Cdc42* during wing development (Sotillos and Campuzano, 2000). In addition, *in vitro* GAP assays have demonstrated that both CYK-4 and MgcRacGAP have substantially higher GAP activity towards Rac1 and Cdc42 compared with Rho1 (Toure *et al.,* 1998; Jantsch-Plunger *et al.,* 2000; Kawashima *et al.,* 2000). However, as *Rho1* is the only Rho family member identified to be essential for cytokinesis in these various model systems, it was proposed that this RacGAP targets Rho1 for inactivation

in-vivo, with temporal/spatial localisation dictating this specificity (Jantsch-Plunger *et al.*, 2000). Currently it remains unclear which Rho family GTPase(s) RacGAP50C and its orthologs target *in-vivo* to regulate cytokinesis.

This chapter describes analyses of genetic interactions involving RacGAP50C as a means of exploring the signalling pathway by which RacGAP50C regulates cytokinesis. Various *RacGAP50C* constructs were generated to enable the genetic interaction tests, including an inducible RNAi construct (*RacGAP50C*^{RNAi}).

6.2 Results

6.2.1 *en::Gal4* driven expression of an inducible *RacGAP50C* hair-pin construct disrupts cytokinesis and actin nucleation in the wing.

RNAi has recently become a widely applied technique, used to effectively 'silence' a target gene via a post-transcriptional mechanism. The observation made in Chapter Three, that cytokinesis could be disrupted in *Drosophila* S2 cells treated with *RacGAP50C* dsRNA, suggests that a significant amount of RacGAP50C is degraded and re-synthesised each mitotic cycle. Therefore, because of the dynamic turnover, it should be possible to silence the endogenous *RacGAP50C in vivo* with an inducible *RacGAP50C*^{RNAi} construct. The *RacGAP50C*^{RNAi} construct was created by a head-to-head cloning of two overlapping PCR products that, when transcribed, produce a fold-back region of double stranded RNA corresponding to nucleotides 248-1125 of the *RacGAP50C* open reading frame (Figure 6.1, A). Over-expression of this construct using the *engrailed* promoter (*en::Gal4*) (drives expression in the posterior compartment) or *scalloped* promoter (*sd::Gal4*) (drives expression in the entire wing), resulted in a disruption to the wing morphology.

Figure 6.1 A schematic of *UAS::RacGAP50C* constructs generated.

A *RacGAP50C* RNAi construct (*UAS::RacGAP50C*^{RNAi}) was generated by a head to head cloning of two overlapping PCR products, corresponding to the 5' region of the *RacGAP50C* coding sequence (A). When transcribed, a fold back region corresponding to nucleotides 248-1125 is predicted to occur. Thick arrows indicate homologous sequences. (B-D) schematic representation of N-terminal Myc-tagged *UAS::RacGAP50C* constructs. (B) wild-type *RacGAP50C*, (C) *RacGAP50C*$^{\Delta EIE}$, (D) *RacGAP50C*$^{\Delta YRL}$. Domains of RacGAP50C are indicated on the wild-type construct (CC- coiled coil domain (green), C1-phorbol ester and diacylglycerol binding domain (blue), GAP- GTPase activating domain (hatched)). (C) Amino acid sequence alignments of part of the first GAP subdomain of RacGAP50C with orthologs and the *D. melanogaster* Rotund, human N-chimaerin and Cdc42-GAP, GAP proteins. Critical conserved catalytic residues, individually deleted in the RacGAP50C constructs in this study are indicated by boxes.

A *UAS::RacGAP50C^{RNAi}*

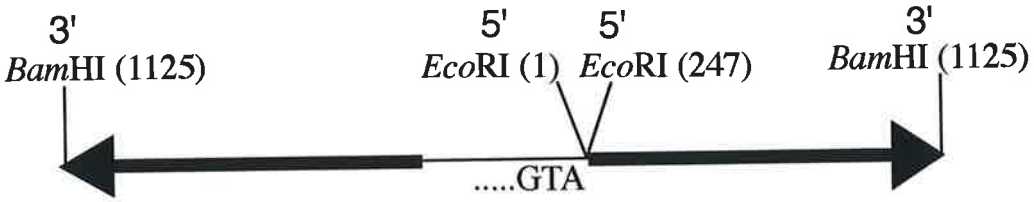

B *UAS::myc-RacGAP50C*

C *UAS::myc-RacGAP50C$^{\Delta EIE}$*

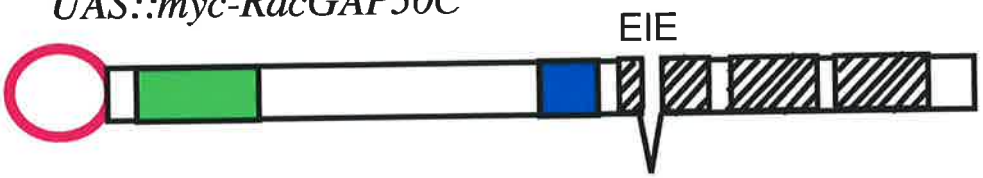

D *UAS::myc-RacGAP50C$^{\Delta YRL}$*

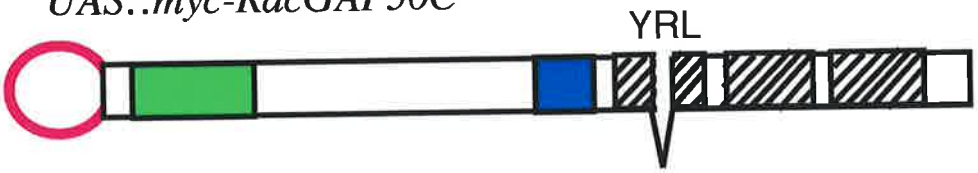

E

		EIE	YRL
RacGAP50C	392	PMIPALIVHCVNEIEARGLTEVGLYRLSSSEREYKALKEQF	
mMgcRacGAP1	361	PMIPAIVVSCVNEIEQRGLTEAGLYRISGCDRTVKELKEKF	
hMgcRacGAP1	360	PMIPSIVVHCVNEIEQRGLTETGLYRISGCDRTVKELKEKF	
CYK-4	434	PMIPAAVIHCVVALEARGLTQEGLYRVPGQVRTVNVLLDEL	
Rotund	158	PMVPALIVHCVTEIEARGLQQEGLYRVSSTREKCKRLRRKL	
hN-Chimaerin	154	TKRPMVVDMCIREIESRGLNSEGLYRVSGFSDLIEDVKMAF	
hCdc42-GAP	152	EPIPIVLRETVAYLQAHALTTEGIFRRSANTQVVREVQQKY	

The adult wing tissue is comprised of a highly ordered hexagonal array of epithelial cells, each producing one distally pointing hair (trichome). *en::Gal4* or *sd::Gal4* driven expression of the *RacGAP50C*^{RNAi} construct results in an easily identifiable disruption caused by an increase in the number (as many as six) of trichomes per cell (Figure 6.2 B, B', D and D'). This phenotype results from the disruption of the mechanism that restricts the site of actin nucleation. A mild disruption to the planar cell polarity (PCP) was also observed in the *RacGAP50C*^{RNAi} wings (Figure 6.2 B' and D'). Both the defect in epithelial polarity and wing hair number are similar phenotypes to those observed in flies carrying a null allele of the Rho effector *Drok* (Winter *et al.,* 2001).

A closer inspection of the cells expressing the *RacGAP50C*^{RNAi} construct identified a disruption to cell division. Firstly, wings expressing the *RacGAP50C*^{RNAi} construct using the *en::Gal4* driver had less than half the normal number of cells in the posterior compartment (Figure 6.2, E). The cellular morphology of pupal wing discs expressing the *RacGAP50C*^{RNAi} construct was also examined. The *mCD8-GFP* construct was coexpressed to mark the cell membranes, and phalloidin was used to examine the trichomes. Examination of the *RacGAP50C*^{RNAi} pupal wing discs revealed that the cells were significantly larger and contained multiple trichomes (Figure 6.3, E and F). Examination of the nuclei, which were in the same area but at a different focal depth, revealed that each cell was typically binucleate and the nuclei appeared to have a disrupted morphology (Figure 6.3, D). Dissociation of third instar larval wing discs also revealed a disruption to cytokinesis at this earlier stage (Figure 6.3, G).

As expected with the broad range of expression driven throughout the body with the *engrailed* promoter, lethality generally occurs in flies expressing the *RacGAP50C*^{RNAi} construct at elevated levels. Disruption of actin-based structures outside of the wing were also seen, including bent scutellum bristles and loss of humeral bristles on the postpronotum (Figure 6.4, B and D).

Figure 6.2 Expression of the *RacGAP50C*^{RNAi} construct disrupts wing morphology.

(A-D) Adult wings, (A'- D') and higher magnification of the posterior region of corresponding wing shown in A-D. (A) wild-type adult wing, (B) *en::Gal4* expression of the *RacGAP50C*^{RNAi} construct at 25°C, (C) and 18°C. (D) *sd::Gal4* expression of the *RacGAP50C*^{RNAi} construct at 25°C. (A and A') Wild-type wing tissue is comprised of an epithelial bilayer, with each cell producing a single trichome hair that projects distally. (B) *en::Gal4* expression of the *RacGAP50C*^{RNAi} construct at 25°C disrupted wing morphology in the posterior half of the wing (below the drawn line). (B') Higher magnification reveals a lower density of trichomes in the posterior region, with many cells appearing to produce multiple trichomes (circled). (C and C') The same *en::Gal4* driven *RacGAP50C*^{RNAi} construct at 18°C produced a much more subtle phenotype. (D and D') *sd::Gal4* expression of the *RacGAP50C*^{RNAi} at 25°C produced a disruption to the entire wing, with higher magnification again revealing a reduced trichome density with many cells producing multiple trichomes, as well as showing disruptions to planar cell polarity. (E) Counting the number of cells in a posterior region of wings expressing the *RacGAP50C*^{RNAi} construct with the *en::Gal4* driver at 25°C, revealed that there are less than half the normal number of cells compared to wild-type. Standard errors bars are displayed.

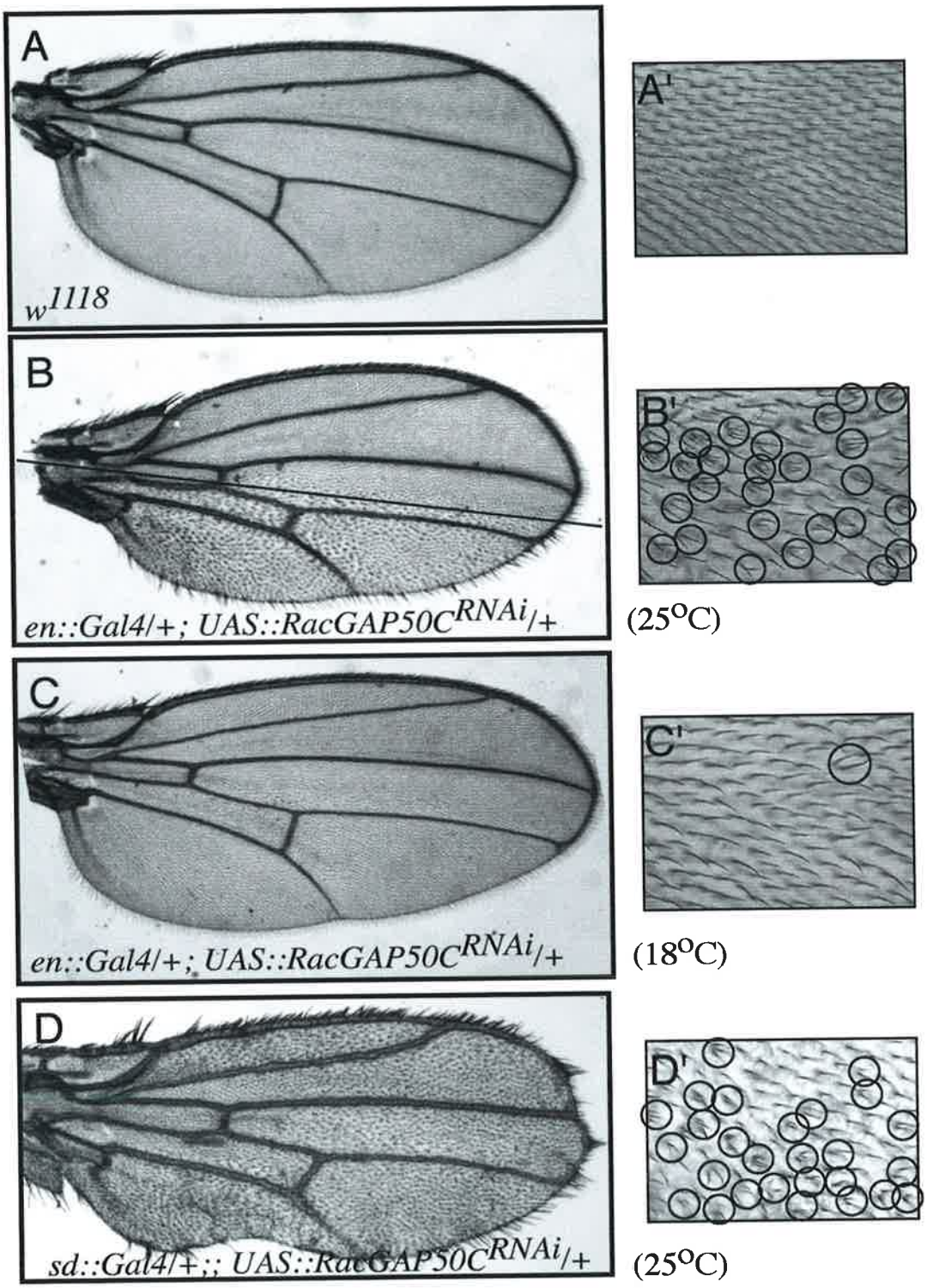
A
w1118
A'
B
en::Gal4/+; UAS::RacGAP50C RNAi /+
B'
(25°C)
C
en::Gal4/+; UAS::RacGAP50C RNAi /+
C'
(18°C)
D
sd::Gal4/+;; UAS::RacGAP50C RNAi /+
D'
(25°C)
E
No. of cells per field
60
50
40
30
20
10
0
WT
RacGAP50C RNAi

Figure 6.3 Expression of the inducible *RacGAP50C*^{RNAi} construct disrupts cytokinesis.

Morphology of wild-type (A-C) and *RacGAP50C*^{RNAi} expressing (D-F) pupal wing discs, 36 hours after pupal formation. Nuclei were stained with Hoechst 33258 (A and D), cell membranes were outlined by expressing the *UAS::mCD8-GFP* construct (B and E), and F-actin structures were stained with Phalloidin (red), and merged with the GFP fluorescence (green) (C and F). The *RacGAP50C*^{RNAi} expressing cells were significantly larger and produced multiple trichomes (E and F). Examination of the nuclei, which were in a different focal plane, revealed fewer nuclei in the same sized field of view in the *RacGAP50C*^{RNAi} tissue, and cells were typically binucleate (compare A with C and D with F). (G) Dissociation of third instar larval wing discs expressing *RacGAP50C*^{RNAi} and *mCD8-GFP* also identified some multinucleate cells. Nuclei detected with Hoechst 33258 are red, and GFP fluorescence is green.

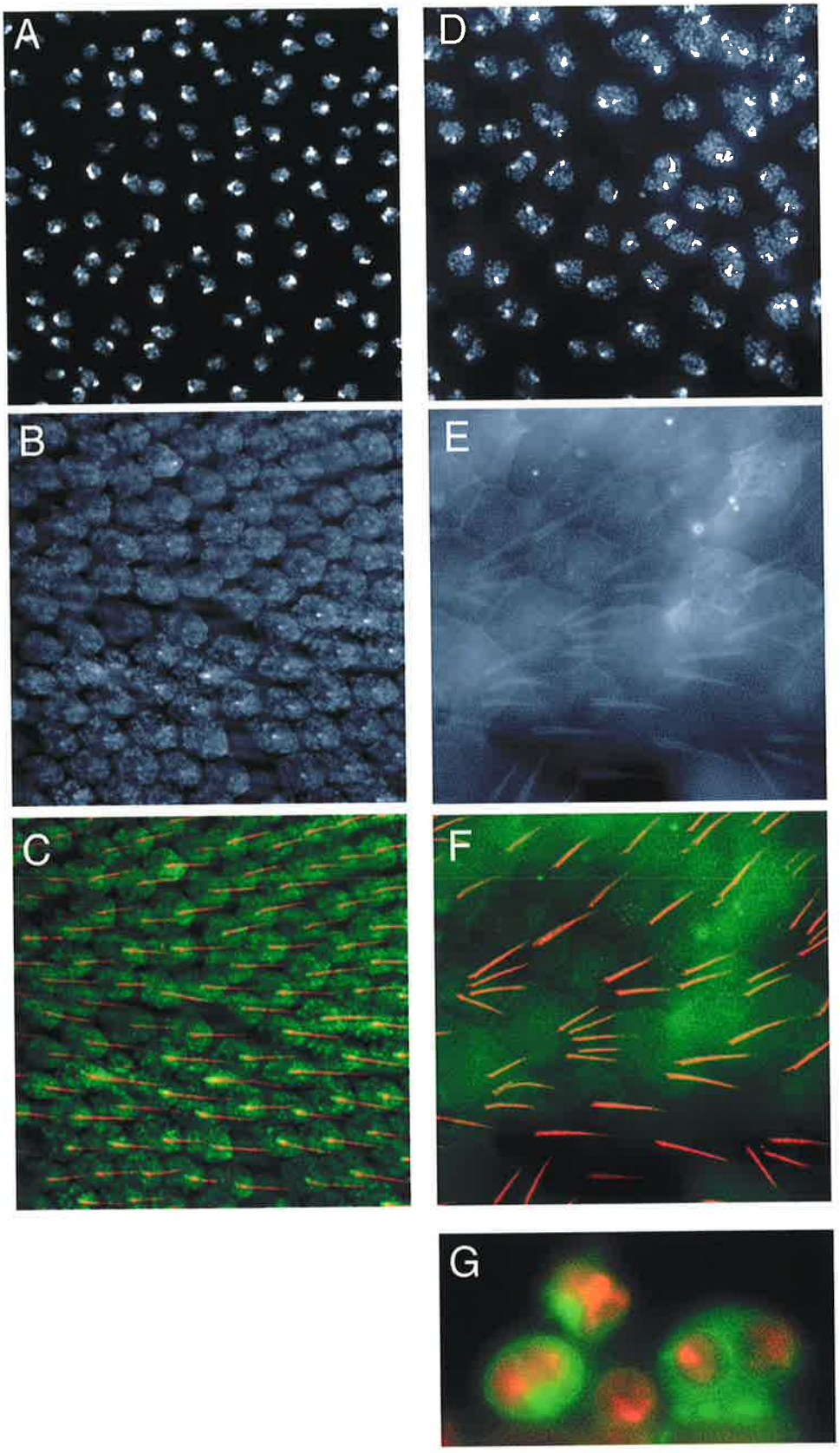
A
D
B
E
C
F
G

Figure 6.4 Other *engrailed*-expressing tissues are affected in *en::RacGAP50C*^{RNAi} flies.

Morphology of actin-based structures in other *en::Gal4* expressing tissues. (A and C) wild-type flies. (B and D) flies expressing the *RacGAP50C*^{RNAi} construct with *en::Gal4*. In some instances flies expressing the *RacGAP50C*^{RNAi} at elevated levels were observed to have their posterior scutellum bristles abnormally bent inwards (B, arrow), and humeral bristles missing (D, arrow).

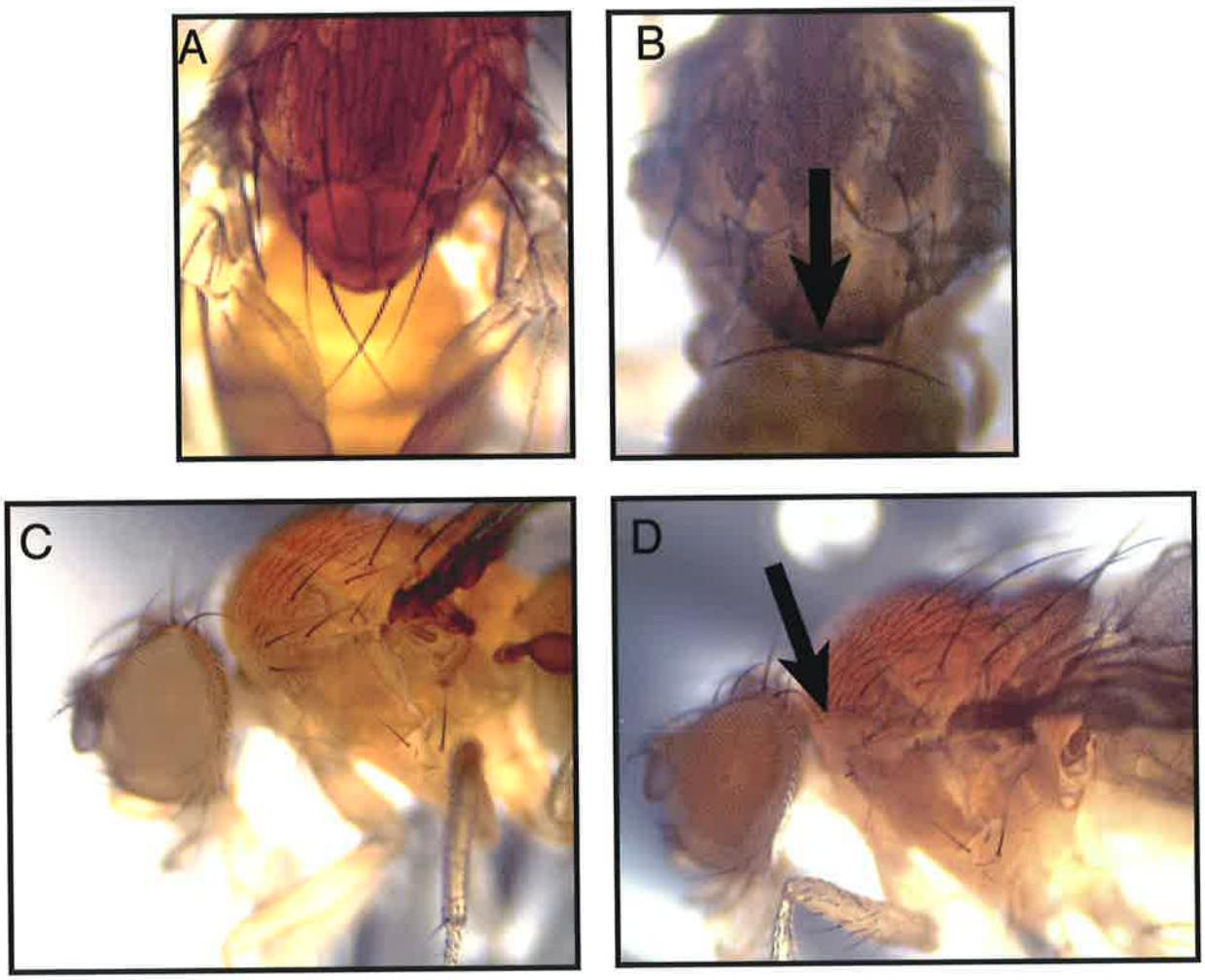
A
B
C
D

6.2.2 Expression of the *RacGAP50C*^{RNAi} construct generates a hypomorphic phenotype

If RacGAP50C plays an essential role in all cytokinesis throughout development, expression of the *RacGAP50C*^{RNAi} construct with the *en::Gal4* promoter would be expected to produce a considerably more disrupted phenotype. The level of *RacGAP50C* silencing was therefore assessed.

Morphological disruptions, caused by the over-expression of transgenes in *Drosophila* using the *S. cerevisiae Gal4/UAS* expression system are generally dose dependent. The disruption caused to the wing, by over-expressing the *RacGAP50C*^{RNAi} construct, was assessed at various temperatures. At 18°C, where expression of the transgene would be expected to be less than that produced at 25°C, the disruption to the wing morphology is subtle (Figure 6.2, C). Conversely, increased expression of the transgene produced by development at 30°C resulted in a significant enhancement of the wing phenotype (data not shown). Additionally, elevated expression of the transgene product by the sequential addition of multiple copies of the *RacGAP50C*^{RNAi} constructs or driver, results in an equivalent enhancement of the phenotype (Figure 6.5, A, B and C). Flies driving four copies of the *RacGAP50C*^{RNAi} construct from two *sd::Gal4* drivers, generates a wing hinge with only a small amount of wing tissue. Two null alleles of *RacGAP50C* (DH15 and AR2) became available at the end of this study. Flies heterozygous for either of these *RacGAP50C* alleles, depleting the endogenous *RacGAP50C* further, were able to enhance the *RacGAP50C*^{RNAi} cytokinetic phenotype (Figure 6.5 E and F).

6.2.3 The GAP domain of RacGAP50C appears essential for cytokinesis.

cyk-4 mutant *C. elegans* embryos exhibit disrupted bundling of central spindle MTs during anaphase/telophase, and a failure to correctly localise the kinesin-like motor protein ZEN-4 (Jantsch-Plunger *et al.*, 2000). A functional role for the CYK-4/ZEN-4 protein complex in bundling MT's has also been demonstrated *in vitro*, without the

Figure 6.5 The *RacGAP50C*^{RNAi} construct generates a hypomorphic phenotype.

(A-C) Disruption of wing morphology caused by increasing the *RacGAP50C*^{RNA} expression with the *sd::Gal4* driver as indicated. Increasing the expression level of the RNAi construct resulted in a corresponding increase in the severity of the disruption caused to the wing. (D) Ectopic expression of the *RacGAP50C*^{RNAi} construct with the *en::Gal4* driver at 25°C. (E and F) Enhancement of the*RacGAP50C*^{RNAi} phenotype, by halving the endogenous *RacGAP50C* dose with the *RacGAP50C* mutant alleles *RacGAP50C*^{AR2} and *RacGAP50C*^{DH15} (E and F).

A

Sd::Gal4/+;; UAS::RacGAP50C^{RNAi}/ +

B

Sd::Gal4/Sd::Gal4;; UAS::RacGAP50C^{RNAi}, UAS::RacGAP50C^{RNAi}/ +

C

Sd::Gal4/Sd::Gal4;; UAS::RacGAP50C^{RNAi} UAS::RacGAP50C^{RNAi}/ UAS::RacGAP50C^{RNAi}, UAS::RacGAP50C^{RNAi}

D

en::Gal4/+; UAS::RacGAP50C^{RNAi}/+

E

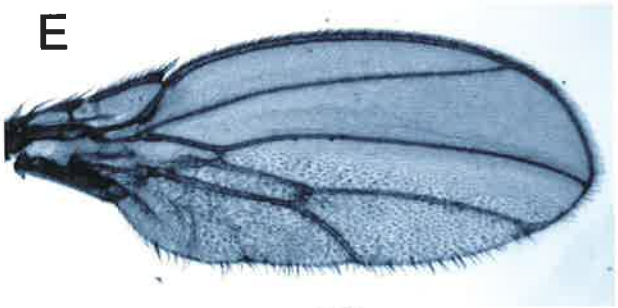

en::Gal4/RacGAP50C^{AR2}; UAS::RacGAP50C^{RNAi}/+

F

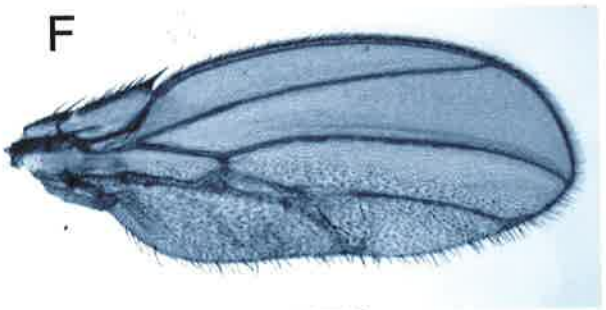

en::Gal4/RacGAP50C^{DH15}; UAS::RacGAP50C^{RNAi}/+

influence of any other protein, including Rho family GTPases (Mishima *et al.,* 2002). Although this RacGAP is capable of targeting Rac1 and Cdc42, as shown by *in vitro* GAP assays (Toure *et al.,* 1998; Jantsch-Plunger *et al.,* 2000; Kawashima *et al.,* 2000) and genetic interactions (Sotillos and Campuzano, 2000), targeting may not necessarily be important in cytokinesis. This study examines whether a functional GAP domain is required by RacGAP50C to regulate cytokinesis. As demonstrated above, expression of the *RacGAP50C*^{RNAi} construct generates a hypomorphic phenotype that is extremely sensitive to dose. Supplying the system with more RacGAP50C, by expressing a wild-type *myc-RacGAP50C* construct (Figure 6.1, B), was able to strongly suppress the *RacGAP50C*^{RNAi} phenotype (Figure 6.6, B).

In vitro studies, involving GTPase activating proteins, have allowed the identification of functionally critical GAP domain residues (Ahmed *et al.,* 1994; Leonard *et al.,* 1998). It has been shown that the deletion constructs ΔEIE (166-168) of *n*-Chimaerin (Ahmed *et al.,* 1994) and the homologous amino acids in the Cdc42-GAP, ΔYLQ (164-166) (Leonard *et al.,* 1998), generate a protein which is still capable of binding the target GTPase with high affinity, but which has a catalytically inactive GAP domain. Also, disruption of an adjacent highly conserved arginine residue produced a similar inactive GAP protein (Ahmed *et al.,* 1994; Leonard *et al.,* 1998). Structural analysis has suggested that this highly conserved arginine residue is the key catalytic residue for the GAP function (Rittinger *et al.,* 1997), while the disruption of the less conserved ΔEIE peptide is predicted to displace this catalytic arginine (Leonard *et al.,* 1998). To address whether the GAP domain was necessary for cytokinesis, two putative dominant negative *RacGAP50C* constructs were coexpressed with the *RacGAP50C*^{RNAi} construct. Based on the *in vitro* binding studies described above, critical residues of the RacGAP50C GAP domain were deleted via site-directed mutagenesis, generating *RacGAP50C*$^{\Delta EIE}$ (amino acids 404-406) and *RacGAP50C*$^{\Delta YRL}$ (amino acids 416-418) (Figure 6.1, C, D and E).

Expression of the myc-tagged *RacGAP50C*$^{\Delta EIE}$ and *RacGAP50C*$^{\Delta YRL}$ constructs with the *en::Gal4* or *sd::Gal4* drivers did not produce any observable disruption to the wing. This is in contrast to similar transgenic stocks (ΔEIE and R417Q) generated by

Figure 6.6 The GAP domain of RacGAP50C appears to be essential for cytokinesis

(A) *RacGAP50C*^{RNAi} phenotype, at 25°C. (B) Co-expression of a Myc-tagged wild-type RacGAP50C construct, resulted in a suppression of the disrupted wing phenotype. (C and D) Co-expression of the *RacGAP50C*^{RNAi} construct with Myc-tagged RacGAP50C constructs with catalytically inactive GAP domains, *RacGAP50C*$^{\Delta EIE}$ (C), and *RacGAP50C*$^{\Delta YRL}$ (D), were unable to rescue the *RacGAP50C*^{RNAi} phenotype.

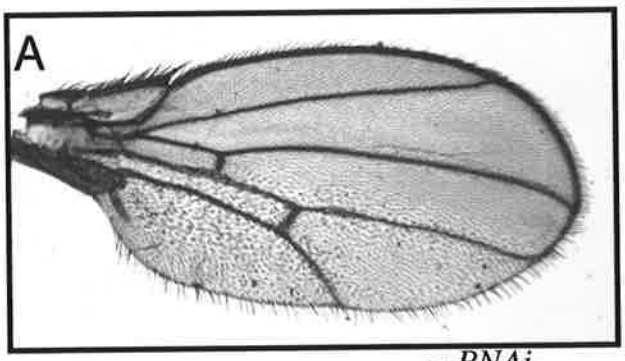

en::Gal4/+; UAS::RacGAP50C^{RNAi}/+

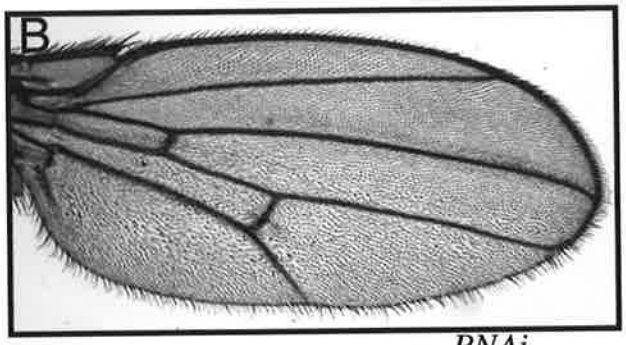

en::Gal4/+; UAS::RacGAP50C^{RNAi},/UAS::MYC-RacGAP50C

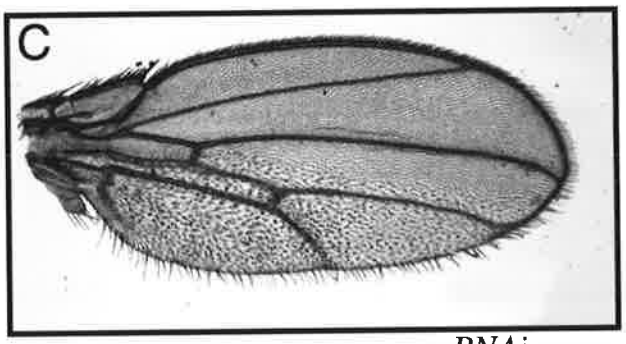

en::Gal4/+; UAS::RacGAP50C^{RNAi},/UAS::MYC-RacGAP50C$^{\Delta EIE}$

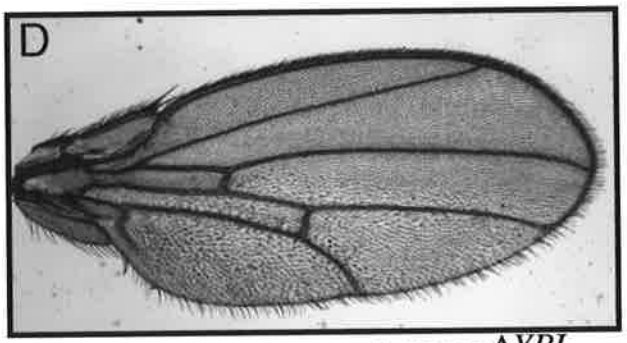

en::Gal4/UAS::MYC-RacGAP50C$^{\Delta YRL}$; UAS::RacGAP50C^{RNAi},/+

Sotillos and Campuzano (2000), which exhibit a loss of wing tissue, an increase in vein width, extra sensory organs, enlarged cells and a disruption to the number and polarity of the trichomes. This difference is unlikely to be due to differences in expression levels, as expression of multiple myc-tagged copies was still unable to generate a phenotype. One possibility is that the N-terminal *myc*-tag causes a steric hindrance to the extreme N-terminal PAV and PBL interaction domains, thus reducing the severity caused by over-expressing this construct.

In contrast to the *en::Gal4* driven expression of wild-type RacGAP50C, co-expression of the putative dominant negative *RacGAP50C* constructs, *myc-RacGAP50C*$^{\Delta EIE}$ and *myc-RacGAP50C*$^{\Delta YRL}$, did not have any significant effect on the *RacGAP50C*^{RNAi} phenotype, even when multiple copies were coexpressed (Figure 6.6, C and D). All transgenic lines were tested with immunostaining and western blot analysis, and observed to be expressing the transgene (data not shown), suggesting that a functional GAP domain is required by RacGAP50C to regulate cytokinesis.

6.2.4 *RacGAP50C* genetically interacts with *pbl*

Previous chapters have discussed the identification and characterisation of the residues necessary for an interaction between RacGAP50C and PBL. To test the biological significance of this PBL RhoGEF-RacGAP50C interaction, genetic interactions between the *RacGAP50C*^{RNAi} construct and various *pbl* constructs were examined.

en::Gal4 driven expression of wild-type *pbl* produced no obvious disruption to the wing morphology (Figure 6.7, B), but appeared to result in some overgrowth of the wing tissue in the posterior region. Co-expression of the *RacGAP50C*^{RNAi} construct produced a complex disruption to the wing morphology, exhibiting a loss of wing tissue in the posterior region, which included the disruption or even complete loss of the posterior cross-vein and L4 and L5 veins (Figure 6.7, C). As previously discussed in chapter three, the N-terminus of PBL was found to be capable of interacting with RacGAP50C in a yeast two-hybrid assay. Expression of the N-terminus of PBL, (*pbl*$^{1\text{-}298}$) should result in competition with the endogenous PBL binding to RacGAP50C.

Figure 6.7 *RacGAP50C* genetically interacts with *pbl*.

(A) The *RacGAP50C*^{RNAi} phenotype produced by the *en::Gal4* driver at 25°C. Phenotype produced by *en::Gal4* ectopic expression of: (B), full-length wild-type *pbl* ; (C), co-expression of *RacGAP50C*^{RNAi} and wild-type *pbl* ; (D), N-terminus of pbl (*pbl*$^{1-298}$); (E), co-expression of *pbl*$^{1-298}$ and *RacGAP50C*^{RNAi}; (F), a *pbl* construct containing an N-terminal truncation (*pbl*$^{\Delta RADECL/RBCTI}$); (G), coexpression of *pbl*$^{\Delta RADECL/RBCTI}$ and *RacGAP50C*^{RNAi}; (H), a dominant negative *pbl* construct (*pbl*$^{\Delta DH}$); (I), and coexpression of *pbl*$^{\Delta DH}$ and *RacGAP50C*^{RNAi}. Expression of wild-type *pbl* did not result in any obvious disruption to wing morphology (B), but when coexpressed with the *RacGAP50C*^{RNAi} construct, a complex phenotype was observed, with some loss of wing tissue and a disruption to vein development in the posterior compartment (C). Although expression of *pbl*$^{1-298}$ was able to disrupt wing morphology (D), no genetic interactions were observed between the *RacGAP50C*^{RNAi} and *pbl*$^{1-298}$ constructs (E). Expression of *pbl*$^{\Delta RADECL/RBCTI}$ produced a very subtle phenotype, disrupting formation of half of the cross-veins (F). However, coexpression with the *RacGAP50C*^{RNAi} resulted in the significant loss of wing tissue (G). Expression of the dominant negative *pbl* construct, *pbl*$^{\Delta DH}$, disrupted the posterior wing morphology (H). Coexpression of *pbl*$^{\Delta DH}$ and *RacGAP50C*^{RNAi} resulted in a strong synergistic interaction, and the loss of most posterior wing tissue (I).

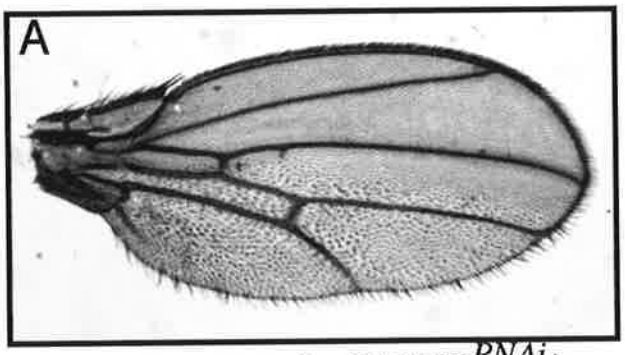

en::Gal4/+; UAS::RacGAP50C^{RNAi}/+

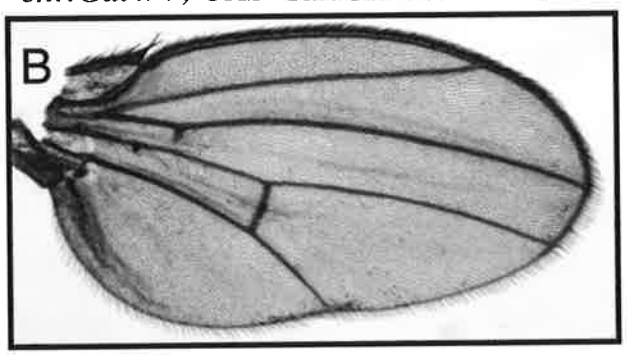

en::Gal4/UAS::pbl

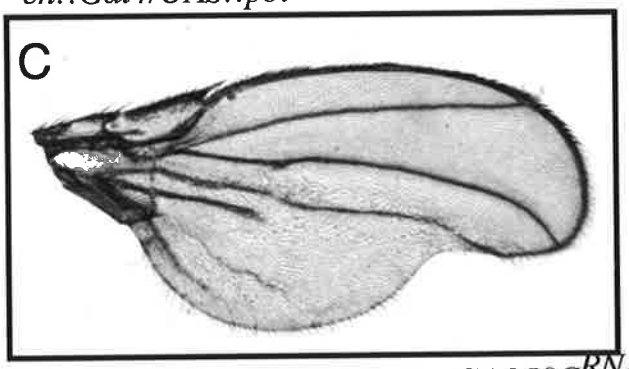

en::Gal4/UAS::pbl; UAS::RacGAP50C^{RNAi}/+

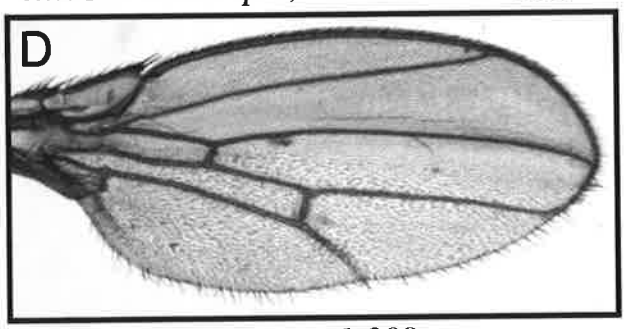

en::Gal4/+; UAS::pbl$^{1-298}$/+

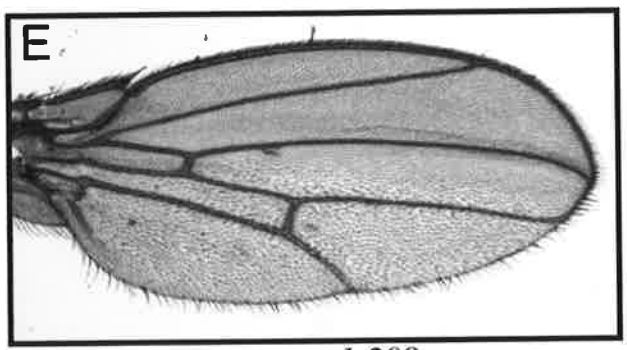

en::Gal4/+; UAS::pbl$^{1-298}$/
UAS::RacGAP50C^{RNAi}

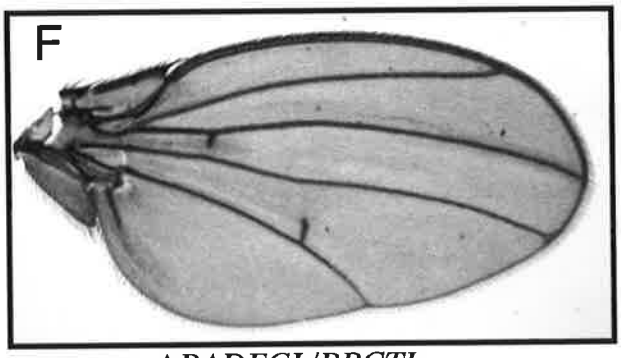

UAS::pbl$^{\Delta RADECL/BRCTI}$/+; en::Gal4/+

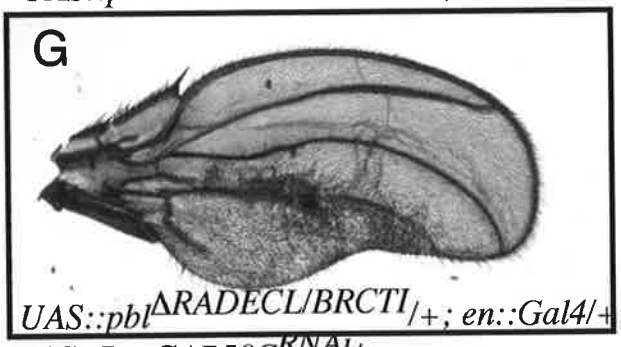

UAS::pbl$^{\Delta RADECL/BRCTI}$/+; en::Gal4/+;
UAS::RacGAP50C^{RNAi}/+

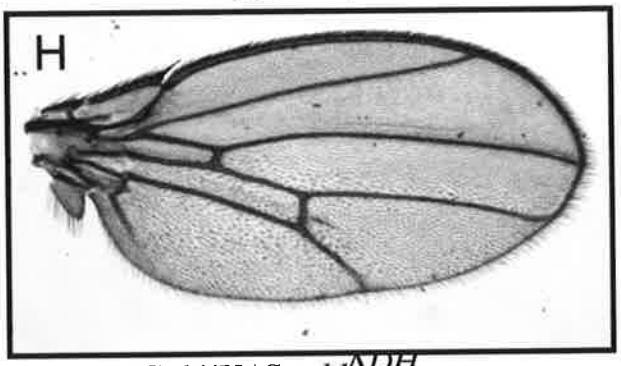

en::Gal4/UAS::pbl$^{\Delta DH}$

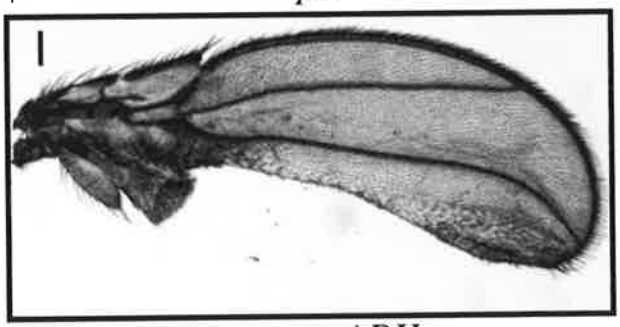

en::Gal4/UAS::pbl$^{\Delta DH}$.
UAS::RacGAP50C^{RNAi}/+

A construct expressing this N-terminal peptide should therefore act as a dominant negative. *en::Gal4* driven expression of $pbl^{1\text{-}298}$ causes a disruption to the posterior wing morphology, resulting in fewer cells which possess multiple trichomes (Figure 6.7, D), similar to that seen with *en::Gal4* driven expression of the $RacGAP50C^{RNAi}$ construct. Coexpression of the $pbl^{1\text{-}298}$ and $RacGAP50C^{RNAi}$ constructs did not result in any modification of the phenotypes (Figure 6.7, E). A *pbl* construct, possessing the entire PBL protein apart from the RADECL/BRCTI domains (which were shown in chapter three to be capable of interacting with RacGAP50C), was also tested for a genetic interaction with *RacGAP50C*. This construct would presumably still be capable of interacting with Rho1 but not with RacGAP50C. *en::Gal4* driven expression of this $pbl^{\Delta RADECL/BRCTI}$ construct produced a very subtle phenotype, resulting in the absence of half of the cross-veins (Figure 6.7, F). However, coexpression of this construct with the $RacGAP50C^{RNAi}$ construct generated a significant enhancement, and a substantial loss of wing tissue in the posterior part of the wing (Figure 6.7, G). A further dominant negative *pbl* construct ($pbl^{\Delta DH}$) was tested for a genetic interaction with *RacGAP50C*. This construct has 53 amino acids deleted from the catalytic region of the Dbl homology (DH) domain, and has previously been shown to disrupt cytokinesis in the developing eye (Prokopenko *et al.,* 1999; O'Keefe *et al.,* 2001). *en::Gal4* driven expression of the $pbl^{\Delta DH}$ construct in the posterior region of the wing results in a disruption with fewer cells and multiple trichomes (Figure 6.7, H), similar to that seen in $RacGAP50C^{RNAi}$ expressing wings. Coexpression of this dominant negative *pbl* construct with the $RacGAP50C^{RNAi}$ construct generated a strongly synergistic phenotype, resulting in the loss of the majority of the wing tissue in the posterior half of the wing (Figure 6.7, I).

6.2.5 *RacGAP50C* genetically interacts with *Rac1*

RacGAP50C encodes a putative GTPase activating protein that is essential for cytokinesis. As shown above, the GAP domain appears to be essential for rescuing the $RacGAP50C^{RNAi}$ phenotype, and therefore the inactivation of a Rho family member appears to be necessary for successful cytokinesis. Genetic interactions between various Rho family members and *RacGAP50C* were therefore investigated.

D. melanogaster possesses eight Rho family members (*Rho1, RhoL, Rac1, Rac2, Mig2-like (Mtl), Cdc42, RhoBTB,* and *CG12102*), of which only five have null alleles. Genetic interactions involving mutant alleles of these five Rho family members ($Rho1^{720}$, $Cdc42^{4}$, $Rac1^{J11}$, $Rac2^{\Delta}$ and Mtl^{Δ}) were examined to see if they could modify the $RacGAP50C^{RNAi}$ phenotype. Loss of one copy of any one of these Rho family alleles, as well as loss of one copy each of $Rac1^{J11}$, $Rac2^{\Delta}$, Mtl^{Δ}, did not modify the phenotype (Figure 6.8).

A genetic interaction between RacGAP50C and the over-expression of various Rho family members was examined next. Previous studies have shown that specific substitutions of critical catalytic residues in GTPases can create constitutively active or dominant inhibitory proteins. The dominant inhibitory molecules are believed to act by competing with the endogenous GTPase for GEF binding, but are unable to signal to downstream effectors, while constitutively active GTPases are GTP hydrolysis defective. Various Rho family GTPase constructs, including wild-type, constitutively active and dominant negative constructs, were tested for genetic interactions with the various *RacGAP50C* constructs. Expression of most of these GTPase constructs with the *en::Gal4* or *sd::Gal4* driver caused lethality, or produced no observable disruption to the wing morphology. *sd::Gal4* driven expression of wild-type *Rac1* is lethal at 25°C, and partially lethal at 18°C. The escaper flies that did emerge at 18°C had a very disrupted wing (Figure 6.9, A). Both the lethality and disrupted morphology of the wing could be suppressed with the co-expression of a wild-type *myc-RacGAP50C*, in a dose dependent manner (Figure 6.9, C and E). Additionally, *sd::Gal4* driven expression of a dominant negative form of *Rac1* ($Rac1^{N17}$) at 18°C, results in a much narrower wing (Figure 6.9, B). This phenotype was greatly enhanced by the coexpression of the wild-type *myc-RacGAP50C*-construct, resulting in the additional loss of wing tissue from the anterior and posterior margins (Figure 6.9, D and F). The coexpression of the $myc\text{-}RacGAP50C^{\Delta EIE}$ and $myc\text{-}RacGAP50C^{\Delta YRL}$ constructs had no effect on the $Rac1^{N17}$ phenotype (Figure 6.9, G). These results clearly demonstrate that RacGAP50C is capable of targeting Rac1 for inactivation, and is consistent with Sotillos and Campuzano (2000). However, induced expression of the Rac1 GTPase

Figure 6.8 Heterozygous Rho family members are unable to modify the *RacGAP50C*^{RNAi} phenotype.

(A) The *RacGAP50C*^{RNAi} phenotype produced by the *en::Gal4* driver at 25°C. No significant modification of the RNAi phenotype was observed in a heterozygous genetic background of: (B) *Rac1*^{J11}; (C) *Rac1*^{J11}, *Rac2*$^{\Delta}$; (D) *Rac1*^{J11}, *Rac2, Mtl*$^{\Delta}$; (E) *Cdc42*^{4} and (F) *Rho1*^{72O}.

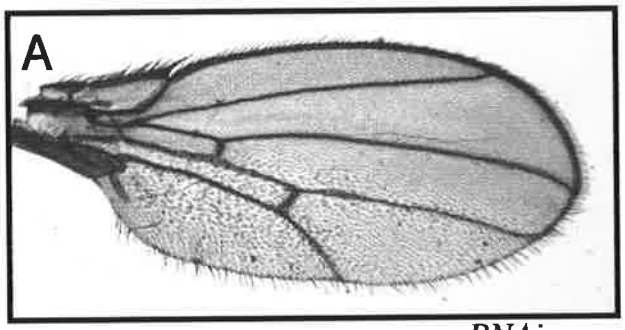

en::Gal4/+; UAS::RacGAP50C^{RNAi}/+

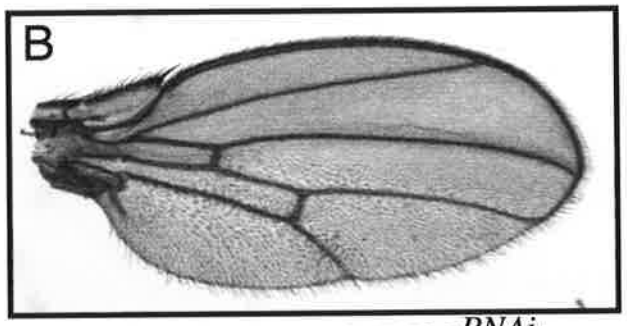

en::Gal4/+; UAS::RacGAP50C^{RNAi}/ Rac1^{J11}

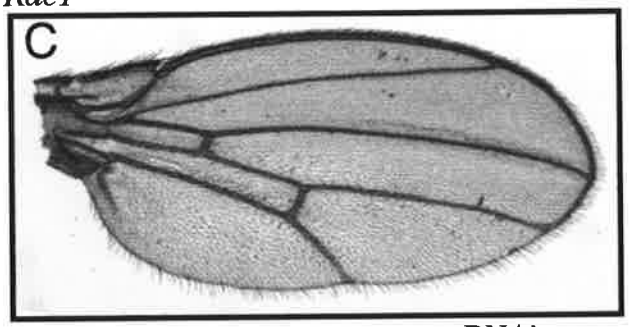

en::Gal4/+; UAS::RacGAP50C^{RNAi}/ Rac1^{J11}, Rac2$^{\Delta}$

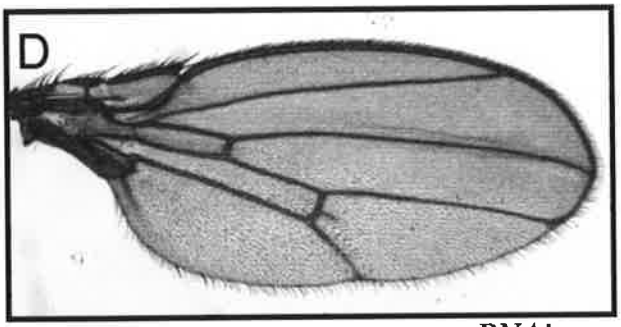

en::Gal4/+; UAS::RacGAP50C^{RNAi}/ Rac1^{J11}, Rac2$^{\Delta}$, MTL$^{\Delta}$

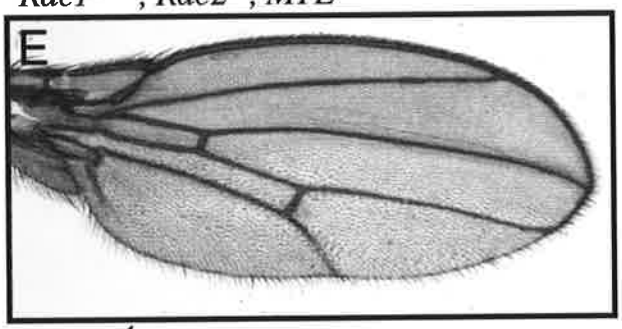

Cdc42^{4}/+; en::Gal4/+; UAS::RacGAP50C^{RNAi}/+

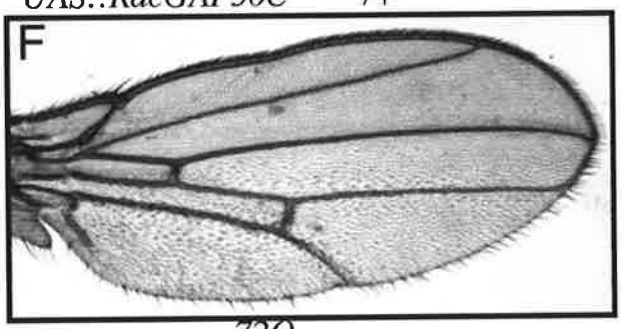

en::Gal4/Rho1^{72O}; UAS::RacGAP50C^{RNAi}/+

Figure 6.9 *RacGAP50C* genetically interacts with *Rac1*.

Ectopic expression of both wild-type *Rac1* (A) and $Rac1^{N17}$ (B) with the *sd::Gal4* driver at 18°C, disrupted wing formation. Co-expression of one (C and E) or two (E and F) copies of a Myc-tagged wild-type RacGAP50C was capable of suppressing the disrupted wing morphology caused by ectopic expression of wild-type *Rac1* (C and E), and enhancing the $Rac1^{N17}$ wing disruption (D and F). (G) Ectopic co-expression of the catalytically inactive $RacGAP50C^{\Delta YRL}$ construct had no effect on the $Rac1^{N17}$ wing phenotype.

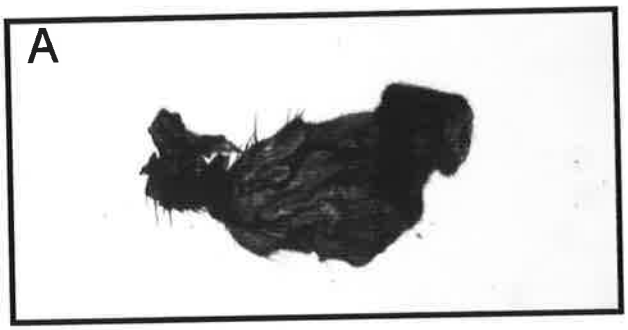

sd::Gal4/+; UAS::Rac1/+

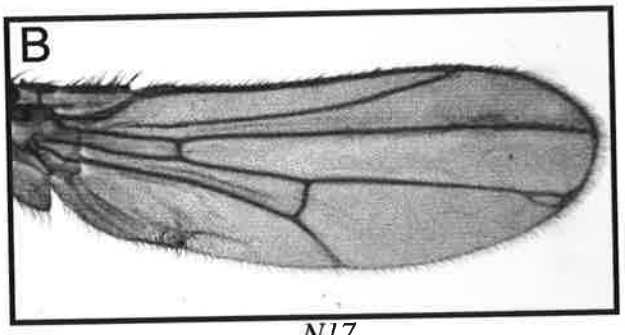

sd::Gal4; UAS::Rac1^{N17}/+

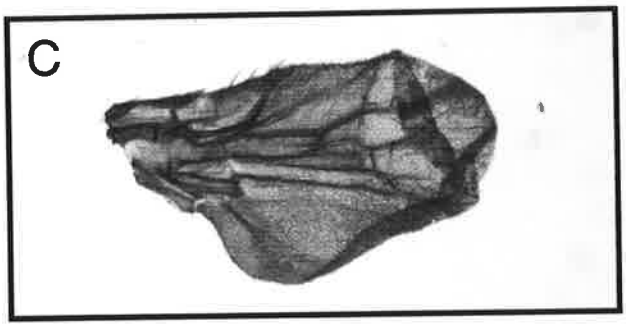

sd::Gal4/+; UAS::Rac1/+;
UAS::MYC-RacGAP50C/+

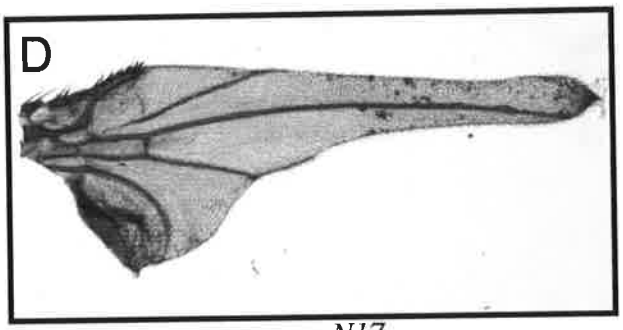

sd::Gal4/+; UAS::Rac1^{N17}/+;
UAS::MYC-RacGAP50C/+

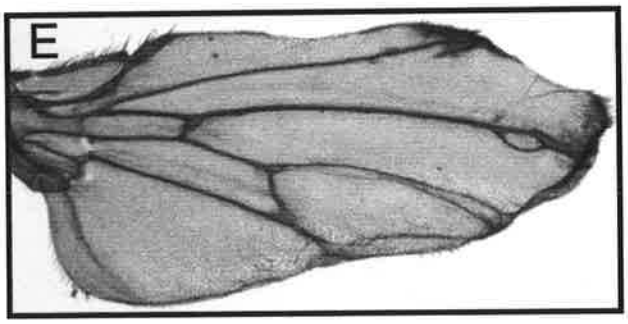

sd::Gal4/+; UAS::Rac1/+;
UAS::MYC-RacGAP50C,
UAS::MYC-RacGAP50C/+

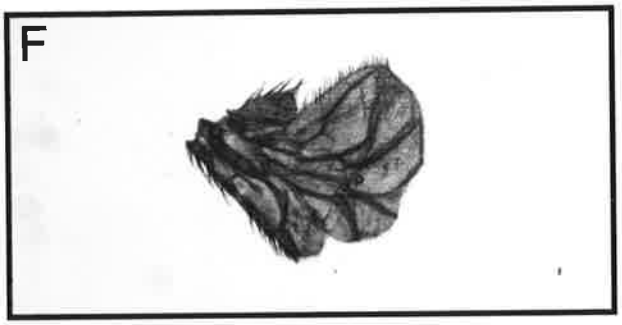

sd::Gal4/+; UAS::Rac1^{N17}/+;
UAS::MYC-RacGAP50C,
UAS::MYC-RacGAP50C/+

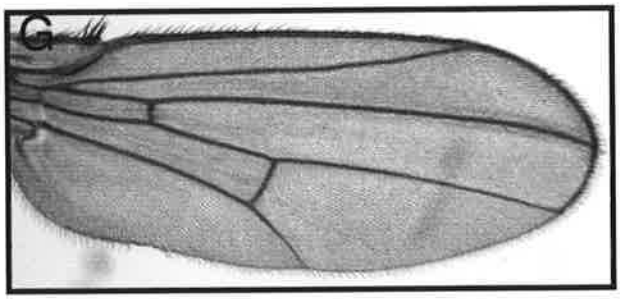

sd::Gal4/+; UAS::Rac1^{N17}/
UAS::MYC-RacGAP50C$^{\Delta YRL}$

may simply create an artificial environment, and fail to specifically address which Rho family GTPase RacGAP50C targets during cytokinesis.

6.2.6 Genetic interactions with candidate RacGAP50C-interacting proteins.

RacGAP50C has previously been shown to genetically interact with Rac1 and Cdc42, and the downstream effector PAK (Sotillos and Campuzano, 2000). Various null alleles of candidate interactors were tested for a genetic interaction with the $RacGAP50C^{RNAi}$ phenotype. These included effectors of Rho signalling: *rok, citron, zip, sqh, dia;* effectors of Rac signalling: *Pak, dock, Sif, mbc, trio, PKN;* and components essential for cytokinesis: *chic, pnut, polo, pav, mhc* and *18w*. None of these null alleles when heterozygous significantly altered the $RacGAP50C^{RNAi}$ phenotype. However, *en::Gal4*-induced expression of a myc-tagged Rac1-activating GEF, *trio*, caused a disruption to the posterior region of the wing, which included the production of ectopic veins, a phenotype characteristic of over-expressing wild-type Rac1. Co-expression of the wild-type *trio* and $RacGAP50C^{RNAi}$ constructs with the *en::Gal4* driver resulted in a significantly enhanced phenotype (Figure 6.10, B). Over-expression of the GEF Trio is likely to cause inappropriate activation of its target GTPase, producing an artificial environment. However, the enhanced phenotype generated with the $RacGAP50C^{RNAi}$ construct suggests that RacGAP50C functions as the GAP for the Rho family member that is activated by Trio.

6.3 Discussion

Previous studies have shown that RacGAP50C and its *C. elegans* ortholog CYK-4 and mammalian ortholog MgcRacGAP, have higher GAP activity towards Rac1 and Cdc42 than for Rho1. However Rho1 is currently the only Rho family member identified as being essential for cytokinesis in these model organisms. It still remains uncertain whether RacGAP50C regulates the level of active Rho1 *in vivo* during cytokinesis, or perhaps inactivates another Rho family member, allowing cytokinesis to proceed.

Figure 6.10 The *RacGAP50C*^{RNAi} phenotype is enhanced by the Rac activator Trio.

(A) Ectopic expression of a Myc-tagged wild-type Trio construct with the *en::Gal4* driver at 25°C, disrupted vein formation in the posterior half of the wing. (B) Ectopic co-expression of the Myc-tagged *trio* and *RacGAP50C*^{RNAi} constructs produced a synergistic enhanced phenotype, resulting in the loss of tissue in the posterior half of the wing.

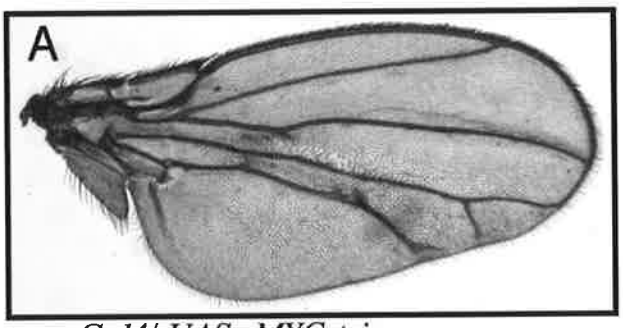

en::Gal4/ UAS::MYC-trio

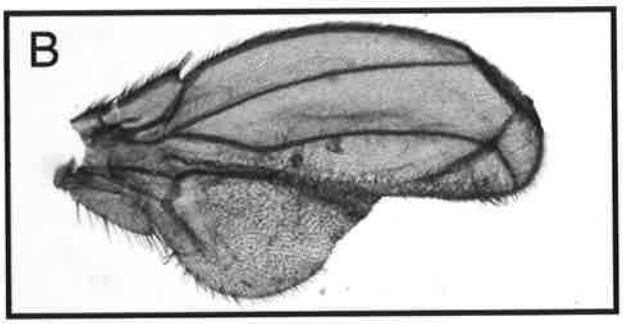

en::Gal4/ UAS::MYC-trio; UAS::RacGAP50C^{RNAi}

The Rho family GTPase that RacGAP50C targets during cytokinesis was investigated using various *RacGAP50C* expression constructs, including dominant negative RacGAP50C proteins and an inducible RNAi construct capable of disrupting cytokinesis. *en::Gal4* driven expression of the *RacGAP50C*^{RNAi} construct resulted in disruption of the adult wing morphology. Examination of the cellular morphology revealed a cytokinetic phenotype, with the loss of over half the normal number of cells, which were enlarged and typically binucleate. These enlarged cells were also observed to have multiple trichomes, a phenotype previously shown to occur in abnormally large wing cells, caused by the failure to restrict the prehair initiation site (Adler *et al.*, 2000). Co-expression of a wild-type *RacGAP50C* was capable of rescuing the *RacGAP50C*^{RNAi} phenotype, while *RacGAP50C* constructs that possessed targeted deletions of critical catalytic residues in the GAP domain were unable to modify the cytokinetic phenotype. *en::Gal4* driven expression of wild-type and GTPase activation-defective *RacGAP50C* constructs should presumably be able to correctly bind the normal endogenous interacting proteins such as PBL, PAV and the target Rho family GTPase. Thus the failure to rescue the cytokinetic defect by the GTPase-activation defective RacGAP50C proteins suggests that inactivation of a Rho family member by RacGAP50C is an essential requirement for cytokinesis. It remains a formal possibility that the deletions generated in the RacGAP50C$^{\Delta EIE}$ and RacGAP50C$^{\Delta YRL}$ proteins cause disruptions other than the GTPase activation domain, creating structural defects and thus a loss of functional activity. However, similar GAP domain disruptions in RacGAP50C have previously been created, and were able to function in genetic interactions (Sotillos and Campuzano, 2000).

The *RacGAP50C*^{RNAi} construct should specifically silence the endogenous *RacGAP50C*, so the disrupted phenotype produced is presumably due to the inappropriate activation of its target Rho family GTPase(s). However, genetic interactions involving the *RacGAP50C*^{RNAi} construct and various mutant alleles of candidate Rho family members failed to identify any significant modification of the *RacGAP50C*^{RNAi} phenotype. This could be a result of the hypomorphic *RacGAP50C*^{RNAi} phenotype being insensitive to modification by various heterozygous null candidates, despite the fact that halving the dose of endogenous *RacGAP50C* resulted in a significant enhancement. Alternatively, it may be that the candidate alleles tested are not the target of RacGAP50C mediated

regulation during cytokinesis. It is possible that one of the untested novel Rho family GTPases is the target of RacGAP50C, or perhaps several Rho family members (perhaps a combination of Cdc42 and Rac GTPases) are targeted by RacGAP50C, so that functional redundancy prevents modification of the *RacGAP50C*^{RNAi} phenotype.

An alternative way to test for such interactions is to examine genetic interactions involving the over-expression of Rho family members. As cross-activation and inhibition between the Rho family members can occur, care must be taken when interpreting the results produced by these constructs. For instance, over-expression of dominant negative Rac proteins results in a disruption to the PCP in both the wing and eye (Eaton *et al.,* 1996; Fanto *et al.,* 2000). However, no defects in the PCP were observed in null mutants of Rac1 or even in clones of the triple null mutant *Rac1*, *Rac2* and *Mtl* (Hakeda-Suzuki *et al.,* 2002). With this reservation in mind, it is potentially significant that the *sd::Gal4* driven expression of wild-type *RacGAP50C* was identified to interact with *Rac1*, in a way that would be consistent with RacGAP50C being the inactivating GAP protein. Genetic interactions between *Rac1* and *RacGAP50C* have previously been reported to be important in regulating the EGFR/Ras signalling pathway during patterning of the *D. melanogaster* wing (Sotillos and Campuzano, 2000). Consistent with RacGAP50C specifically targeting Rac1, a strong enhancement was observed between *RacGAP50C* and the Rac family GEF *trio*. However, none of the Rac family members have been shown to be necessary for cytokinesis, and the over-expression of wild-type or constitutively active *Rac1* does not inhibit cytokinesis (L. Luo, personal communication), therefore regulation of Rac1 cannot be the key event of RacGAP50C activity during cytokinesis.

RacGAP50C and *pbl* were also shown to genetically interact, confirming the importance of an *in vivo* interaction. Strong synergistic enhancement of the *RacGAP50C*^{RNAi} phenotype was observed with *en::Gal4* driven expression of dominant negative forms of *pbl* (*pbl*$^{\Delta RADECL/\ BRCT1}$ and *pbl*$^{\Delta DH}$). The fact that these interactions are synergistic and not antagonistic, suggests that RacGAP50C does not act opposite to PBL to inactive Rho1. If RacGAP50C targeted Rho1 for inactivation, over-expression of the *RacGAP50C*^{RNAi} should have suppressed the dominant negative *pbl* phenotype.

These data lead to two likely scenarios. Firstly, PBL and RacGAP50C target the same GTPase (Rho1), but at different times. For example, PBL may activate Rho1 early in anaphase to initiate cortical constriction, while RacGAP50C inactivates Rho1 later during telophase, to restrict constriction and stabilise the ingressed furrow once it reaches the bundled central-spindle. This theory would be consistent with the observations of extensive cortical furrowing in the *cyk-4* mutant embryos. A second possibility is that PBL and RacGAP50C target separate GTPases (Rho1 and, possibly, members of the Rac family respectively). The cooperative targeting of the GAP and the GEF could down-regulate Rac1 GTPase activity, allowing the activation of Rho1, and thus initiating cytokinesis. This would be consistent with biochemical studies involving mammalian cells, which have shown that under certain circumstances activation of Rac1 can inhibit the activation of Rho1 (Sander *et al.,* 1999; Zondag *et al.,* 2000).

en::Gal4 driven expression of the N-terminus (BRCT domain containing region) of *pbl* ($pbl^{1\text{-}298}$) appeared to disrupt the number of cells produced, but surprisingly no genetic interactions were observed with the $RacGAP50C^{RNAi}$ construct. Despite being over-expressed, this N-terminal PBL fragment may not be able to correctly localise to the contractile ring, and therefore may be unable to interfere with the endogenous PBL-RacGAP50C complex. This PBL fragment lacks the C-terminal PH domain, which from other studies has been implicated in correct cortical targeting (Lemmon *et al.,* 1997). Although the N-terminus of Ect-2 is capable of correctly localising to the midbody (Tatsumoto *et al.,* 1999), this is likely to involve different mechanisms of targeting to that of PBL. As discussed in chapter three, a conserved interaction was demonstrated between the human MgcRacGAP and N-terminus of Ect2. MgcRacGAP and Ect2 appear to colocalise on the mitotic spindles, central spindle and midbody (Tatsumoto *et al.,* 1999; Hirose *et al.,* 2001). Therefore, unlike PBL, Ect-2 is likely to be associated in a Ect-2-MgcRacGAP-CHO1/MKLP1 protein complex throughout mitosis, so that the N-terminal Ect-2 fragment can correctly localise independent of its GEF domain.

Although the genetic interactions studied did not identify the signalling pathway through which RacGAP50C acts during cytokinesis, a number of important observations were made. The GAP domain of RacGAP50C appears essential for its

role in cytokinesis. RacGAP50C was found to be capable of targeting Rac1 for inactivation, but the significance of this interaction during cytokinesis remains unclear. *RacGAP50C* was also identified to act antagonistically with the RacGEF *trio*. Strong genetic interactions between *RacGAP50C* and *pbl* constructs were also demonstrated, supporting the significance of this protein-protein interaction *in vivo*.

6.3.1 Future directions

6.3.1.1 Identification of the RacGAP50C target GTPase.

Genetic interactions presented here, as well as by other groups, have shown RacGAP50C is capable of targeting Rac1 and Cdc42. Although Rac does not appear to play an essential role in cytokinesis in humans, *C. elegans* or *Drosophila*, activated Cdc42 has been shown to disrupt cytokinesis in *Xenopus* (Drechsel *et al.*, 1997) and cause disruptions to cellularisation in *Drosophila* embryos (Crawford *et al.*, 1998). *en::Gal4* driven expression of the $RacGAP50C^{RNAi}$ construct was able to disrupt cytokinesis in a dose dependent manner. Despite this fact genetic interactions described here failed to clearly indicate which Rho family GTPase is targeted by RacGAP50C during cytokinesis. Although halving the dose of the candidate GTPases *Rho1*, *Rac1*, *Rac2*, *Mtl*, *Cdc42*, and combinations of *Rac1*, *Rac2* and *Mtl*, had no significant effect on the phenotype, the generation of mutant clones of the target GTPase may be required to suppress the $RacGAP50C^{RNAi}$ phenotype. Due to the hypomorphic nature of the $RacGAP50C^{RNAi}$ phenotype, clones may only need to be produced late in larval/pupal development, minimising the disruption to other actin-based events. Therefore, future studies directed at identifying suppressors of this phenotype would likely yield good candidates for the target of normal RacGAP50C activity during cytokinesis.

Another means of investigating which Rho GTPase is targeted by RacGAP50C, is to examine genetic interactions involving the RacGEF *trio*. *en::Gal4* driven expression of wild-type *trio* was capable of significantly enhancing the $RacGAP50C^{RNAi}$ phenotype. Although the *D. melanogaster* Trio has been shown to act as a GEF for Rac1, Rac2 and Mtl during photoreceptor axon pathfinding (Newsome *et al.*, 2000), this activation occurs through only one of the two GEF domains. The target for the second GEF

domain is currently unknown. However, the mammalian Trio has a separate Rac-specific and Rho-specific GEF domain (Debant *et al.,* 1996). Therefore expression of *trio* could potentially activate both Rho1 and the Rac GTPases, creating a very complicated genetic environment to interpret the results. Nevertheless, whether the phenotype produced by over-expression of *trio* can be suppressed by the removal of candidate Rho family GTPases should still be examined, as this may point to the target for RacGAP50C.

6.3.1.2 Localisation of PBL constructs.

The genetic interactions identified between *pbl* and *RacGAP50C* are highly suggestive of an important *in vivo* interaction between these two proteins. Although the *en::Gal4* driven expression of the *pbl* constructs such as $pbl^{\Delta RADECL/\ BRCT1}$ and $pbl^{\Delta DH}$ had strong synergistic interactions with the $RacGAP50C^{RNAi}$ phenotype, interestingly the pbl^{1-298} construct did not interact. It would be important to identify the subcellular localisation of these expressed *pbl* constructs, as well as observe if there is any disruption to the localisation of the endogenous RacGAP50C.

Chapter Seven: A genetic screen to identify components involved in *pbl* signalling.

7.1 Introduction

As discussed earlier, *pbl* encodes a protein that has a set of conserved domains characteristically found in Rho family GEFs. PBL is capable of interacting genetically and with the Rho1 GTPase (Prokopenko *et al.*, 1999). Rho1 is also the only Rho family member identified to play an essential role in cytokinesis in *C. elegans*, mammals and *Drosophila* (O'Connell *et al.*, 1999; Prokopenko *et al.*, 1999; Jantsch-Plunger *et al.*, 2000). Immediate downstream effectors of Rho include Citron kinase, Rho kinase and the forming-homology protein Diaphanous, all of which regulate actin cytoskeleton dynamics. Thus it is likely that the biological function of PBL involves Rho mediated regulation of the actin cytoskeleton during cell division.

Rho GTPases are involved in signalling to multiple downstream targets in various developmental and morphological contexts. One approach to identifying components of a particular signalling pathway is to screen for second sight mutations that dominantly modify a pre-existing mutant phenotype. Ectopic expression or loss of function mutations of genes can lead to morphological disruptions in structures such as the eye. In some cases the genetic background can be adequately sensitive, so that disruptions in potential regulators or effectors can modify the disrupted phenotype. The usefulness of this particular type of screen was first demonstrated in the identification of components involved in the Ras signalling pathway (Simon *et al.*, 1991).

Ectopic expression of a full-length wild-type *pbl* cDNA in cells posterior to the morphogenetic furrow using the *GMR-gal4* driver produces a dominant global roughening of the eye (Prokopenko *et al.*, 1999; O'Keefe *et al.*, 2001). This phenotype

is characterised by a disruption to both the ommatidial and bristle organisation. This *GMR-pbl* rough eye phenotype has previously been used to identify second site mutations that dominantly enhance or suppress this rough eye phenotype, using the Spradling lethal P-element collection and Bloomington Stock centre deficiencies covering the second and third chromosomes. Although a large proportion of the deficiency stocks enhanced the rough eye phenotype, only two deficiencies were capable of suppressing the rough eye phenotype. These deficiency stocks, *Df(2R)Jp8* and *Df (2L)E110,* uncovered the candidate genes *Rho1* and the actin-binding protein *chicadee* respectively. Null alleles of both *Rho1* and *chic* produce a strong dominant suppression of the *GMR-pbl* rough eye phenotype. Other candidate mutant alleles tested that were capable of suppressing the rough eye phenotype included the Rho-kinase allele rok^2 and the regulatory light chain of non-muscle myosin, *spaghetti-squash*, allele sqh^1. All of these dominant supressors identified can be envisaged to fit into the same pathway involving Rho-mediated actin/ myosin reorganisation during cytokinesis. Thus the *GMR-pbl* rough eye phenotype appears to be sensitive to dominant modifiers at second site locations.

This chapter describes a random mutagenesis screen conducted on the major autosomes, for strong dominant suppressors of the *GMR-pbl* rough eye phenotype. This would hopefully identify candidate genes involved in the PBL-mediated signalling pathway during cytokinesis.

7.1.1 EMS mutagenesis of *D. melanogaster*

The approach used to identify dominant suppressors of the *GMR-pbl* rough eye phenotype involved a random mutagenesis of the major autosomes of *Drosophila* (Figure 7.1). The autosomal second and third chromosomes of *Drosophila* represent approximately 75% of the overall *D. melanogaster* genome, and approximately 80% of the total euchromatic genomic DNA. Random point mutations were generated throughout the genome using the potent chemical mutagen, ethyl methylsulfonate (EMS).

Wild-type males, carrying isogenised second and third chromosomes, were fed a glucose diet laced with EMS. These males, carrying the mutagenised sperm, were

crossed to *GMR-pbl* females to separate the individual gametes. Males produced in the F1 progeny were screened for a strong dominant suppression of the rough eye phenotype. This approach failed to screen for dominant modifiers on the X chromosome, which would have required more complicated fly crosses to select and maintain the modifier. Males that displayed a dominant suppression were selected and crossed back to *GMR-pbl; isoIII* females to confirm that the suppressor mutation was germ-line transmissible.

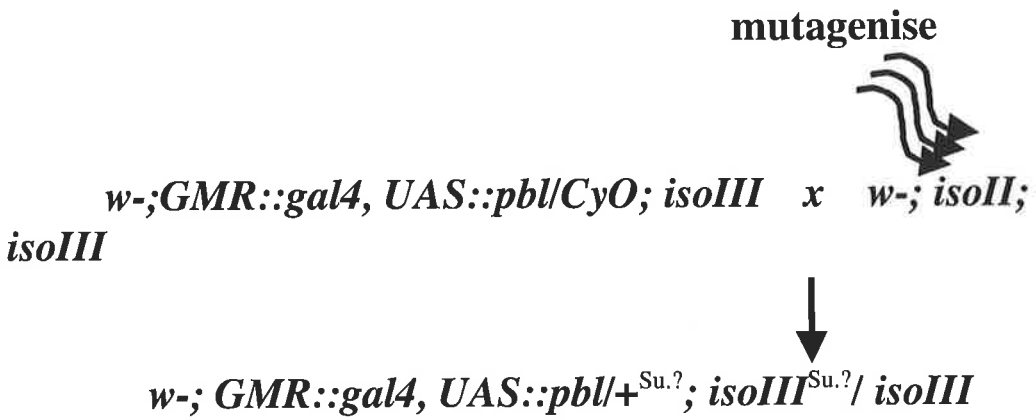

Figure 7.1 Scheme for identifying dominant suppressors of the *GMR-pbl* rough eye phenotype.

Wild-type males were mutagenised with EMS, and crossed to virgin *GMR-pbl* females at 25°C. Males from the F1 generation, carrying the *GMR-pbl* transgene, were examined for strong suppression of the rough eye phenotype, and selected for further analysis.

7.2 Results

7.2.1 Suppressors of *GMR-pbl*

Approximately 9300 male progeny of the mutagenised males, carrying the *GMR-pbl* construct, were examined for their ability to dominantly suppress the external rough eye phenotype. This resulted in the identification of seven independent modifiers, which were capable of varying levels of suppression, ranging from near wild-type to a moderate suppression (Figure 7.2). Each mutant was localised to a particular chromosome, and a balanced stock generated. Viability of homozygous mutants were

tested and shown that apart from the suppressor Su(*GMR-pbl*)2.1, the rest carried a recessive lethal. Although the lethality may not be linked with the suppressor mutation, the recessive lethality was used as the basis to test for allelism among the mutants. This identified five complementation groups (Table 7.1), (Su(*GMR-pbl*)2.1 and Su(*GMR-pbl*)2.2 formed one complementation group, Su(*GMR-pbl*)2.3 and Su(*GMR-pbl*)2.4 formed a second complementation group, while the others appeared to represent single suppressor alleles). All second chromosome suppressors stocks were recessive lethal, and were tested for complementation with the *Rho1* null alleles ($Rho1^{72O}$ *and* $Rho1^{72R}$). The suppressor line Su(*GMR-pbl*)2.3 was identified as the sole suppressor that failed to complement the *Rho1* null allele. However, the suppressor line Su(*GMR-pbl*)2.4, which failed to complement Su(*GMR-pbl*)2.3, does complement the *Rho1* null allele. This suggests that Su(*GMR-pbl*)2.3and Su(*GMR-pbl*)2.4 may share a common second sight lethal mutation, and therefore may not be part of the same complementation group. The probability of hitting the same second site lethal independent of the suppressor is extremely low, and therefore the shared lethal mutation may be a chromosomal disruption or a synthetic lethality between the second site lethals.

Each *GMR-pbl* suppressor line was tested for its ability to modify the rough eye phenotype caused by expression in the developing eye of a dominant negative *pbl* construct, $GMR\text{-}pbl^{\Delta DH}$ (Prokopenko *et al.*, 1999). The suppressor Su(*GMR-pbl*)2.5 from chromosome two and Su(*GMR-pbl*)3.1 and Su(GMR-pbl)2.1 from chromosome three, moderately to strongly enhanced the rough eye phenotype, while all other *GMR-pbl* suppressor lines strongly suppressed the dominant negative eye phenotype to an almost wild-type appearance (data not shown). This is surprising, especially for the case of the *Rho1* allele Su(*GMR-pbl*)2.3. *Rho1* null alleles strongly suppress the *GMR-pbl* rough eye phenotype but enhance the dominant negative eye phenotype, therefore Su(*GMR-pbl*)2.3 appears not to genetically act in the same way as a *Rho1* null allele.

Figure 7.2 Suppressors of the *GMR-pbl* rough eye phenotype.

Scanning electron micrographs of the dominantly suppressed *GMR-pbl* rough eye phenotype. (A) wild-type; (B) *GMR-pbl* rough eye phenotype. This general rough eye is characterised by an increased number of bristles. Suppression of the *GMR-pbl* rough eye phenotype with (C) Su(*GMR-pbl*)2.1; (D) Su(*GMR-pbl*)2.2; (E) Su(*GMR-pbl*)2.3; (F) Su(*GMR-pbl*)2.4; (G) Su(*GMR-pbl*)2.5; (H) Su(*GMR-pbl*)3.1 and (I) Su(*GMR-pbl*)3.2.

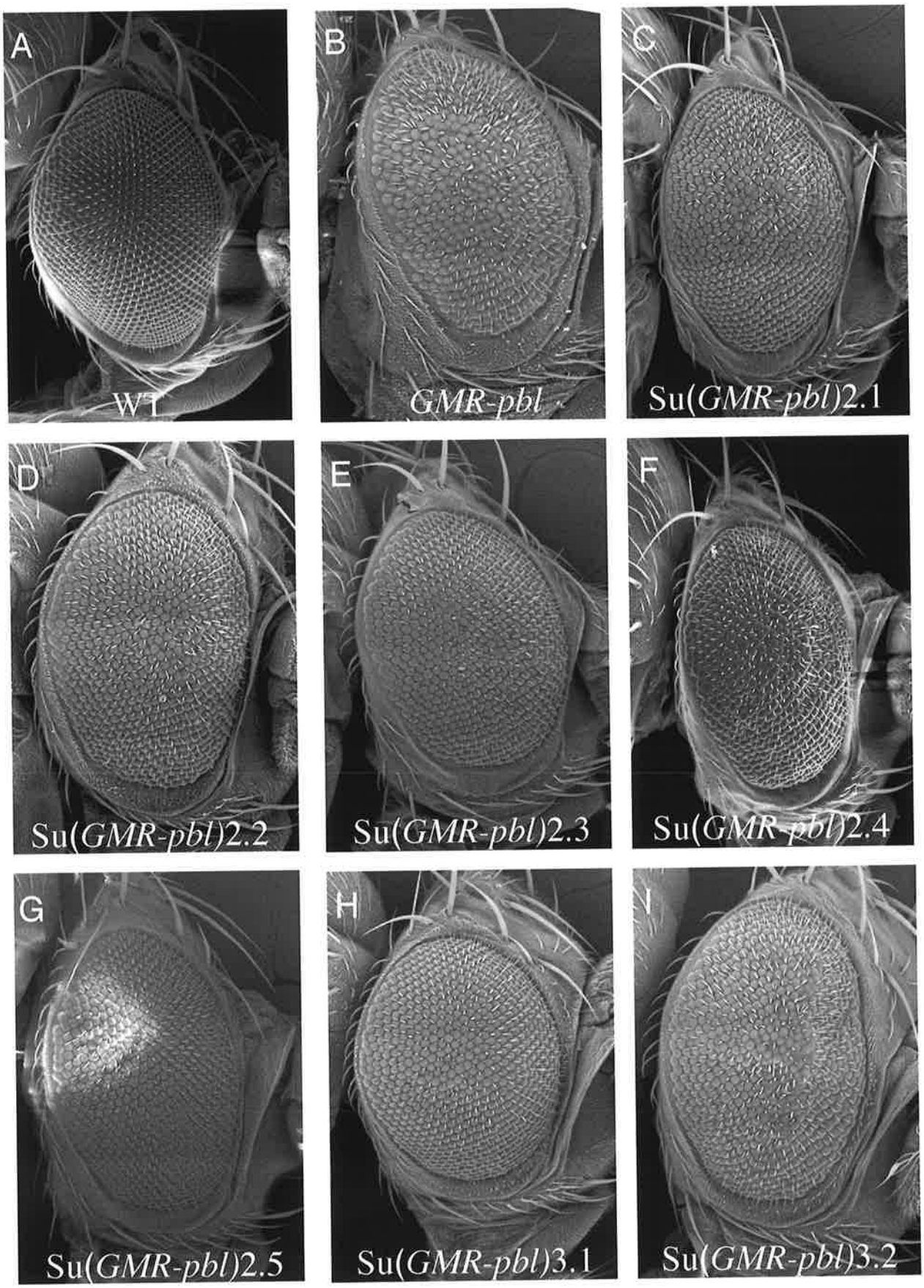
A
WT
B
GMR-pbl
C
Su(GMR-pbl)2.1
D
Su(GMR-pbl)2.2
E
Su(GMR-pbl)2.3
F
Su(GMR-pbl)2.4
G
Su(GMR-pbl)2.5
H
Su(GMR-pbl)3.1
I
Su(GMR-pbl)3.2

Table 7.1 Dominant genetic modifiers of *GMR-pbl*

Suppressor	ID ref. #	Chrom.	Genetic Loci	Candidate Gene(s)	*GMR-pbl*	*GMR-pblΔDH*
Complementation group I						
Su(*GMR-pbl*)2.1	XVI-II②	II	23C	*Lilliputian*	S+++	S++++
Su(*GMR-pbl*)2.2	LVII-II①	II			S+++	S++++
Complementation group II						
Su(*GMR-pbl*)2.3	XXXV-I①	II	52E3-4	*Rho1*	S++++	S++++
Su(*GMR-pbl*)2.4	LIX-II③	II			S+++	S++++
Complementation group III						
Su(*GMR-pbl*)2.5	XIII-I①	II	27.5-29		S++	E++
Complementation group IV						
Su(*GMR-pbl*)3.1	LI-II①	III			S++++	E++
Complementation group V						
Su(*GMR-pbl*)3.2	XXVII-I①	III			S++	E+++

S++++ very strong suppression (WT); S+++ strong suppression; S++ moderate suppression
E++++ very strong enhancment (WT); E+++ strong enhancement; E++ moderate enhancement

7.2.2 Molecular Analysis

The chromosomal position of Su(*GMR-pbl*)2.5 was mapped by mitotic recombination and deficiency analysis. Chromosomes generated from a random mutagenesis generally possess multiple lethals, therefore recombination mapping has the advantage of mapping the allele on the basis of its suppressor phenotype and not lethality (Figure 7.3). Su(*GMR-pbl*)2.5 was identified to have a recombination distance of 33% from *aristaless*, 28% from *black* and 50% from *speck*. This maps the suppressor to the cytological map position of 27.5-29 on chromosome 2. All deficiency stocks tested within this region complemented the lethality of the suppressor (Table 7.2). There are several possibilities to explain these

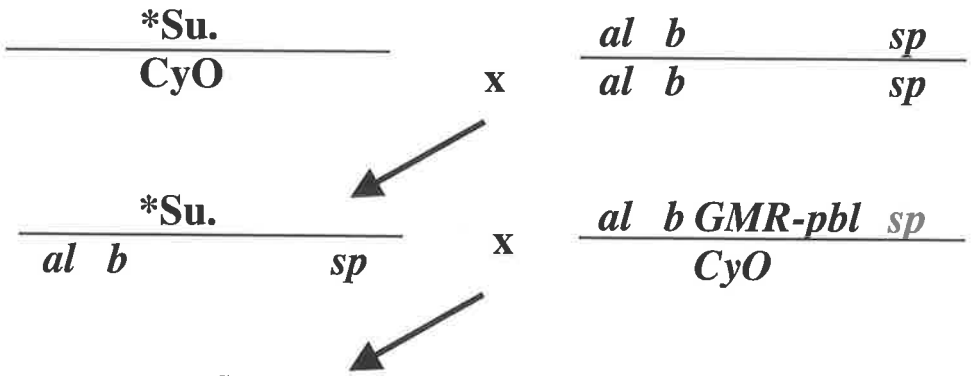

Figure 7.3 Procedure used to map Su(*GMR-pbl*)2.5

Crossing scheme used to map the second chromosome suppressor Su(*GMR-pbl*)2.1 via mitotic recombination. (*Su:suppressor allele; *al*:*aristaless*; *b*:*black*; sp:*speck*)

results. Firstly the suppressor may be positioned in one of the three gaps not uncovered by deficiencies within this region. Further gaps may also be present due to the imprecise cytological mapping of the deficiency breakpoints. Alternatively the mitotic recombination may not have correctly refined the cytological position of the suppressor. The suppressor may also be in the 27.5-29 region but may not be a recessive lethal.

The two alleles that make up complementation group I, Su(*GMR-pbl*)2.2 and Su(*GMR-pbl*)2.1, were also mapped by mitotic recombination followed by deficiency complementation, refining the location of the suppressor to cytological region 23. This was further narrowed down by smaller deficiencies and then with lethal *P*-element insertions within this region. Both alleles failed to complement the lethal stock *l(2)23Cc*, and all three were subsequently identified to fail to complement *P*-element stocks that disrupted the maternal pair-rule gene *lilliputian* ($lilli^{k054331}$ and $lilli^{00632}$).

Table 7.2 Complementation of Su(*GMR-pbl*)2.5 with deficiency stocks

Deficiency stock	Region disrupted	Comp./fail to comp.
Df(2L)Dwee-delta5	27A-28A	complemented
Df(2L)Spd^{l2}	27C01-28A	complemented
Df(2L)spd	27D-28C	complemented
Df(2L)XE-3801	27E02-28D01	complemented
Df(2L)XE-2750	28B02-28D03	complemented
Df(2L)Trf-C6R31	28DE	complemented
Df(2L)TE29Aa-11	28E04-29C01	complemented
Df(2L)N22-14	29C01-30C09	complemented
Df(2L)N22-5	29D01-30D01	complemented
Df(2L)30A-C	29F07-30C05	complemented

Recombination mapping involving the suppressor alleles of complementation group II failed to show any specific linkage with any marker. The third chromosome suppressors, Su(*GMR-pbl*)3.1 and Su(GMR-pbl)2.1, were tested for complementation with the null candidate alleles of *pbl, pav* and *mbc*. However, all crosses revealed complementation between these alleles and the suppressors.

7.3 Discussion

Ectopic expression of wild-type *pbl* in cells posterior to the morphogenetic furrow results in the disruption of the exterior morphology of the eye. This rough eye phenotype was used as the basis of a screen to identify regulatory and effector molecules involved in PBL signalling. Several candidate alleles (*Rho1, chic, sqh* and *rok*) have previously been identified to suppress the *GMR-pbl* rough eye phenotype. This chapter presents research conducted to identify novel components involved in *pbl* signalling. A random EMS mutatgenesis of the second and third chromosomes identified seven strong suppressors of *GMR-pbl* that fit into at least five complementation groups.

From the original seven suppressors identified, genetic analysis revealed that two of the very strong suppressing alleles, that make up complementation group I, were *lilliputian*

alleles. Lilliputian is a maternal pair-rule gene that acts in cytoskeletal regulation, segmentation and morphogenesis (Tang *et al.,* 2001). *Lilliputian* has previously been identified in many eye modification screens as a dominant suppressor (Dickson *et al.,* 1996; Neufeld *et al.,* 1998; Rebay *et al.,* 2000). As discussed by Tang and colleagues (2001), *lilli* appears to act as a factor required for *GMR* transcriptional activation. This is also evident in the fact that both *lilliputian* alleles were strong dominant suppressors of both *GMR-pbl* and *GMR-pblΔDH* rough eye phenotype.

Candidate modifiers would be expected to exert opposite effects on the *GMR-pbl* or the *GMR-ΔDHpbl* phenotypes. For example, removing one copy of *Rho1* dominantly suppresses the phenotype caused by the ectopic expression of wild-type *pbl* but enhances the dominant negative rough eye phenotype. This suggests that the *GMR-pbl* suppressors Su(*GMR-pbl*)2.5, Su(*GMR-pbl*)3.1 and Su(GMR-pbl)2.1, are more likely to represent candidate proteins involved in *pbl*-mediated signalling. The remaining suppressors, that dominantly suppress both the rough eye phenotypes of *GMR-pbl* and *GMR-ΔDHpbl*, may be non-specific regulators of *Gal4::UAS* expression systems, like *lilliputian*. The suppressor Su(*GMR-pbl*)2.3 fails to complement *Rho1* and both strongly suppress the *GMR-pbl* rough eye phenotype. However, Su(*GMR-pbl*)2.3, unlike the null *Rho1* alleles, suppresses the dominant negative *pbl* rough eye phenotype. Thus, Su(*GMR-pbl*)2.3 fails to act genetically like a null *Rho1* allele, or even a possible hypomorphic *Rho1* allele. One possibility is Su(*GMR-pbl*)2.3 is not a *Rho1* allele, but instead a synthetic lethality occurs with *Rho1*. The other member of complementation group II, Su(*GMR-pbl*)2.4, appears even more likely not to be a *Rho1* allele, due to its complementation of the *Rho1* mutant allele and the observation that it suppressors the *GMR-ΔDHpbl* rough eye phenotype. Sequencing the genomic region of *Rho1* in both Su(*GMR-pbl*)2.3 and Su(*GMR-pbl*)2.4 suppressor lines could be used to determine if there are any *Rho1* molecular lesions. In the case of Su(*GMR-pbl*)2.3, if it turns out to be a *Rho1* allele, the molecular lesion could be of significant interest, due to its unusual genetic interactions with *pbl.*

Rho1 had previously been identified as the only strong suppressor of the *GMR-pbl* rough eye phenotype. The number of *Rho1* alleles identified from the screen should be an indication of the level of saturation. Present results indicate that potential only one

suppressor (Su(*GMR-pbl*)2.3) is a *Rho1* allele. This, as well as the evidence suggesting that the majority of suppressors are single allele complementation groups, indicates the low level of genome coverage achieved in this screen.

Future work will require the mapping of the remaining suppressors and further investigation of any potential candidates. As stated above, based solely on the dominant modifier effects, the suppressor lines Su(*GMR-pbl*)2.5, Su(*GMR-pbl*)3.1 and Su(GMR-pbl)2.1 are prime candidates for regulating *pbl* signalling. Previous studies have shown that the *GMR-pbl* phenotype appears sensitive enough to identify modifiers involved in PBL-mediated Rho1 activation. A continuation of the screen could be helpful in the identification of more components in this signalling pathway. With the release of new and more *P*-element stocks, these may be a more effective way to quickly identify candidate modifiers, and could easily include stocks positioned on the X chromosome.

Chapter Eight: General discussion and future directions.

8.1 Introduction

The *Drosophila melanogaster pbl* gene encodes a putative Rho family GEF that is essential for cytokinesis. Cytokinesis fails in the 14th and subsequent mitoses in homozygous *pbl* mutants (Hime and Saint, 1992; Lehner, 1992). Evidence suggests that PBL mediated activation of Rho1 at the contractile ring is required for the correct formation and function of contractile ring components (Prokopenko *et al.,* 1999). As well as possessing the DH/PH GEF domain, PBL also contains tandem N-terminal BRCT domains. Previous studies involving other proteins have shown that BRCT domains act as protein-protein interaction domains and are found in proteins that play a role in DNA damage sensing and repair (Bork *et al.,* 1997; Callebaut and Mornon, 1997).

In this thesis the role of the N-terminal domains of PBL was investigated. This region of PBL was found to interact with the Rho family GAP protein, RacGAP50C. Further experiments revealed that RacGAP50C was essential for cytokinesis and formed an *in vivo* complex with the kinesin–like motor protein, Pavarotti. During anaphase/telophase, the majority of the RacGAP50C-PAV complexes localise to the midzone region of cortically localised central spindle MTs. Furthermore, genetic interaction studies identified strong interactions between *RacGAP50C* and both *pbl* and *Rac1*. These results have led me to propose a model, whereby the PAV-RacGAP50C-PBL complex positions the contractile ring and regulates cortical furrowing.

8.2 PBL interacts with a number of proteins with both nuclear and cytoplasmic functions.

pbl is essential for cytokinesis in *Drosophila*. PBL activates Rho1 through its DH/PH GEF domain, to coordinate the formation and function of the contractile ring (Prokopenko *et al.,* 1999). In addition to this cytoplasmic role, evidence suggests that PBL may also have a nuclear function. A hypomorphic allele of *pbl* has been shown to be hypersensitive to irradiation (Harley, 2002). During late telophase PBL accumulates in the nucleus and remains there until metaphase of the next cell cycle (Prokopenko *et al.,* 1999). PBL also contains two tandem highly conserved BRCT domains in the N-terminus, which are found in other proteins that play roles in DNA repair pathways. Taken as a whole, this evidence supports the idea of a separate nuclear function for PBL. To explore the role of these predicted nuclear N-terminal PBL domains, a yeast two-hybrid screen was conducted to identify candidate interacting proteins. This screen identified a number of proteins with potential nuclear and cytoplasmic roles.

Although the N-terminus of PBL may be capable of interacting with several proteins during different stages of cell division or within different intracellular pools, it is likely that only a few of these proteins identified are true *in vivo* PBL interactors. RacGAP50C was the only candidate interactor that was studied in depth. RacGAP50C was shown to exist as a complex with PBL *in vivo*. Of the remaining candidate interactors identified, Armadillo (the *Drosophila* ortholog of β-catenin) appears to be a worthy candidate for further investigations. It is known that *armadillo* has conserved roles in cadherin-catenin based cytoskeletal interactions (Peifer, 1993), but has also been identified to genetically interact with *pbl* (Greaves *et al.,* 1999). Future work involving the other candidate interactors should begin by confirming the presence of an *in vivo* protein complex with PBL. Coimmunoprecipitations, such as that conducted with RacGAP50C, could be performed to confirm the presence of such a protein complex. Alternatively, mass-spectrometry studies of proteins pulled down in PBL immunoprecipitation experiments could complement the yeast two-hybrid interactor results, as well as identify other proteins that complex with, but not necessarily bind directly to, PBL.

8.3 The role of RacGAP50C during cytokinesis.

The *D. melanogaster RacGAP50C*, like the *C. elegans cyk-4* and mammalian *MgcRacGAP* (Jantsch-Plunger *et al.,* 2000; Hirose *et al.,* 2001; Van de Putte *et al.,* 2001; Mishima *et al.,* 2002), is essential for cytokinesis. Significant levels of multinucleate cells were generated in *Drosophila* S2 cultured cells treated with *RacGAP50C* RNAi, as well as *in vivo* with the ectopic expression of an inducible *RacGAP50C* RNAi construct. Observations of *cyk-4* mutant embryos revealed that they were capable of initiating but not completing furrow ingression (Jantsch-Plunger *et al.,* 2000). This suggests that this RacGAP is required during the late stage of cytokinesis, possibly involved in stabilisation of the ingressed furrow, resolving the midbody MTs, or vesical transport/deposition for abscission. Comparative analysis of cytokinetic mutant phenotypes of orthologous nematode and fruit-fly genes reveals significant differences. For instance, the *C. elegans* kinesin-like motor protein *zen-4* plays an essential role in maintaining the bundled central spindle MTs during cytokinesis and, similar to the *cyk-4* mutant embryos, *zen-4* mutant embryos can still initiate but fail to complete cortical furrowing (Raich *et al.,* 1998). The *D. melanogaster* ortholog of *zen-4* is the *pararotti* (*pav*) gene. Homozygous *pav* mutant embryos also have a reduction in the level of central spindle MT bundling. However, contractile ring components fail to assemble and no cortical furrowing is observed (Adams *et al.,* 1998), suggesting a much earlier defect in cytokinesis.

It is now widely accepted that different mechanisms are involved during cytokinesis of cells in large invertebrate embryos, such as *C. elegans*, compared with smaller animal cells (Murata-Hori and Wang, 2002). Formation of the cleavage furrow and initiation of furrowing in *C. elegans* embryos, like the echinoderm embryos studied by Rappaport, relies on a stimulatory signal generated primarily from astral MTs (Rappaport, 1985). However, in cultured mammalian cells and *D. melanogaster* cells, the primary stimulus is produced by the bundled central spindle MTs (Cao and Wang, 1990; Wheatley and Wang, 1996; Giansanti *et al.,* 1998). Evidence therefore suggests that disrupting *RacGAP50C* in *D. melanogaster* cells would disrupt the formation of the contractile ring and no cortical furrowing would be observed. This is supported by recent analysis of RNAi treated *Drosophila* S2 cells (Somma *et al.,* 2002). However, the exact cytokinetic defect in *RacGAP50C* mutants remains to be determined.

Initial examinations of the *RacGAP50C* mutant alleles *RacGAP50C*^{AR2} and *RacGAP50C*^{DH15}, did not reveal any disruption to the epithelial cell divisions during the early embryonic divisions. This is likely to reflect a high maternal contribution. Examination of cortical furrowing in the absence of RacGAP50C may need to be conducted using a different technique. The disruption to cytokinesis could be generated by RNAi treatment of *Drosophila* S2 cells. Although the disruption produced by RNAi may not be fully penetrant and a small amount of residual protein may still be sufficient to allow the initiation of some cortical furrowing. Therefore, a large number of cells would need to be examined, to determine the phenotype in the absence of RacGAP50C. The effect of cortical furrowing in the absence of RacGAP50C could also be examined in cells injected with anti-RacGAP50C antibodies.

Another significant difference between the *C. elegans* and *D. melanogaster* systems involves the actual analysis of cytokinetic phenotypes. The initial divisions of the *C. elegans* embryos are studied live, showing fine morphological detail using Nomarski microscopy, while *D. melanogaster* phenotypes are generally characterised in fixed tissue preparations. The disadvantage with fixed tissues is that subtle morphological detail such as a partial furrowed cortex may not be obvious and fixation techniques may not preserve such cell shapes. The use of a biological tool such as GFP tagged Spaghetti-Squash (myosin II regulatory light chain), would allow the visualisation of equatorial cortical movements during anaphase/ telophase. These studies have been initiated in our labortory and should provide a better understanding of cytokinesis in *D. melanogaster*.

8.4 RacGAP50C localises to the central spindle microtubules and the midbody during anaphase/telophase.

The intracellular localisation of MgcRacGAP and CYK-4 has previously been studied and reported. Both orthologs localise to the central spindle region and midbody during the late stages of mitosis (Jantsch-Plunger *et al.*, 2000; Hirose *et al.*, 2001; Kitamura *et al.*, 2001; Mishima *et al.*, 2002). Immunological studies revealed that RacGAP50C has a similar localisation pattern in *D. melanogaster* cells.

In mammalian cells MgcRacGAP and the mammalian ortholog of PBL, Ect2, appear to colocalise throughout mitosis (Tatsumoto *et al.*, 1999; Hirose *et al.*, 2001). Ect2 and MgcRacGAP were shown to interact in a yeast two-hybrid assay and due to their apparent identical localisations, may associate throughout mitosis. However, in *D. melanogaster* embryonic epithelial cells, PBL has a significantly different localisation to that reported for Ect2. Instead of localising to MTs, PBL is observed to localise to the equatorial cortex during anaphase/ telophase (Prokopenko *et al.*, 1999). This suggests that an interaction between PBL and RacGAP50C may occur at the time of contractile ring ingression, where an interaction between the cortex and bundled MTs is postulated to occur. Alternatively an interaction between these two proteins could occur in the nucleus of interphase cells. The nuclear versus cytoplasmic interaction could be determined with co-immunoprecipitation experiments using nuclear versus cytoplasmic cellular fractions. The visualisation of the proteins interacting within living cells could also address this question. This could be investigated using fluorescence resonance energy transfer (FRET) analysis.

One significant difference in localisation was observed between RacGAP50C and its orthologs MgcRacGAP and CYK-4. Despite having an apparently identical intracellular localisation, three-dimensional projections of late anaphase/early telophase cells revealed that the majority of RacGAP50C localised to punctate spots at the midzone of cortically localised MTs. This RacGAP50C localisation appeared to be on the inner face of the contractile ring, as seen by colocalisation studies performed with PBL, the contractile ring components PNT and Anillin, and the MT binding protein PAV.

It was initially thought that the BRCT domains of PBL were involved in a separate nuclear role, however a more exciting proposal is that the function of these domains is to interact with RacGAP50C during anaphase/telophase to coordinate the reorganisation of both the microtubule and actin cytoskeletons during cytokinesis.

8.5 RacGAP50C interacts with the kinesin-like motor protein Pavarotti

Localisation of the *C. elegans* RacGAP50C ortholog, CYK-4, and the PAV kinesin-like motor protein ortholog ZEN-4, have been shown to be interdependent (Jantsch-Plunger *et al.*, 2000). Recently, an *in vivo* complex between this RacGAP and kinesin-like motor protein, termed centralspindlin, has been shown to exist in both *C. elegans* and mammalian tissues and to bundle MTs *in vitro* (Mishima *et al.*, 2002). Various models for how the centralspindlin complex mediates MT bundling have been proposed (Mishima *et al.*, 2002). According to one model, individual centralspindlin complexes interact with multiple MTs to bundle them. A second model proposes that separate centralspindlin complexes, on separate MTs, interact to form multimeric higher order structures.

In this study, a conserved complex between RacGAP50C and the kinesin-like motor protein PAV was identified in *Drosophila* embryonic tissues. Both proteins were found to colocalise to the cortical MTs during anaphase/telophase and RacGAP50C was shown to require PAV for correct localisation. Two-hybrid assays revealed that the N-terminus of RacGAP50C, adjacent to the PBL interacting domain, was both necessary and sufficient for the interaction with PAV. The N-terminus of the *C. elegans* CYK-4 has also recently been shown to be necessary for interacting with ZEN-4, as well as for homodimerisation (Mishima *et al.*, 2002). It is curious that the N-terminus of this RacGAP is critical with respect to a number of protein interactions. It is possible that the formation of a RacGAP homodimer is a prerequisite for further interactions with the kinesin-like motor protein or PBL. Alternatively, PBL and PAV may compete with each other for binding to RacGAP50C.

8.6 RacGAP50C interacts genetically with *Rac1* and *pbl*

The identification of the Rho family GTPase that is targeted for inactivation by RacGAP50C is essential for fully understanding the signalling mechanisms involved during cytokinesis. Previous studies have shown that MgcRacGAP and CYK-4 are capable of inactivating Rac1 and Cdc42, with a much higher affinity than Rho1 in *in*

vitro GAP assays (Toure *et al.*, 1998; Jantsch-Plunger *et al.*, 2000; Kawashima *et al.*, 2000). *RacGAP50C* has also been shown to genetically interact with *Rac1* and *Cdc42* during wing vein formation (Sotillos and Campuzano, 2000). The difficulty with identifying the *in vivo* target of RacGAP50C is that Rho family members are involved in a wide range of actin-based reorganisation events and are capable of cross-activating and inhibiting other members. Ectopic expression of these proteins and effectors is likely to cause inappropriate activation or suppression of other Rho family signalling pathways.

In this study, an inducible *RacGAP50C* RNAi construct (*RacGAP50C*^{RNAi}) was used to disrupt *RacGAP50C* function *in vivo*. Expression of this construct disrupted cytokinesis in a dose dependent manner, suggesting that this phenotype may provide a good assay to identify the target Rho family GTPase. Surprisingly, no modification of the *RacGAP50C*^{RNAi} phenotype was achieved with mutants in the candidate Rho family members tested. A number of explanations are possible. Firstly, despite the dose dependent sensitivity of the RNAi construct, the mutant phenotype may not be suitably sensitive to be modified in a heterozygous candidate gene environment. Therefore, suppressing modifications may need to be assayed by clonal analysis of mutations in the various Rho family members. Secondly, the target Rho family member may not have been tested, as several novel Rho family members remain to be tested. Furthermore, functional redundancy may also occur between various Rho family members, thus masking genetic interactions.

Although removing one copy of candidate Rho family members failed to modify the *RacGAP50C*^{RNAi} phenotype, strong genetic interactions were observed when *Rac1* and wild-type *RacGAP50C* were ectopically expressed. RacGAP50C was capable of suppressing the phenotype produced by ectopic expression of *Rac1* and enhanced the phenotype produced by ectopic expression of the dominant negative Rac1, *Rac1*^{N17}. These interactions clearly demonstrate that RacGAP50C is capable of targeting Rac1 *in vivo* for inactivation, consistent with previous reported genetic interactions (Sotillos and Campuzano, 2000). However, it is currently unclear in which biological context this interaction is relevant. When over-expressing a protein, an artificial environment is generated. This may result in proteins interacting where normally they would not.

Furthermore, the relationship between the different Rac members adds further complications. A functional redundancy exists between Rac1, Rac2 and Mtl, but no disruption to cytokinesis has been reported in flies homozygous for all three *Rac* genes (*Rac1, Rac2* and *Mtl*) (Hakeda-Suzuki *et al.,* 2002; Ng *et al.,* 2002), suggesting that the activity of these small GTPases is not required for cytokinesis. However, the likely function of RacGAP50C is to inactivate a Rho family GTPase, allowing cytokinesis. Therefore, a disruption to cytokinesis would only be observed by inappropriately activating the target GTPase. However, ectopic expression of constitutively active GTPases is likely to generate general actin cytoskeletal disruptions, which could indirectly disrupt cytokinesis, thus making interpretation of the cellular phenotypes difficult.

The *RacGAP50C*^{RNAi} construct is capable of genetically interacting with various *pbl* constructs. An enhanced disruption to the *RacGAP50C*^{RNAi} wing phenotype was observed with expression of PBL carrying an N-terminus (RacGAP50C interacting domain) deletion. This suggests that the PBL-RacGAP50C interaction is a necessary and important regulatory interaction in the control of cytokinesis. A significantly strong synergistic interaction was also observed with the expression of PBL carrying a deletion within the DH domain, which has previously been shown to disrupt cytokinesis (Prokopenko *et al.,* 1999; O'Keefe *et al.,* 2001). This suggests that RacGAP50C does not function as the GAP opposite PBL in the regulation of Rho1 activity during cytokinesis. If RacGAP50C targeted Rho1 for inactivation during cytokinesis, the dominant negative PBL phenotype should be rescued by depleting the system of RacGAP50C using the *RacGAP50C*^{RNAi} construct. Instead, a significant enhancement was observed, resulting in the loss of almost all tissue. This suggests that RacGAP50C targets a different Rho family GTPase, which has an inhibitory effect on Rho mediated signalling during cytokinesis. The identity of this GTPase remains to be confirmed.

8.7 Is the PBL-RacGAP50C-PAV complex the stimulatory signal that regulates the coordination of MT and actin cytoskeletons during cytokinesis?

The mechanism that positions the contractile ring and initiates furrowing remains to be elucidated. A number of studies have shown that the stimulatory signal derives from the overlapping MTs of the central spindle (Cao and Wang, 1996; Wheatley and Wang, 1996; Murata-Hori and Wang, 2002). The research presented in this thesis led to the discovery that RacGAP50C-PAV complexes in the central spindle midzone region are localised to cortical MTs. I propose a novel model in which the PAV-RacGAP50C-PBL interactions are necessary for the positioning and regulation of the contractile ring. The arrival of the RacGAP50C-PAV complex to the central spindle would enable the establishment of an interaction with PBL. This PAV-RacGAP50C-PBL complex would then be capable of initiating cytokinesis, via RacGAP50C-targeted inactivation of an unknown Rho family GTPase and PBL-mediated activation of Rho1 downstream targets (citron kinase, diaphanous) (Figure 8.1). This model combines previous reports that have discussed the importance of both the contractile ring and central spindle and lends strong support to the model put forward by Gatti and colleagues that the integrity of the central spindle and contractile ring are interdependent (Gatti *et al.*, 2000; Somma *et al.*, 2002). The localisation of PAV-RacGAP50C (centralspindlin) complexes to the midzone of cortically associated MTs immediately prior to cortical furrowing suitably positions this complex to stimulate the assembly and/or furrowing of the contractile ring at the equatorial plane. The localisation of the PAV-RacGAP50C complex is independent of cortically associated PBL, so it is possible that PBL is recruited to the contractile-ring by the PAV-RacGAP50C complex. Perhaps the interaction between PBL and RacGAP50C is purely mechanical and the functional requirement of this interaction is to generate the correct GTPase signalling environment during cytokinesis. The importance of this interaction could be addressed by substituting the interacting domains of PBL and RacGAP50C with independent interacting domains and observing whether the protein complex can still perform its endogenous biological role during cytokinesis. The discovery that the PAV and PBL interaction domains of RacGAP50C are adjacent to each other and that this region is also involved in

Figure 8.1 The PAV-RacGAP50C-PBL complex provides a molecular model for the positioning and regulation of the contractile-ring.

I propose that the PAV-RacGAP50C MT midzone-localised complex positions the contractile ring and coordinates cytoskeletal remodelling during cytokinesis. (A) RacGAP50C specifies the site for contractile ring formation by localising to the midzone of the central spindle and cortical MTs, through the activity of the plus end-directed kinesin-like motor protein, PAV. (B) At the midzone, cortically localised PBL interacts with the RacGAP50C-PAV complexes, allowing the activation of Rho1 signalling pathways, including the FH protein Diaphanous and citron kinase needed for cortical furrowing. RacGAP50C is postulated to inactivate a Rho family member(s), needed for the removal of an inhibitory signal preventing PBL-mediated activation of Rho1.

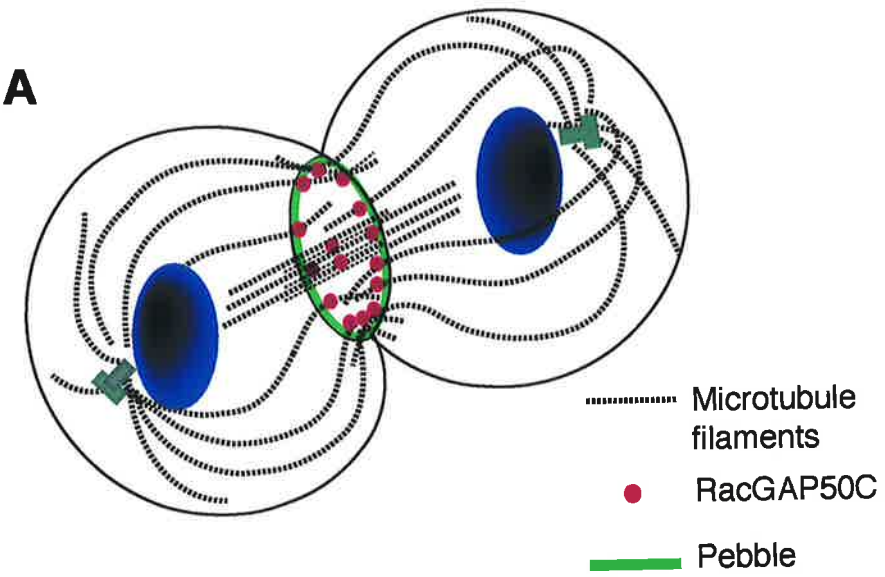
A
Microtubule filaments
RacGAP50C
Pebble

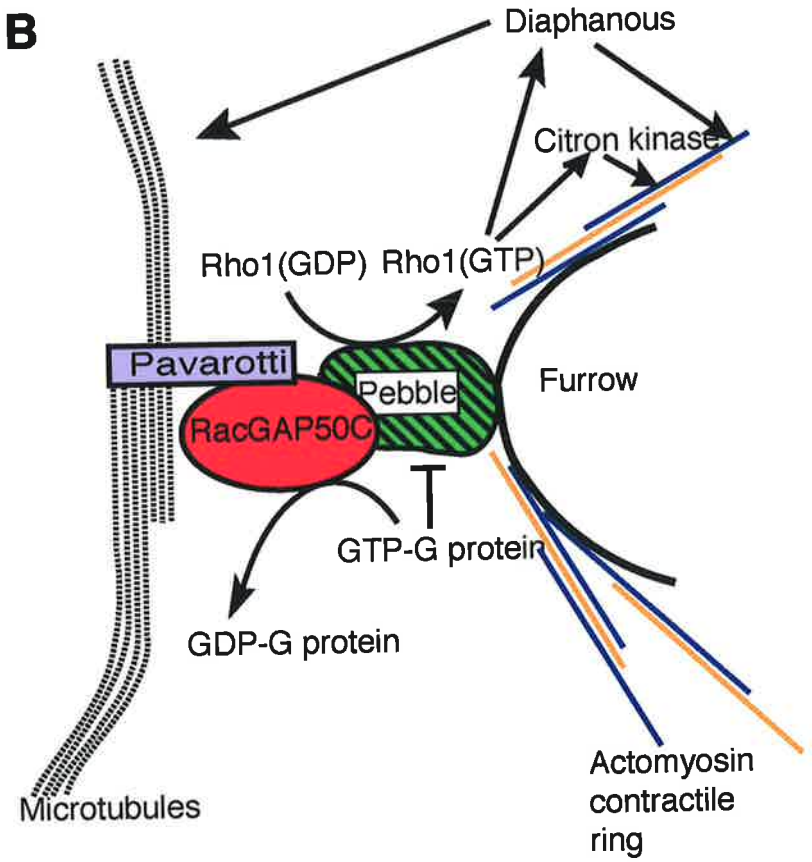
B
Diaphanous
Citron kinase
Rho1(GDP)
Rho1(GTP)
Pavarotti
Pebble
RacGAP50C
Furrow
GTP-G protein
GDP-G protein
Microtubules
Actomyosin contractile ring

homodimerisation, suggests competition for binding may exist between these proteins. Upon completion of the initial MT bundling, PBL, which may have a higher affinity for RacGAP50C, would displace PAV and thus form a new functional complex required for the next stage of signalling cytokinesis, while the constriction of the cortex would generate the midbody.

The only inconsistencies with this model lie with the cytokinetic mutant phenotypes observed in *C. elegans*. Unlike most other animal cells, extensive cortical furrowing in *C. elegans* embryos can still be initiated in the apparent absence of a central spindle, suggesting that the central spindle is not needed for the formation or initiation of the contractile ring, but instead plays a much later role in cytokinesis. Although CYK-4 has been reported to colocalise to the central spindle midzone during anaphase/telophase (Jantsch-Plunger *et al.,* 2000), it is possible that the localisation at the midzone region of cortically associated astral MTs was missed. Infact, ZEN-4, which has been shown to form the centralspindlin complex with CYK-4, was originally reported to localise to the central spindle (Raich *et al.,* 1998), but has since been reported to also localise ahead of the leading edge of the ingressing furrow (Jantsch-Plunger and Glotzer, 1999). The amount of CYK-4/ZEN-4 protein detected at the midzone region of the central spindle in *C. elegans* may have been so intense relative to the staining at the midzone of the astral MTs, that the localisation at the cortex was overlooked. The localisation of CYK-4 during anaphase/telophase, particularly on cortically associated astral MTs, therefore warrants further investigation. The initial furrowing followed by the failure to complete cytokinesis in *cyk-4* and *zen-4* mutant embryos may occur due to a residual amount of CYK-4/ZEN-4 complexes. As discussed above the involvement of the CYK-4/ZEN-4 complexes with astral MTs may have been missed. Therefore the *C. elegans* *cyk-4* and *zen-4* mutant phenotypes should be reinvestigated within a mutant background that is devoid of astral MTs, thereby confirming any interaction with the astral MTs. There are alternative explanations as to why the cytokinetic phenotypes observed in *C. elegans* appear significantly different to that of other animal cells. It is possible that the PBL-RacGAP50C complex is not required for the initiation of furrowing, but plays a role later in cytokinesis, or that significant differences exist between the mechanisms involved in accomplishing cytokinesis in *C. elegans* embryos compared to *Drosophila* epithelial cells. An uncharacterised ortholog of *pbl*, *let-21*,

also exists in *C. elegans*. Future studies involving the disruption of *let-21* should be investigated and would provide valuable information as to the mechanisms involved in *C. elegans* cytokinesis. It would be of considerable importance to observe if cortical furrowing can still occur in *let-21* disrupted embryos, and whether LET-21 is cortically associated like PBL, or localises to the central spindle like Ect2.

In retrospect, this work has provided the first molecular model to potentially account for the positioning and activation of cytokinesis in animal cells.

8.8 Summary

This thesis describes the identification of a conserved PAV-RacGAP50C-PBL interaction in *D. melanogaster*. All three of these proteins are essential for cytokinesis. The Pav-RacGAP50C complex localises to the midzone region of cortically associated MTs during anaphase/telophase. It is at this stage that an interaction between RacGAP50C and the cortically associated PBL RhoGEF appears to occur. Genetic interactions suggest that RacGAP50C targets a Rho family GTPase, but, due to functional redundancy amongst the Rac's, may target several for inactivation during cytokinesis. This interaction possibly relieves an inhibitory signal, allowing PBL mediated activation of the Rho1 signalling pathway during cytokinesis. Although yet to be proven, the timed arrival of the conserved
RacGAP50C-PAV complex to the central spindle at anaphase and the physical association between the Rho family GAP, RacGAP50C, and the PBL RhoGEF, is suggestive evidence that the PAV-RacGAP50C-PBL complex produces the stimulatory signal that initiates and regulates cytokinesis. This study has therefore provided a key novel molecular model for cytokinesis regulation that can be tested in future studies.

References

Adachi, H., Takahashi, Y., Hasebe, T., Shirouzu, M., Yokoyama, S. and Sutoh, K. (1997). "*Dictyostelium* IQGAP-related protein specifically involved in the completion of cytokinesis." *Journal of Cell Biology* **137**(4): 891-8.

Adam, J. C., Pringle, J. R. and Peifer, M. (2000). "Evidence for functional differentiation among *Drosophila* septins in cytokinesis and cellularization." *Molecular Biology of the Cell* **11**(9): 3123-35.

Adams, R. R., Tavares, A. A., Salzberg, A., Bellen, H. J. and Glover, D. M. (1998). "*pavarotti* encodes a kinesin-like protein required to organize the central spindle and contractile ring for cytokinesis." *Genes and Development* **12**(10): 1483-94.

Adler, P. N., Liu, J. and Charlton, J. (2000). "Cell size and the morphogenesis of wing hairs in *Drosophila*." *Genesis* **28**: 82-91.

Ahmed, S., Lee, J., Wen, L.-P., Zhao, Z., Ho, J., Best, A., Kozma, R. and Lim, L. (1994). "Breakpoint cluster region gene product-related domain of n-Chimaerin. Discrimination between Rac-binding and GTPase activating residues by mutational analysis." *The Journal of Biological Chemistry* **269**(26): 17642-17648.

Amano, M., Ito, M., Kimura, K., Fukata, Y., Chihara, K., Nakano, T., Matsuura, Y. and Kaibuchi, K. (1996). "Phosphorylation and activation of myosin by Rho-associated kinase (Rho-kinase)." *Journal of Biological Chemistry* **271**(34): 20246-9.

Arar, C., Ott, M.-O., Toure, A. and Gacon, G. (1999). "Structure and expression of murine *mgcRacGAP*: its developmental regulation suggests a role for the Rac/ MgcRacGAP signalling pathway in neurogenesis." *Journal of Biochemisty* **343**: 225-230.

Arbeitman, M. C., Furlong, E. E. M., Iman, F., Johnson, E., Null, B. H., Baker, B. S., Krasnow, M. A., Scott, M. P., Davis, R. W. and White, K. P. (2002). "Gene expression during the life cycle of *Drosophila melanogaster*." *Science* **297**: 2270-2275.

Ausubel, S. F., Brent, R. E., Kingston, R. E., Moore, D., Seidman, J. G., Smith, J. A. and Struhl, K. (1994). "Current Protocols in Molecular Biology." *NEW YORK: WILEY, 1994.*

Bahler, J., Steever, A. B., Wheatley, S., Wang, Y. l., Pringle, J. R., Gould, K. L. and McCollum, D. (1998). "Role of polo kinase and Mid1p in determining the site of cell division in fission yeast." *Journal of Cell Biology* **143**(6): 1603-16.

Balch, W. E. (1990). "Small GTP-binding proteins in vesicular transport." *Trends in Biochemical Sciences* **15**: 473-477.

Bamburg, J. R. (1999). "Proteins of the ADF/cofilin family: essential regulators of actin dynamics." **15**: 185-230.

Bardin, A. J., Visintin, R. and Amon, A. (2000). "A mechanism for coupling exit from mitosis to partitioning of the nucleus." *Cell* **102**: 21-31.

Barrett, K., Leptin, M. and Settleman, J. (1997). "The Rho GTPase and a putative RhoGEF mediate a signaling pathway for the cell shape changes in *Drosophila* gastrulation." *Cell* **91**(7): 905-15.

Bateman, J. and Van Vactor, D. (2001). "The Trio family of guanine-nucleotide-exchange factors: regulators of axon guidence." *Journal of Cell Science* **114**: 1973-1980.

Bezanilla, M., Forsburg, S. L. and Pollard, T. D. (1997). "Identification of a second myosin-II in *Schizosaccharomyces pombe*: Myp2p is conditionally required for cytokinesis." *Molecular Biology of the Cell* **8**: 2693-2705.

Bi, E., Maddox, P., Lew, D. J., Salmon, E. D., McMillan, J. N., Yeh, E. and Pringle, J. R. (1998). "Involvement of an actomyosin contractile ring in *Saccharomyces cerevisiae* cytokinesis." *Journal of Cell Biology* **142**(5): 1301-12.

Bluemink, J. G. and Laat, S. W. D. (1973). "New membrane formation during cytokinesis in normal and cytochalasin B-treated eggs of *Xenopus laevis*.1. Electron microscope observations." *Journal of Cell Biology* **59**: 89-108.

Boguski, M. S. and McCormick, F. (1993). "Proteins regulating Ras and its relatives." *Nature* **366**: 643-654.

Bonaccorsi, S., Giansanti, M. G. and Gatti, M. (1998). "Spindle self-organization and cytokinesis during male meiosis in *asterless* mutants of *Drosophila melanogaster*." *Journal of Cell Biology* **142**(3): 751-61.

Bork, P., Hofmann, K., Bucher, P., Neuwald, A. F., Altschul, S. F. and Koonin, E. V. (1997). "A superfamily of conserved domains in DNA damage-responsive cell cycle checkpoint proteins." *Faseb Journal* **11**(1): 68-76.

Bourne, H. R., Sanders, D. A. and McCormick, F. (1990). "The GTPase superfamily: a conserved switch for diverse cell functions." *Nature* **348**: 125-132.

Burgess, R. W., Deitcher, D. L. and Schwarz, T. L. (1997). "The synaptic protein syntaxin1 is required for cellularization of *Drosophila* embryos." *Journal of Cell Biology* **138**(4): 861-75.

Byers, B. and Goetsch, L. (1976). "A highly ordered ring of membrane-associated filaments in budding yeast." *Journal of Cell Biology* **69**: 717-721.

Callebaut, I. and Mornon, J. P. (1997). "From BRCA1 to RAP1: a widespread BRCT module closely associated with DNA repair." *FEBS Lett.* **400**: 25-30.

Cao, L. G. and Wang, Y. L. (1990). "Mechanism of the formation of contractile ring in dividing cultured animal cells. II. Cortical movement of microinjected actin filaments." *Journal of Cell Biology* **111**(5 Pt 1): 1905-11.

Cao, L. G. and Wang, Y. L. (1996). "Signals from the spindle midzone are required for the stimulation of cytokinesis in cultured epithelial cells." *Molecular Biology of the Cell* **7**(2): 225-32.

Carlsson, L., Nystrom, L. E., Sundkvist, I., Markey, F. and Lindberg, U. (1977). "Actin polymerizability is influenced by profilin, a low molecular weight protein in non-muscle cells." *Journal of Molecular Biology* **115**: 465-483.

Carmena, M., Riparbelli, M. G., Minestrini, G., Tavares, A. M., Adams, R., Callaini, G. and Glover, D. M. (1998). "*Drosophila* polo kinase is required for cytokinesis." *Journal of Cell Biology* **143**(3): 659-71.

Chang, F., Woollard, A. and Nurse, P. (1996). "Identification and characterisation of fission yeast mutants defective in actin ring assembly and placement." *Journal of Cell Biology* **109**: 131-142.

Chant, J. and Stowers, L. (1995). "GTPase cascades choreographing cellular behavior: movement, morphogenesis, and more." *Cell* **81**(1): 1-4.

Chung, C. Y. and Firtel, R. A. (1999). "PAKa, a putative PAK family member, is required for cytokinesis and the regulation of the cytoskeleton in *Dictyostelium discoideum* cells during chemotaxis." *Journal of Cell Biology* **147**(3): 559-76.

Clemens, J. C., Worby, C. A., Simonson-Leff, N., Muda, M., Maehama, T., Hemmings, B. A. and Dixon, J. E. (2000). "Use of double-stranded RNA interference in *Drosophila* cell lines to dissect signal transduction pathways." *Proceedings of the National Academy of Sciences of the United States of America* **97**(12): 6499-503.

Conklin, E. G. (1917). "Effects of centrifugal forces on the structure and development of the eggs of *Crepidula*." *J Exp Zool* **22**: 311-419.

Conner, S. D. and Wessel, G. M. (1999). "Syntaxin is required for cell division." *Molecular Biology of the Cell* **10**(8): 2735-43.

Cook, T. A., Nagaski, T. and Gundersen, G. G. (1998). "Rho guanosine triphosphate mediates the selective stabilisation of microtubules induced by lysophosphatidic acid." *Journal of Cell Biology* **141**: 175-185.

Cooke, C. A., Heck, M. M. and Earnshaw, W. C. (1987). "The inner centromere protein (INCENP) antigens: movement from the inner centromere to midbody during mitosis." *Journal of Cell Biology* **105**: 2053-2067.

Crawford, J. M., Harden, N., Leung, T., Lim, L. and Kiehart, D. P. (1998). "Cellularization in *Drosophila melanogaster* is disrupted by the inhibition of rho activity and the activation of Cdc42 function." *Developmental Biology* **204**(1): 151-64.

Crevel, G., Huikeshoven, H., Cotterill, S., Simon, M., Wall, J., Philpott, A., Laskey, R. A., McConnell, M., Fisher, P. A. and Berrios, M. (1997). "Molecular and cellular characterisation of CRP1, a *Drosophila* chromatin decondensation protein." *Journal of Structural Biology* **118**: 9-22.

Daub, H., Gevaert, K., Vandekerckhove, J., Sobel, A. and Hall, A. (2001). "Rac/Cdc42 and p65PAK regulate the microtubule-destabilizating protein stathmin through phosphorylation at serine 16." *Journal of Biological Chemistry* **276**: 1677-1680.

De Lozanne, A. and Spudich, J. A. (1987). "Disruption of the *Dictyostelium* myosin heavy chain gene by homologous recombination." *Science* **236**: 1086-1091.

Debant, A., Serra-Pages, C., Seipel, K., O'Brien, S., Tang, M., Parkhurst, S. M. and Streuli, M. (1996). "The multidomain protein Trio binds the LAR transmembrane tyrosine phosphatase, contains a protein kinase domain, and has separate rac-specific and rho-specific guanine nucleotide exchange factor domains." *Proceedings of the National Academy of Sciences of the United States of America* **93**: 5466-5471.

Di Cunto, F., Imarisio, S., Hirsch, E., Broccoli, V., Bulfone, A., Migheli, A., Atzori, C., Turco, E., Triolo, R., Dotto, G. P., Silengo, L. and Altruda, F. (2000). "Defective neurogenesis in citron kinase knockout mice by altered cytokinesis and massive apoptosis." *Neuron* **28**(1): 115-27.

Dickson, B. J., Straten, A., Dominguez, M. and Hafen, E. (1996). "Mutations modulating Raf signalling in *Drosophila* eye development." *Genetics* **142**: 163-171.

Drechsel, D. N., Hyman, A. A., Hall, A. and Glotzer, M. (1997). "A requirement for Rho and Cdc42 during cytokinesis in *Xenopus* embryos." *Current Biology* **7**(1): 12-23.

Dumontier, M., Hocht, P., Mintert, U. and Faix, J. (2000). "Rac1 GTPases control filopodia formation, cell motility, endocytosis, cytokinesis and development in *Dictyostelium*." *Journal of Cell Science* **113 (Pt 12)**: 2253-65.

Duronio, R. J. and O'Farrell, P. H. (1995). "Developmental control of the G1 to S transition in *Drosophila*:cyclin E is a limiting downstream target of E2F." *Genes and Development* **15**: 1456-1468.

Dutartre, H., Davoust, J., Gorvel, J. P. and Chavrier, P. (1996). "Cytokinesis arrest and redistribution of actin-cytoskeleton regulatory components in cells expressing the Rho GTPase CDC42Hs." *Journal of Cell Science* **109 (Pt 2)**: 367-77.

Eaton, S., Wepf, R. and Simons, K. (1996). "Roles for Rac1 and Cdc42 in planar polarization and hair outgrowth in the wing of *Drosophila*." *Journal of Cell Biology* **135**: 1277-1289.

Eberharter, A., Ferrari, S., Langst, G., Straub, T., Imhof, A., Varga-Weisz, P., Wilm, M. and Becker, P. B. (2001). "Acf1, the largest subunit of CHRAC, regulates ISWI-induced nucleosome remodelling." *EMBO* **20**: 3781-3788.

Eda, M., Yonemura, S., Kato, T., Watanabe, N., Ishizaki, T., Madaule, P. and Narumiya, S. (2001). "Rho-dependent transfer of Citron-kinase to the cleavage furrow of dividing cells." *Journal of Cell Science* **114**(18): 3273-84.

Edwards, D. C., Sanders, L. C., Boku, S. and Gill, G. N. (1999). "Activation of LIM-kinase by Pak1 couples Rac/Cdc42 GTPase signalling to actin cytoskeletal dynamics." *Nature Cell Biology* **1**: 253-259.

Epp, J. A. and Chant, J. (1997). "An IQGAP-related protein controls actin-ring formation and cytokinesis in yeast." *Current Biology* **7**(12): 921-9.

Fanto, M., Weber, U., Strutt, D. I. and Mlodzik, M. (2000). "Nuclear signaling by Rac and Rho GTPases is required in the establishment of epithelial planar polarity in the *Drosophila* eye." *Current Biology* **10**(16): 979-88.

Field, C. and Kellogg, D. (1999). "Septins: cytoskeletal polymers or signalling GTPases?" *trends in Cell Biology* **9**: 387-394.

Field, C. M., al-Awar, O., Rosenblatt, J., Wong, M. L., Alberts, B. and Mitchison, T. J. (1996). "A purified Drosophila septin complex forms filaments and exhibits GTPase activity." *Journal of Cell Biology* **133**(3): 605-16.

Field, C. M. and Alberts, B. M. (1995). "Anillin, a contractile ring protein that cycles from the nucleus to the cell cortex." *Journal of Cell Biology* **131**(1): 165-78.

Fishkind, D. J., Silverman, J. D. and Wang, Y. L. (1996). "Function of spindle microtubules in directing cortical movement and actin filament organization in dividing cultured cells." *Journal of Cell Science* **109 (Pt 8)**: 2041-51.

Fishkind, D. J. and Wang, Y. L. (1993). "Orientation and three-dimensional organization of actin filaments in dividing cultured cells." *Journal of Cell Biology* **123**(4): 837-48.

Frazier, J. A., Wong, M. L., Longtine, M. S., Pringle, J. R., Mann, M., Mitchison, T. J. and Field, C. (1998). "Polymerization of purified yeast septins: evidence that organized filament arrays may not be required for septin function." *Journal of Cell Biology* **143**(3): 737-49.

Fujiwara, K. and Pollard, T. D. (1978). "Simultaneous localization of myosin and tubulin in human tissue culture cells by double antibody staining." *Journal of Cell Biology* **77**(1): 182-95.

Gatti, M., Giansanti, M. G. and Bonaccorsi, S. (2000). "Relationships between the central spindle and the contractile ring during cytokinesis in animal cells." *Microscopy Research and Technique* **49**(2): 202-8.

Genova, J. L., Jong, S., Camp, J. T. and Fehon, R. G. (2000). "Functional analysis of Cdc42 in actin filament assembly, epithelial morphogenesis, and cell signaling during *Drosophila* development." *Developmental Biology* **221**(1): 181-94.

Gerisch, G. and Weber, I. (2000). "Cytokinesis without myosin II." *Current Opinion in Cell Biology* **12**: 126-132.

Giansanti, M. G., Bonaccorsi, S., Williams, B., Williams, E. V., Santolamazza, C., Goldberg, M. L. and Gatti, M. (1998). "Cooperative interactions between the central spindle and the contractile ring during *Drosophila* cytokinesis." *Genes and Development* **12**(3): 396-410.

Giansanti, M. G., Gatti, M. and Bonaccorsi, S. (2001). "The role of centrosomes and astral microtubules during asymmetric division of Drosophila neuroblasts." *Development* **128**(7): 1137-45.

Giet, R. and Glover, D. M. (2001). "*Drosophila* aurora B kinase is required for histone H3 phosphorylation and condensin recruitment during chromosome condensation and to organize the central spindle during cytokinesis." *Journal of Cell Biology* **152**(4): 669-82.

Glotzer, M. (1997). "The mechanism and control of cytokinesis." *Current Opinion in Cell Biology* **9**: 815-823.

Glotzer, M. (2001). "Animal cell cytokinesis." *Annual Review of Cellular and Developmental Biology* **17**: 351-386.

Goldschmidt-Clermont, P., Machesky, L. M., Doberstein, S. K. and Pollard, T. D. (1991). "Mechanism of the interaction of human platelet profilin with actin." *Journal of Cell Biology* **113**: 1081-1089.

Greaves, S., Sanson, B., White, P. and Vincent, J. P. (1999). "A screen for identifying genes interacting with armadillo, the *Drosophila* homolog of beta-catenin." *Genetics* **153**: 1753-1766.

Grigliatti, T. (1986). *Drosophila*: a practicle approach, IRL Press Oxford.

Gunsalus, K. C., Bonaccorsi, S., Williams, E. V., Verni, F., Gatti, M. and Goldberg, M. L. (1995). "Mutations in twinstar, a *Drosophila* gene encoding a cofilin/ADF homologue, result in defects in centrosome migration and cytokinesis." *Journal of Cell Biology* **131**(5): 1243-59.

Hakeda-Suzuki, S., Ng, J., Tzu, J., Dietzl, G., Sun, Y., Harms, M., Nardine, T., Luo, L. and Dickson, B. J. (2002). "Rac function and regulation during *Drosophila* development." *Nature* **416**: 438-442.

Harden, N., Lee, J., Loh, H. Y., Ong, Y. M., Tan, I., Leung, T., Manser, E. and Lim, L. (1996). "A *Drosophila* homolog of the Rac- and Cdc42- activated serine/threonine kinase PAK is a potential focal adhesion and focal complex protein that colocalises with dynamic actin structures." *Molecular and Cellular Biology* **16**: 1896-1908.

Harden, N., Ricos, M., Ong, Y. M., Chia, W. and Lim , L. (1999). "Participation of small GTPases in dorsal closure of the *Drosophila* embryo: distinct roles for Rho subfamily proteins in epithelial morphogenesis." *Journal of Cell Science* **112**: 273-284.

Harley, A. S. (2002). Analysis of a nuclear role for *pebble*, a gene required for cytokinesis in *Drosophila*. Faculty of Science. Adelaide, University of Adelaide.

Hart, M. J., Callow, M. G., Souza, B. and Polakis, P. (1996). "IQGAP1, a calmodulin-binding protein with a rasGAP-related domain, is a potential effector for cdc42Hs." *EMBO* **15**: 2997-3005.

Hendrickson, T. W., Yao, J., Bhadury, S., Corbett, A. H. and Joshi, H. C. (2001). "Conditional mutations in gamma-tubulin reveal its involement in chromosome segrgation and cytokinesis." *Molecular Biology of the Cell* **12**: 2469-2481.

Herrmann, S., Amorim, I. and Sunkel, C. E. (1998). "The POLO kinase is required for multiple stages during spermatogenesis in *Drosophila melanogaster*." *Chromosoma* **107**: 440-451.

Hill, C. S., Wynne, J. and Treisman, R. (1995). "The Rho family GTPases RhoA, Rac1, and CDC42Hs regulate transcriptional activation by SRF." *Cell* **81**(7): 1159-70.

Hime, G. and Saint, R. (1992). "Zygotic expression of the *pebble* locus is required for cytokinesis during the postblastoderm mitoses of *Drosophila*." *Development* **114**(1): 165-71.

Hirose, K., Kawashima, T., Iwamoto, I., Nosaka, T. and Kitamura, T. (2001). "MgcRacGAP is involved in cytokinesis through associating with mitotic spindle and midbody." *Journal of Biological Chemistry* **276**(8): 5821-8.

Jantsch-Plunger, V. and Glotzer, M. (1999). "Depletion of syntaxins in the early *Caenorhabditis elegans* embryo reveals a role for membrane fusion events in cytokinesis." *Current Biology* **9**(14): 738-45.

Jantsch-Plunger, V., Gonczy, P., Romano, A., Schnabel, H., Hamill, D., Schnabel, R., Hyman, A. A. and Glotzer, M. (2000). "CYK-4: A Rho family GTPase activating protein (GAP) required for central spindle formation and cytokinesis." *Journal of Cell Biology* **149**(7): 1391-404.

Julian, M., Tollon, Y., Lajoie-Mazenc, I., Moisand, A., Mazarguil, H., Puget, A. and Wright, M. (1993). "gamma-Tubulin participates in the formation of the midbody during cytokinesis in mammalian cells." *Journal of Cell Science* **105 (Pt 1)**: 145-56.

Jurgens, G., Wieschaus, E., Nusslein-Volhard, C. and Kluding, H. (1984). "Mutations affecting the pattern of the larval cuticle in *Drosophila melanogaster*." *Roux's Archives of Developmental Biology* **193**: 283-295.

Kaitna, S., Mendoza, M., Jantsch-Plunger, V. and Glotzer, M. (2000). "Incenp and an aurora-like kinase form a complex essential for chromosome segregation and efficient completion of cytokinesis." *Current Biology* **10**(19): 1172-81.

Karess, R. E., Chang, X. J., Edwards, K. A., Kulkarni, S., Aguilera, I. and Kiehart, D. P. (1991). "The regulatory light chain of nonmuscle myosin is encoded by spaghetti-squash, a gene required for cytokinesis in Drosophila." *Cell* **65**(7): 1177-89.

Kawashima, T., Hirose, K., Satoh, T., Kaneko, A., Ikeda, Y., Kaziro, Y., Nosaka, T. and Kitamura, T. (2000). "MgcRacGAP is involved in the control of growth and differentiation of hematopoietic cells." *Blood* **96**(6): 2116-24.

Kim, J. H., Kang, J. S. and Chan, C. S. (1999). "Sli15 associates with the ipl1 protein kinase to promote proper chromosome segregation in *Saccharomyces cerevisiae*." *Journal of Cell Biology* **145**: 1381-1394.

Kimura, K., Ito, M., Amano, M., Chihara, K., Fukata, Y., Nakafuku, M., Yamamori, B., Feng, J., Nakano, T., Okawa, K., Iwamatsu, A. and Kaibuchi, K. (1996). "Regulation of myosin phosphatase by Rho and Rho-associated kinase (Rho-kinase)." *Science* **273**(5272): 245-8.

Kimura, K., Tsuji, T., Takada, Y., Miki, T. and Narumiya, S. (2000). "Accumulation of GTP-bound RhoA during cytokinesis and a critical role of ECT2 in this accumulation." *Journal of Biological Chemistry* **275**(23): 17233-6.

Kinoshita, M., Kumar, S., Mizoguchi, A., Ide, C., Kinoshita, A., Haraguchi, T., Hiraoka, Y. and Noda, M. (1997). "Nedd5, a mammalian septin, is a novel cytoskeletal component interacting with actin-based structures." *Genes and Development* **11**(12): 1535-47.

Kishi, K., Sasaki, T., Kuroda, S., Itoh, T. and Takai, Y. (1993). "Regulation of cytoplasmic division of Xenopus embryo by rho p21 and its inhibitory GDP/GTP exchange protein (rho GDI)." *Journal of Cell Biology* **120**(5): 1187-95.

Kitamura, T., Kawashima, T., Minoshima, Y., Tonozuka, Y., Hirose, K. and Nasoka, T. (2001). "Role of MgcRacGAP/Cyk4 as a regulator of the small GTPase Rho family in cytokinesis and cell differentiation." *Cell Structure and Function* **26**: 645-651.

Knoblich, J. A., Sauer, K., Jones, L., Richardson, H., Saint, R. and Lehner, C. F. (1994). "Cyclin E controls S phase progression and its down-regulation during *Drosophila* embryogenesis is required for the arrest of cell proliferation." *Cell* **77**: 107-120.

Koonin, E. V., Altschul, S. F. and Bork, P. (1996). "BRCA1 protein products: functional motifs." *Nature Genetics* **13**: 266-267.

Kosako, H., Goto, H., Yanagida, M., Matsuzawa, K., Fujita, M., Tomono, Y., Okigaki, T., Odai, H., Kaibuchi, K. and Inagaki, M. (1999). "Specific accumulation of Rho-associated kinase at the cleavage furrow during cytokinesis: cleavage furrow-specific phosphorylation of intermediate filaments." *Oncogene* **18**(17): 2783-8.

Krendel, M., Zenke, F. T. and Bokoch, G. M. (2002). "Nucleotide exchange factor GEF-H1 mediates cross-talk between microtubules and the actin cytoskeleton." *Nature Cell Biology* **4**: 294-301.

Kuriyama, R., Dragas Granoic, S., Maekawa, T., Vassilev, A., Khodjakov, A. and Kobayashi, H. (1994). "Heterogeneity and microtubule interaction of the CHO1 antigen, a mitosis-specific kinesin-like protein. Analysis of subdomains expressed in insect sf9 cells." *Journal of Cell Science* **107**: 3485-3499.

Kuriyama, R., Gustus, C., Terada, Y., Uetake, Y. and Matuliene, J. (2002). "CHO1, a mammalian kinesin-like protein, interacts with F-actin and is involved in the terminal phase of cytokinesis." *The Journal of Cell Biology* **156**(5): 783-790.

Kuroda, S., Fukata, M., Kobayashi, K., Nakafuku, M., Nomura, N., Iwamatsu, A. and Kaibuchi, K. (1996). "Identification of IQGAP as a putative target for the small GTPases, Cdc42 and Rac1." *Journal of Biological Chemistry* **271**(38): 23363-7.

Larochelle, D. A., Vithalani, K. K. and De_Lozanne, A. (1996). "A novel member of the rho family of small GTP-binding proteins is specifically required for cytokinesis." *Journal of Cell Biology* **133**(6): 1321-9.

Lecuit, T. and Wieschaus, E. (2000). "Polarized insertion of new membrane from a cytoplasmic reservoir during cleavage of the *Drosophila* embryo." *Journal of Cell Biology* **150**(4): 849-860.

Lee, K. S., Yuan, Y. L., Kuriyama, R. and Erikson, R. L. (1995). "Plk is an M-phase-specific protein kinase and interacts with a kinesin-like protein, CHO1/MKLP-1." *Molecular and Cellular Biology* **15**(12): 7143-51.

Lehner, C. F. (1992). "The pebble gene is required for cytokinesis in *Drosophila*." *Journal of Cell Science* **103 (Pt 4)**: 1021-30.

Lemmon, M. A., Falasca, M., Ferguson, K. M. and Schlessinger, J. (1997). "Regulatory recruitment of signalling molecules to the cell membrane by pleckstrin-homology domains." *trends in Cell Biology* **7**: 237-242.

Lenzen, C., Cool, R. H., Prinz, H., Kuhlmann, J. and Wittinghofer, A. (1998). "Kinetic analysis by fluorescence of the interaction between Ras and the catalytic domains of the guanine nucleotide exchange factor Cdc25Mm." *Biochemistry* **37**: 74207430.

Leonard, D. A., Lin, R., Cerione, R. A. and Manor, D. (1998). "Biochemical studies of the mechanism of action of the Cdc42-GTPase-activating protein." *The Journal of Biological Chemistry* **273**(26): 16210-16215.

Longtine, M. S., DeMarini, D. J., Valencik, M. L., Al-Awar, O. S., Fares, H., De Virgilio, C. and Pringle, J. R. (1996). "The septins: roles in cytokinesis and other processes." *Current Opinion in Cell Biology* **8**(1): 106-19.

Longtine, M. S., Fares, H. and Pringle, J. R. (1998). "Role of the yeast Gin4p protein kinase in septin assembly and the relationship between septin assembly and septin function." *Journal of Cell Biology* **143**(3): 719-36.

Lowy, D. R. and Willumsen, B. M. (1993). "Function and regulation of Ras." *Annual Review of Biochemisty.* **62**: 851-891.

Lutz, D. A., Hamaguchi, Y. and Inoue, S. (1988). "Micromanipulation studies of the asymmetric positioning of the maturation spindle in *Chaetopterus sp.* oocytes:I. Anchorage of the spindle to the cortex and migration of a displaced spindle." *Cell Motility and the Cytoskeleton* **11**: 83-96.

Mabuchi, I., Hamaguchi, Y., Fujimoto, H., Morii, N., Mishima, M. and Narumiya, S. (1993). "A rho-like protein is involved in the organisation of the contractile ring in dividing sand dollar eggs." *Zygote* **1**(4): 325-31.

Mabuchi, I. and Okuno, M. (1977). "The effect of myosin antibody on the division of starfish blastomeres." *Journal of Cell Biology* **74**(1): 251-63.

Madaule, P., Eda, M., Watanabe, N., Fujisawa, K., Matsuoka, T., Bito, H., Ishizaki, T. and Narumiya, S. (1998). "Role of citron kinase as a target of the small GTPase Rho in cytokinesis." *Nature* **394**: 491-4.

Maekawa, M., Ishizaki, T., Boku, S., Watanabe, N., Fujita, A., Iwamatsu, A., Obinata, T., Ohashi, K., Mizuno, K. and Narumiya, S. (1999). "Signalling from Rho to the actin cytoskeleton through protein kinases ROCK and LIM-kinase." *Science* **285**: 895-898.

Magie, C. R., Meyer, M. R., Gorsuch, M. S. and Parkhurst, S. M. (1999). "Mutations in the Rho1 small GTPase disrupt morphogenesis and segmentation during early *Drosophila* development." *Development* **126**(23): 5353-64.

Matuliene, J. and Kuriyama, R. (2002). "Kinesin-like protein CHO1 is required for the completion of cytokinesis in mammalian cells." *Molecular Biology of the Cell* **13**: 1832-1845.

McCollum, D. and Gould, K. L. (2001). "Timing is everything: regulation of mitotic exit and cytokinesis by the MEN and SIN." **11**(2): 89-95.

Miki, T., Smith, C. L., Long, J. E., Eva, A. and Fleming, T. P. (1993). "Oncogene ect2 is related to regulators of small GTP-binding proteins." *Nature* **362**(6419): 462-5.

Minestrini, G., Mathe, E. and Glover, D. M. (2002). "Domains of the Pavarotti kinesin-like protein that direct its subcellular distribution: effects of mislocalisation on the tubulin and actin cytoskeleton during *Drosophila* oogenesis." *Journal of Cell Science* **115**: 725-736.

Minet, M., Nurse, P., Thuriaux, P. and Mitchison, J. M. (1979). "Uncontrolled septation in a cell division cycle mutant of the fission yeast *Schizosaccharomyces pombe*." *Journal of Bacteriology* **137**: 440-446.

Mishima, M., Kaitna, S. and Glotzer, M. (2002). "Central spindle assembly and cytokinesis require a kinesin-like protein/RhoGAP complex with microtubule bundling activity." *Developmental Cell* **2**: 41-54.

Moore, M. S. and Blobel, G. (1993). "The GTP-binding protein Ran/TC4 is required for protein import into the nucleus." *Nature* **365**: 661-663.

Moriyama, K., Iida, K. and Yahara, I. (1996). "Phosphorylation of Ser-3 of cofilin regulates its essential function on actin." *Genes Cells* **1**: 73-86.

Mullins, J. M. and McIntosh, J. R. (1982). "Isolation and initial characterization of the mammalian midbody." *Journal of Cell Biology* **94**(3): 654-661.

Murata-Hori, M. and Wang, Y. (2002). "Both midzone and astral microtubules are involved in the delivery of cytokinesis signals: insights from the mobility of aurora B." *Journal of Cell Biology* **159**: 45-53.

Murray, A. W., Solomon, M. J. and Kirschner, M. W. (1989). "The role of cyclin synthesis and degradation in the control of maturation promoting factor activity." *Nature* **339**(6222): 280-6.

Nagaoka, R., Abe, H., Kusano, K. and Obinata, T. (1995). "Concentration of cofilin, a small actin-binding protein, at the cleavage furrow during cytokinesis." *Cell Motility and the Cytoskeleton* **30**(1): 1-7.

Neufeld, P. N., Tang, A. H. and Rubin, G. M. (1998). "A genetic screen to identify components of the *sina* signalling pathway in *Drosophila* eye development." *Genetics* **148**: 277-286.

Neufeld, T. P. and Rubin, G. M. (1994). "The Drosophila peanut gene is required for cytokinesis and encodes a protein similar to yeast putative bud neck filament proteins." *Cell* **77**(3): 371-9.

Newsome, T. P., Schmidt, S., Dietzl, G., Keleman, K., Asling, B., Debant, A. and Dickson, B. J. (2000). "Trio combines with dock to regulate Pak activity during photoreceptor axon pathfinding in *Drosophila*." *Cell* **101**(3): 283-94.

Ng, J., Nardine, T., Harms, M., Tzu, J., Goldstein, A., Sun, Y., Dietzl, G., Dickson, B. J. and Luo, L. (2002). "Rac GTPases control axon growth, guidance and branching." *Nature* **416**: 442-446.

Nislow, C., Lombillo, V. A., Kuriyama, R. and McIntosh, J. R. (1992). "A plus-end-directed motor enzyme that moves antiparallel microtubules in vitro localizes to the interzone of mitotic spindles." *Nature* **359**(6395): 543-7.

Nobes, C. D. and Hall, A. (1995). "Rho, rac, and cdc42 GTPases regulate the assembly of multimolecular focal complexes associated with actin stress fibers, lamellipodia, and filopodia." *Cell* **81**(1): 53-62.

O'Connell, C. B., Wheatley, S. P., Ahmed, S. and Wang, Y. L. (1999). "The small GTP-binding protein rho regulates cortical activities in cultured cells during division." *Journal of Cell Biology* **144**(2): 305-13.

O'Keefe, L. (2001). Genetic analysis of the role of *pebble* during cytokinesis in *Drosophila*. Molecular Biosciences. Adelaide, University of Adelaide.

O'Keefe, L., Somers, W. G., Harley, A. and Saint, R. (2001). "The Pebble GTP exchange factor and the control of cytokinesis." *Cell Structure and Function* **26**: 619-626.

Oda, H., Uemura, T., Shiomi, K., Nagafuchi, A., Tsukita, S. and Takeichi, M. (1993). "Identification of a *Drosophila* homologue of alpha-catenin and its association with the armadillo protein." *Journal of Cell Biology* **121**: 1133-1140.

Oegema, K., Savoian, M. S., Mitchison, T. J. and Field, C. M. (2000). "Functional analysis of a human homologue of the *Drosophila* actin binding protein anillin suggests a role in cytokinesis." *Journal of Cell Biology* **150**(3): 539-52.

Ohashi, K., Hosoya, T., Takahashi, K., Hing, H. and Mizuno, K. (2000). "A *Drosophila* homolog of LIM-kinase phosphorylates cofilin and induces actin cytoskeletal reorganization." *Biochemical and Biophysical Research Communications* **276**(3): 1178-85.

Opas, J. and SoÇtyÑska, M. S. (1978). "Reorganization of the cortical layer during cytokinesis in mouse blastomeres." *Experimental Cell Research* **113**(1): 208-11.

Ory, S., Munari-Silem, Y., Fort, P. and Jurdic, P. (2000). "Rho and Rac exert antagonistic functions on spreading of macrophasge-derived multinucleated cells and are not required for actin fibre formation." *Journal of Cell Science* **113**: 1177-1188.

Palazzo, A. F., Cook, T. A., Alberts, A. S. and Gundersen, G. G. (2001). "mDia mediates Rho-regulated formation and orientation of stable microtubules." *Nature Cell Biology* **3**: 723-729.

Palmieri, S. J. and Haarer, B. K. (1998). "Polarity and division site specification in yeast." *Current Opinions in Microbiology* **1**(6): 678-86.

Palmieri, S. J., Nebl, T., Pope, R. K., Seastone, D. J., Lee, E., Hinchcliffe, E. H., Sluder, G., Knecht, D., Cardelli, J. and Luna, E. J. (2000). "Mutant Rac1B expression in *Dictyostelium*: effects on morphology, growth, endocytosis, development, and the actin cytoskeleton." *Cell Motility and the Cytoskeleton* **46**(4): 285-304.

Pan, J. Y., Fieles, W. E., White, A. M., Egerton, M. M. and Silberstein, D. S. (2000). "Ges, a human GTPase of the Rad/Gem/Kir family, promotes endothelial cell sprouting and cytoskeleton reorganisation." *Journal of Cell Biology* **149**: 1107-1116.

Pantaloni, D. and Carlier, M. F. (1993). "How profilin promotes actin filament assembly in the presence of thymosin beta 4." *Cell* **75**: 1007-1014.

Parry, D. H. and O'Farrell, P. H. (2001). "The schedule of destruction of three mitotic cyclins can dictate the timing of events during exit from mitosis." *Current Biology* **11**(9): 671-83.

Peifer, M. (1993). "The product of the *Drosophila* segment polarity gene *armadillo* is part of a multi-protein complex resembling the vertebrate adherens junction." *Journal of Cell Science* **105**: 993-1000.

Peifer, M., Pai, L. M. and Casey, M. (1994). "Phosphorylation of the *Drosophila* adherens junction protein Armadillo: roles for wingless signal and zeste-white 3 kinase." *Developmental Biology* **166**: 543-556.

Piel, M., Nordberg, J., Euteneuer, U. and Bornens, M. (2001). "Centrosome-dependent exit of cytokinesis in animal cells." *Science* **291**(5508): 1550-3

.

Powers, J., Bossinger, O., Rose, D., Strome, S. and Saxton, W. (1998). "A nematode kinesin required for cleavage furrow advancement." *Current Biology* **8**(20): 1133-6.

Prokopenko, S. N., Brumby, A., O'Keefe, L., Prior, L., He, Y., Saint, R. and Bellen, H. J. (1999). "A putative exchange factor for Rho1 GTPase is required for initiation of cytokinesis in *Drosophila*." *Genes and Development* **13**(17): 2301-14.

Raich, W. B., Moran, A. N., Rothman, J. H. and Hardin, J. (1998). "Cytokinesis and midzone microtubule organization in *Caenorhabditis elegans* require the kinesin-like protein ZEN-4." *Molecular Biology of the Cell* **9**(8): 2037-49.

Rappaport, R. (1961). "Experiments concerning the cleavage stimulus in sand dollar eggs." *J Exp Zool* **148**: 81-89.

Rappaport, R. (1968). "Geometrical relations of the cleavage stimulus in flattened, perforated sea urchin eggs." *Embryologia* **10**: 115-130.

Rappaport, R. (1985). "Repeated furrow formation from a single mitotic apparutus in cylindrical sand dollar eggs." *Journal of Experimental Zoology* **234**: 167-171.

Rappaport, R. and Rappaport, B. (1983). "Cytokinesis: Effects of blocks between the mitotic apparatus and the surface on the furrow establishment in flattened *Echinoderm* eggs." *The Journal of Experimental Zoology* **227**: 213-227.

Rebay, I., Chen, F., Hsiao, F., Kolodziej, P. A., Kuang, B. H., Laverty, T., Suh, C., Voas, M., Williams, A. and Rubin, G. M. (2000). "A genetic screen for novel components of the Ras/Mitogen-activated protein kinase signalling pathway that interact with the *yan* gene of *Drosophila* identifies split ends, a new RNA recognition motif-containing protein." *Genetics* **154**(2): 695-712.

Reed, S. I. (1996). "G1/S regulatory mechanisms from yeast to man." *Prog. Cell Cycle Res.* **2**: 15-27.

Ren, X. D., Kiosses, W. B. and Schwartz, M. A. (1999). "Regulation of the small GTP-binding protein Rho by cell adhesion and the cytoskeleton." *EMBO* **18**: 578-585.

Ridley, A. J. and Hall, A. (1992). "The small GTP-binding protein rho regulates the assembly of focal adhesions and actin stress fibres in response to growth factors." *Cell* **70**(3): 389-99.

Ridley, A. J., Paterson, H. F., Johnston, C. L., Diekmann, D. and Hall, A. (1992). "The small GTP-binding protein rac regulates growth factor-induced membrane ruffling." *Cell* **70**(3): 401-10.

Rieder, C. L. and Salmon, E. D. (1998). "The vertebrate cell kinetochore and its roles during mitosis." *trends in Cell Biology* **8**: 310-318.

Rittinger, K., Walker, P., Eccleston, J. F., Nurmahomed, K., Owen, D., Laue, E., Gamblin, S. and Smerdon, S. (1997). "Crystal structure of a small G protein in complex with the GTPase-activating protein rhoGAP." *Nature* **388**: 693-697.

Rivero, F., Illenberger, D., Somesh, B. P., Dislich, H., Adams, N. and Meyer, A. K. (2002). "Defects in cytokinesis, actin reorganisation and the contractile vacuole in cells deficient in RhoGDI." *EMBO* **21**: 4539-4549.

Royal, I., Lamarche Vane, N., Lamorte, L., Kaibuchi, K. and Park, M. (2000). "Activation of Cdc42, Rac, PAK, and Rho-kinase in response to hepatocyte growth factor differentially regulates epithelial cell colony spreading and dissociation." *Molecular Biology of the Cell* **11**: 1709-1725.

Sakata, H., Rubin, J. S., Taylor, W. G. and Miki, T. (2000). "A Rho-specific exchange factor Ect2 is induced from S to M phases in regenerating mouse liver." *Hepatology* **32**(2): 193-9.

Salzberg, A., Prokopenko, S. N., He, Y., Tsai, P., Pal, M., Maroy, P., Glover, D. M., Deak, P. and Bellen, H. J. (1997). "P-element insertion alleles of essential genes on the third chromosome of *Drosophila melanogaster*: mutations affecting embryonic PNS development." *Genetics* **147**(4): 1723-41.

Sambrook, J., Fritsch, E. F. and Maniatis, T. (1989). "Molecular Cloning: A laboratory manual." *2nd edition, Cold Spring Harbor Laboratory Press, 1989.*

Sander, E. E., ten Klooster, J. P., van Delft, S., van der Kammen, R. A. and Collard, J. G. (1999). "Rac downregulates Rho activity: reciprocal balance between both GTPases determines cellular morphology and migratory behaviour." *Journal of Cell Biology* **147**: 1009-1022.

Sanders, L. C., Matsumura, F., Bokoch, G. M. and de Lanerolle, P. (1999). "Inhibition of myosin light chain kinase by p21-activated kinase." *Science* **283**: 2083-2085.

Santama, N., Krijnse-Locker, J., Griffiths, G., Noda, Y., Hirokawa, N. and Dotti, C. G. (1998). "KIF2beta, a new kinesin superfamily protein in non-neuronal cells, is associated with lysosomes and may be implicated in their centrifugal translocation." *EMBO* **17**: 5855-5867.

Savoian, M. S. and Rieder, C. L. (2002). "Mitosis in primary cultures of *Drosophila melanogaster* larval neuroblasts." *Journal of Cell Science* **115**: 3061-3072.

Schmidt, S., Sohrmann, M., Hofmann, K., Woollard, A. and Simanis, V. (1997). "The Spg1p GTPase is an essential, dosage-dependent inducer of septum formation in *Schizosaccharomyces pombe*." *Genes and Development* **11**(12): 1519-34.

Schumacher, J. M., Golden, A. and Donovan, P. J. (1998). "AIR-2: An Aurora/Ipl1-related protein kinase associated with chromosomes and midbody microtubules is required for polar body extrusion and cytokinesis in *Caenorhabditis elegans* embryos." *Journal of Cell Biology* **143**(6): 1635-46.

Severson, A. F., Hamill, D. R., Carter, J. C., Schumacher, J. and Bowerman, B. (2000). "The aurora-related kinase AIR-2 recruits ZEN-4/CeMKLP1 to the mitotic spindle at metaphase and is required for cytokinesis." *Current Biology* **10**(19): 1162-71.
Shannon, K. B. and Li, R. (1999). "The multiple roles of Cyk1p in the assembly and function of the actomyosin ring in budding yeast." *Molecular Biology of the Cell* **10**(2): 283-96.

Shou, W., Seol, J. H., Shevchenko, A., Baskerville, C., Moazed, D., Chen, Z. W. S., Jang, J., Shevchenko, A., Charbonneau, H. and Deshaies, R. J. (1999). "Exit from mitosis is triggered by Tem1-dependent release of the protein phosphatase Cdc14 from nucleolar RENT complex." *Cell* **97**: 233-244.

Shu, H. B., Li, Z., Palacios, M. J., Li, Q. and Joshi, H. C. (1995). "A transient association of gamma-tubulin at the midbody is required for the completion of cytokinesis during the mammalian cell division." *Journal of Cell Science* **108 (Pt 9)**: 2955-62.

Sigrist, S., Jacobs, H., Stratmann, R. and Lehner, C. F. (1995). "Exit from mitosis is regulated by *Drosophila* fizzy and the sequential destruction of cyclins A, B and B3." *Embo Journal* **14**(19): 4827-38.

Simon, M. A., Bowtell, D. D., Dodson, G. S., Laverty, T. R. and Rubin, G. M. (1991). "Ras1 and a putative guanine nucleotide exchange factor perform crucial steps in signalling by the sevenless protein tyrosine kinase." *Cell* **67**(4): 701-16.

Sisson, J. C., Field, C., Ventura, R., Royou, A. and Sullivan, W. (2000). "Lava lamp, a novel peripheral golgi protein, is required for *Drosophila melanogaster* cellularization." *Journal of Cell Biology* **151**(4): 905-18.

Skop, A. R., Bergmann, D., Mohler, W. A. and White, J. R. (2001). "Completion of cytokinesis in *C. elegans* requires a brefeldin A-sensitive membrane accumulation at the cleavage furrow apex." *Current Biology* **11**: 735-746.

Smith, L. G. (2001). "Plant cell division: building walls in the right places." *Nature Reviews of Molecular and Cellular Biology* **2**: 33-39.

Somlyo, A. P. and Somlyo, A. V. (1994). "Signal transduction and regulation in smooth muscle." *Nature* **372**: 231-236.

Somma, M. P., Fasulo, B., Cenci, G., Cundari, E. and Gatti, M. (2002). "Molecular dissection of cytokinesis by RNA interference in *Drosophila* cultured cells." *Molecular and Cellular Biology* **13**: 2448-2460.

Song, K., Mach, K. E., Chen, C. Y., Reynolds, T. and Albright, C. F. (1996). "A novel suppressor of *ras1* in fission yeast, *byr4*, is a dose-dependent inhibitor of cytokinesis." *Journal of Cell Biology* **133**: 1307-1319.

Sotillos, S. and Campuzano, S. (2000). "*DRacGAP*, a novel *Drosophila* gene, inhibits EGFR/Ras signalling in the developing imaginal wing disc." *Development* **127**(24): 5427-38.

Speliotes, E. K., Uren, A., Vaux, D. and Horvitz, H. R. (2000). "The survivin-like *C. elegans* BIR-1 protein acts with the Aurora-like kinase AIR-2 to affect chromosomes and the spindle midzone." **6**(2): 211-23.

Strutt, D. I., Weber, U. and Mlodzik, M. (1997). "The role of RhoA in tissue polarity and Frizzled signalling." *Nature* **387**(6630): 292-5.

Sumi, T., Matsumoto, K., Takai, Y. and Nakamura, T. (1999). "Cofilin phosphorylation and actin cytoskeletal dynamics regulated by rho- and Cdc42-activated LIM-kinase 2." *Journal of Cell Biology* **147**: 1519-1532.

Tang, A. H., Neufeld, T. P., Rubin, G. M. and Muller, H.-A. J. (2001). "Transcriptional regulation of cytoskeletal functions and segmentation by a novel maternal pair-rule gene, *lilliputian.*" *Development* **128**: 801-813.

Tatsumoto, T., Xie, X., Blumenthal, R., Okamoto, I. and Miki, T. (1999). "Human ECT2 is an exchange factor for Rho GTPases, phosphorylated in G2/M phases, and involved in cytokinesis." *Journal of Cell Biology* **147**(5): 921-8.

Toure, A., Dorseuil, O., Morin, L., Jegou, B., Reibel, L. and Gacon, G. (1998). "MgcRacGAP, a new human GTPase-activiating protein for Rac and Cdc42 similar to *Drosophila rotundRacGAP* gene product, is expressed in male germ cells." *Journal of Biological Chemistry* **273**(11): 6019-23.

Van de Putte, T., Zwijsen, A., Lonnoy, O., Rybin, V., Cozijnsen, M., Francis, A., Baekelandt, V., Kozak, C. A., Zerial, M. and Huylebroeck, D. (2001). "Mice with a homozygous gene trap vector insertion in *mgcRacGAP* die during pre-implantation development." *Mechanisms of Development* **102**(1-2): 33-44.

Verheyen, E. M. and Cooley, L. (1994). "Profilin mutations disrupt multiple actin-dependent processes during Drosophila development." *Development* **120**(4): 717-28.

Volker, A., Stierhor, Y. D. and Jurgens, G. (2001). "Cell cycle-independent expression of the *Arabidopsis* cytokinesis-specific syntaxin KNOLLE results in mistargeting to the plasma membrane and is not sufficient for cytokinesis." *Journal of Cell Science* **114**(16): 3001-12.

Waizenegger, I., Lukowitz, W., Assaad, F., Schwarz, H., Jurgens, G. and Mayer, U. (2000). "The *Arabidopsis* KNOLLE and KEULE genes interact to promote vesicle fusion during cytokinesis." *Current Biology* **10**(21): 1371-4.

Walczak, C. E., Mitchison, T. J. and Desai, A. (1996). "XKCM1: a *Xenopus* kinesin-related protein that regulates microtubule dynamics during mitotic spindle assembly." *Cell* **84**: 37-47.

Waterman-Storer, C. M., Worthlylake, R. A., Liu, B. P., Burridge, K. and Salmon, E. D. (1999). "Microtubule growth activates Rac1 to promote lamellipodial protrusions in fibroblasts." *Nature Cell Biology* **1**: 45-50.

Weber, I., Gerisch, G., Heizer, C., Murphy, J., Badelt, K., Stock, A., Schwartz, J. M. and Faix, J. (1999). "Cytokinesis mediated through the recruitment of cortexillins into the cleavage furrow." *Embo Journal* **18**(3): 586-94.

Wheatley, S. P., Carvalho, A., Vagnarelli, P. and Earnshaw, W. C. (2001). "INCENP is required for proper targeting of Survivin to the centromeres and the anaphase spindle during mitosis." *Current Biology* **11**(11): 886-90.

Wheatley, S. P. and Wang, Y. (1996). "Midzone microtubule bundles are continuously required for cytokinesis in cultured epithelial cells." *Journal of Cell Biology* **135**(4): 981-9.

Williams, B. C., Riedy, M. F., Williams, E. V., Gatti, M. and Goldberg, M. L. (1995). "The *Drosophila* kinesin-like protein KLP3A is a midbody component required for central spindle assembly and initiation of cytokinesis." *Journal of Cell Biology* **129**(3): 709-23.

Winter, C. G., Wang, B., Ballew, A., Royou, A., Karess, R., Axelrod, J. D. and Luo, L. (2001). "*Drosophila* Rho-associated kinase (Drok) links Frizzled-mediated planar cell polarity signaling to the actin cytoskeleton." *Cell* **105**(1): 81-91.

Yamaguchi, Y., Katoh, H., Yasui, H., Mori, K. and Negishi, M. (2001). "RhoA inhibits the nerve growth factor-induced Rac1 activation through Rho-associated kinase-dependent pathway." *Journal of Biological Chemistry* **276**: 18977-18983.

Yamano, H., Gannon, J. and Hunt, T. (1996). "The role of proteolysis in cell cycle progression in *Schizosaccharomyces pombe*." *Embo Journal* **15**(19): 5268-79.

Zang, J. H., Cavet, G., Sabry, J. H., Wagner, P., Moores, S. L. and Spudich, J. A. (1997). "On the role of myosin-II in cytokinesis; division of *Dictyostelium* cells under adhesive and nonadhesive conditions." *Molecular Biology of the Cell* **8**: 2612-2629.

Zondag, G. C., Evers, E. E., ten Klooster, J. P., Janssen, L., van der Kammen, R. A. and Collard, J. G. (2000). "Oncogenic Ras downregulates Rac activity, which leads to increased Rho activity and epithelial-mesenchymal transition." *Journal of Cell Biology* **149**: 775-782.

Addendum: Amendments to thesis

1) Page 12, line 3 replace "normal cells" with "these cells"
2) Page 12, line 24 replace "mitotic spindles" with "mitotic microtubules"
3) Page 16, line 9 replace "activates" with "inactivates"
4) Page 21, line 7,11 replace "effectors" with "regulators"
5) Page 21, line 7 replace "GTP/GDP exchange" with "GTP/GDP hydrolysis"
6) Figure 1.2 replace "GTP" with "GDP" and vice versa where the GEF is shown diagrammatically to catalyse the reaction
7) Page 25, line 18 replace "IQGAP and PAK" with "and the Rac/Cdc42 effectors IQGAP and PAK"
8) Page 29, line 9 replace "exchange assays" with "GTPase assays"
9) Page 120 insert "(A and B)" at the start of the figure legend
10) Page 159 replace title 7.2.2 "Molecular Analysis" with "Genetic Analysis"
11) Pages 159-160 replace "mitotic recombination" with "meiotic recombination"